A Chemical Biology Investigation of Neutrophil Extracellular Traps

Zur Erlangung des akademischen Grades eines

Doktors de Naturwissenschaften

(Dr. ret. nat.)

von der Fakultät Chemie

der Technischen Universität Dortmund

angenommene

Dissertation

von

Masters in Chemistry

Nancy E. Martinez

aus

Amarillo, Texas. United States of America

Dekan: Prof. Dr. Roland Winter

1. Gutachter: Prof. Dr. Dr. Herbert Waldmann
2. Gutachter: Prof. Dr. Carsten Watzl
3. Wissenschaftliche Mitarbeiter: Dr. Matthias Müller

This work was carried out under the supervision of Prof. Dr. Dr. Herbert Waldmann at the Faculty of Chemistry of the Technical University of Dortmund and at the Max Planck Institute of Molecular Physiology in Dortmund with close collaboration with Prof. Arturo Zychlinsky at the Max Planck Institute for Infection Biology in Berlin from August 2008 to August 2013.

Dedicated to my parents Daniel and Elvira
to my guardian angel Maty, R.I.P.
to my family and friends
For keeping me grounded while I accomplish my dreams

“Everything on Earth has a purpose, every disease an herb to cure it, and every person a mission….”

Morning Dove
Salish

Abstract

Neutrophils are short-lived leukocytes that migrate to sites of infection where they phagocytose, degranulate, and form Neutrophil Extracellular Traps (NETs). During NET formation, the nuclear lobules of neutrophils disappear, the chromatin expands and, decorated with neutrophilic granule proteins are expelled. NET formation requires the generation of reactive oxygen species (ROS) by nicotinamide adenine dinucleotide phosphate (NADPH) oxidase, which is activated by the protein kinase C (PKC) activator phorbol-12-myristat-13-acetate (PMA). Bacteria, fungi, viruses, and microbial components and other immune cells are the physiological stimuli of NETs. NETs can be pathogenic, for example in sepsis, cancer, autoimmune and cardiovascular diseases. Therefore, the identification of NET formation inhibitors is of high interest. The focus of the project is the application of chemical biology techniques to study NET formation and identify small molecule inhibitors.

A semi-automated high content phenotypic screen was developed using human neutrophils that can identify inhibitors of NET formation. For this purpose, established small molecule compound libraries were screened. The identified small molecule hit compounds were grouped into four categories based on their influence on nuclear morphology and cell viability. These groups are: group 1: viable cells with small nuclei; group 2: viable cells with large nuclei; group 3: dead cells with small nuclei; and group 4: dead cells and NET formation. Since this is the first assay of NETosis to be reported, it was patented.

After the screening of commercial compound libraries, GW5074, a c-Raf kinase inhibitor that stopped NET formation with group 1 characteristics was identified. To investigate if the Raf-MEK-ERK pathway is involved in NET formation, specific kinase inhibitors, GW5074 (c-Raf), U0126 (MEK), Staurosporine (PKC) kinase inhibitors and the ERK inhibitory peptide (ERK) were tested. They were all identified as group 1 phenotype inhibitors. Ras, an upstream protein from Raf, was excluded as a key protein involved in the NET formation mechanism after testing indirect Ras inhibitors. Additionally, the involvement of the ERK pathway upstream of NADPH oxidase was proven. It was shown that anti-apoptotic proteins are expressed to allow NETosis to occur and are regulated by MAPK signaling pathway. The neutrophils phagocytic and degranulation functions were shown to be uneffected in the presence of inhibitors. This work was published in Nature Chemical Biology (Hakkim et al., 2011).

In addition to the ERK signaling pathway, the involvement of the eicosanoid pathway in NET formation was established. Arachidonic acid, diaglycerol and platelet activation factor, known activators of the eicosanoid pathway, were identified as triggers of NET formation. Furthermore, it was demonstrated that lipoxygenase (LOX) is required for NETosis by using specific LOX inhibitors that blocks NET formation. The COX signaling pathway was excluded due to the lack of inhibitory activity of the COX specific compounds. Traditionally in innate immunology, lipid signalling is known

to be involved in cell-to-cell communication. For NETosis, the involvment of this role it was confirmed by the identification of lipid bodies present on the NETs. It is hypothesized that the lipid bodies are composed of a signaling lipid. This work needs to be further established and is beyond the scope of this thesis. Our results elucidated a new function in leukocytes, leading to possibilities to develop a novel field in neutrophil biology.

After screening the MPI Dortmund in-house-compound library, tetrahydroisoquinolines (THIQs) were identified as a novel class of NET formation inhibitors. THIQs inhibit NETosis at low micromolar concentration independent of the NET formation stimulus and at different stages of NET formation. Cells treated with THIQ 1 displayed decondensed nuclei and the phenotype was assigned to group 2, making this an inhibitor with a unique profile. As before, the influence of THIQs on the oxidative burst was studied. THIQs do not affect ROS formation suggesting that they act downstream of ROS formation. Next, the THIQs were biochemically tested on proteins that are involved in the mechanism of NET formation. Interestingly, none of these proteins were shown to be direct targets for the THIQs. Based on the structure activity relationship (SAR) of 100 THIQs, tool compounds suited for target identification were designed and synthesized. With these compounds, affinity-based proteomic experiments were performed on human neutrophil lysates. Unfortunately, no proteins were identified that were selectively enriched with the active probe in comparison to the control. The cellular target of the THIQs might not be a cytosolic soluble protein and is yet to be identified.

A hallmark of many immune disorders is the overproduction and lack of degradation of NETs. NET formation inhibitors are considered promising candidates for the treatment of one autoimmune disease, systematic lupus erythematosus (SLE). Therefore, SLE patient-derived neutrophils were used to evaluate the ability of THIQs to inhibit NET formation in a physiologically highly relevant setting. THIQs inhibited NET formation efficiently in non-activated and PMA-activated SLE patient neutrophils. These results clearly indicate that THIQs have great potential as tool compounds and as a starting point for the development of novel small molecule therapeutics.

The study of the neutrophil NET formation enigma is a perfect example wherein a chemical biology approach can be applied successfully. A robust assay protocol was established allowing NET formation to be studied quickly and could be scaled up to a high throughput setup. Two novel signalling mechanisms were identified and added to the overall mechanism of NETosis. A novel small molecule NET inhibitor compound class was identified and added to the general toolbox developed by us and others to study NETs.

Zusammenfassung

Neutrophile sind kurzlebige Leukozyten, die zu Infektionsorten wandern, wo sie phagoyztieren, degranulieren und sogenannte *Neutrophil Extracellular Traps* (NETs, deutsch: Neutrophile Extrazelluläre Fallen) bilden. Während der NET-Formation lösen sich die nuklearen Lobuli der Neutrophilen auf, das Chromatin dehnt sich aus und wird zusammen mit neutrophilen Granulaproteinen in den extrazellulären Raum ausgestoßen. Bakterien, mikrobielle Komponenten, Pilze, Viren und andere Immunzellen gehören zu den physiologischen Aktivatoren der NET-Formation. Die Bildung von NETs kann außerdem durch den Proteinkinase C (PKC) Aktivator Phorbol-12-myristat-13-acetat (PMA) induziert werden, der die Nicotinamid-Adenin-Dinukleotidphosphat (NADPH) -Oxidase katalysierte Bildung von reaktiven Sauerstoffspezies (ROS) und so letztlich NET-Formation bewirkt. Die Formation von NETs kann auch in Krankheiten involviert sein, unter anderem in Sepsis, Krebs und Autoimmun- sowie Herz-Kreislaufkrankheiten. Aus diesem Grund ist die Identifizierung von NET-Bildungsinhibitoren von großem Interesse. Der Schwerpunkt dieses Projektes ist es kleine Moleküle, welche die NET-Formation inhibieren zu identifizieren und diese im Sinne eines Chemischen Biologie basierten Ansatzes zu nutzen um die Formation von NETs zu genauer zu untersuchen.

Ein semi-automatisierter, multiparametrischer phenotypischer *Screen* zur Identifizierung von Inhibitoren der NET-Formation in humanen Neutrophilen wurde entwickelt und mehrere Substanzbibliotheken wurden in dem neuartigen Assay getestet. Die aktiven Substanzen wurden dann, basierend auf dem von ihnen induzierten Phänotypen in eine von vier Kategorien eingeteilt. Diese Kategorien waren: 1) Lebende Zellen mit kleinem Nucleus, 2) Lebende Zellen mit großem Nucleus, 3) Tote Zellen mit kleinem Nucleus, und 4)Tote Zellen die NETs gebildet haben. Dieser Assay war der erste seiner Art und wurde daher patentiert.

In dem *Screening* von kommerziellen Substanzbibliotheken wurde GW5074, ein bekannter c-Raf Kinase Inhibitor, als Inhibitor der NET-Formation der Kategorie 1 identifiziert. Daher wurden weitere Inhibitoren des Raf-MEK-ERK Signalwegs auf ihren Effekt auf die NET-Formation hin untersucht. Die getesteten Substanzen GW5074 (c-Raf Inhibitor), U0126 (MEK-Inhibitor), Staurosporin (PKC Inhibitor) und das *ERK inhibitory peptide* (ERK Inhibitor) induzierten alle einen Kategorie 1 Phänotyp. Direkte Inhibitoren von Ras, einem dem Raf-MEK-ERK Signalweg vorgeschaltetem Protein, zeigten keinen Effekt, somit konnte eine Schlüsselfunktion von Ras in der NET-Bildung ausgeschlossen werden. Darüber hinaus wurde die Beteiligung des ERK-Weges *upstream* der NADPH-Oxidase nachgewiesen. Es wurde gezeigt, dass die Expression von anti-apoptotischen Proteinen zur NET-Formation notwendig ist und dass dies durch den MAPK Signalweg kontrolliert wird. Die phagozytotische Aktivität und die Degranulierung von Neutrophilen bleibt durch die Inhibitoren der NET-Formation unberührt. Diese Ergebnisse wurden in Nature Chemical Biology veröffentlicht (Hakkim et al., 2011).

Neben dem ERK-Signalweg wurde die Beteiligung des Eicosanoid-Weges in der NET-Bildung etabliert. Arachidonsäure, Diacylglycerin und Thrombozytenaktivierungsfaktor, bekannte Aktivatoren des Eicosanoidwegs, wurden als Auslöser der NET-Bildung identifiziert. Durch die Verwendung spezifischer Lipoxygenase (LOX) Inhibitoren konnte darüber hinaus gezeigt werden, dass LOX-Aktivität für die NET-Formation notwendig ist. Cyclooxigenase (COX) konnte unter Verwendung des selben Ansatzes als Schlüsselprotein ausgeschlossen werden. Aus der klassischen Immunolgie ist bekannt, dass *Lipid-Signalling* in der Zell-zu-Zell-Kommunikation eine wichtige Rolle spielt. Dies konnte in diesem Projekt durch den Nachweis von *Lipid Bodies* auf NETs auch für die NET-Formation bestätigt werden. Die genaue Rolle und Zusammensetzung dieser *Lipid Bodies* in NETs benötigt weitere Forschung und liegt außerhalb des Rahmens dieser Arbeit. Unsere Ergebnisse zeigen eine neue Funktion von Leukozyten, was zu Möglichkeiten der Entwicklung eines neuartigen Feldes in der Biologie der Neutrophilen führt.

In dem Screening der internen Substanzbiblitohek des MPI Dortmund wurden Tetrahydroisoquinoline (THIQs) als ein neuartige Klasse von Inhibitoren der NET-Formation identifiziert. THIQs sind wirksam in Konzentrationen im niedirgen millilmolaren Bereich und inhibieren die Bildung von NETs unabhängig vom Stimulus der NET-Formation und in verschiedenen Stadien. THIQ 1 ist der einzige Inhibitor, der einen Kategorie 2 Phänotyp mit dekondensierten Nuclei bewirkt. THIQs haben keinen Effekt auf die Bildung von ROS und in weiteren biochemischen Experimenten konnte kein direkter Einfluß auf bekannte, in die Bildung von NETs involvierte Proteine beobachtet werden. Basierend auf Untersuchungen bezüglich der Struktur-Wirkungsbeziehung von 100 THIQs wurden daraufhin Sonden zur Affinätschromatographie-basierten Identifikation der THIQ-Zielproteine entworfen und synthetisiert. Die in den anschließenden Pulldown-Experimenten konnten jedoch keine potentiellen Zielproteine identifiziert werden und somit ist das zelluläre Ziel der THIQs, be idem es sich eventuell um ein nicht-zytosolisches Protein handeln könnte, noch offen.

Die Überproduktion und mangelhafte Degradation von NETs ist ein Kennzeichen vieler Autoimmunerkrankungen, insbesondere von Systemischen Lupus erythematodes (SLE). Inhibitoren der NET-Formation stellen daher ein vielversprechendes Ziel für dessen Behandlung dar. Die Wirksamkeit der THIQs auf nicht-aktivierte und PMA-stimulierte NET-Formation konnte in diesem Projekt erfolgreich an Neutrophilen von SLE-Patienten gezeigt werden. Die Wirksamkeit dieser Substanzen in einem physiologisch relevanten Modell unterstreicht das Potential dieser neuartigen Klasse von Inhibitoren der NET-Formation als funktionelles Molekül zur Erforschung der NET-Formation und als Startpunkt für Entwicklung neuartiger Medikamente.

Die Erforschung der NET-Formation in Neutrophilen ist ein perfektes Beispiel in dem ein chemisch-biologischer Ansatz erfolgreich angewendet werden kann. In diesem Projekt wurde ein

robustes Assayprotokoll zur Evaluation der NET-Formation etabliert und in ein Hochdurchsatzformat übertragen. Dadurch konnte eine Rolle von zwei Signalwegen in der Formation von NETs gefunden werden. Außerdem wurde eine neuartige Klasse von kleinen Molekülen mit der Fähigkeit die Formation von NETs zu inhibieren identifiziert, die auch Wirksamkeit in SLE-Patientenzellen Wirksamkeit zeigt.

Abbreviations

ABAH:	4-Aminobenzoic acid hydrazide
BPI:	Bactericidal/permeability- increasing protein
BSA:	Bovine serum albumin
C5a:	Complement component 5a
CA:	*Candida albicans*
C/EBP:	CCAAT/enhancer-binding protein
CG:	Capthepsin G
CGD:	Chronic Granulomatous Disease
COX:	Cyclooxygenase
cRaf:	Proto-oncogene serine/threonine-protein kinase, MAP kinase kinase kinase
CXCL:	C-X-C motif chemokine ligand
CXCR:	C-X-C motif chemokine receptor
DAG:	Diacylglycerol
DC:	Dendritic cells
DFP:	Diisopropyl flourophosphate
DMSO:	Dimethyl sulfoxide
DNA:	Deoxyribonucleic acid
DNase:	Deoxyribonuclease
DPI:	Diphenyleneiodonium chloride
EGF:	Epidermal Growth Factor
ERK:	Extraceullar-signalling regulated kinases
Fig.:	Figure
fMLP:	*N*-Formylmethionyl-leucyl-phenylalanine
GCSF:	Granulocyte colony stimulating factor
GMCSF:	Granulocyte macrophage colony-stimulating factor
GO:	Glucose oxidase
GPCR:	G protein–coupled receptors
hCAP-18:	Human cathelicidin
HCT:	High content screening
HL60:	Human promyelocytic leukemia cells
HOCl:	Hydrogen hypochlorite
H_2O_2:	Hydrogen peroxide
HTS:	High Throughput Screening
ICAM:	Intercellular adhesion molecules
IFN:	Interferon
IL:	Inter-leukins

iNOS:	Nitric oxidase synthase
LBR:	Lamin B receptor
LDC:	Lead discovery Center
LDH:	Lactate dehydrogenase
LL-37:	Human cathelicidin
LOPAC:	Library of pharmacologically active compounds
LOX:	Lypoxygenase
LPS:	Lipopolysaccharide
LSS:	Low spin supernatant
MAP:	Mitogen-activated protein
MEK:	Mitogen-activated protein kinase kinase
MOI:	Multiplicity of infection
MPO:	Myeloperoxidase
MS:	Multiple sclerosis
MST:	Microscale thermophoresis
NADPH:	Nicotinamide adenine dinucleotide phosphate
NE:	Neutrophil elastase
NET:	Neutrophil extracellular traps
NGAL:	Neutrophil gelatinase-associated lipocalin
NK:	Natural killer cell
NO:	Nitric Oxide
NOX:	NADPH oxidase protein family
NP:	Natural Product
O:	Oxygen
PAD:	Peptidyl arginine deiminase
PAMP:	Pathogen-associated molecular patterns
PFA:	Paraformaldehyde
PHA:	Pelger-Hüet Anomaly
PKC:	Protein kinase C
PMA:	Phorbol-12-myristate-13-acetate
PMN:	Polymorphonuclear cells/leukocytes
PMSF:	Phenylmethanesulfonyl fluoride
PR3:	Proteinase 3
RB:	RIKEN beads
RNA:	Ribonucleic acid
RNAi:	RNA interference
ROS:	Reactive oxygen species

SAR:	Structure Activity Relationship
SEM:	High resolution scanning microscope
SILAC:	Stable isotope labeling by amino acids in cell culture
SLE:	Systematic lupus erythematosus
SOD:	Superoxide dismutase
THIQ(s):	Tetrahydroisoquinoline(s)
TLR:	Toll-like receptor
TIR:	Toll/interleukin-1
TNF:	Tumor necrosis factor
TRAP:	Thrombin receptor activated peptide
UV:	Ultra-violet light

Contents

Chapter 1: General Introduction

1.1 Chemical biology and disease

In science, the objective is to investigate natural phenomena and part of the challenge is to create solutions to problems that arise during the process. The development of new tools and new technologies is essential. Chemical biology is the division of science where chemical tools, usually small molecule probes, are used to study biological systems and events (Altmann et al., 2009). The possibilities and flexibility that they provide are diverse and in particular small molecules derived from nature – in essence natural products - have proven their value since the beginning of chemistry and biology (Doweyko and Doweyko, 2009; Eder et al., 2014; Wetzel et al., 2011). The use of small molecules provides the possibility for full control over concentration, duration of exposure, protein modulation and phenotype manipulation. Another advantage is that these tools allow for rapid effect recording of effect and swift clearance. Being able to remove the tool compound quickly is a great advantage over permanent modifications such as gene knock-out or knock-downs, if these are even possible. Such genetic modifications are often lethal to the host limiting their use (Ziegler et al., 2013).

Today, the focus for chemical biology is on finding solutions to problems such as better treatment for cancer; overcoming antibiotic resistance; engineering microbes that can function as small molecule factories; shortening the drug development pipeline or using technology for smarter, accurate and painless diagnostics (Kostic et al., 2016b). In order to study such complex processes, collaboration between many different scientific fields are required. Different disciplines that collaborate in a chemical biology project range from synthetic organic chemistry to immunology, from molecular biology and pharmacology, to biochemistry and bioorganic chemistry (Bucci et al., 2010; Kostic et al., 2016a, b). A good example of a chemical biology approach is the application of “click” chemistry. The organic chemistry process of a click reaction is a diverse procedure that allows the generation of complex conjugated molecules performed *in-situ* in biological systems. Whether it is copper catalyzed or by Staudinger ligation, it has been applied in several fields such as bioconjugation, drug discovery, and materials science (Nwe and Brechbiel, 2009; Thirumurugan et al., 2013). The Bertozzi’s group successfully performed an *in vivo* biorthogonal chemistry click reaction in live cells, mice, and in zebrafish. This work provides labeling tools for imaging and target validation (Agarwal et al., 2015; Chang et al., 2010; Cohen et al., 2010).

Besides chemical biology approaches with specifically designed tools, nature has always been a good source of inspiration for small molecule probe design. Natural products are highly optimized for their purpose through evolution, making them excellent starting points for novel biological active compounds. Wetzel et.al. has depicted a natural compound scaffold tree to categorize scaffolds of interest with high potential of biological activity (Wetzel et al., 2009). Large numbers of libraries have been synthesized based on these scaffolds (Doweyko and Doweyko, 2009). A good example where such small molecules are used is in the study of reactive oxygen

species (ROS) (Dickinson and Chang, 2011). The generation of ROS is a fast complicated process making it challenging to study. Several small molecule tool compounds have been developed such as diphenyleneiodonium chloride (DPI), apronin, and pyrocatechol respectively an inhibitor, a scavenger and an activator of ROS formation. A common application of well-established compounds, inhibitors or activators, is use as controls. In research performed in ROS generation, small molecules are used as controls. These molecules allow for rapid manipulation of ROS formation unlike gene knockouts (Bolt et al., 2009; Saladino et al., 2008).

As the scientific challenges increase in difficulty so do the complexity of the tools that are required. Studying a complex autoimmune disease or cancer requires the use of biological systems that result in complicated readouts. The use of stem cells and primary human cells for screening clearly fits these criteria, since it is far from simple. As it will be described in this thesis, we are the first to apply a combination of novel proposed (i.e. primary cell screens, new techniques of proteomics) and traditional solutions to a physiological problem, the study of neutrophil extracellular traps.

Chapter 2: Aim of the Project

Neutrophil Extracellular Trap (NET) formation is a recently discovered response carried out by neutrophils in order to trap pathogens as part of the native immune response. Many details concerning the mechanism of action of this newly discovered type of cell death are still unknown. Their properties make neutrophils complicated cells to handle and there is no permanent cell line that can mimic NET formation. This means conventional procedures are not feasible and therefore we required the development of novel techniques and assays to study the phenomena. We postulated that chemical inhibitors of NET formation would allow us to identify key regulators of NETosis. Furthermore this work will lead to a better understanding of NET formation.

The focus of this project is to identify small molecule modulators of NET formation and their molecular targets. These small molecule tools will be used to investigate the mechanisms and proteins involved in the generation of NETs. The study of NETs requires a collaboration of specialized biology and chemistry groups and consequently we started a collaboration between the Zychlinsky's group (Max Planck Institute for Infection Biology in Berlin) and the Waldmann's group (Max Planck Institute of Molecular Physiology in Dortmund). The work described in this thesis has been performed both in Berlin and in Dortmund.

Chapter 3: Neutrophils

White blood cells are the first cells that protect the human body against invading pathogens and are equipped with various defense mechanisms, sometimes at the cost of their own existence (Nathan, 2006). White blood cell is the colloquial name for the leukocytes. If the white cells are classified according to their cell structure they are named granulocytes. The most abundant type of granulocytes are neutrophils. Granulocytes consist of neutrophils, eosinophils and basophils and are part of the innate immune system. All granulocytes contain many lysosomes and secretory vesicles and are classified based on their chemical differences and function (Rivera et al., 2016). Neutrophils constitute more than ninety percent of the granulocytes in circulation and according to early studies the bone marrow produces $9x10^8$ neutrophils/kg of body weight per day (Dancey et al., 1976; Gunzer, 2014). Many of the immune cells are terminal cells, i.e cells that will not undergo cell division. These terminal cells, neutrophils, reside in the blood for approximately eight hours.

3.1 Morphology

Neutrophils were first named by Paul Ehrlich in the late nineteenth century (Amulic et al., 2012) for their capacity to retain neutral dyes. Their main physical characteristic is their lobulated nuclei giving them the name of “polymorphous nucleus” which caused them to be classified as polymorphonuclear cells (PMNs) by Elie Metchnikoff in 1893. The terms neutrophil and PMN are used interchangeably in this dissertation.

Why do neutrophils have lobulated nuclei? To this day, there is no definite explanation (Figure 1). One of the earlier theories was postulated by Metchnikoff and states that the lobulated nucleus facilitates passage to different sites in the body through blood vessels and small pores. No definite proof has been found to support this (Chou et al., 2010) and the notion may be incorrect because some experiments using human promyelocytic leukemia cells (HL60) cells, with the Pelger-Hüet anomaly (PHA) round nuclei phenotype, show the unaffected ability to cross membranes (Olins and Olins, 2004, 2005). Another possible explanation for the lobulated nuclei is the enhancement of phagocytosis since it provides more space in the cytoplasm for accepting pathogens (Carvalho et al., 2015). Notably, there has been no real evidence dictating an evolutionary need for polymorphonucleus.

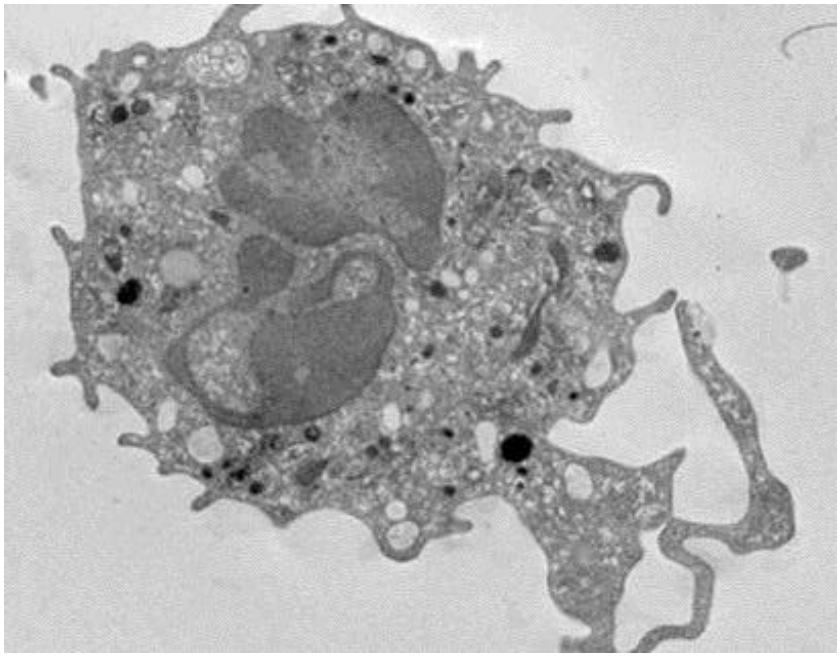

Figure 1. Transition electron microscopy image of a neutrophil (Fuchs et al., 2007).

3.2 Neutrophils source

Neutrophils differentiate from precursor cells named hematopoetic stem cells in a process called myelopoiesis. This differentiation is a stepwise process starting with division into a multipotent precursor which further divides into a myeloid or a lymphoid progenitor. Subsequently, most of the differentiated myeloid cells become part of the innate immune response. Alternatively, those cells that differentiated from the common myeloid progenitors become part of the adaptive immune system (Bardoel et al., 2014; Borregaard, 2010). In the case of neutrophils their common progenitor is the myeloid cell or myeloblast, specifically, the granulocyte/macrophage progenitor cell and this differentiation process is termed granulopoiesis (**Figure 2**). Granulopoiesis is highly regulated by cytokine release (Bugl et al., 2012). The main cytokine involved are the granulocyte colony-stimulating factor (G-CSF) and granulocyte macrophage colony-stimulating factor (GM-CSF) (Mayadas et al., 2014). Inter-leukins (IL) regulate G-CSF production in peripheral tissues triggered with IL-23, IL-17, and the levels of G-CSF known as the G-CSF feedback loop. IL-23 is produced by macrophages and dendritic cells (DC) and induces the production of IL-17 by T helper cells, T lymphocytes and natural killer cells. This results in the neutrophil differentiation followed by the expression of G-CSF. Macrophages produce IL-23 after the clearing of apoptotic neutrophils, hence this process depends on the amount of neutrophils in circulation (Bardoel et al., 2014; Mayadas et al., 2014; Stark et al., 2005). An additional means of generating neutrophils is via emergency granulopoiesis (Basu et al., 2000) which is a reaction to the presence of foreign pathogens. The pathway is dependent on the particular pathogen. For example in the case of *Listeria*

monocytogenes GCSF is required for a neutrophil rapid response (Bardoel et al., 2014; Papayannopoulos and Zychlinsky, 2009b). However, it is not the case for *Candida albicans* where interleukin-1 (IL-1) is used (Altmeier et al., 2016; Basu et al., 2000). It is certain that when it comes to maintenance, the neutrophil numbers are controlled by constant exposure to pathogens. For instance, germ-free mice suffer from serious neutropenia (low number of neutrophils) (Bugl et al., 2013). In brief, homeostasis of neutrophils is regulated by the amount of available neutrophils. The number of available PMNs is dependent on phagocytosis, PMNs numbers in bone marrow, or external pathogens that trigger inflammatory responses.

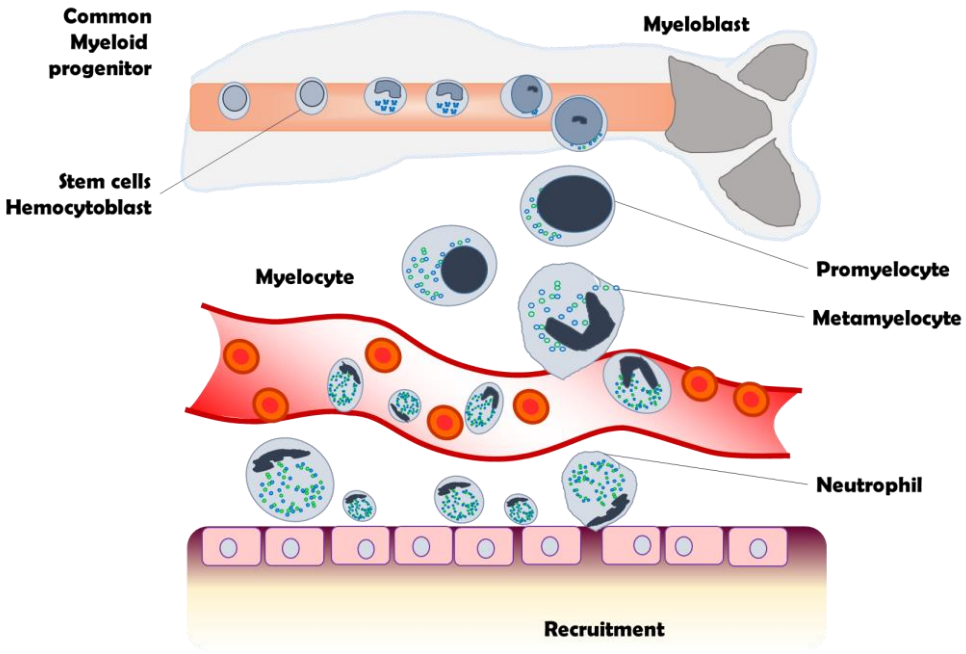

Figure 2. Neutrophil Granulopoiesis. The transition of the myeloid cell in the bone marrow to full maturation in the blood stream. Image modified from Kruger, et. al. (Kruger et al., 2015).

3.3 Neutrophil Response

After maturation, neutrophils migrate to sites of inflammation. PMNs are the first cells to infiltrate infected tissue and compose more than sixty percent of cells at the site of infection (Brinkmann and Zychlinsky, 2007; Papayannopoulos and Zychlinsky, 2009a). They are terminal cells and do not undergo cell division and as a result, as “ready-to-go” cells, they have to be able to pass through different environments and tissues to the target locations. In doing so they have alternative ways to use and re-use their weapons. The role that the neutrophil will perform is completely dependant on the activation, i.e. stimulus. Stimulants include bacterial derived pathogen-associated molecular patterns (PAMPs), i.e. lipopolysaccharide (LPS) and N-Formylmethionyl-leucyl-phenylalanine (fMLP). Also, chemoattractants and cytokines, i.e. tumor

necrosis factor (TNF)-α, interleukin (IL)-1β, IL-8, and IL-17; adhesion molecules produced by endothelial cells, i.e. P-selectins and E-selectins and the integrin superfamily intercellular adhesion molecules (ICAMs) can recruit neutrophils (**Figure 2 and 3**) (Borregaard, 2010; Kruger et al., 2015; Mayadas et al., 2014).

3.3.1 How does the Neutrophil Response Work?

Neutrophils are abundant and widely distributed throughout the body. Primary chemokines coordinate the equilibrium of the neutrophil release and retention. PMNs are released from bone marrow by stromal cells that produce C-X-C motif chemokine ligand (CXCL)-12 which is recognized by the C-X-C-motif chemokine receptor (CXCR)-4 on PMNs and induces neutrophil mobilization (**Figure 2**). The two main chemokines receptors expressed in neutrophils are CXCR1 and CXCR2 which are responsible for retention and release of cytokines, respectively (Kruger et al., 2015; Martin et al., 2003). CXCR2 is the receptor for CXCL1, CXCL2, CXCL3, CXCL5, CXCL6 and CXCL8, all of which chemokines are responsible for neutrophil homeostasis in response to neutrophil number by releasing myeloid cells (Nauseef and Borregaard, 2014).

Myeloid cells (pre-neutrophil cells) are released from bone marrow when a disease state is detected. These cells are capable of recognizing a series of signals that lead directly to employment of their “attack” mechanisms and then on to maturation into neutrophils.

The steps of the traditional adhesion cascade are (**Figure 3)**:

a) Capture: the initial attachment of the neutrophil to the endothelium close to inflammatory sites and performed by selectins;

b) Rolling: neutrophils roll along the endothelium mediated by selectins;

c) Firm adhesion: integrin-mediated rolling is stopped, adhesion and spreading of the cells occurs;

d) Crawling/transmigration: mediated by integrin’s and in which the neutrophil crawls through the endothelial space or tissue reaching the site of infection/inflammation.

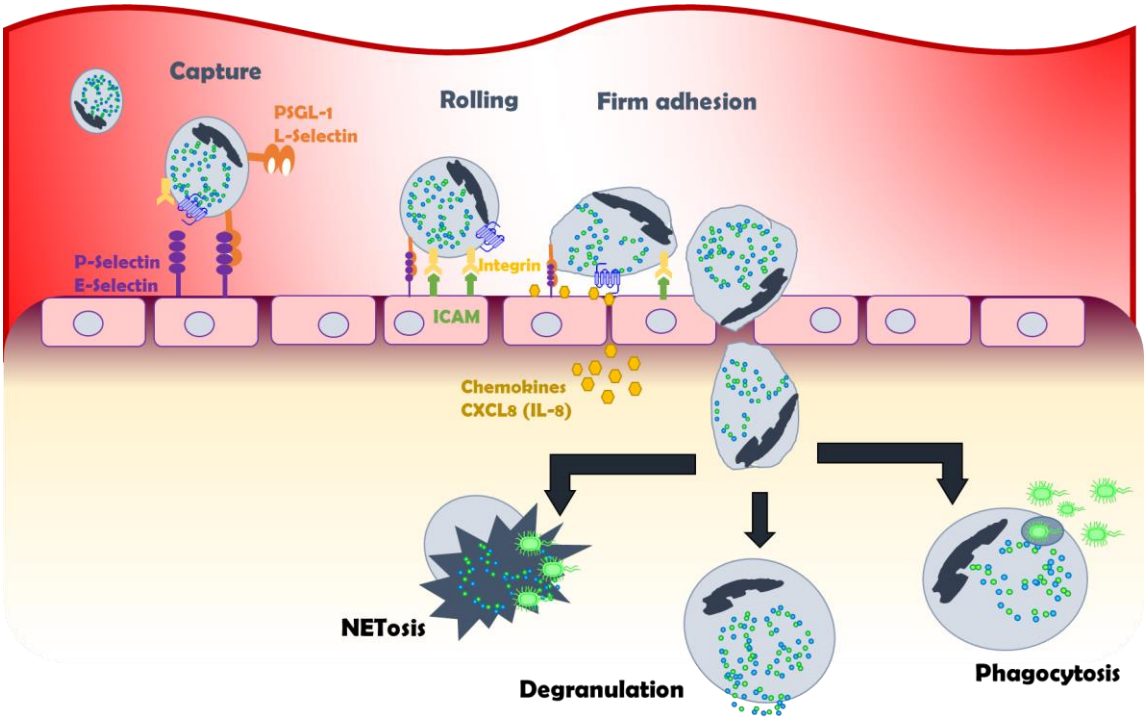

Figure 3. Neutrophil recruitment and function. Once the neutrophil gets released, it captures, rolls and goes through the epithelial layer. Here it performs its function of phagocytosis, degranulation or NETosis. Image based on images from Amulic, et. al and Mayadas, et. al. (Amulic et al., 2012; Mayadas et al., 2014).

3.4 Neutrophils Components

Since neutrophils are the first line of defense against the invading pathogens, the chemical weapons used by neutrophils to kill bacteria substances are highly toxic. These substances are located, transported, and used by the neutrophil in a controlled manner to avoid unnecessary damage to healthy tissue. PMNs have developed special organelle-based storage and transport system and these organelles are called granules.

3.4.1 Granules

The neutrophil's arsenal is composed of granular proteins, secretory vesicles, antimicrobial peptides, and antimicrobial proteins. The granules can be divided in three major types, azurophilic (primary), specific (secondary) and gelatinase (tertiary) granules. The secretory vesicles are usually referred to as a type of granule; and usually classified as the fourth group (Amulic et al., 2012; Borregaard, 2010).

Azurophilic granules are also known as primary or peroxidase-positive granules, named after their ability to take up dye azure A (Amulic et al., 2012). They are the first type of granule upon maturation and are the largest in size (~0.3 µm in diameter) but also the last to mobilize. Some of

these primary granules include the following proteases: myeloperoxidase (MPO), lysozyme, inducible nitric oxidase synthase (iNOS), β-glucoronidase, bactericidal/permeability-increasing protein (BPI), and the serine containing proteases: neutrophil elastase (NE), cathepsin G (CG), proteinase 3 (PR3) (Faurschou and Borregaard, 2003).The secondary granules or specific granules are smaller (~0.1 μm in diameter) and are the second ones to mature. Their main component is the glycoprotein lactoferrin and they contain a wide range of antimicrobial proteins including neutrophil gelatinase-associated lipocalin (NGAL), human cathelicidin (hCAP-18) and lysozyme. The tertiary type of granule, or gelatinase granules, are the smallest and the last to be formed during maturation. They are composed of a few antimicrobials and used mainly for storage of metalloproteases, i.e. gelatinase and, leukolysin. The last class of organelles are the secretary vesicles. These are not granules by definition, though they are often classified in the granules (**Figure 4**). They are formed during endocytosis at the last stage of neutrophil maturation. Secretory vesicles are a reservoir for the membrane molecules and are used during neutrophil migration.

3.4.2 Antimicrobial peptides and proteins

An additional component of the neutrophil's arsenal are the antimicrobial peptides and proteins, which are relatively small, <10 kDa, and produced in abundance. Over 800 have been identified (Reddy et al., 2004). These peptides have become the focus of many studies and, most of the work performed with these peptides is based on *in vitro* experiments. The identification of neutrophilic antimicrobial proteins allowed their classification into three main categories: cationic, enzymatic, and the class of 'depriving' proteins (Amulic et al., 2012; Brogden, 2005).

Cationic peptides comprise the main group of peptides in neutrophils and usually bind to negatively charged microbial cell membranes producing pores, thereby causing membrane permeabilization. Cationic peptides can also inhibit DNA and RNA biosynthesis or can disrupt bacterial biofilms. These peptides include defensins, mainly α-defensins, and cathelicidins. Defensins have multiple disulfide bonds that under physiological conditions change structure and become more active (Schroeder et al., 2011). Their main function is to permeabilize the bacterial wall via formation of pores and to inhibit RNA and DNA synthesis. LL-37 is the most intensively researched of all the cathelicidins. LL-37 stimulates neutrophil chemotaxis, increases chemokine receptor expression, induces cytokine production, decreases apoptosis as well as potentiating other immune cells, for example dendritic cells (Lande et al., 2011; Lande et al., 2007; Mayadas et al., 2014). The other class of neutrophil components are antimicrobial proteins which are categorized as either cationic proteins, proteolytic enzymes or metal chelator proteins. The cationic proteins include bactericidal, or permeability-increasing protein (BPI), that binds to lipopolysaccharide (LPS) resulting in an increase in cell permeability and hydrolysis of bacterial phospholipids (Canny and Levy, 2008), and histones, which besides their major role in DNA packaging are excellent antimicrobials. The second class of antimicrobial proteins are the proteolytic enzymes that

participate in the dismantling of the bacterial cell wall. Important proteins in this group include lysozyme, serine proteases, and azurocidin. The serine proteases Proteinase 3 (PR3), neutrophil elastase (NE) and Capthepsin G (CG) are highly regulated by serpins and only released under specific conditions (Campanelli et al., 1990; Weinrauch et al., 2002). Finally, metal chelator proteins function as antimicrobial proteins by chelating the pathogen metal load and thereby limiting bacterial growth. As examples lactoferrin binds iron while calprotectin is active in binding zinc (Amulic et al., 2012).

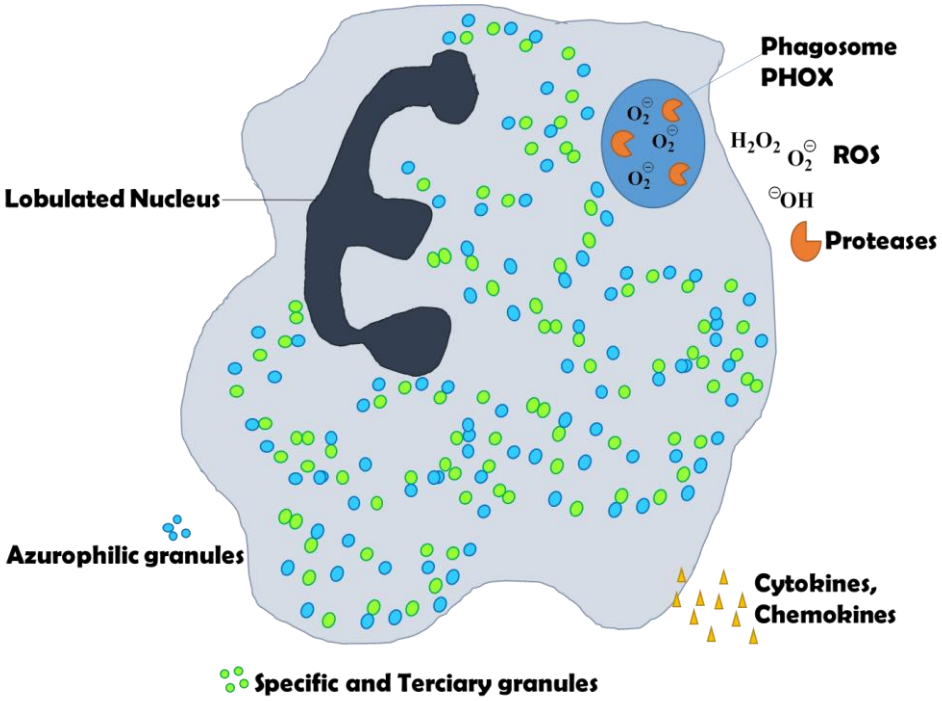

Figure 4. Neutrophil components. Neutrophils have a polymorphous nucleus; azurphilic, specific and tertiary granules and phagosomes. Phagosomes are equipped with proteases that release ROS. Neutrophils also express receptors for cytokines and chemokines that enables the communication to other cells.

3.4.3 Reactive Oxygen Species

Reactive oxygen species (ROS) are a collection of oxygen-based reactive molecules which include radical species (O_2•-, and OH•), non-radical hydrogen peroxide (H_2O_2) and hypochlorous acid (HOCl) (Hayyan et al., 2016). ROS generation in neutrophils is a cascade starting with a respiratory burst, or other increase in oxygen consumption, to produce superoxide (O_2•-) by nicotinamide adenine dinucleotide phosphate (NADPH) oxidase. This enzyme reduces oxygen into superoxide (O_2-) (Mayadas et al., 2014). In turn, superoxide dismutase (SOD) converts O_2- into (H_2O_2) (Fuchs et al., 2007; Metzler et al., 2011) and myeloperoxidase (MPO) converts H_2O_2 to (HOCl) (Hampton et al., 1998). NADPH oxidase complex is composed of $p47^{phox}$, $p67^{phox}$, and $p40^{phox}$ that migrate to the membrane and form the complex by binding with membrane proteins

gp91phox (NOX2) gp22phox and GTPase Rac (Rac1 and Rac2) (Kleniewska et al., 2012). Besides ROS generation, NAPDH oxidase regulates inflammation by activating redox cascades that signal to other cells (Seger, 2010). Superoxide is involved with the change in ionic flux in the phagosome (Reeves et al., 2002) (**Figure 4**).

The main function of ROS is eliminating antimicrobial activity through decarboxylation, deamination or peroxidation (Bardoel et al., 2014). Indirectly ROS can kill pathogens by modulation of phagocyte proteinase activity (Williams, 2006). ROS is involved in signaling via the oxidation of cysteine residues of several proteins, change in the ionic influx and signaling to host molecules (Amulic et al., 2012; Winterbourn et al., 2006). Another important ROS species is nitric oxide (NO), a short-lived and highly reactive molecule produced by inducible nitric oxidase synthase (iNOS) and found in primary granules of neutrophils (Evans et al., 1996). Additionally, superoxide reacts with NO thereby producing high levels of peroxynitrite.

Regulation is a highly sensible step in ROS generation, since an overproduction will result in uncontrollable oxidation and high damage to regular tissue. On the other hand, inhibiting ROS production in neutrophils can be dangerous, for example in the case of chronic granulomatous disease (CGD) which is caused by a mutation in the NADPH oxidase complex. These patients cannot produce ROS and are consequently very inefficient in killing pathogens leading to severe infections (Kuhns et al., 2010; Winkelstein et al., 2000).

3.5 Neutrophil Defense Mechanisms

PMNs can interact with other cells, both immune and non-immune. Neutrophils communicate with macrophages, B and T lymphocytes, mesenchymal stem, dendritic and natural killer cells, and platelets. As mentioned previously, PMNs communicate with endothelial cells when translocating throughout the body (Scapini and Cassatella, 2014). In the following section, the mechanisms in which the neutrophil responds in a sites of infection. This will include the secretion of cytokines, degranulation, phagocytosis, and generation of neutrophil extracellular traps.

3.5.1 Phagocytosis

Phagocytosis is the process of pathogen ingestion by the neutrophil. It takes place in a vacuole in the neutrophil called a phagosome. Phagocytosis is the major mechanism that neutrophils employ to fight infections. Phagocytosis is a very fast process, considering it includes such major changes as physical uptake of particle, intracellular signaling cascades, and major cytoskeletal rearrangements (**Figure 3**) (Amulic et al., 2012; Vieira et al., 2002). For example, it takes as little as 20 seconds for IgG-opsonized particles to be phagocytosed by neutrophils (Segal et al., 1980).

Phagocytosis is triggered by the pattern-recognition receptors of microorganisms, or by opsonic receptors, i.e. FcɣRs, C-type lectin receptors, or complement receptors. After activation, the particle

or pathogen is taken up while the phagosome granules fuse and NADPH oxidase complex is assembled and becomes active (Lee et al., 2003).

This process called phagosome maturation is an extremely toxic combination for bacteria. Compared to the phagosome of macrophages, the neutrophil phagosome is neutral, with alkaline periods during which serine proteases, i.e. NE and CG, are activated (Jankowski et al., 2002). Ion channels play a major role in phagosomal maturation, in which cytosolic calcium ions are essential. Potassium (K+) channels activate, in response to the NADPH oxidase, the release of granular proteases. Phagocytic receptors are triggered by immune complexes or by tissue damage (Amulic et al., 2012; Lee et al., 2003; Mayadas et al., 2014).

3.5.2 Degranulation

Degranulation is the release of antimicrobial molecules (previously described in Section 3.4) in response to a stimulus. Many immune cells are capable of degranulation, for example granulocytes, mast cells, T- cells and natural killer (NK) cells (**Figure 3**). In human neutrophils, granules are more than just storage-units that become activated during inflammation. Granules mobilize once the cell has activated in response to pathogen invasion or an inflammatory response. The secretory vesicles are the particles that take most advantage of the degranulation process compared to the azurophilic granules or gelatinase granules since they are harder to mobilize and more likely to be expelled via exocytosis (Faurschou and Borregaard, 2003; Lominadze et al., 2005).

In section **3.3.1**, the main steps of the neutrophil recruitment and maturation were described. During capture, when the neutrophil interacts with the endothelium, in response to the selectin and chemoattractant interaction, the secretory vesicles mobilize (**Figure 3**). The merging of the secretory vesicles with the plasma membrane exposes the components to the external environment resulting in the step known as firm adhesion. Once the PMNs start to travel through the endothelial space, a process called transmigration or crawling (both terms are used interchangeably in the literature). Signaling leads to the mobilization of gelatinase granules. The metalloproteases released during this process aid the traverse movement of the neutrophil. Once the PMN reaches the site of infection, oxidative burst occurs and the azurophilic and specific granules mobilize and kill pathogens (Amulic et al., 2012; Faurschou and Borregaard, 2003; Mayadas et al., 2014).

Chapter 4: Neutrophils Extracellular Traps

In 2004, Zychlinsky and colleagues reported the first visual recording by microscopy of the release of extracellular chromatin fibers decorated with cytoplasmic granules and histones produced by a neutrophil. This is the official discovery of the neutrophil extracellular trap (NET) (Brinkmann et al., 2004). For quite some time, scientists have described extracellular fiber like structures present in their samples. Due to the lack of advanced microscopy techniques they were considered as artifacts. Since then, the process of NET formation was coined NETosis. NEtosis describes a new form for neutrophils to confine infections that results in expulsion of extracellular DNA traps (Brinkmann et al., 2004; Fuchs et al., 2007; Steinberg and Grinstein, 2007).

Neutrophils are not the only cells that can undergo extracellular trap formation. Cells like are eosinophils (Yousefi et al., 2008), mast cells (von Kockritz-Blickwede and Nizet, 2009), monocytes and macrophages (Chow et al., 2010) all share similarities in molecular mechanism. Upon activation, neutrophils undergo drastic nuclear changes, i.e., chromatin decondensation and nuclear envelop disintegration, cytoskeleton rearrangement and release DNA extracellularly (Brinkmann et al., 2004; Fuchs et al., 2007; Hakkim et al., 2011; Urban et al., 2009) (**Figure 5**).

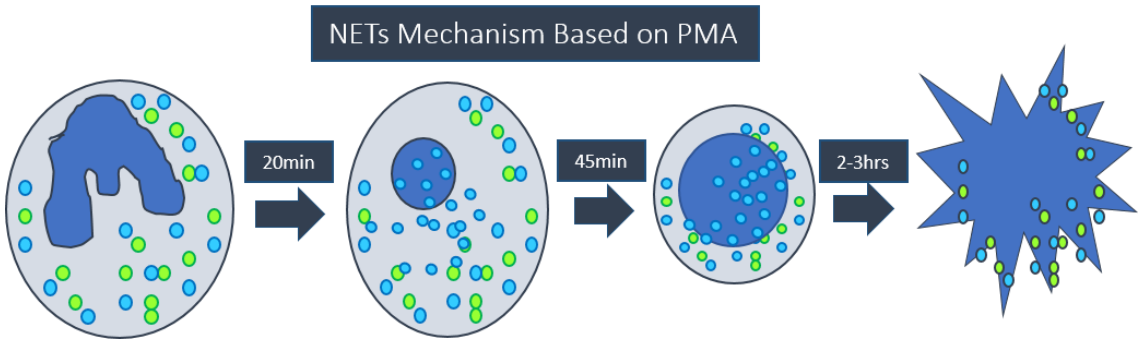

Figure 5. Morphological changes during Neutrophil extracellular trap (NET) formation. Upon stimulation with PMA, neutrophils undergo a series of drastic changes, specifically in the nucleus. In the first 20 minutes ROS are released and azurophilic granules migrate to the nucleus where the nucleus gets delobulated followed by chromatin decondensation. Finally, the chromatin is released extracellularly.

4.1 How do NETs work?

NET formation is a programmed cell death mechanism that can be monitored via three methods: quantification of extracellular DNA using a dye that binds double stranded DNA, such as Picogreen after deoxyribonuclease (DNase) treatment; morphologically, i.e. monitoring DNA using DNA-binding dyes with a microscope; molecular mechanisms, using known processes involved in NET formation like oxidative burst or cell death.

The unique neutrophil nuclear morphology was introduced in the previous chapter and the focal peculiarity was the multi-lobulated shape. Undoubtedly, transformation in nuclear morphology will

be the most dramatic change to be monitored in the phenomenon of NET formation (Carvalho et al., 2015; Fuchs et al., 2007). During NETosis the nucleus rearranges and the nuclear lobules are lost, accompanied by chromatin decondensation, a detachment of the inner from the outer nuclear membrane and a simultaneous disintegration of the granules. This is followed by disintegration of the nuclear envelope causing the cytoplasm and nucleoplasm to mix homogenously. The final step is the ejection of the cellular content into the extracellular space (Fuchs et al., 2007).

Recently, thanks to modern microscopic techniques, several proteins and processes have been connected to NETosis. Three main classes of NET formation mechanisms were described in literature: ROS-dependent, ROS-independent and the non-cell death mechanism. B. Yipp and P. Kubes introduced the terms of suicidal vs. vital NETosis (Yipp and Kubes, 2013). The main characteristic of suicidal NETosis is the activation of Protein Kinase C that results in cell death. During vital NETosis which is activated by direct microbe exposure, rupture of the outer cell membrane does not occur. Another difference is the timeframe, in suicidal NETs occur between 90 and 180 min. In the case of vital NETs occur in 5 to 60 min (Yipp and Kubes, 2013). Many other research groups have generated their own interpretation of the formation of NETs. Yousefi et. al. differentiates between NET formation vs NETosis which correlates to the difference between suicidal and vital NETosis (Yousefi and Simon, 2016). The terms NETosis, NET formation and NET generation will be used interchangeably in this thesis.

4.1.1 Mechanisms of NET formation

The ROS dependent mechanism was the first type of NETosis described. This ROS dependent mechanism was studied by activating neutrophils with PMA. NADPH oxidase catalyzes the conversion of O_2 to O_2^-. Followed by conversion of O_2^- to H_2O_2 by SOD catalysis, which inturn is catalyzed by MPO catalyzes to producing HOCl from H_2O_2 (Patel et al., 2010; Urban et al., 2009). These redox reactions have two main purposes: cell signaling and bacterial killing. The ROS cell signaling is for the mobilization and maturation of granules. Simultaneously, ROS production recruits other immune cells (Campos et al., 2007; van der Linden and Meyaard, 2016).

While studying NETosis, Remijsen observed vacuolization in CGD patient cells and hypothesized that the vacuolization was caused by autophagy (Remijsen et al., 2011) which is the lysosome-regulated disintegration of intracellular components allowing organelle and protein regeneration for maintenance of cytoplasmic homeostasis (Rubinsztein et al., 2012). Remijsen and colleagues proved that autophagy plays a role in NETosis by monitoring the distribution of the microtubule-associated protein light chain 3 (LC3) which is transfered into the vacuoles in a pattern typical for autophagy. Also, they were able to stop the process by using traditional autophagy inhibitors such as wortmanin. They postulate that vacuolization typical for autophagy is necessary to allow the mixing of the chromatin with the granules before being expelled outside of the cell.

Epigenetics plays a role in NETosis. Reported in literature is the histone hypercitrullination which mediates the chromatin unfolding via deamination of the histones through conversion of the arginine side chains in histones to citrullines. The hypercitrullination is regulated via the peptidyl arginine deiminase-4 (PAD4). PAD4 replaces the arginines, which are positively charged, with an uncharged citrulline and directly affects the rapid nuclear decondensation (Cooper et al., 2013).

ROS generation releases granules such as NE and MPO, where NE migrates to the nucleus 60 minutes after stimulation. Once in the nucleus NE digests histones, specifically degrading histones H2B and H4 leading to DNA decondensation (Papayannopoulos et al., 2010). Slower than NE, MPO migrates to the nucleus after 120 min stimulation and also aids in DNA decondensation (Metzler et al., 2011; Papayannopoulos et al., 2010). Additionally MPO was found to be required for the release of NE from the granules in the cytosol during NET formation (Metzler et al., 2014). Hypercitrullination together with the NE histone degradation have been identified as required for chromatin decondensation.

The suicidal part of the NETosis has been the topic of much controversy. Many immunologists have stated that the cell sacrifice is a high price to pay and seems extreme, especially in combination with the complications related to release of cell contents into the tissue environment.

Non-cell death ETosis, also known as vital NETosis, has been reported (Clark et al., 2007). Here an extracellular DNA release was observed while the cell membrane of the PMNs remained complete. A detailed mechanism of this ETosis was described by Kubes and colleagues who reported that vesicles with DNA are passed though the cytoplasm, merged with the plasma membrane and expelled out of the cell with no membrane perforation (Pilsczek et al., 2010; Yipp and Kubes, 2013). The non-cell death NETosis does employ ROS, although the role of this compound has not been specified its involvement has been proven to be essential for granular mobilization, cellular response and inflammation. Other cells were also found to perform ETosis. Yousefi and colleagues reported a “catapult-like” expulsion of mitochondrial DNA by eosinophils keeping the cells viable. This cell death has also been termed as vital NETosis. This ETosis can be stimulated by IL-5 and LPS and is inhibited by the NADPH oxidase inhibitor DPI (Yousefi et al., 2009). The mayor activators are bacteria, in particular gram-positive bacteria, such as *Staphylococcus aureus* (Pilsczek et al., 2010).

The last NET formation mechanism that has been reported is ROS-independent NET formation. This is by far the most controversial mechanism since it is the most occult of all three mechanisms. There has been no experimental proof that supports the exclusion of ROS. This ROS- independent NETosis mechanism is based on calcium-influx and the activation of calcium- influenced pathways. This is a huge contradiction to well-established data reported in the literature for years. The finfings in the literature state that stimulating cells, including PMNs, with ionomycin causes ROS generation

(Walker et al., 1991). They activated NET formation with ionomycin in differentiated human promyelocytic leukemia (HL-60) cells and neutrophils (Parker et al., 2012). Using the same cell system, Douda et. al. later demonstrated that calcium induced NETosis requires mitochondrial ROS and the involvement of the SK3 ion channel. They proved that different kinase mechanisms are involved. When NETosis is activated by PMA, ERK is required while when activated by calcium ionophore A23187, AKT is the required kinase. They changed the name of the mechanism to NADPH-oxidase-independent NETosis rather than ROS-independent (Douda et al., 2015).

4.2 What are NETs composed of?

NETs are composed of DNA, serving as a backbone, decorated with antibacterial proteins. The chromatin fibers were studied via high resolution scanning electron microscopy and were described as smooth fibers that are approximately 15 nm in diameter with globular structures of 30 to 50nm. The globular structures are conformed of antibacterial neutrophil proteins (Brinkmann and Zychlinsky, 2007). Urban and colleagues performed a proteomic study of NETs. As the interest in NETs has grown so has the list of identified NET proteins. Table 2 displays the proteins that compose NETs (Urban et al., 2009).

Table 2. Summary of the protein composition of NETs.

Cellular localization	Protein name	Gene name Swissprot/TREMBL
Granules	Neutrophil elastase*[a]	ELA2/P08246
	Lactotransferrin [a]	LTF/P02788
	Azurocidin [a]	AZU1/P20160
	Cathepsin G [a]	CTSG/P08311
	Myeloperoxidase [a]	MPO/P05164
	Leukocyte proteinase 3 [a]	PR3/P24158
	Lysozyme C [a]	LYZ/P61626
	Neutrophil defensin 1 and 3 [a]	DEFA-1 and -3 P59665, P59666
	Bactericidal permeability-increasing protein	BPI/P17213
Nucleus	Histone 1	H1F0/P07305
	Histone H2A * [a]	H2A/Q9NV63+
	Histone H2B [a]: a) Histone H2B* [a] b) Histone H2B-like [a]	H2B/Q16778+ H2B/Q3KP43,Q6GMR5
	Histone H3* [a]	H3/Q71DI3+
	Histone H4* [a]	H4/P62805+
	Myeloid cell nuclear differentiation antigen [a]	MNDA/P41218
Cytoplasm	S100 calcium-binding protein A8* [a]	S100A8/P05109
	S100 calcium binding protein A9 [a]	S100A9/P06702
	S100 calcium-binding protein A12 [a]	S100A12/P80511
Cytoskeleton	Actin (P and/or R) [a]	ACTB, ACTG1 P60709, P63261
	Myosin-9 [a]	MYH-9/P35579
	Alpha-actinin (1 and/or -4) [a]	ACTN1, ACTN4 P12814, O43707
	Plastin-2 [a]	LCP1/P13796
	Cytokeratin-10 [a]	KRT-10/P13645
	Fibronectin	FN1/P02751
Peroxisomal	Catalase [a]	CAT/P04040
Glycolytic enzymes	Alpha-enolase [a]	ENO1/P06733+
	Transketolase [a]	TKT/P29401
Membrane/Secreted	Cathelicidin	CAMP CAP18 FALL39
	LL-37	P49913

*Most abundant proteins found on NETs. [a] Proteins identified via proteomic approach by Urban, C. et.al. (Urban et al., 2009).

4.2.1 Neutrophil Elastase

In earlier chapters neutrophil elastase (NE) was introduced as a neutrophil-specific protein. Consequently it is of high interest to study the role of NE in the context of NETosis (Bardoel et al., 2014). NE cleaves a variety of proteins, i.e. enterobacterial virulence factors, quite specifically, and protects against both gram-positive and gram-negative bacteria and fungal infections (Weinrauch et al., 2002). Papayanoupolous et al. demonstrated that NE is required in the formation of NETs via histone degradation. NE antibodies are used as the main marker for the identification of NETs together with a nuclear dye in all microscopy experiments. Interestingly, NE knock out mice are hardly used as a direct proof for NET mechanistic studies since humans with NE mutations suffer strong infections and NE knockout in mice leads to neutropenia. Neutropenia leads to a separate series of defects in mice and therefore introduces issues that might not be linked directly to the effects of NE on NET mechanisms (Amulic et al., 2012).

4.2.2 Myeloperoxidase

Myeloperoxidase (MPO), like NE, is a very abundant neutrophil protein stored in azurophilic granules (Schultz and Kaminker, 1962). MPO is an important component in the oxygen-dependent killing by neutrophils through the production of oxidants. MPO catalyses the conversion of hydrogen peroxide to hypochlorous acid (H_2O_2 to HOCl) which is a very potent antimicrobial agent (Klebanoff, 2005). Unlike NE, MPO-deficiency is not common in humans and has minor effects with regard to the overall health of the patient. Infections are the main concern for MPO-deficient patients since they have defective intercellular killing. The most common infection is caused by *Candida albicans* that can occasionally cause serious health effects. This stability has led to the use of MPO-deficient human patients and MPO-deficient mice for NETosis studies. The MPO work was led by Metzler et. al. where joint studies of NE and MPO were addressed and led to the finding that both proteins translocate to the nucleus and aid in DNA decondensation (Metzler et al., 2014; Petrides and Nauseef, 1998).

4.3 What triggers NETs?

Neutrophil mechanisms were discussed in section **3.5** and activators of those mechanisms were briefly mentioned. It is no coincidence that NET formation is triggered by similar stimuli. Often NETosis is seen as the last resort of the cell and the stimuli are often presented in high concentrations or in combination with other stimuli. NETosis is activated by PAMPs of a wide range of microbes including bacteria, fungi, virii and eukaryotes. **Table 3** summarizes the known pathogenic stimuli of NET formation and **table 4** summarizes the known molecular, non-bacterial stimuli for NETosis.

Table 3. Known pathogens that induce NET formation.

Microorganism	Name	Type	NETosis Type
Fungus	*Aspergillus fumigatus*		Suicidal (Bruns, lung 2010)
	Candida albicans	Yeast	Suicidal, Vital (Urban et al., 2009)
	Cryptococcus gatti	Yeast	Suicidal (Springer et al., 2010)
	Cryptococococuss neoformans	Yeast	Suicidal (Urban et al., 2009)
Bacteria	*Enterococcus faecalis*	Gram positive	Suicidal (Lippolis et al., 2006)
	Listeria monocytogenes	Gram positive	Vital, Suicidal (Ermert et al., 2009)
	Mycobacterium canetti	Gram positive	Vital (Ramos-Kichik et al., 2009)
	Mycobacterium tuberculosis	Gram positive	Vital (Ramos-Kichik et al., 2009)
	Staphylococcus aureus	Gram positive	Vital, Suicidal (Brinkmann et al., 2004; von Kockritz-Blickwede and Nizet, 2009)
	Streptococcus dysgalactiae	Gram positive	Vital (Lippolis et al., 2006)
	Streptococcus pneumoniae	Gram positive	Vital, Suicidal (Beiter et al., 2006; Crotty Alexander et al., 2010)
	Streptococcus pyogenes	Gram positive	Vital (Buchanan et al., 2006; von Kockritz-Blickwede and Nizet, 2009)
	Escherichia coli	Gram negative	Suicidal (Lippolis et al., 2006; Webster et al., 2010)
	Haemophilus influenza	Gram negative	Suicidal (Hong et al., 2009)
	Helibactor pylori	Gram negative	Suicidal (Hakkim et al., 2011)
	Klebsiella pneumonia	Gram negative	Suicidal (Papayannopoulos et al., 2010)
	Pseudomonas aeruginosa	Gram negative	Suicidal (von Kockritz-Blickwede and Nizet, 2009)
	Serratia marcescens	Gram negative	Suicidal (Lippolis et al., 2006)
	Shigella flexneri	Gram negative	Suicidal (Brinkmann et al., 2004)
Virus	*Human Immunodeficiency Virus-1 (HIV-1)*		(Saitoh et al., 2012)
Eukaryota	*Eimeria bovis*	Parasite	(Behrendt et al., 2010)
	Leishmania amazonensis	Trypanosoma	(Guimaraes-Costa et al., 2009)

Table 4. Known non-bacterial stimuli of Neutrophil Extracellullar Traps

Stimuli	Pathway / Component	NETosis Type	Reference
Single			
Phorbol 12-myristate 13-acetate (PMA)	PKC ERK ROS Histone citrullination NE and MPO relocation Actin (Guimaraes-Costa 2009)	Suicidal	(Brinkmann et al., 2004; Hakkim et al., 2011)
Platelet activation factor (PAF)	PKC ERK ROS	Suicidal	(Hakkim et al., 2011)
1-2-dioctanoyl-sn-gylcerol (diacylglycerol (DAG) analog)	PKC ERK ROS	Suicidal	(Hakkim et al., 2011)
Lipopolysaccharide (LPS)	ROS PAD4 Histone citrullination Actin	NA	(Li et al., 2010; Ramos-Kichik et al., 2009)
Calcium ionophore	ROS PAD4	NA	(Wang et al., 2009)
Glucose oxidase (GO)	ROS	Suicidal	(Fuchs et al., 2007; Oehmcke et al., 2009)
Nitric oxide donors	ROS	Suicidal	(Patel et al., 2010)
Hydrogen peroxide	ROS PAD4 Histone citrullination	Suicidal	(Li et al., 2010)
Interleukin-8 (IL-8)	PAD4 Actin	NA	(Ramos-Kichik et al., 2009)
Leukotoxin	CD18	NA	
Tumor necrosis factor (TNF) α	Histone citrullination PAD	NA	(Wang et al., 2009)
M1-protein-fibrinogen complex	ROS Cathelicidin	NA	(Lauth et al., 2009; Oehmcke et al., 2009)
Statins	ROS Histones	NA	(Chow et al., 2010)
Panton-Valentin leukocidin	ROS	Viable	(Pilsczek et al., 2010)
Uric acid	ROS	Viable	(Arai et al., 2014)
Mixtures			
Granulocyte macrophage colony stimulating factor (GM-CSF) + C5a	ROS Mitochondrial DNA	Viable	(Yousefi et al., 2009)
GM-CSF + LPS	ROS Mitochondrial DNA	Viable	(Yousefi et al., 2009)
Cells			
Thrombin receptor activated peptide (TRAP) activated platelets	ROS TXA_2 ERK	Viable	(Caudrillier et al., 2012)

4.4 NETs purpose

Neutrophils are filled with many antimicrobial proteins to eradicate infections (section **3.4**). NETs additionally assist antimicrobial activity by pathogen trapping, immobilization and exposure of antimicrobial components to trapped pathogens (Brinkmann et al., 2004). Whether this effort is enough to kill bacteria directly is much up for debate. Proof of trapping has been tested with several bacterial strains and mutated bacteria, monitored by electron microscope, immunofluorescence microscopy, and flow chambers with microscopy (Goldmann and Medina, 2012). Several bacterial strains such as *Staphylococcus aureus*, *Shigella flexneri*, *Salmonella typhimurium* and *Escherichia Coli* bind to extracellular DNA *in vitro* (Beiter et al., 2006; Brinkmann et al., 2004). The ultimate proof of NETs biological relevance is their effect on the evolution of bacterial organisms, either by, the evolution of processes of evasion or the evolution of other specific defense mechanisms in an effort to avoid capture within NETs. *Streptococcus* strains, i.e. *S. pyogenes*, *S. pneumonie, (Beiter et al., 2006) S. aureus*, have evolved to produce DNases that dismantle the NETs DNA backbone (Buchanan et al., 2006; Walker et al., 2007). *Pseudomonas aeruginosa* uses the DNA to form biofilms and repurposes the granular proteins (Mulcahy et al., 2008; Walker et al., 2005). Trapping is not exclusive to bacteria as Saitoh et. al. showed via super-resolution structured illumination microscopy that HIV activates NETs via toll-like receptors (TLR) 7 and TLR8. They also found HIV particles trapped in the NETs that were released upon DNase treatment (Saitoh et al., 2012). To strengthen the NET antimicrobial purpose, ROS generation is prolonged when neutrophils undergo NETosis compared to when they undergo regular apoptosis (Mayadas et al., 2014).

4.5 The dark side of NETs

In recent decades, life expectancy has increased significantly. However therapeutic and disease-treatment challenges remain in the fields of chronic diseases like cardiovascular diseases, obesity, diabetes, chronic pain, persistent inflammation and autoimmune diseases. For many of these chronic illnesses no reliable diagnosis and treatments are available due to the complexity of the disease. Discoveries such as NET formation gave new mechanistic insights for cardiovascular, inflammatory and autoimmune diseases.

Many diseases arise when there is a fault in homeostasis maintenance, such as uncontrolled NET formation. The role of NETs in disease and their physiological relevance are exploratory. In infectious diseases, NETosis is thought to be beneficial due to their antibacterial components and ability to trap bacteria. There are other benefits. In the case of chronic granulomatous disease (CGD) patients suffer from a genetic deficiency in NADPH oxidase and cannot effectively fight infections and CGD patients suffering from chronic *Aspergillus nidulans infections* where able to clear the infection when NET formation was restored via gene therapy (Bianchi et al., 2009).

However, for many autoimmune and inflammatory diseases, NET formation is detrimental as NET components contribute to the pathology of the disease and in many cases increase the severity of inflammation.

When NET formation increases in an uncontrolled manner, its components lead to auto-antibody generation, large amounts of ROS release, artery and vein clogging due to chromatin's sticky nature, and recruitment of immune cells. In chronic obstructive pulmonary disease (COPD) patients' sputum is highly viscous and decreases lung function due to NET components (Porto and Stein, 2016). Another example is cystic fibrosis patients with from chronic lung infections. Here, NET components serve as biofilms building blocks for *P. aeruginosa* (Hoiby et al., 2010). **Table 5** summarizes the NET's involvement in diseases.

Table 5. Role of NETs in disease

Disease	NET Effect	Reference
Autoimmune		
Systematic lupus erythematosus (SLE)	? NETs No NET clearance ? Immune cell recruitments ? Immune response	(Garcia-Romo et al., 2011; Hakkim et al., 2011; Lood et al., 2016)
Vasiculitis	? NETs Damaging NET components ? Immune cell recruitments ? Immune response	(Kessenbrock et al., 2009)
Rheumatoid arthritis	? NETs Damaging NET components ? Immune cell recruitments ? Immune response	(Dwivedi et al., 2012; Khandpur et al., 2013)
Colitis	? NETs Damaging NET components ? Immune cell recruitments ? Immune response	(Bennike et al., 2015)
Venous and cardiological disease		
Atherosclerosis	? Immune cell recruitments ? Immune response ? NETs	(Knight et al., 2014; Warnatsch et al., 2015)
Thrombosis	? NETs ? Blockage/viscosity ? Immune cell recruitments ? Immune response	(Fuchs et al., 2010)
Lung disease		
Pneumonia	? NETs Bacterial trapping (S. pneumoniae) Bacterial biofilms (H. influenzae) Damaging NET components	(Hong et al., 2009; Wartha et al., 2007)
Chronic obstructive pulmonary disease (COPD)	? NETs Damaging NET components ? Blockage/viscosity ? Immune cell recruitments ? Immune response	(Obermayer et al., 2014; Qiu et al., 2003)
Asthma	? NETs ? Blockage/viscosity Damaging NET components	(Dworski,R. allergic 2011)
Respiratory syncytial virus bronchiolitis	? NETs ? Blockage/viscosity ? Immune cell recruitments	(Cortjens, B. airway 2015)
Tuberculosis	Bacterial trapping ? Immune cell recruitments Damaging NET components	(Ramos-Kichik, V. extracellular 2009)
Transfusion-related acute lung injury (TRALI)	? NETs ? Blockage/viscosity	(Caudrillier, A. transfusion 2012)
Cystic fibrosis	Bacterial biofilms ? Immune response ? Blockage/viscosity	(Dwyer et al., 2014; Papayannopoulos et al., 2011)
Other disease		
Chronic granulomatosus disease (CGD)	No NETs	(Bianchi et al., 2009)
Sepsis	? NETs ? Immune response ? Blockage/viscosity	(Clark et al., 2007)
Preeclampsia	? NETs ? Blockage/viscosity ? Immune cell recruitments ? Immune response	(Hahn et al., 2012)
Kidney injury	? NETs ? Immune response Damaging NET components	(Jansen et al., 2017)

Note: ↑ = Increase

4.5.1 NETs and autoimmune diseases

It has been a long time since Paul Ehrlich described autoimmunity as “horror autotoxicus”. In autoimmune disease, homeostasis is disrupted by the immune system attacking the body because it is unable to differentiate between self-molecules and foreign molecules. Specifically, antibodies and T-cells attack the host causing inflammation and organ failure. A common identifier of autoimmune disease is anti-neutrophil cytoplasmic antibodies (ANCAs) directed at intracellular proteins such as C-ANCA proteinase 3(PR3), C-ANCA atypical (BPI, MPO, CG), P-ANCA (MPO) and atypical ANCA (multiple specificities). The multiple specificities include catalase, enolase, actin, lactorefferrin, lysozyme, defensing, cathepsin G and elastase (Savige et al., 2000). Neutrophils have been implicated in many autoimmune diseases and their involvements vary as much as their multifaceted responsibilities. Consequently, titers of ANCA antibodies vary in each autoimmune disease. For instance, in Wegener’s granulomatosis the titers of the ANCA antibodies are 80-90% C-ANCA; for cystic fibrosis (not an autoimmune disease) 80% C-ANCA atypical; microscopic polyangiitis 50% P-ANCA and for more complicated diseases such as rheumatoid arthritis is it identified by a collection of atypical ANCAs (Savige et al., 2000). These convoluted diagnostic parameters illustrate the complexity of autoimmune diseases. Therefore, new insights, such as the discovery of NET formation and their role in the autoimmune diseases, are highly valuable in designing and formulating improved treatments.

4.5.1.1 Vasculitis

Vasculitis is the name for a collection of diseases where blood vessels are affected by necrotic inflammation. The organs that suffer damage are mainly the lungs and kidneys, with to a lesser extent the skin, upper airways, brain and heart. In the case of small vessel vasculitis, MPO and PR3 ANCA-antibodies are used for the diagnosis (Nemeth and Mocsai, 2012). Kessenbrock et. al. showed that NETs are involved in small vessel vasiculitis. MPO and PR3, both components of NETs, are the main drivers of this disease. As NET formation is increased uncontrollably, so are the numbers of MPO and PR3, resulting in an increasing of the titers of ANCA-antibodies. These increased ANCA-antibodies titers activate the immune response which results in inflammation and cell debri released from NETosis. ANCA-activated NETosis further activates other immune cells such as myeloid dendritic cells which further contribute to the illness (Bardoel et al., 2014; Kessenbrock et al., 2009).

In the case of atherosclerosis, another venous disease where the arterial vessels are damaged, cholesterol crystals were found to induce NETosis. Here, NETs are found to primarily recruit macrophages. In the case where the NETosis was inhibited, the vesicular damage was reduced (Warnatsch et al., 2015).

4.5.1.2 Systematic lupus erythematosus (SLE)

Systematic lupus erymatosus (SLE), also known as Lupus, is an autoimmune multi-symptomatic disease typically affecting several vital organs in the body and with a disease progress characterised by flares' in which the patient experiences increased malady. In SLE, the immune system fails to regulate antibody generation and starts attacking several organs and tissues. SLE is frequently a diagnostic nightmare and is often misdiagnosed because symptoms can be so varied and similar to other diseases. There is no conclusive test that can unmistakably identify SLE (Yu and Su, 2013). The severity of the disease is not taken lightly since patients with SLE can have symptoms that range from the unthreatening, skin rashes, all the way to life threatening nephritis (kidney inflammation).

In recent years, more attention has been given to cell types and antibody titers used to diagnose lupus. SLE patients produce high levels of autoantibodies against nuclear antigens. Additional to the ANCA antibodies, frequently used to detect autoimmune diseases, antibodies against double stranded DNA (anti-dsDNA) are detected. High titers in anti-dsDNA have been directly correlated with nephritis and SLE disease activity. Other antibodies that are present in the serum of lupus patients are anti-histones, antibodies against single stranded DNA (anti-ssDNA), ribonucleoprotein (anti-ribonucleoprotein) and ribosomes (anti-ribosomal) (Wu and Mohan, 2007). Pascual and colleagues have created a SLE genetic signature of 1564 transcripts of specific upregulated gene expression (Garcia-Romo et al., 2011). Moreover, they identified low-density neutrophils that express anti-ribonucleoprotein (anti-RNP), cathelicidin (LL-37), high-mobility group protein 1 (HMGB1) and histone markers and are abundant in the population of SLE patients (Bennett et al., 2003).

For many years medical doctors have diagnosed and treated SLE patients with very little success and with generally a low understanding of the disease itself. However after the discovery of NETs, the similarities between the disease symptoms of SLE and the components of NETs, i.e. the extracellular chromatin and anti-dsDNA, appeared to be more than just coincidental and in a few short years several research groups identified the link between SLE and NETosis. They identified that SLE patients make more NETs compared to healthy people and display spontaneous NET formation (without a stimuli) (Jorch and Kubes, 2017; Lood et al., 2016). The DNA of these NETs triggers dendritic cells to produce type I interferon which results in increased NET production (Garcia-Romo et al., 2011; Lande et al., 2011). Not only do SLE patients make more NETs, they are also not able to degrade them efficiently due to the antigens present in the SLE patient sera and DNase I deficiencies (Hakkim et al., 2010). Over-production of NETs and impaired clearance of NET component are now part of the etiology of SLE. Other components of the NETs mechanism are currently being studied with a view to improving the treatment of SLE. For example, PAD4 Cl-

amidine was used to decrease autoantibodies in lupus- prone mice (Knight et al., 2013). After years of research, SLE has become the leading NET-associated disease.

4.5.1.3 Rheumatoid Arthritis

Rheumatoid arthritis (RA) is a progressive destructive autoimmune disease targeting joints. In RA patients joint synovial lining is changed to pannus, which is a combination of synovial fibroblast and immune cells (Shelef et al., 2013). For many years, the main factor of RA was IgG that recognizes self IgM antibodies. Only recently has the presence of anti-citrullinated protein autoantibodies (ACPA) been identified as a major factor involved in RA onset. ACPA is a specific marker for RA and NETs have been identified as a source of these auto-antigens. In the NET formation mechanism citrullization is essential for decondensation of the chromatin. During this process neighboring or passing cells can take up the citrullinated proteins generating the autoantibodies and immune complexes. In addition, serum from RA patients has been identified with NETosis triggers *in vitro* (Dwivedi et al., 2012; Khandpur et al., 2013). Taking everything into consideration these factors create an inflammatory cycle since these immune complexes trigger NET formation and neutrophil recruitment.

4.6 What makes NETs difficult to study?

In previous chapters, all the different aspects of neutrophils and NETs have been addressed. Since 2004, when NET formation was discovered, there has been a large amount of research focused on the biological relevance of NETosis. What makes these studies difficult is that cells undergoing NETosis, especially neutrophils, are sensitive, terminal and short-lived (Gunzer, 2014). In literature, it is well documented that *ex vivo* treatment and behavior of PMNs differs from their *in vivo* behavior. These issues also apply when investigating NET formation.

Over the last years, molecular biology has seen major steps in the development of new genetic techniques i.e. RNA interference (RNAi), and CRISPR-based interference (Adamson et al., 2016). Nevertheless, these techniques are useless when it comes to mimicking the diverse function that neutrophils have *in vivo* (Nathan, 2006). Neutrophil-like cell lines, i.e. HL-60 and NB4, can be differentiated to closely resemble neutrophils although they lack certain neutrophil specific cytokines. Specifically, when it comes to NET formation there is no cell line that can undergo NETosis. Regarding mice models, NADPH oxidase and neutrophil elastase knockout mice have been bred, but these mice are challenged with serious infections (Amulic et al., 2012).

Altogether, chemical biology provides an excellent solution when it comes to addressing neutrophils and NETosis. Ideally, the identification of a small molecule NET formation inhibitor can be a great tool to further study neutrophil function and more specifically NET formation. An additional important use for the NET inhibitor would be a pharmaceutical application aimed at NET-dependent diseases.

Chapter 5: Results and Discussion Section 1: NET Screen

5.1 Introduction to screening

For more than two decades, screening has been the main technique for the identification of small molecules in pharma. In the early 2000s, high-throughput screening (HTS) was introduced and companies spend millions of dollars on building extended compound libraries (Erlanson et al., 2016). These screening campaigns led to many pharmaceutical leads; nevertheless, it also resulted in many failed projects based on false positives. Ideally, in search of leads nature inspired and derived chemical scaffold should also be screened (Sundberg, 2000). These issues have been recognized in recent years. Scaffold variety has been introduced with fragment-based drug discovery (FBDD), natural product-inspired libraries (Biology-oriented synthesis, BIOS), and computational predictions (Erlanson et al., 2016; Wetzel et al., 2011). In addition, screening has evolved from simple biochemical assays to complex high-content cell-based and whole organism screening. By changing the traditional approach disrupting the purified protein-compound to primary cells, permanent cell cultures, and whole organism made screens more predictive and closer to *in vivo* settings.

Steven A. Haney describes high-content screening (HCS) as the application of biochemical and/or morphological parameters to study cells in a desired manner resulting in an improved drug discovery pipeline, both in speed as in quality (Haney et al., 2006). HCS is ideal for hit identification beyond small molecules, e.g. peptides or RNAi. A typical HTS protocol consists of exposing cells to substances and collecting the simple readout usually involving single-fluorescence readout. In HCS, the analysis is more sophisticated due to automated image fluorescence analysis. In recent years, there has been a constant improvement in screening techniques. For instance, high-throughput fluorescence microscopy combined with flow cytometry provides single cell resolution. This single-cell measurement can be 2 or more parameters for one cell and it can be easily applied to a population of cells resulting in a qualitative and quantitative readout (Horvath et al., 2016). In previous screens, cell-sub-populations were completely dismissed due to the yes-or-no readouts for the entire cell. The HCS screens allow sub-cellular localization with multichannel fluorescence readouts that provide relevant information of certain cell organelles or they target genetically modified proteins affected by active small molecule (Kapoor et al., 2016). The challenge of HCS screens is the data analysis. Caie et. al. developed an automated high-content analysis where a multivariate clustering generated a fingerprint signature profile for compounds with biological similarity for different mechanistic classes (Caie et al., 2010). This chemical biology-driven advancement for the pursuit of biological active molecules has allowed more complex targets to be successfully pursued with small molecules.

This chapter addresses the establishment of the first cell-based screen to obtain novel small molecule NET inhibitors. The NET assay can be considered an early version a high-content screen

due to the complexity of the microscopy readout. The elegance of the screen relies on its simplicity where one dye produces two different readouts.

5.2 Development of an assay to detect inhibitors of NET formation.

This is the first chemical screen to study neutrophil extracellular trap (NET) formation. This work was pioneered by Abdul Hakkim and Tobias Fuchs. Consequently, many optimizations were performed during the development of a robust assay. NET formation is a novel biological phenomenon and many aspects are still unknown. As previously mentioned, there is no model cell line that mimics neutrophil NET formation, except for purified neutrophils. Due to the short-life and nature of the neutrophils the assay needs to be performed uninterrupted until the cells are fixed. The assay starts with neutrophil gradient purification from fresh human blood. This purification was established in the Zychlinsky lab by Tobias Fuchs and Abdul Hakkim using Histopaque 1119 and Percol where neutrophils were obtained in the >95% purification by flow cytometer quantification (Aga et al., 2002).

The NET assay is constructed on the morphological changes of the nuclei undergoing NET formation which was previously reported in 2007 (Fuchs et al., 2007). The assay detects the formation of four main neutrophil nuclear morphologies. The first is the lobulated nuclei, which is the natural state of the neutrophil (**Figure 6 A and E**). Upon activation, the nucleus rearranges within the first 60 minutes leading to the second stage which is delobulation. In this stage chromatin concentrates into a small circle (**Figure 6 B and F**). The third stage (called decondensation) is characterized by enlarged nuclei and internal mixing of granules and cellular components occurs (**Figure 6 C and G**). The final stage is the release of the chromatin to the extracellular space, which is labeled NETs (**Figure 6 D and H**). This sequence of nuclear morphologies was confirmed by detailed microscopy, see **Figure 6 E-H**. It is to be noted that each stage has a particular set of physiological parameters such as size, intensity and circularity that can be measured. The nuclear changes such as size and shape are quantified after the image analysis of the collected images from the automatic microscope. By employing this method, the exact stage in which the NET inhibitors stop NET formation can be determined. This will provide an insight into the cellular process that a particular compound targets and can narrow down the search for its protein target. There is an advantage if a vital DNA dye is employed, i.e. non-cell permeable dye, since it is possible to obtain a second readout such as cell death.

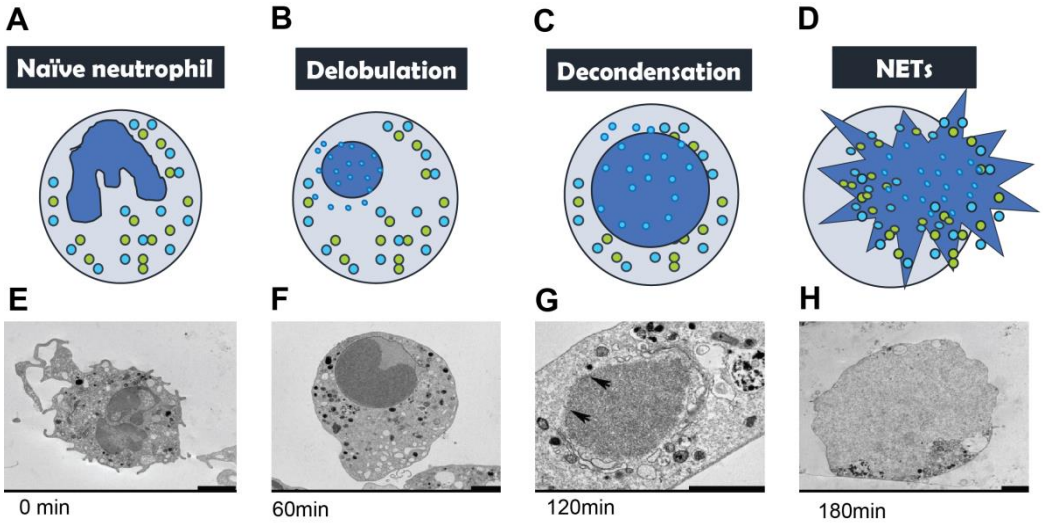

Figure 6. Different nuclear morphologies in NET formation. (A-D) Cartoon representations of different morphologies present during NET formation during time course. (E-H) Transmission electron microscope images of neutrophils upon activation with PMA and fixed at different times. At 0 minutes neutrophils have a small and lobulated nuclei (A and E). After 60 minutes the nuclei delobulate and display small and rounded morphology (B and F). At 120 minutes the nuclei continue to expand and are large and rounded illustrated by black arrows (C and G). At 180 minutes the nuclei are very large and of an irregular shape as in NETs (D and H) (Fuchs et al., 2007).

The chosen dye is SYTOX Green. SYTOX Green intercalates with DNA and it is membrane impermeable so it is excluded from live cells. The half-life of neutrophils is short, although it is important to know the exact period of time when the cells are viable and can be used. Neutrophils from two healthy donors were purified at the same time and stored under the same medium conditions. The cell populations were compared under unstimulated and PMA stimulated conditions and at different times after activation and temperatures. SYTOX green was used to determine cell death (**Figure 7**). The results show that for both donors storing the cells at 4^{o}C increased cell death compared to those stored at 25^{o}C. Neutrophils of both donors showed increased cell death on average by 10% upon PMA stimulation. From this experiment, it can be concluded that the cells can be stored for up to six hours at room temperature without cell death.

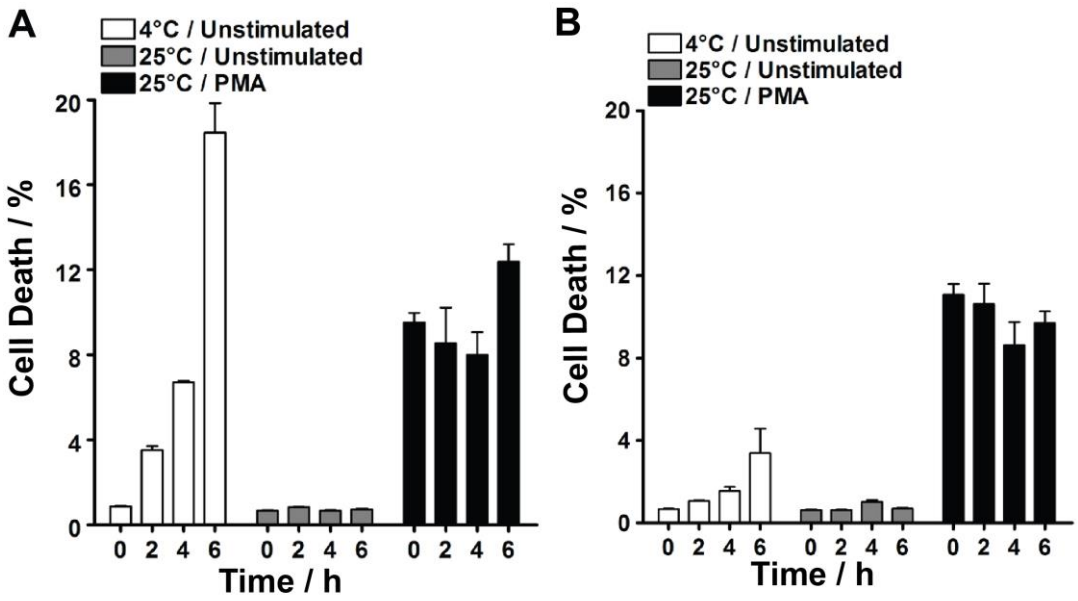

Figure 7. Optimization of neutrophil storage shows similar trends regardless of the donor. Neutrophils were obtained by two different donors in parallel and stored in complete medium at 4°C or 25°C, donor 1 (A) and donor 2 (B). Cells were left unstimulated or were stimulated with 40 nM PMA for the indicated times. Cell death was measured with SYTOX Green.

To validate if indeed SYTOX Green is only entering dead cells upon fixation with paraformaldehyde (PFA), cells were fixed with 2% PFA and incubated for 10min and 60min with and with and without detergent (0.1% of Triton-X). Unstimulated cells with no fixation were used as a negative control and cells exposed to detergent served as a positive control. Detergent-exposed cells have compromised cell membranes allowing the dye to enter the cell easily. After SYTOX Green staining, cells that were only fixed with PFA were not stained with SYTOX Green, whereas cells showed high fluorescence in presence of detergent (**Figure 8 A**).

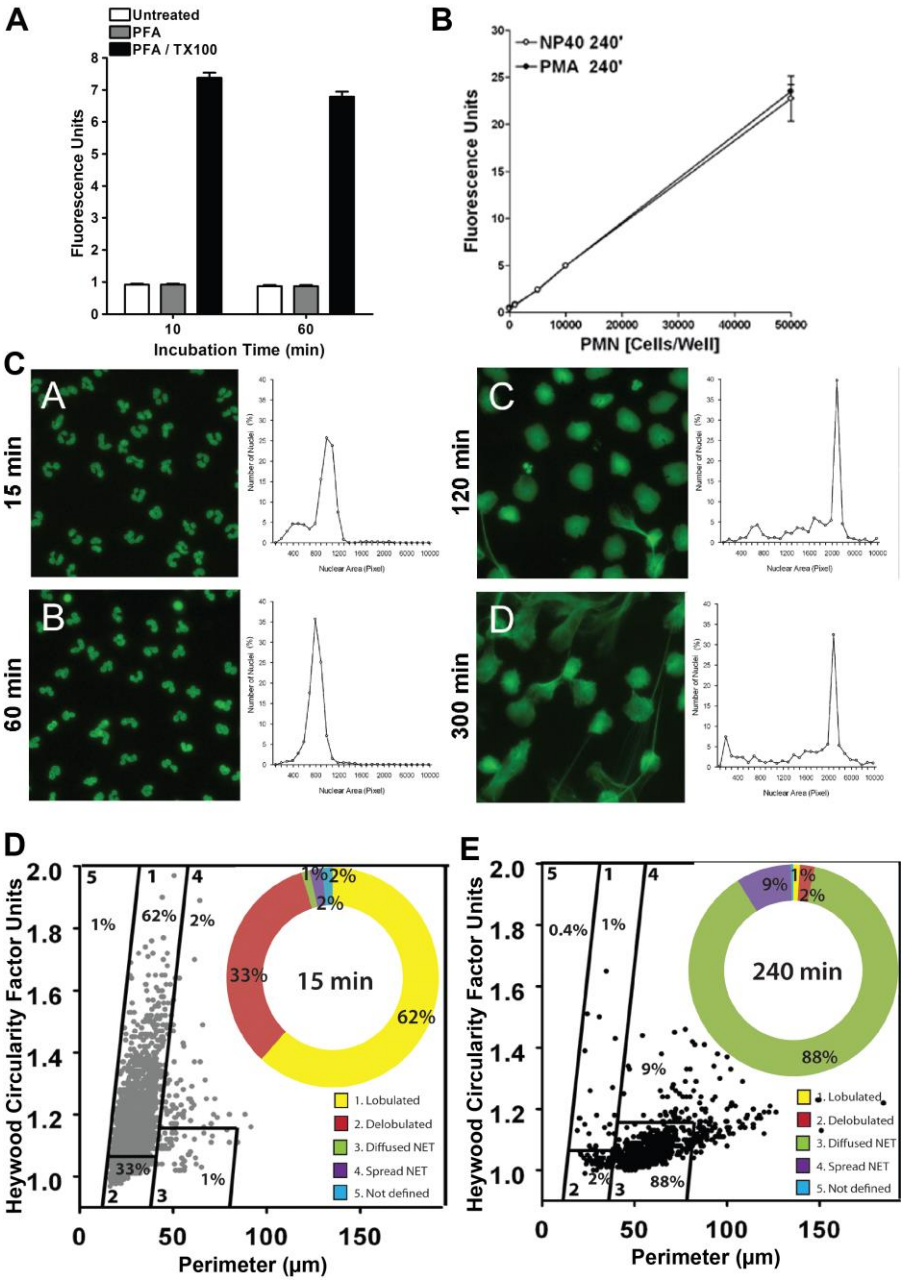

Figure 8. Methodology for NET formation assay quantification of cell viability and nuclear morphology. (A) PFA fixation does not effect SYTOX Green staining. Cells were untreated, fixed with or without Triton-X. Cells were incubated for 10 to 60 min, stained with SYTOX Green and fluorescence was measured. (B) Quantification of neutrophil cell death with SYTOX Green. Different numbers of neutrophils were seeded and activated with PMA for 240 min or incubated with the nonionic detergent NP-40. (C) Analysis of distinct nuclear morphologies during NET formation. Neutrophils were activated with PMA for 15 (A), 60 (B), 150 (C), and 300 min (D), fixed, permeabilized with Triton X-100 and stained with SYTOX Green. (A), delobulated at <100 pixels (B), decondensed at 2000 pixels (C), and NETs at 2000 pixels, respectively. (D-E) Graphical phenotype representation using the Heywood circularity factor. The neutrophil nuclei images obtained in (C) were analyzed using a dot plot graph analysis of perimeter versus Heywood circularity factor. Each dot represents a nucleus. Gates were set to distinguish lobulated and delobulated nuclei, and diffused and spread NETs. (D) Nuclear morphology 15 minutes after activation with PMA. (E) Nuclear morphology 15 minutes 240 minutes after activation with PMA (Hakkim et al., 2011) .

To test if the method was quantitative, neutrophils were seeded at different concentrations. Cells were exposed to the non-ionic detergent NP-40 to permeabilize the cells, resulting in cell death. Another set of cells was activated with PMA, also resulting in cell death. Both conditions resulted in similar dose-dependent responses after 240 min of PMA addition (**Figure 8 B**). The fluorescence measured is proportional to the amount of cells that were plated confirming that the fluorescent readout is indeed quantitative.

Next, the quantification of the morphologies was addressed based on the four main morphologies discussed above (**Figure 6**). The first parameter is the size of the nuclear area at different time points that corresponded to the main morphologies. After the cells were activated with PMA and incubated for a given time cells were fixed with PFA, permeabilized with 0.1% Triton-X and stained with SYTOX Green. Microscopy pictures were obtained with a 10X objective using a Scan^R automated microscope. Hakkim established an algorithm on the Scan^R image analysis software was applied and optimized for the SYTOX Green signal and the elaborate thresholds for the nuclear size of each morphology. To obtain images corresponding to the naïve state, cells were activated for 15 min with 40 nM of PMA to guarantee adhesion and these nuclei showed the lobulated morphology (**Figure 8 C**). Analysis showed that the prominent size of a lobulated nucleus is 1000 pixels, (**Figure 8C**). The second nuclear morphology, delobuated, comes after 60 min of activation (**Figure 8 C**). In the image the nuclei appear to be rounded and nuclear size corresponding to 800 pixels. The cells seem to have reduced the nuclear size by 200 pixels while displaying increased circularity. The following two nuclear morphologies are decondensed at 120 min and NETs at 300 min. The size of the nuclei was increased significantly to 2000 pixels and NETs are the same in pixel size. The nuclear change in the circularity is quite drastic. At 120 min the nucleus is round and large and at 300 min the nucleus is completely has been expelled and the circularity is lost. Size is not the only parameter that was taken into consideration, the perimeter of the nuclei was analysed using the Heywood circularity factor (HCF). HCF designates the ratio of the perimeter to the circularity of a given area. Round nuclei will have a HCF of 1, where a larger and more irregular shape, i.e. NETs, is expected to have a higher HCF (**Figure 8 D-E**). The final algorithm classified the images as follows: nuclei with a pixel size from 100 to 200 pixels and a HCF of 1 to 2 were classified as lobulated (**Figure 8C A**). Nuclei with the size of <100 pixels and a HCF of 1 classified as delobulated (**Figure 8C B**). Nuclei with 2000 pixels and a larger HCF were termed decondensed. Finally, the nuclei with 2000 pixels or higher and a very large HCF were classified as NETs (**Figure 8C C and D**). The algorithm was verified manually to confirm that the quantification represented the images.

The analysis was performed using the Scan^R image analysis algorithm as developed by Abdul Hakkim and Tobias Fuchs. Later, I developed another algorithm using free software Cell Profiler and Cell Analyst. The same parameters were taken into account in the pipeline developed

with the initial training of Marc Bickle from the screening facility Max Planck Institute of Molecular Cell Biology and Genetics in Dresden. Cell Profiler is a self-learning program and improves its algorithm based on the image input. Consequently, the algorithm becomes increasingly accurate by as more test images are added. Based on the previous experience, NET formation was halted by using NET inhibitors at the same stages mentioned in previous paragraphs. This facilitated the generation of the pipelines. Cell Profiler is strongly dependant on the images. A pipeline was created for each microscope that was used and in some instances modifications were performed per experiment.

Many additional issues were addressed such as the optimal conditions in which to obtain and maintain the cells, time, automatization of the microscopy and the scale up to a full high-throughput screen. Finally, a robust NET screening cascade was obtained for evaluation and medium-sized small molecule libraries were screened. **Figure 9** shows the workflow of the NET screen as it was performed either manually, semi-automatically or automatically. The workflow starts with fresh human blood and finishes with the screening plates fixed and ready for microscopy analysis. The entire workflow must be performed within a single day due to the nature of the cells. The isolation of the neutrophils requires around 2 hours (**Figure 9 Step 1**). The plating of the compounds and seeding of the cells, including the 30 min compound pre-incubation, requires the subsequent hour to 3 hours depending on the number of compound to be tested (**Figure 9 Step 2-4**). Upon PMA activation, a 4 hours incubation time at 37^{o}C is required to allow NET formation. Finally, the cells are stained with SYTOX green and fixed with PFA.

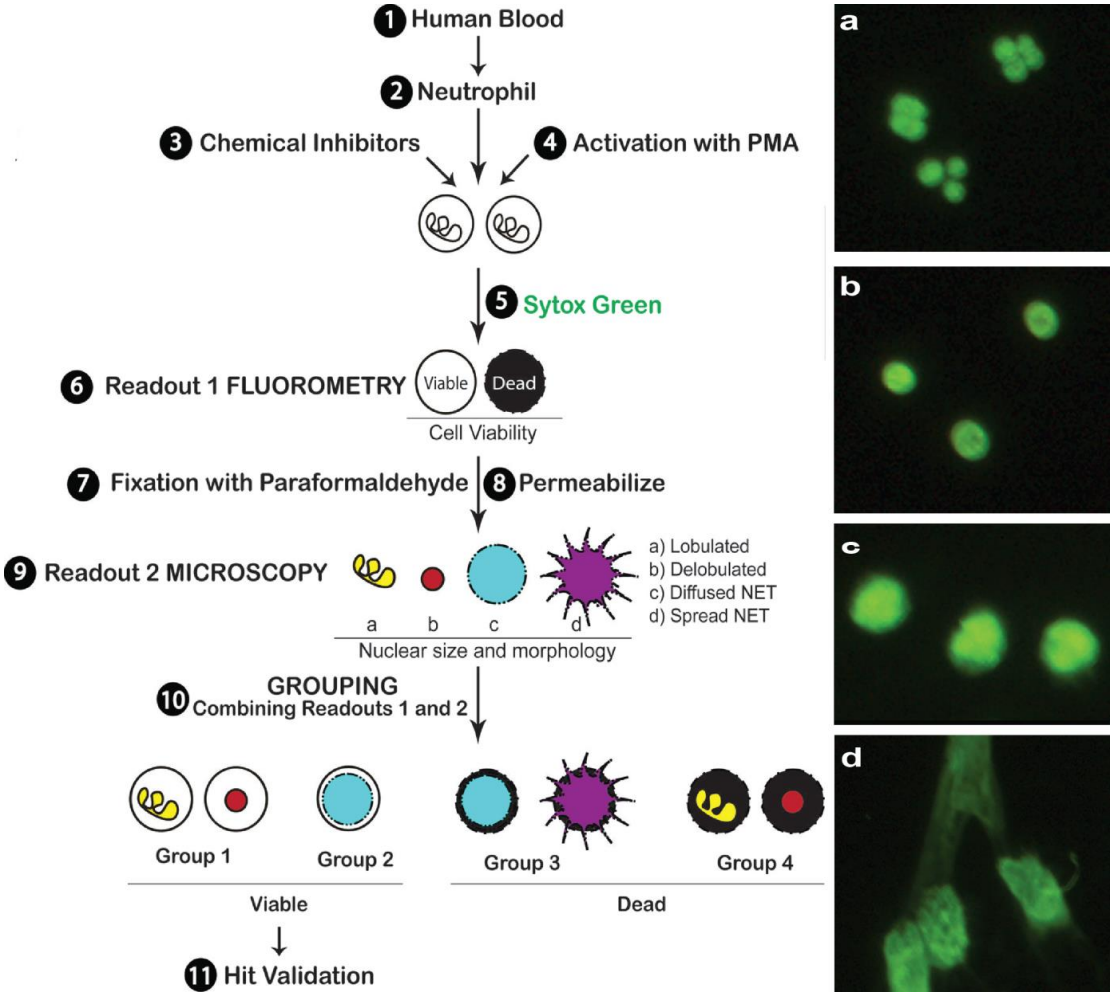

Figure 9. Screening protocol and morphology classification. (1) Neutrophils were isolated from Human peripheral blood using a density gradient (2). $1x10^4$ neutrophils were seeded (3). Cells were activated with PMA (40 nM) for 240 min (4). Neutrophils were fixed with PFA (2% (w/v)) and stained with the cell-impermeable DNA dye SYTOX Green (5 and 6, respectively). At this step only dead neutrophils were stained. Fluorescence was determined to assess cell viability (7). Neutrophils were permeabilized to allow homogenous staining of all cells (8). Pictures of nuclear morphologies were taken by an automated microscopy system and classified into four distinctive morphologies (9 a-d). The compounds were grouped (10) based on both readouts (steps 7 and 9). Compounds yielding viable cells with small nuclei (lobulated or rounded) were in group 1, and those producing cells with large nuclei were in group 2. Non-inhibitors were in group 3, and dead cells with small nuclei were in group 4. Final step is hit validation (11). Figure modified from Nature Chemical Biology 2011 (Hakkim et al., 2011).

With a working assay established, commercial libraries of annotated compounds were then screened. The libraries were obtained from Sigma Aldrich, the library of 1280 pharmacologically active compounds (LOPAC), and MicroSource, a US drug compound collection composed of 1380 FDA approved drugs. The hits from these libraries of compounds with known targets can give insights into which enzymes and receptors are involved in the mechanisms responsible for NET formation.

5.3 First hit evaluation

The LOPAC library of 1280 compounds was screened using the protocol described in the previous paragraph in a semi-automated manner. The compounds were pipetted in 384-well plates so that the final concentration was 100µM using an automated pipetting device and subsequent steps were performed manually (**Figure 9**), with 10^4 neutrophils plated per well and activated with 40 nM PMA and then incubated for 240 min at 37^{o}C. The complete library was screened twice and the compounds were analyzed as previously established. The main interest is in compounds that fall in group 1 and 2. Since there are five readouts (cell death and four morphologies), screening large number of compounds generates vast amounts of data and simplification is required. It was decided to reduce the five readouts to a two number system (one for cell death and one for morphology). The morphology readout was simplified by combining the lobulated and delobuted percentages in one number that indicate the percentage of small nuclei. Compounds with higher than 50 % small nuclei were classified as group 1 compounds and those with a less than 50 % small nuclei are classified as group 2. All compounds causing cell death in more than 50 % of cells were immediately discarded as toxic compounds. The screening campaign resulted in 38 compounds that showed cell death in less than 50 % of cases, coupled with NET formation inhibition. This corresponds to a hit rate of 3 %.

The next step was investigating the known biological activity and the potential involvement of the hit compounds in the NET formation mechanism. Indeed, it was observed that compounds with known modes of action, related to NET formation, were among the set of hits. Once classified according to activity, three main target groups could be distinguished (**Figure 10**). First, inhibitors of fatty acid metabolism were identified as NET formation inhibitors, e.g. resveratrol (**B135, Figure 10**), a known COX inhibitor. COX inhibitors are powerful anti-inflammatory drugs and are often used in the treatment of autoimmune diseases. However, a direct link between COX inhibitors and NETs had not been reported. Unexpectedly, GPCR and cell cycle kinase inhibitors were identified. GPCR pharmacology in neutrophil biology is a so far unexplored subject in the relative new field of neuroimmunology. The most intriguing set of hits were the kinase inhibitors that target kinases involved in the oncogenic signaling pathways. Much is known about these kinases in other cell types linking them to cell death and cell division. Neutrophils are terminal cells and the cell division mechanisms are considered to be deactivated. The identification of these kinase inhibitors as NET formation inhibitors shows how much neutrophil and NET biology is to be explored.

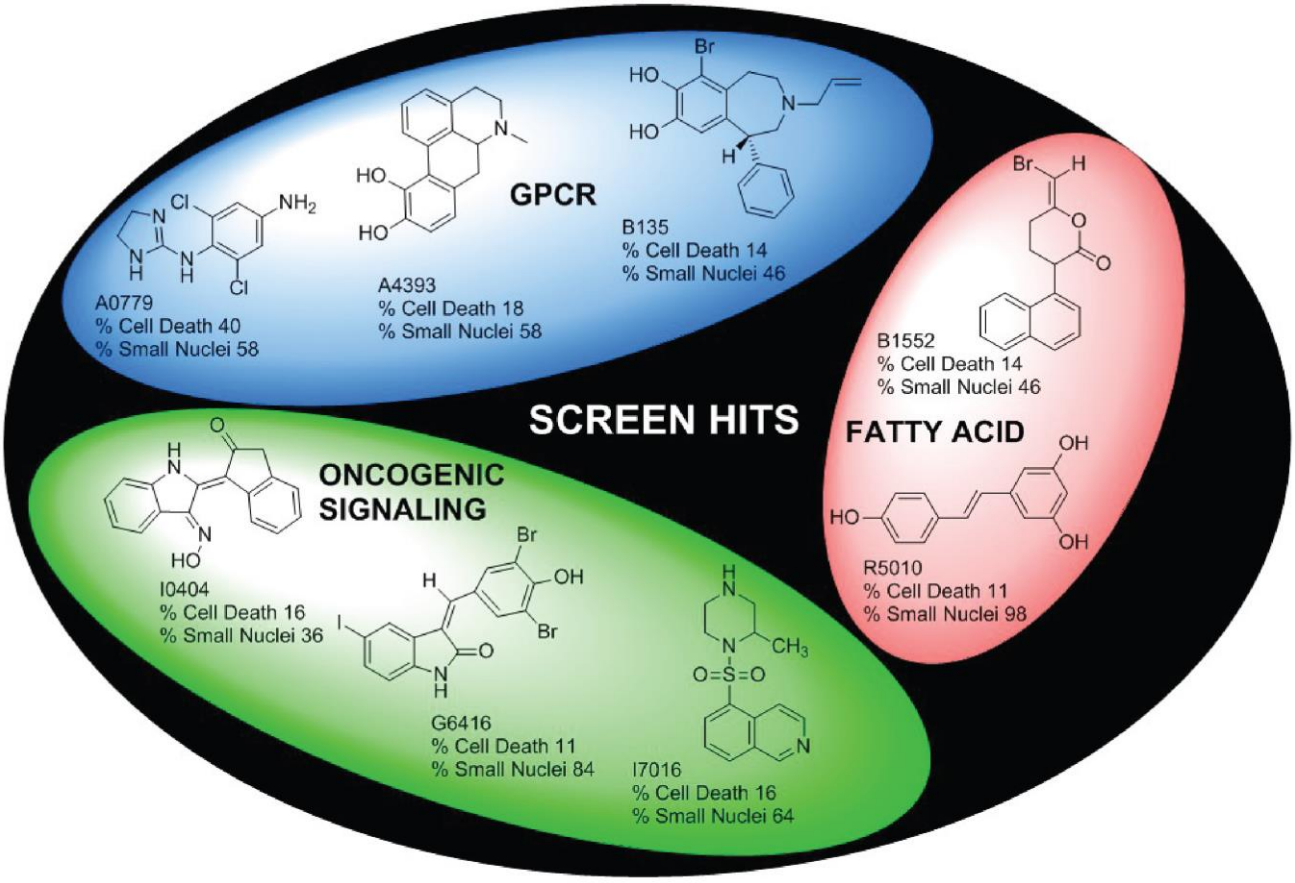

Figure 10. Evaluation of screening hits. Hit compounds were classified according to their biological activity and three main inhibitor groups stood out GPCRs, fatty acid and cell cycle (A). Neutrophils were pre-incubated with 100 µM of the compounds for 20 min at 37°C followed by stimulation with 40 nM PMA and further incubation for 240 min to allow NET formation. Cells were stained with SYTOX Green to detect death cells Data are mean values ± s.d. (N=1, n=2). US: unstimulated cells.

Chapter 6: Results and Discussion Section 2: Involvement of the Raf/ERK/MEK pathway

6.1 Hypothesis

After the identification of kinase inhibitors as NET formation inhibitors, we set out to investigate the involvement of the ERK pathway in NETosis. The kinase inhibitors involved in the ERK signaling pathway showed a group 1 NET inhibitor phenotype. Since group 1 inhibitor is likely to arrest NET formation at an early stage based on our knowledge of the NET mechanism. The involvement of the ERK signaling pathway is hypothesized that it will be in the early stages of NETosis.

6.2 Inhibitors of the ERK Pathway inhibit NET formation

Experiments described in this section were performed alongside with Abdul Hakkim.

Resulting from the LOPAC library screening, kinase inhibitors involved in oncogenic signaling pathways were found to inhibit NET formation effectively. The RAF protein, also known as mitogen activated protein (MAP) kinase kinase kinase, is a member of the MAP kinase cascade together with MAP kinase kinase (MEK) and extracelullar-signalling regulated kinases (ERK) proteins. This pathway is linked to the regulation guanosine nucleotide binding (G) protein, Ras. Ras is involved in cell proliferation, growth, and differentiation and has been known as a powerful oncogene for many years (Roberts and Der, 2007). Therefore, all MAP kinases in the pathway have been investigated as drug targets. The mechanisms activating this pathway are a series of phosphorylations, i.e. Ras indirectly activates the kinase activity of Raf by phosphorylation. Next, Raf phosphorylates and thereby activates MEK resulting in activation of ERK which relocates to the nucleus. Activated ERK regulates many crucial biological processes for example it increases cell survival by activating anti-apoptotic proteins such as Bcl-XL and Mcl-1 which regulate the negative feedback loop to Ras-Raf-MEK kinases, and cell vacuolization in autophagy (Cagnol and Chambard, 2010). The research on the effect of the kinases on the regulation of cell survival and apoptosis has produced several efficient and specific inhibitors that were introduced in the previous paragraph. In **Figure 11**, the sequential Ras-Raf-MEK-ERK pathway is depicted together with the structures of each inhibitor. All this work has been performed in mammalian cells that undergo cell division, posing the obvious question of the role of RAS-Raf-MEK-ERK signaling in terminal cells such as neutrophils. Although, there is not much research performed on the subject, the ERK ability to lengthening cell lifespan can be the reason for using upregulating this signaling pathway. For an activated neutrophil, with a life span of only a few hours, a continuous signal for cell survival can be vital in keeping the PMN alive until the source of infection is found.

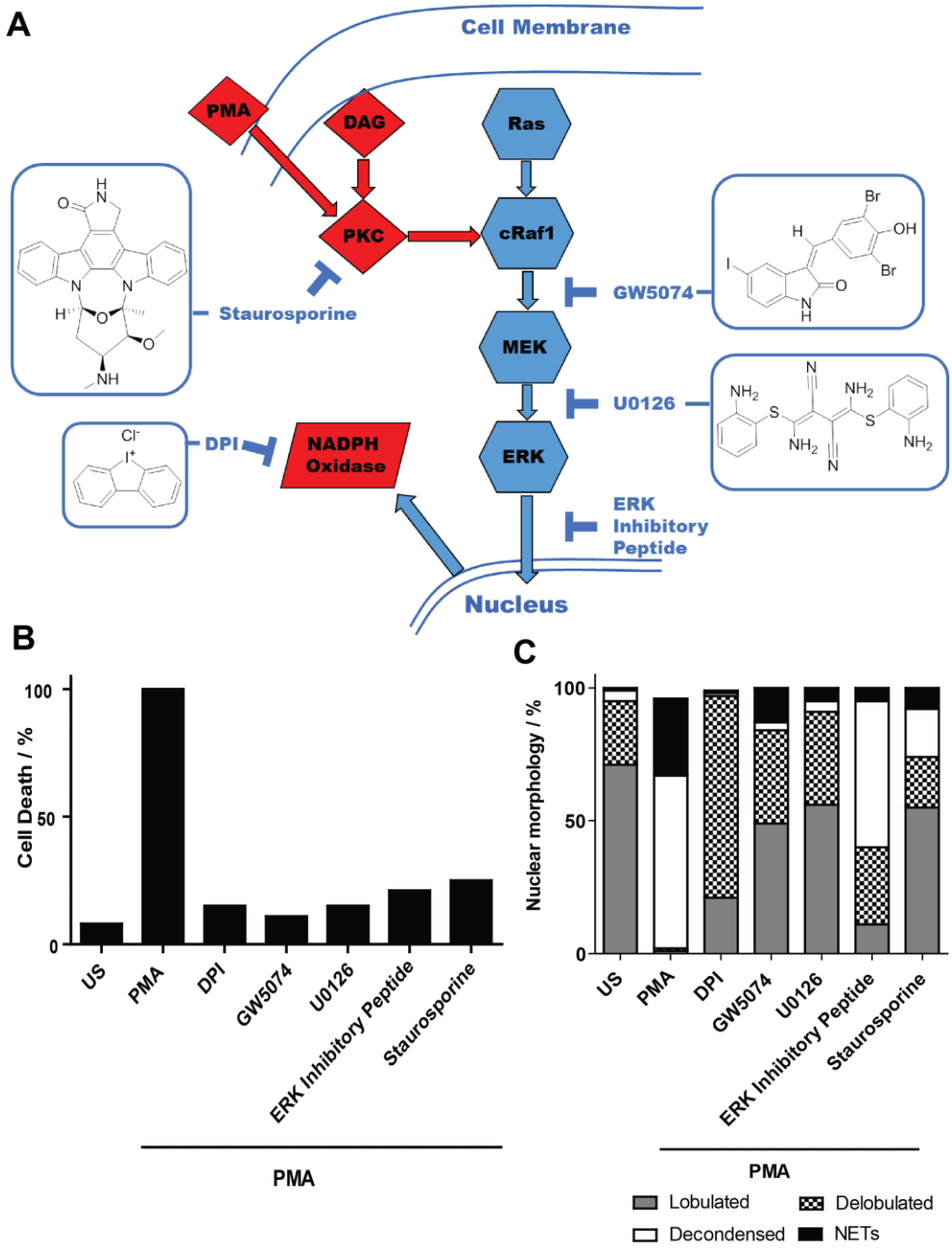

Figure 11. Investigation of the involvement of the Raf-MEK-ERK pathway in NET formation. (A) Ras/MEK/ERK pathway and known inhibitors. MEK pathway inhibitors stop NETosis. (B and C) Neutrophils were pre-incubated with 100 µM of the compounds for 20 min at 37°C followed by stimulation with 40 nM PMA and further incubation for 240 min to allow NET formation. Cells were stained with SYTOX Green to detect dead cells (B). Data are mean values ± s.d. (N=3, n=3, *P < 0.05 unpaired two tailed Student t-test). US: unstimulated cells. Nuclear morphology was analyzed after fixation and permeabilization using automated microscopy (C).

To test this hypothesis, neutrophils were exposed to the different MAPK inhibitors and were activated to undergo NETosis by using PMA. One of the interesting hits was the cRaf-1 inhibitor GW5074 (LOPAC code 6416) produced a 11 % cell death and 84 % small nuclei (**Figure 10**) corresponding to a group 1-type NET inhibitors (Lackey et al., 2000). To investigate the relevance of the Ras-Raf-MEK-ERK pathway in the context of NET formation mechanism, the following kinase inhibitors were subjected to experiments that validate their inhibitory role on NETosis; U0126, a MEK inhibitor, and an ERK2 inhibitory peptide (Favata et al., 1998). DPI was used as a positive control since NADPH oxidase is involved in the NET formation pathway and is downstream of ERK (O'Donnell et al., 1993). Staurosporine, a potent PKC inhibitor, was used as a control (Tamaoki et al., 1986).

NET formation was inhibited quite efficiently resulting in a group 1 morphology for all compounds, except for the ERK inhibitory peptide which showed a group 2 morphology (**Figure 11B and 11C**). This data clearly shows that the Raf-MEK-ERK pathway is involved in NETosis. Next, Ras protein was investigated, which is upstream of Raf, as a disruptor of NETosis. At the time there was no direct Ras inhibitor known and several indirect strategies to disrupt Ras oncogene signaling had been used. The Waldmann group has developed palmostatin B, an acyl protein thioesterase (APT1/2) inhibitor, and BMS3 and ABT, inhibitors of RabGGTase. Palmostatin B inhibits APT resulting in interference with Ras intracellular localization (Dekker et al., 2010). BMS3 is a dual inhibitor of FTase and RabGGTase and ABT inhibits RabGGTase (Bon et al., 2011; Stigter et al., 2012). The three inhibitors disrupt the post-translational modifications of Ras. The indirect Ras inhibitors failed to inhibit NET formation at all concentrations tested (**Figure 12B**).This data discards the direct involvement of Ras in NETosis and it can postulated that the mechanism bypasses Ras (**Figure 12A**). PKC is known to activate Raf directly without the participation of Ras. The involvement of PKC was validated by inhibiting NET formation with staurosporine (**Figure 11B and 11C**).

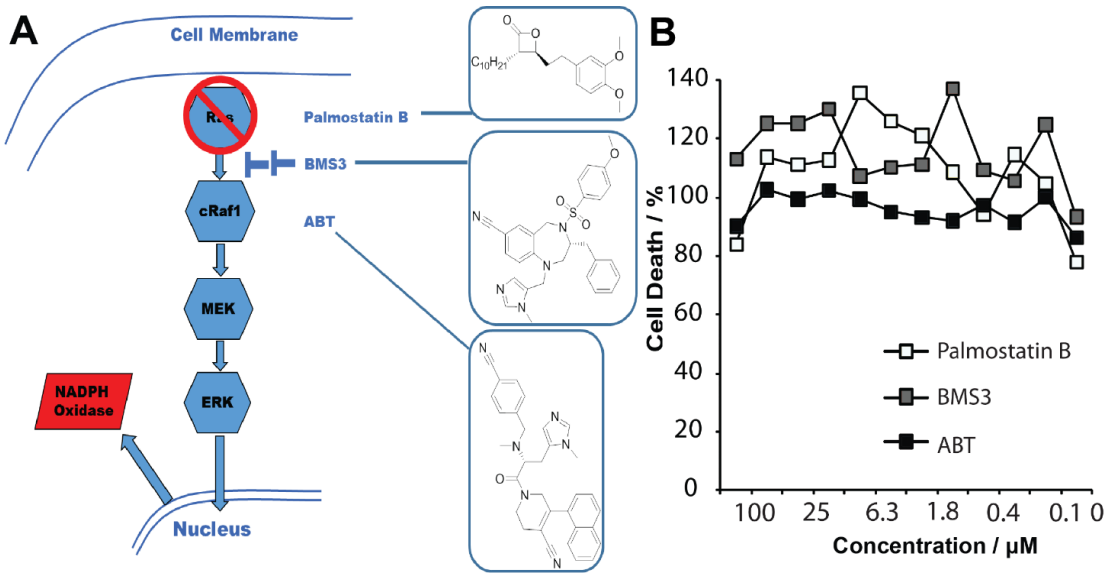

Figure 12. Ras does not participate in NET formation. (A) Canonical Ras-Raf-MEK-ERK pathway sequence and the structures of inhibitors non-direct inhibitors of Ras palmostatin B, BMS3, and ABT. (A) Palmostatin B, BMS3 and ABT failed to inhibit NETosis at several concentrations. Neutrophils were pre-incubated with a serial dilution of the compounds for 20 min at 37°C followed by stimulation with 40 nM PMA and further incubation for 240 min to allow NET formation. Cells were stained with SYTOX Green to detect death cells (B). Data are mean values ± s.d. (N=3, n=2).

Plant-derived phorbol esters, such as PMA, mimic the activity of diacylglycerol (DAG) in cells by activating protein kinase C (PKC) (Emerit and Cerutti, 1981; Niedel et al., 1983). Since PMA is a non-physiological PKC activator, the ability of the physiologically occurring PKC activators such as the lipophilic second messenger diacylglycerol (DAG) or platelet activation factor (PAF) to generate NETs was investigated. Upon stimulation with the lipids DAG analog and PAF, NETosis was observed at a concentration of 3 µM (**Figure 13A and 13B**). When working with lipids, delivery to the cell must be optimized. It is well documented that lipids are not soluble and the use of fatty acid-free bovine serum albumin and solvents other than DMSO such as alcohols are required. The delivery system to the neutrophils, concentration of the lipids, and incubation time were optimized to generate NETs (data not shown). After the optimization it was observed that PAF was not as effective as DAG as a NET formation activator. Interestingly, both activated NET formation at a concentration of 3 µM or higher. Showed a cell death up to 80 % (or higher) compared to the unstimulated control. Lower concentrations were found to be less effective. Once the optimal conditions were found, the cells were pre-treated with GW5074, U0126, Staurosporine kinase inhibitors and the ERK inhibitory peptide. These compounds successfully suppressed NET formation as detected by a decrease in cell death (**Figure 13C and 13E**) and increase in cells with lobulated nuclei (**Figure 13D and 13F**). Similarly, activation of NET formation by PAF was inhibited by the compounds and cells displayed the group 1 phenotype (**Figure 13C and 13D**). GW5074 and

U0126 inhibited NET formation upon activation with DAG, and cells exhibited similar phenotype as well (**Figure 13E and 13F**). In both cases, upon activation with PAF and DAG, MEK inhibitor cells maintained their inhibitory properties and exhibited the small nuclei phenotype. These results demonstrate the efficient inhibition of NET formation by the ERK pathway kinase inhibitor compounds induced by naturally occurring PKC activators.

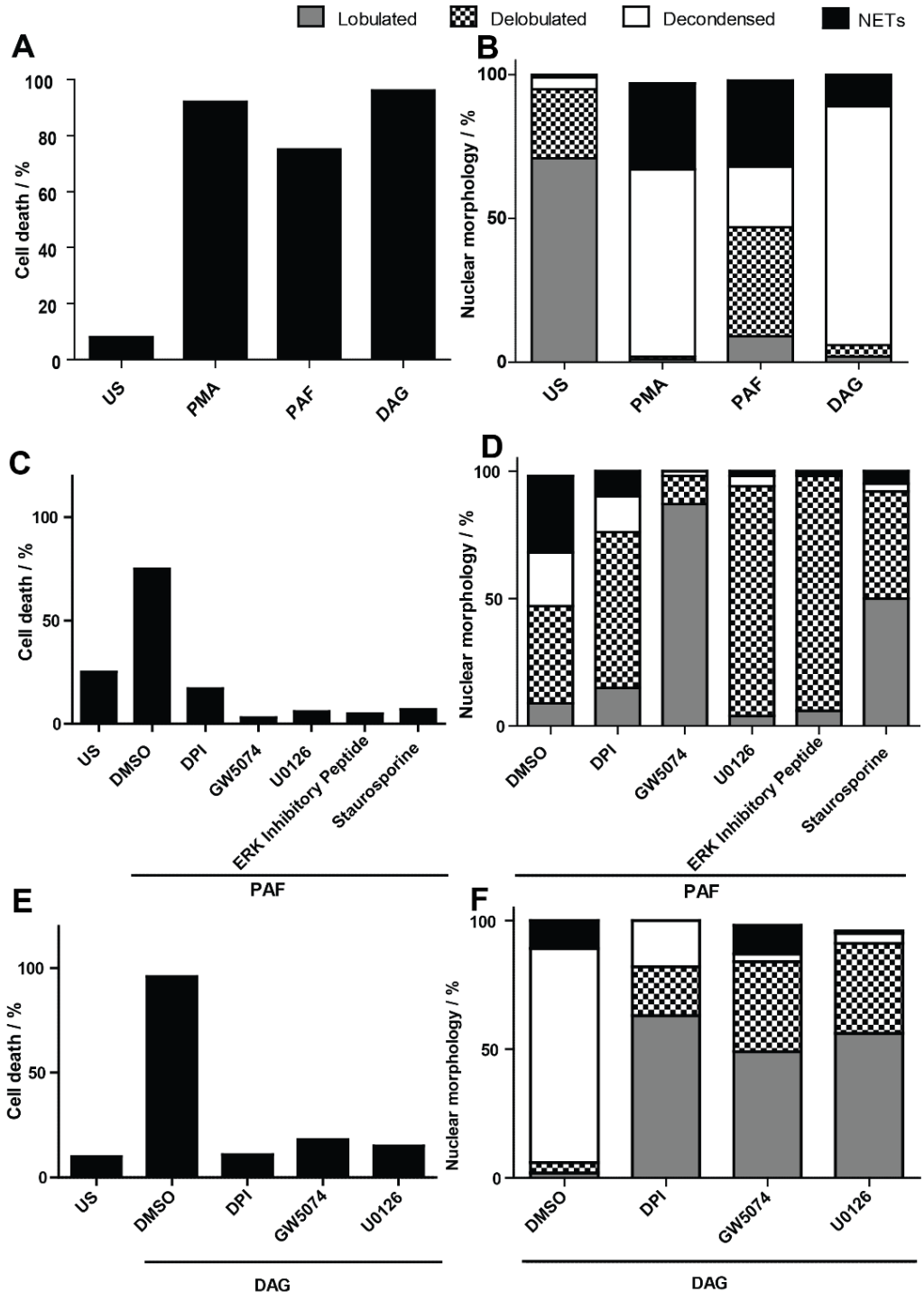

Figure 13. MAPK inhibitors respond to physiological PKC activators. DAG and PAF activate NET formation. Neutrophils were stimulated with 3 µM DAG or 3 µM PAF for 240 min (A-B). Neutrophils were pre-treated with 100 µM of the compounds for 20 min at 37^{o}C prior to stimulation with 3 µM PAF for 240 min (C-D) or 3 µM DAG (E-F). In all cases, cells were stained with SYTOX Green to detect dead cells (A, C and E) followed by fixation and permeabilization. The detailed nuclear morphology was quantified using automated microscopy (B, D and E). Data are mean values ± s.d. (N=3, n=3, *P < 0.05 unpaired two tailed Student t-test). US: unstimulated cells, DAG: Diaglycerol analog: 1–2-dioctanoyl-sn-glycerol, PAF: Platelet Activating Factor.

As mentioned in the introduction, the neutrophil's main function is to control infection by invading pathogens. To confirm, the neutrophils were exposed to *Helicobacter pylori* (*H. pylori*) to activate NETosis. *H. pylori* is a gastric gram negative bacterium known to make biofilms and have an outer layer consisting of lipopolysaccharide (LPS) and phospholipids (Kusters et al., 2006). Both LPS and phospholipids are known to activate NET formation (Brinkmann and Zychlinsky, 2007). In **Figure 14A and 14B**, for the first time it was shown that this gastric bacteria indeed produces NETs to a 20% above basal level. *H. pylori* is not as effective as PMA. Once the cells were pre-incubated with the MAPK signaling inhibitors, NET formation was inhibited and cells displayed group 1 phenotype (**Figure 14C and 14D**). With these experiments it was demonstrated that the Raf-MEK-ERK kinase inhibitors are efficient NET inhibitors, regardless of the employed stimuli.

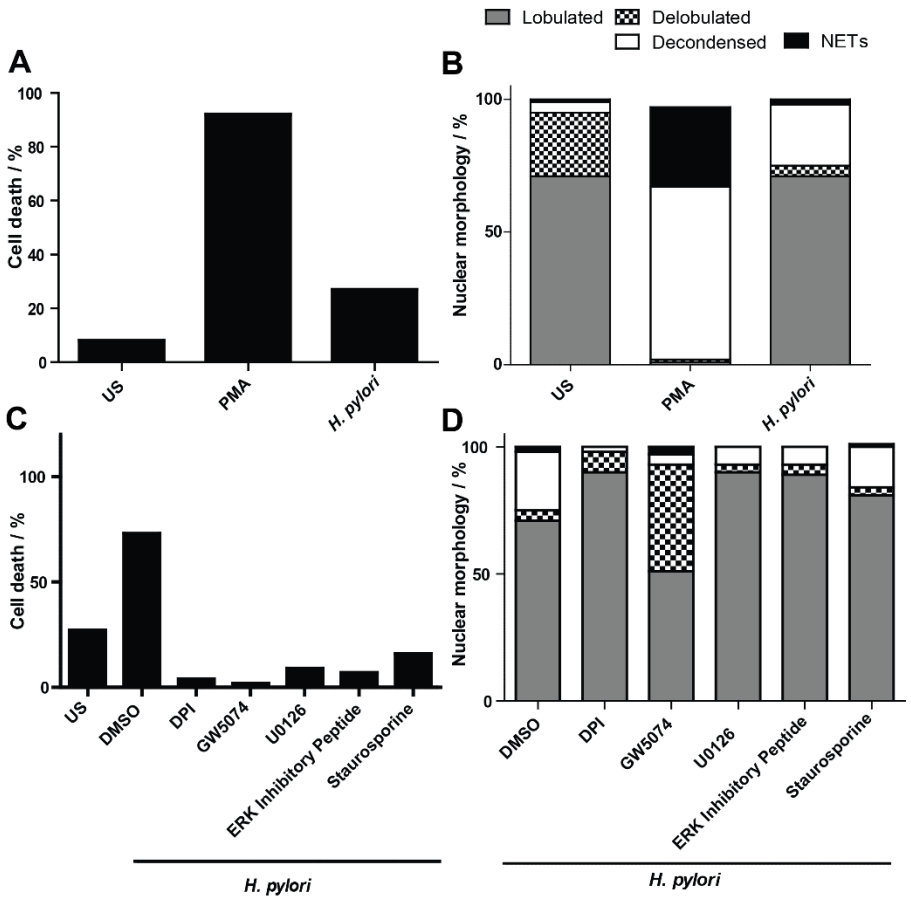

Figure 14. MAPK inhibitors block *H. pylori* NETs. *Helicobacter pylori* type 1 strain P12 was grown on Brain Heart infusion agar plates incubated for 37°C microaerophilic atmosphere. Neutrophils were stimulated with 40 nM of PMA or MOI of 100 of *Helicobacter pylori* for 240 min (A-B. Neutrophils were pre-treated with 100 µM of the compounds for 20 min at 37°C to stimulation MOI of 100 of *H. pylori* for 240 min (C-D). In all cases, cells were stained with SYTOX Green to detect dead cells (A and C) The detailed nuclear morphology was quantified using automated microscopy (B and D). Data are mean values ± s.d. (N=3, n=3, *P < 0.05 unpaired two tailed Student t-test). US: unstimulated cells.

6.3 Raf/ERK/MEK pathway is upstream of NADPH oxidase during NET formation

The Raf-MEK-ERK signaling pathway was proven to be part of NET formation using a chemical biology approach. Small molecule kinase inhibitors were used to disrupt NETosis and the inhibitors were efficient regardless of the stimuli. Therefore, the next step was to investigate the placement of the Raf-MEK-ERK signaling pathway in the overall NET formation mechanism. Reactive oxygen species (ROS) are essential in cell signaling and are fundamental for NET formation. ROS production is measured using an *insitu* peroxidase/luminol assay. Neutrophils were activated with PMA and after fifteen minutes the amount of ROS produced was detected. Staurosporine, GW5074, U0126 and ERK peptide inhibitor blocked ROS generation comparable to DPI, a known NADPH oxidase inhibitor (**Figure 15A**). These data demonstrate that the Raf-MEK-ERK pathway is upstream of NADPH oxidase. This finding is in line with earlier reports where a direct link was

established between phosphorylation of $p47^{phox}$, a NADPH oxidase component, by ERK (El Benna et al., 1996). Next, the involvement of the ERK pathway in NETosis was assessed by detection of phosphorylated-ERK (p-ERK) 1 and 2 by means of immunoblotting, which is the conventional proof of activated ERK pathway. When neutrophils were activated with PMA there was an increase in p-ERK compared to lack of phosphorylation when the cells were unstimulated. Staurosphorine, GW5074 and U0126 blocked the phosphorylation of ERK 1 and 2. The ERK peptide inhibitor only decreased ERK 1 phosphorylation as expected. DPI failed to block phosphorylation of ERK 1 and 2, proving that PMA-based NETosis is upstream of NADPH oxidase. When the cells were activated with *H. pylori* the immunoblotting results showed that the mechanism of *H. pylori* is independent of PKC (**Figure 15B**). Earlier in the chapter it was mentioned that there have been several studies linking the oncogenic potential of the MAPK signaling pathway to cancer cell survival by promotion of expression anti-apoptotic proteins such as Bcl-2, Bcl-XL, Mcl-1 and IAP. MAPK signaling not only increases the survival in cancerous cells, but also in immune cells. In myeloid leukemia, inhibition of ERK signaling causes an expression in anti-apoptotic proteins resulting in an elongated neutrophil survival (Simard et al., 2015). The ERK pathway modulates the expression of Mcl-1, so the expression Mcl-1 anti-apoptotic protein via immunofluorescence was investigated. Indeed there was in expression of the Mcl-1 protein after 120 minutes of PMA activation. As NETosis progresses, Mcl-1 is suppressed (**Figure 15C**). We tested the Mcl-1 expression levels in the presence of the PKC-Raf-MEK-ERK inhibitors and the expression levels of Mcl-1 were partially blocked. This data suggests that apoptosis is stopped by the expression of anti-apoptotic proteins allowing NET formation to continue. All of this regulatory signaling proves that NET formation is a controlled cell death mechanism, and not an uncontrolled cell explosion.

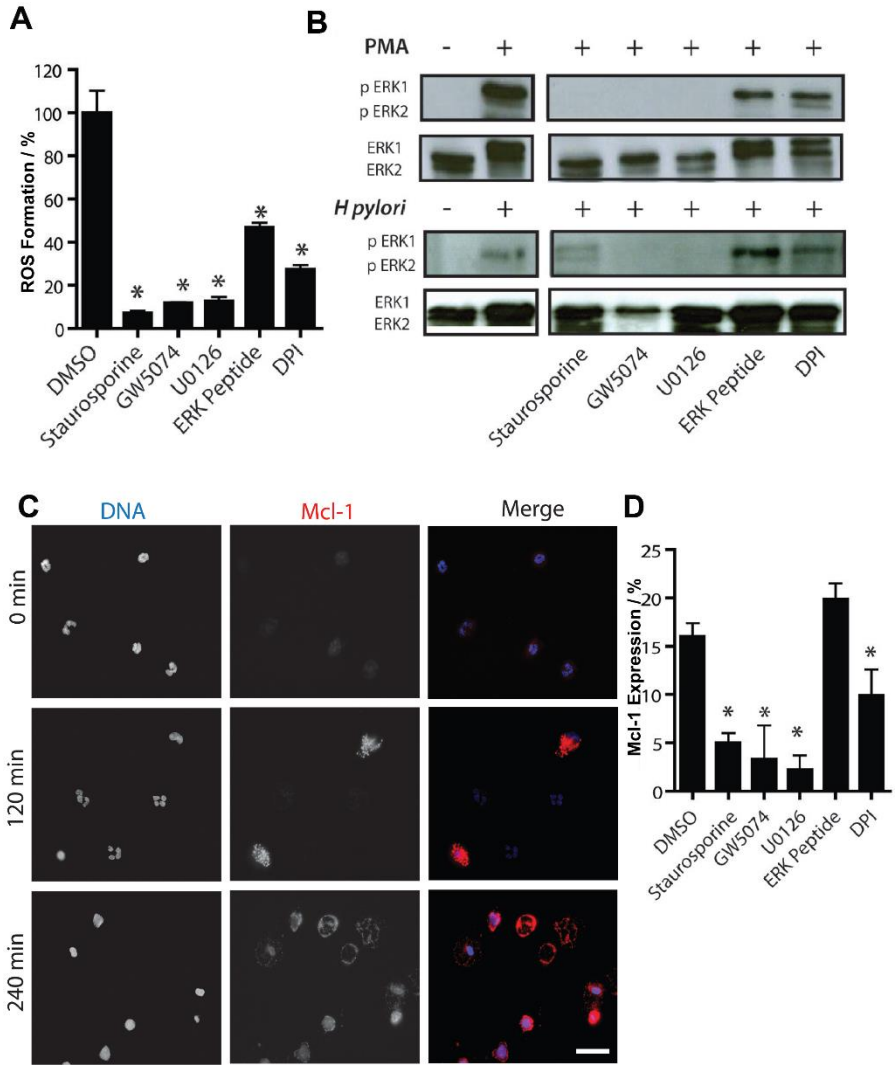

Figure 15. Raf-MEK-ERK pathway is upstream of NADPH oxidase. Influence of MAPK kinase inhibitors on the generation of reactive oxygen species (A). Neutrophils were treated with 100 µM of the compounds for 20 min prior to stimulation with 20 nM PMA to induce an oxidative burst. ROS were detected *in situ* using the luminol/HRP reagent. Data shown correspond to percent of generated ROS after 15 min stimulation with PMA. US: unstimulated cells. Validation of ERK protein by immunobloting analysis in NET Formation. (B) Phospo-ERK (pERK) is present in activated cells and not in unstimulated neutrophils. Anti-apoptotic protein Mcl-1 is expressed allowing NETosis to occur (C and D) (C). (D). Immunofluorescence using anti-Mcl-1 and DNA was stained with Hoechst 33342 and SYTOX. These representative experiments were performed in triplicate and presented as mean ± s.d. Significance **P* < 0.05; n paired, two-tailed Student's *t*-test. The relationship between ROS formation and Mcl-1 expression was tested for significance with a two-way ANOVA, with Bonferroni correction (Hakkim et al., 2011).

A common theme in NET-related diseases is the uncontrolled overproduction of NETs. Many physicians are hesitant to stop immune processes for fear of a full body immunosuppression. An immunosuppressed patient is less than ideal since the patient will suffer constant severe infections. Besides NETosis, phagocytosis and degranulation, other neutrophil functions are essential in maintaining homeostasis and to keep infections under control. Ideally, a small molecule therapeutic

would stop NET formation without affecting the other neutrophil functions. To investigate this we subjected neutrophils again to MAPK inhibitors and studied their effect on degranulation and phagocytosis. As mentioned in the introduction, lactoferrin is a neutrophil granular protein and it is produced during degranulation. Interestingly, the Raf-MEK-ERK signaling inhibitors did not halt lactoferrin production in comparison to cells treated with DMSO (**Figure 16A**). To study phagocytosis, neutrophils were encouraged to phagocytose fluorescent latex beads and the phagocytic activity was measure via flow cytometer. Raf-MEK-ERK signaling inhibitors did not affect the phagocytic activity of neutrophils. There was only a slight change in activity when the cells were exposed to U0126 or DPI (**Figure 16B**). We were able to place the Raf-MEK-ERK pathway upstream of NADPH oxidase and determined that this oncogenic pathway also plays a role that is directly linked with cell death mechanisms. In the case of NET formation neutrophils must bypass other cell mechanism to allow NET formation to occur, e.g. via apoptosis. Finally, we showed that anti-apoptotic proteins are indeed expressed to allow NETosis to occur. The kinase inhibitors used in these experiments in fact open the gate to many future pharmaceutical opportunities as they seem not to affect regular neutrophil cell function.

6.4 Project Conclusion

The first protocol to identify NET inhibitors was described. Using this protocol a library of 1266 commercially available small molecules (LOPAC library from Sigma) was screened. The Raf-MEK-ERK kinase inhibitors were identified as group 1 phenotype inhibitors. These inhibitors were active regardless of the NET formation activator. We were able to prove that group 1 compounds arrest NET formation at an early stage. Also, we show the involvement of the ERK pathway upstream of NADPH oxidase which occurs in the first 20 minutes of NET formation. We showed that anti-apoptotic proteins are expressed to allow NETosis to occur and are regulated by MAPK signaling pathway. Neutrophil phagocytic and degranulation function is maintained in presence of inhibitors (Hakkim et al., 2011).

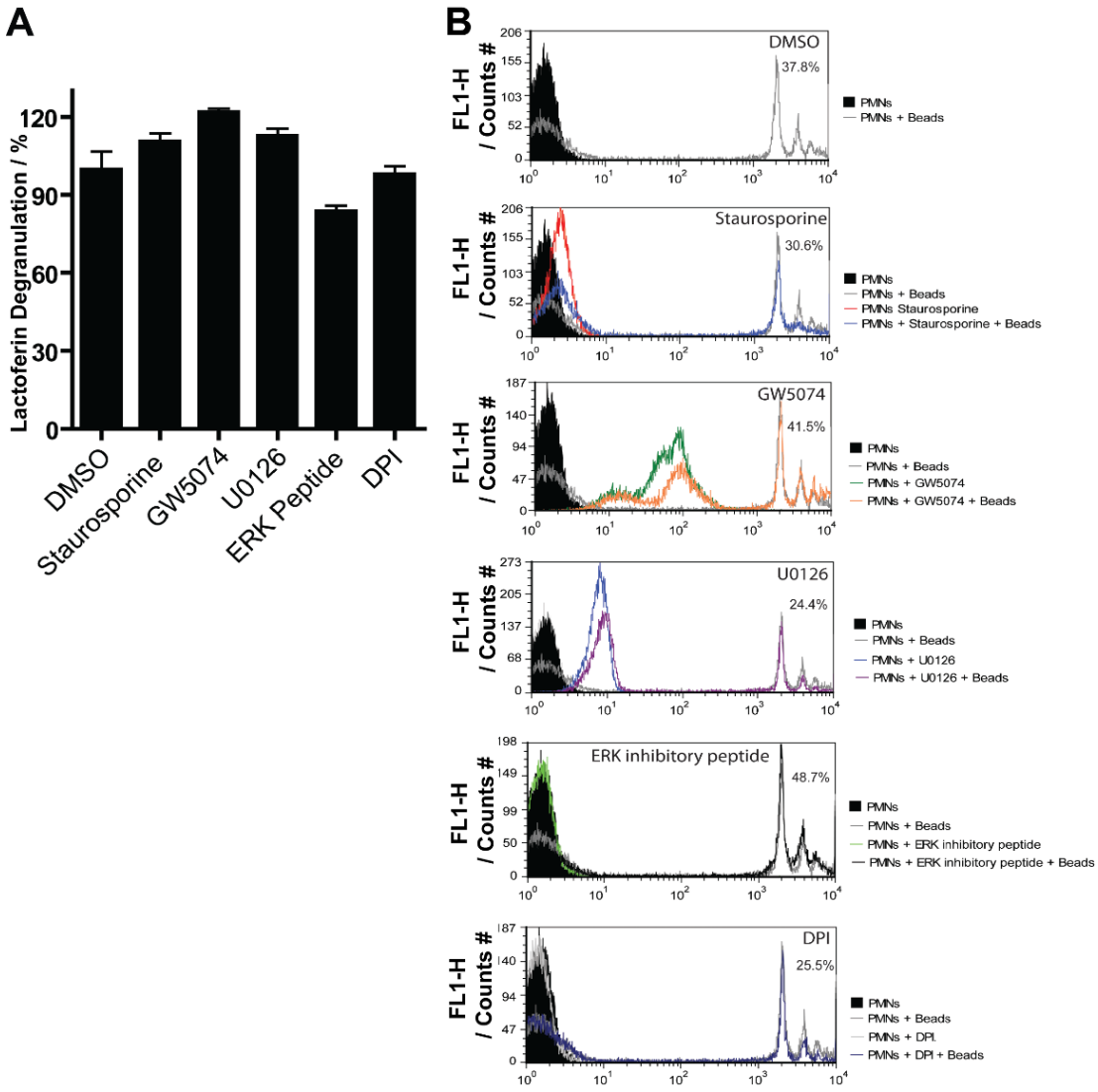

Figure 16. Raf-MEK-ERK inhibitors do not affect phagocytosis or degranulation. MAPK kinase inhibitors do not halt degranulation when neutrophils are activated with *Helicobacter pylori* (A). Neutrophils were pre-incubated with compounds then stimulated MOI of 100 of *Helicobacter pylori* for 90 min. Supernantant was tested for lactoferrin production using an anti-lactoferrin enzyme-linked immunosorbent assay (ELISA). Phagocytosis of fluorescent carboxylated beads is not effected by the MAPK inhibitors. (B) Neutrophils were pre-treated with compound for 30 min in siliconized tubes. Cells were exposed to the green fluorescence latex beads and incubated for 60min for binding and internalization. Cell suspensions were analyzed by flow cytometry and normalized to percent total cell count.

Chapter 7: Results and Discussion Section 3: Role of the Eicosanoid Pathway

Initial experiments described in this section were performed alongside with Abdul Hakkim.

7.1 Hypothesis

As part of the hits, there were inhibitors of the eicosanoid pathway among some of the potent inhibitors. It hypothesized that there is a direct involvement of the eicosanoid pathway in NET formation. NET formation is induced with signaling lipids such as DAG and PAF. This lipid signalling pathway can be incorporated in the traditional view of cell-to-cell communication to NETosis. To further investigate this pathway several inhibitors of the cyclooxygenase (COX) / lipoxygenase (LOX) pathways were screened and identified as NET generation inhibitors. Our results elucidate a new function in leukocytes, contributing to a novel field of study for neutrophil biology.

7.2 Introduction to the eicosanoid pathway

Immune cell trafficking pathways are regulated by signaling lipids (Wymann and Schneiter, 2008). These lipids are synthesized via autocrine or paracrine depending on the regulatory signal (Nathan, 2006). They regulate cell proliferation, apoptosis, metabolism and migration (Wymann and Schneiter, 2008). In the introduction neutrophil migration was discussed and specific phosphoinositides were highlighted for their involvement in this neutrophil migration and invasion. Phosphoinositides can be hydrolyzed by phospholipase C (PLC) to diaglycerol (DAG) where DAG activates protein kinase C (PKC) releasing calcium ions (Ca^{2+}) (Mackay and Twelves, 2007; Wymann et al., 2003). This signaling activates the synthesis and release of several lipids, including lysophosphatidic acid (LPA) and activation of several proteins, for instance G protein-coupled receptors (GPCRs). Together LPA and GPCRs are responsible for release of specific eicosanoids (Futerman and Hannun, 2004). Eicosanoids are a very active type of lipids derived from arachidonic acid (AA). The most predominant lipid categories are lipoxins (LX), leukotrienes (LT), hydroxyeicosatetraenoic acids (HETE), prostaglandins (PG), thromboxanes (TX), resolvins (Rv), and eoxins (EX) (Sala et al., 2010). Eicosanoids have a very short half-life, typically of the order of seconds or minutes, and they bind mainly to GPCRs and nuclear receptors. Besides eicosanoid synthesis, PLA2 produces lysolipids, for example lysophosphatidlcholine (lyso-PC), which is converted to platelet-activation factor (PAF), and is a powerful inflammation activator (Cyster, 2005).

For years it has been known that the imbalance in these lipid signaling pathways contributes to chronic inflammation, autoimmunity, allergy, cancer, atherosclerosis, hypertension, and metabolic and degenerative diseases. Specifically, the main source of inflammation is the release of granular content and the formation of PG, TX, and LT by leukocytes (neutrophils, lymphocytes, macrophages, mast cells and granulocytes) as a result of high levels of Ca^{2+}, cytokines or chemokines. For decades, the treatment for inflammation diseases has been some form of

regulation of the production of these lipids. Aspirin, which was synthesized by Felix Hoffmann at Bayer in 1897, was based on the studies of willow tree leaves used in the treatment of fever and pain relief (Wymann and Schneiter, 2008). This gave birth to modern non-steroidal anti-inflammatory drugs (NSAIDs) which are selective cyclooxygenase (COX) inhibitors. Cyclooxygenase (COX) is an enzyme that converts arachidonic acid into prostaglandin (PG), a principal member of the eicosanoid cascade.

In chronic inflammation, ceramide kinase (CerK) and cystolic phospholipase (cPLA2) release arachidonic acid to activate the GPCRs that, together with chemokines, cytokines and histamine-caused bronchial restriction, is detrimental in late allergies and inflammation (Yedgar et al., 2007).

The role of signaling lipids such as AA, DAG and PAF on neutrophils is well-established. Due to the short-lived nature of both the lipids and neutrophils, all the details of their mechanisms of actions are unknown. Obviously, new techniques such as lipidomics, where LC/MS/MS techniques are applied to the identification and quantification of lipids, and microscopy techniques, are likely to shed more light on lipid function. In the literature the concept of NETs and lipids is limited. In a few findings, including our research, NETs are shown to be generated by PAF and DAG (Clark et al., 2011; Hakkim et al., 2011; Yost et al., 2010).

7.3 Eicosanoid pathway and NET formation

We reported that NET formation can be induced by messenger lipids (Hakkim et al., 2011). The initial reasoning was that platelet activation factor (PAF) and diaglycerol (DAG) are signaling molecules that activate PKC protein. PAF and DAG were used in the assay as physiological alternative to PMA. PAF and DAG are traditionally involved in cell-to-cell communication signaling pathways and they are well known to be involved actively in immune responses. Typically, to activate the generation of PAF or DAG in the cell, neutrophils are stimulated with calcium ions or combinations of granulocyte macrophage colony-stimulating factor (GM-CSF) and N-formulmethionyl-leucyl-phenylanine (fMLP) or calcium with fMLP (Cronstein and Weissmann, 1995). In the case of NETs these combinations did not prove to be good NET formation activators. Nevertheless, we were able to activate the neutrophils with PAF and DAG at concentrations of 3 µM using fatty acid-free BSA as vehicle. In the case of DAG, 1–2-dioctanoyl-*sn*-glycerol was used which is a membrane-permeable DAG analog (**Figure 17 A-B and C-D**). Besides activating PKC, DAG also activates protein kinase D (PKD). Activating the signaling pathways of PKC or PKD as a result of increased ROS activation leads to an induction in survival pathways protecting the cell from apoptosis (Toker, 2005). In the context of NET formation, this signaling keeps the neutrophil alive long enough for NETosis to take place. Phosphatidic acid (PA) is produced by phosphorylation of

DAG-activated kinases. It is known that these enzymes affect signaling to ERK pathway via GTPase (Toker, 2005). This supports our findings that the Raf-MEK-ERK pathway is involved in NET formation.

As mentioned before, the lipid 1-*o*-alkyl-2-acetyl-*sn*-glycero-3-phosphocholine (PAF) activates PKC and this activity negatively regulates the PAF receptor, but this is one of many PAF functions (Ali et al., 1994). Notably PAF is the most established lipid in cell-to-cell communication. It was first established as a messenger protein by specifically binding to its own GPCR, platelet activation factor receptor (PAFR) (Prescott et al., 2000). PAF has both autocrine and intracrine effects. PAF-induced activity is highly regulated upon availability, specific expression of the receptor, which can be sensitized and desensitized, and finally rapid degradation of PAF by acetyl hydrolysis inside and outside the cell. PAF, like many other lipids, has a very short half-life of a few minutes in the blood stream. This tight regulation is attributed to its autocoid nature and efficiency affecting neighboring cells and cells where it is synthesized (Prescott et al., 2000). PAF is known to be synthesized in immune cells, mainly neutrophils, and endothelial cells and the synthesis occurs in periods of acute inflammation response. In neutrophils, it is known to affect the adhesion response by β2 integrin (Harris et al., 2000). In addition to neutrophils, PAF has been linked to neuronal migration and neurotransmitter release (Kato et al., 1994). In the plasma, where PAF acetyl hydrolase has been connected to low density lipoproteins (LDL) and high-density lipoproteins (HDL), it has a role in vascular disease (Tellis and Tselepis, 2014). Similar to DAG signaling mechanisms, PAF has been associated to the ERK signaling pathway upon direct activation of PKC with PAF. As PAF is known to activate the PAF receptor, it was shown to maintain phosphatidylinositol levels. Interestingly, similar to our findings for the NET formation, no activation of Ras was observed (Honda et al., 1994).

Both lipids, DAG and PAF, trigger the eicosanoid pathway and we decided to investigate whether arachidonic acid (AA), the main precursor for this pathway, was able to activate NET formation. Arachidonic acid was used to stimulate neutrophils at 3 µM using fatty acid-free BSA as vehicle to activate NETs. NETs were obtained in 15 to 45 min which is faster than observed for PMA (which takes 2 to 4 hours for NET formation) (**Figure 17 A-B and E**). Overall, AA was shown to be less effective compared to PMA since fewer cells were triggered to produce NETs after 4 hours of incubation. This could be due to the fact that AA is quickly metabolized, as it was mentioned in previous chapters. This would explain why all lipids were most active at 3 µM compared to PMA which is already very active at 40 nM. From studies known in literature it is not clear at what concentrations these lipids should be active. The mechanism in which neutrophils are known to synthesize eicosanoid lipids physiologically after an infection or inflammatory response is depicted in **Figure 17 F**.

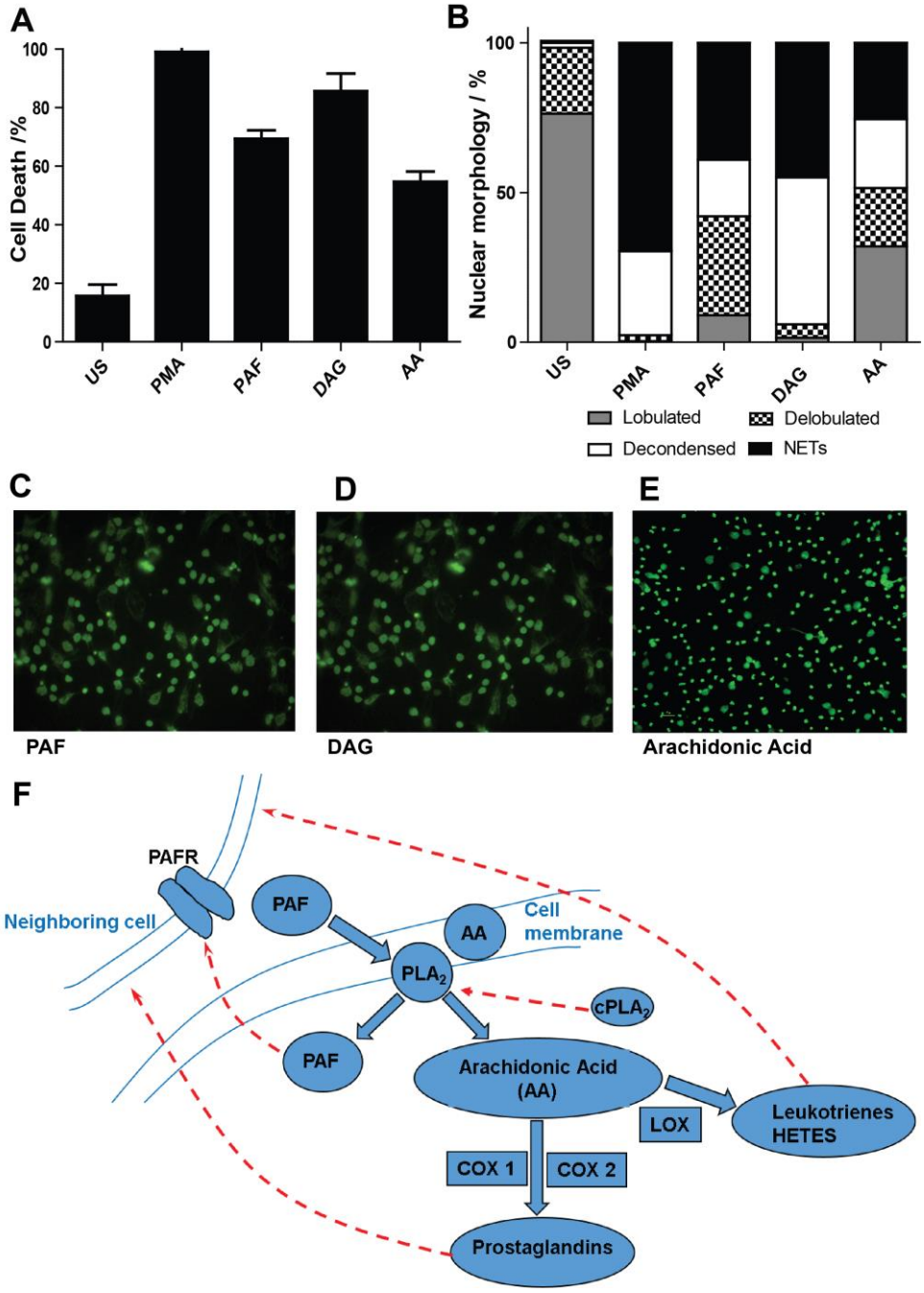

Figure 17. PAF, DAG and AA activate NET formation. Neutrophils were stimulated with 3 µM PAF (A, B and C), 3 µM DAG (A, B and D) or 3 µM AA for 240 min (A, B and E). Cells were stained with SYTOX Green to detect dead cells (A) followed by fixation and permeabilization. The detailed nuclear morphology was quantified (B). Representative images of cells treated with PAF (C), DAG (D) and AA (E). Data are mean values ± s.d. (N=3, n=3). (F) Scheme of transcellular biosynthesis of eicosanoids. US: unstimulated cells. DAG: Diaglycerol analog: 1–2-dioctanoyl-sn-glycerol, PAF: Platelet Activating Factor, AA: Arachidonic acid.

In PMA-activated NET formation there are important regulatory roles for NE and MPO. Next, it was of interest to see if the granular proteins NE and MPO were present in lipid generated NETs.

Since, MPO and NE have been used as NET markers in recent reports (Papayannopoulos et al., 2010) it has become of general practice to demonstrate the expression of the proteins via immunoflouresnce. AA and PAF-induced NETs contained NE and MPO proteins. These results confirm that NETs can be generated upon activation with lipids (**Figure 18**).

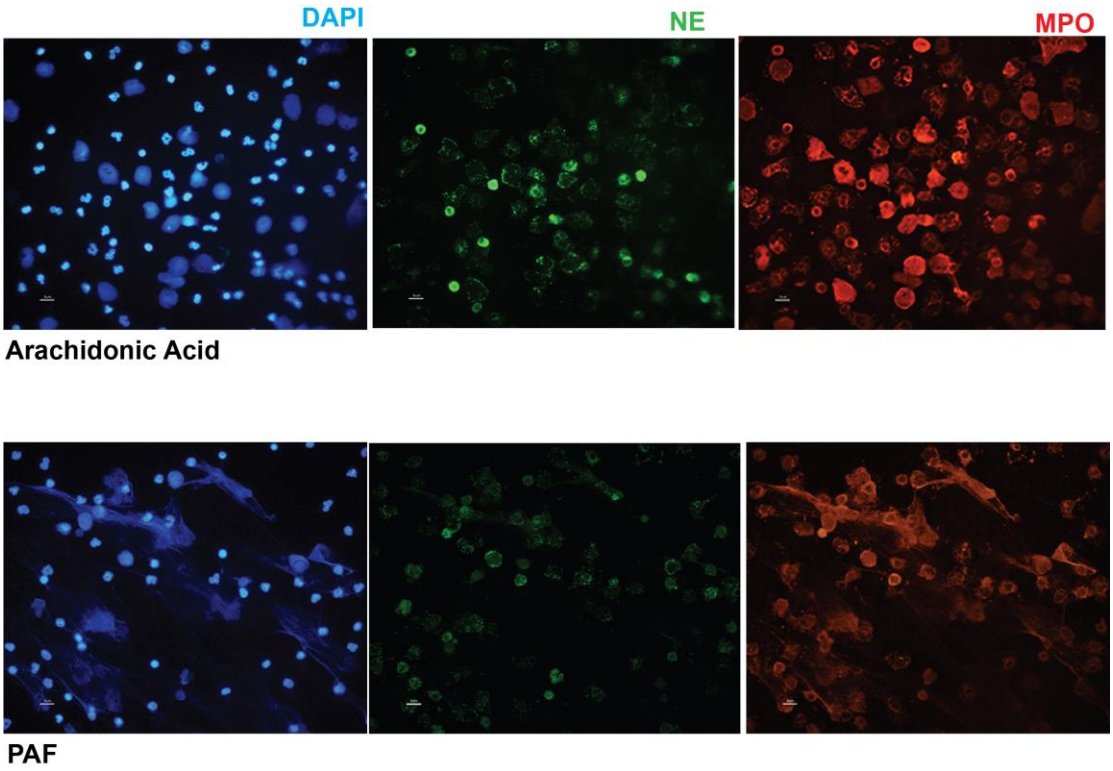

Figure 18. NE and MPO localize in AA and PAF-induced NETs. Neutrophils were stimulated with 3 µM AA or 3 µM PAF for 240 min followed by fixation and permeabilization. Cells were stained with DAPI, anti-NE and or anti-MPO antibodies. PAF: Platelet Activating Factor, AA: Arachidonic acid.

In vivo PMA will not be able to activate NETosis, therefore, it was relevant to show that NETs are generated by physiologically relevant compounds like PKC activators DAG and PAF. In addition, to activating PKC, it is known that PAF and DAG are important signaling lipids for neutrophils and they are involved in cell-to-cell communication. Eicosanoid lipid synthesis is initiated by arachidonic acid and we showed that NETs can be activated with AA.

7.4 LOX inhibitors stop NET formation, but COX inhibitors do not

In addition to the identification of arachidonic acid as a NET activator, the NET screen was expanded to the MicroSource US Drug compound library. The US drug library is a collection of 1360 compounds of FDA-approved pharmaceutical compounds. In both screening campaigns, we identified COX/LOX inhibitors such as resveratrol and curcurmin. In order to identify the signaling

mechanism, in which the eicosanoid pathway is involved in NET formation, additional inhibitors were screened in the NET inhibition screen. The COX/LOX inhibitors suggest a very promising therapeutic component for NET inhibitors. These inhibitors, specifically COX1/2 inhibitors, are common therapeutics for inflammation diseases. These compounds are commonly known as nonsteroidal anti-inflammatory drugs (NSAIDs) and are widely used for pain and inflammatory treatments.

Resveratrol and curcumin are both natural products that are known to have antioxidant properties and have been identified as COX inhibitors. Additional studies showed that they were not specific to COX but showed inhibitory activity for LOX as well. Their promiscuity as ROS scavengers and inhibitors of many other enzymes that are involved in the redox mechanisms has been reported (Fremont, 2000; Jankun et al., 2016). We tested the compounds as positive controls in addition to other dual inhibitors of COX/LOX like nordihydroguaiaretic acid (NGDA) and eicosatetraynoic acid (ETYA) (Kleniewska et al., 2012). These dual inhibitors were most active upon the activation with PMA since 40 to 60 % cell death and large nuclei was observed. This would classify them as group 2-type NET inhibitors (**Figure 19 A-B**). They showed an efficient inhibition at the last stage where NET formation stopped right before the cell ruptures to expel the nuclear content.

Zileuton, MK-866 and PD146196 are specific LOX inhibitors. Zileuton is a 5-LO inhibitor, MK-866 is a 5-LO activating protein (FLAP) inhibitor and PD146196 is 15-LO inhibitor. Both 5-LO inhibitors caused 70% cell death and large nuclei morphology. They are classified as a group 2-type of NET inhibitor. The most efficient NET inhibitor was PD146196 with a cell death of 68% and group 1-type morphology (**Figure 19 C-D**).

Celecoxib and indomethacin were used as selective COX inhibitors. Celecoxib is a COX2 inhibitor used in the treatment of arthritis while indomethacin is a COX inhibitor used for fever and inflammation suppression. Both compounds failed to inhibit NET formation with an observed cell death of 90% or higher and a large nuclei morphology (**Figure 19 F-E**). All COX inhibitors were not found to be inhibitors of NET formation. In addition to these two compounds, other NSAIDs such as diclofenac, meclofenamic and sulindac sulfone were tested and showed no inhibition of NET formation (data not shown).

From the COX/LOX inhibition data it can be concluded that the eicosanoid pathway is indeed involved in NET formation. Dual LOX/COX inhibition confirmed this finding although the lack of selectivity of these compounds needs to be taken into consideration. The selective inhibitors that were used provide new insights into the mechanisms involved in NET formation. Whereas COX enzymes do not influence NET formation, LOX enzymes regulate NETosis. Notably, LOX inhibitors are not the most effective NET formation inhibitors.

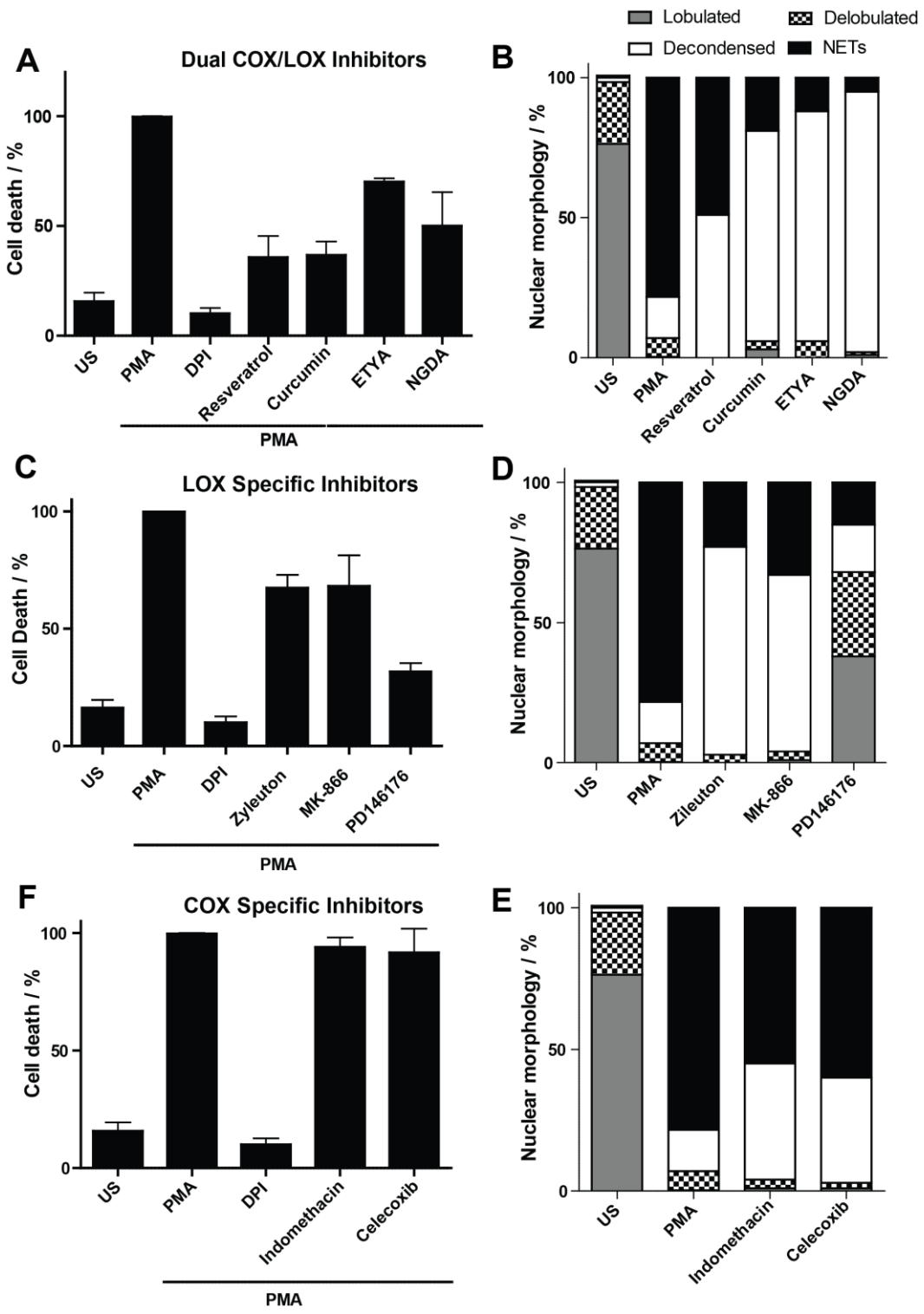

Figure 19. LOX and COX/LOX dual inhibitors stop NET formation. Dual COX/LOX and LOX inhibitors halt NETosis (A-D). COX inihibitors fail to stop NET formation (E-F). Neutrophils were pre-incubated with the compounds for 20 min (30 µM), except for MK-866 (1 µM), by stimulation with 40 nM PMA and further incubation for 240 min to allow NET formation. Cells were stained with SYTOX Green to detect death cells (A, C, and E). Nuclear morphology was analyzed upon fixation and permeabilization using automated microscopy (B, D and F). Data are mean values ± s.d. (N = 3, n = 3). US: unstimulated cells.

Next, the possibility that inhibitors of the arachidonic acid pathway exert their action through ROS generation was explored. Therefore, an oxidative burst assay after the exposure to the compounds was performed. Surprisingly, resveratrol and ETYA failed to inhibitor ROS generation after 30min although it was expected that all dual inhibitors halt ROS formation. The COX inhibitors failed to inhibit ROS generation as well. However, all LOX inhibitors reduced ROS generation placing the involvement of this 5-LO and 15-LO upstream of ROS generation (**Figure 20**). This is in line with previous findings where DAG and PAF were found to activate the ERK pathway (Prescott et al., 2000; Toker, 2005). We show that the ERK pathway is upstream of ROS generation in NET formation. It was hypothesized that this COX/LOX pathway would be involved upstream of ROS. Nevertheless, further experiments would be necessary to confirm this finding.

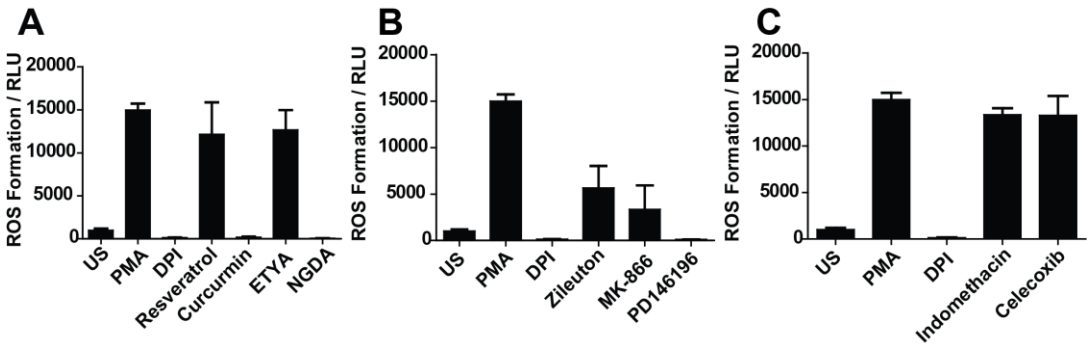

Figure 20. Influence of COX and LOX inhibitors on ROS generation. Neutrophils were treated with 15 µM of the compounds for 20 min prior to stimulation with 20 nM PMA to induce an oxidative burst. ROS were monitored *in situ* using the luminol/HRP reagent every minute for 120 minutes. Data shown correspond to percent of generated ROS after 30 min stimulation with PMA for dual COX/LOX (A), LOX (B), and COX (C) inhibitors. Data are shown as mean values ± s.d. (N=3, n=3). US: unstimulated cells. RLU: relative light units.

The failure of COX-specific inhibitors to halt NETosis supports with earlier reports where neutrophils activated with AA or ERK signaling were completely independent of COX activity (Capodici et al., 1998). In their findings the activity was due to 5-LO. They tested ERK activity, with both indomethacin (COX inhibitor) and zileuton (5-LO inhibitor) upon activation with AA, zileuton affected the ERK activity and indomethacin showed no effect. The results presented here for the different COX and LOX inhibitors follow a similar pattern.

The involvement of lipoxygenases in NETs suggests another interesting role and that is cell-to-cell communication. Lipoxins are produced by the metabolism of arachidonic acid by 12/15-lipoxygenase and 5-lipoxygensae (5-LO). Lipoxin production is a typical response to transcellular metabolism. Traditionally, in neutrophils calcium ions stimulate the production of lipoxin A4 (LXA4) which is later used to activate and communicate with platelets (Edenius et al., 1988). If this is the

case in NET formation, hypothetically, lipoxin synthesis can be triggered to either activate or deactivate NET formation in adjacent cells and signaling to other adjacent cells.

7.5 Novel finding of lipid bodies in NETs

In an attempt to prove the presence of lipids on NETs, oil red O staining was performed. The neutrophils were activated with PMA to generate NETs and fixed on glass slides. The unstimulated neutrophils (used as control) and NETs were stained with SYTOX green, a DNA dye, and oil red O, a classical lipid stain. Oil red O is a soluble diazole dye with an absorption of 518 nm that stains neutral lipids and cholesteryl esters, but not biological membranes (Mehlem et al., 2013). This surprisingly revealed a presence of lipid bodies on the NETs and on the neutrophils as illustrated in **Figure 21**. Lipid bodies are also known as lipid droplets or adiposomes, organelles that are known to be involved in metabolism and lipid storage. In the context of immune cells, specifically inflammation, lipid droplets get triggered by oxidative stress and inflammatory factors, i.e. LPS, pathogens, PAF, eicosanoids, and cytokines (Melo et al., 2011a). Lipid droplets can be used as inflammation markers in disease (Melo et al., 2011b). In the case of NETs, this is the first account in which lipid bodies are seen in NETs. Therefore, their role and composition is unknown.

On the unstimulated cells lipid bodies were surrounding the nucleus and were present in the cytoplasm (**Figure 21 A-B**). Detailed inspection revealed that the lipid bodies on the NETs were located on the strings of the NETs and on the outside rim of cell membrane remnants (**Figure 21 E-G**). After, micrococcal nuclease (MNase)–mediated digestion of the DNA and centrifugation, the lipid bodies were isolated (**Figure 21 C**). After imagining, it was not possible to investigate the lipid bodies further. There was much optimization needed for proper storage and identification techniques.

It can be speculated that the lipid bodies are composed of AA, PAF, leukotrienes or lipoxins which are synthesized during NET formation and are encapsulated in a lipid body. It is known that lipid bodies are composed of a neutral core containing triacylglycerols (TG) and cholesterol esters (CE) surrounded by phospholipids (Deevska and Nikolova-Karakashian, 2017). These fatty acids can be converted to AA or into any other fatty acid intermediate. These lipid bodies decorate the NETs, like the granular proteins, and may serve to send pro-inflammatory signals to adjacent cells. A basis for this hypothesis comes from the image where a NET string connects an adjacent cell and the DNA string is decorated with lipid bodies (**Figure 21 D**). The role of these lipid bodies would be dependent on the type lipid the lipid body is composed.

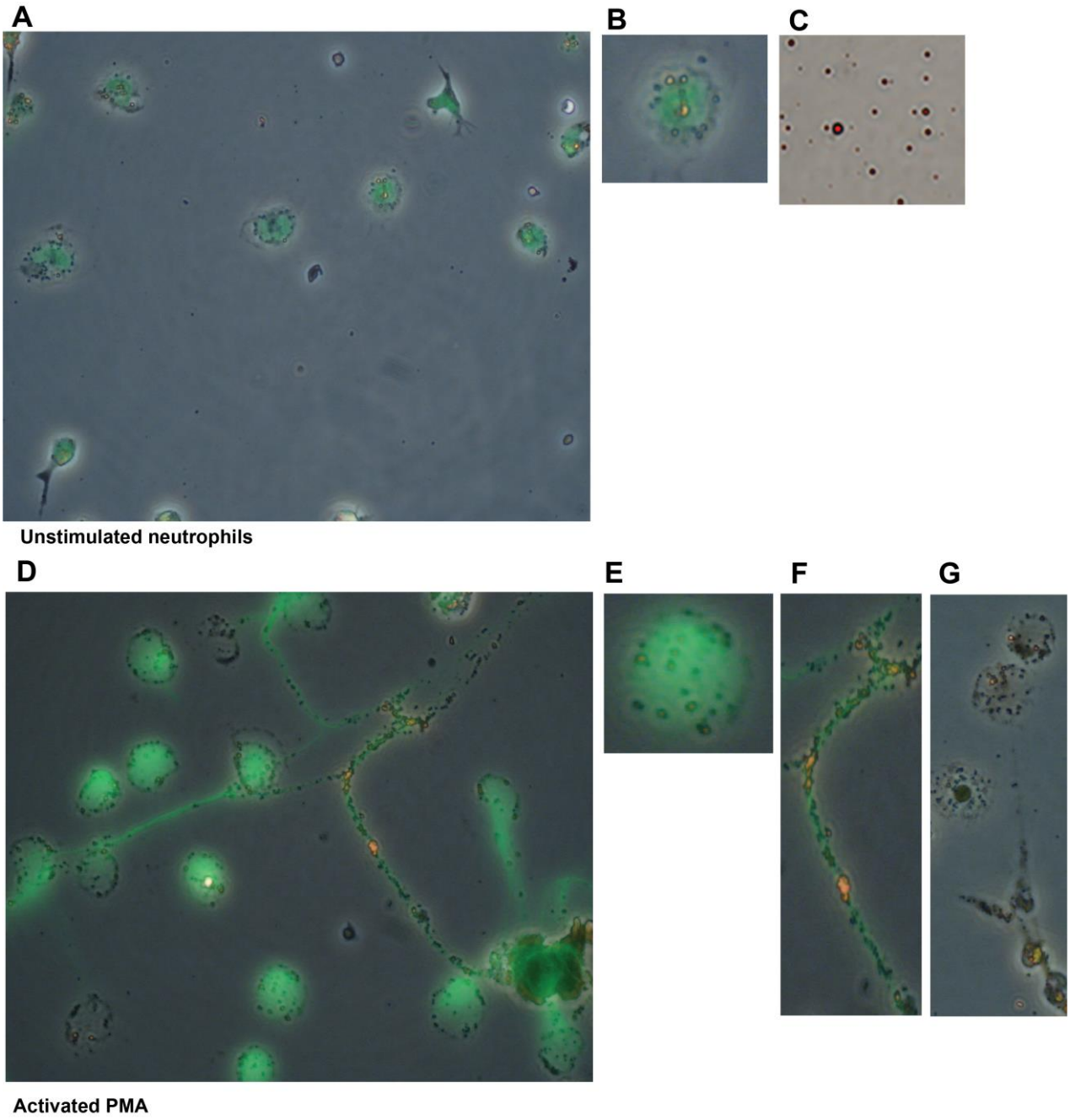

Figure 21. Lipid bodies found in NETs. Unstimulated neutrophils stained with Oil O Red and counterstained with SYTOX green (A-C). Red colored lipid bodies surround the nucleus (B). Lipid bodies (C) Neutrophils activated with PMA have lipid bodies on the periphery of the diffused NETs (D-E). (F-G) Lipid bodies are also found along the NETs. (D, F-G) Lipid bodies are present on the strings of DNA from the NETs that are connecting two different neutrophils.

7.6 Project Conclusion

The involvement of the eicosanoid pathway in NET formation was confirmed. NETs were generated with signaling lipids that are precursors of the eicosanoid synthesis pathway. The LOX inhibitors had an effect on NET formation and COX inhibitors did not. This excludes COX signaling

pathway from the NETosis mechanism. It can be postulated that once the eicosanoid pathway is activated it chooses the lipoxygenase route to synthesize leukotrienes or lipoxins followed by activation of adjacent cells which eventually triggers NET formation. The eicosanoid pathway is a signaling pathway whose primary role is communication and this was confirmed by the finding of lipid bodies on the NETs. We hypothesize that the lipid bodies are composed of a signaling lipid. Our first attempts to identify the composition of the lipid bodies, was via HPLC identification using a 9-antryl diazomethane (ADAM) for identification of eicosanoids. However, this was not successful due to lack of experience and appropriate setup (Moraes et al., 2004). Therefore the content of the detected lipid bodies remains to be determined and their role on NETosis remains to be confirmed.

Chapter 8: Results and Discussion Section 4: Identifying Novel NET Inhibitors

8.1 Hypothesis

The NET phenotypic screening of annotated libraries led to the identification of Raf-MEK-ERK signalling and eicosanoid pathways involved in NET formation. The screen was expanded to the in-house library of natural product-(NP)-inspired compound to identify novel NET inhibitors or new biological targets that will elucidate NETosis. Additionally, these compounds may represent a starting point for development of future therapeutics.

8.2 Identification of novel inhibitors: Aminothiazoles

The screen was expanded to the in-house developed library of 8407 compounds to identify inhibitors of NET formation based on natural product inspired chemical scaffolds. For this compound library, the compounds are based on NP-derived scaffolds and the targets are mostly unknown. The same readouts for the assay as before were used, i.e. nuclear morphology and cell death of neutrophils (**Figure 22**). The compounds were screened at an initial concentration of 100 µM. The screen produced 134 hits a less than 2 % hit rate.

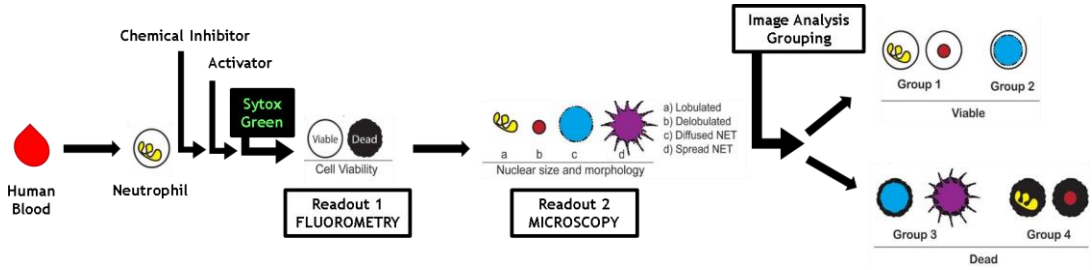

Figure 22. NET screen workflow and inhibitor classification

2-substituted aminothiazoles were identified as novel potent NET inhibitors. At a concentration of 100 µM the compounds blocked NET formation and maintained cell viability. Aminothiazole derivatives were causing two different nuclear morphologies, i.e. group 1 and group 2. The aminothiazole scaffold represents an attractive compound series due to their structure and well established biological activity. Thiazoles are potent compounds found in drugs such as sulfathiazole, an antibacterial agent; ritonavir, an antiviral compound; and abafungin, an antifungal agent (Siddiqui, N. Thiazoles 2009). The most active compounds were **AT4-AT6** from **Table 6**. These three compounds induce the same group 1 phenotype. Compounds **AT15**, **AT2**, and **AT9** (**Table 6**) exhibited a group 2 morphology. The hypothesis is that compounds with a group 2 nuclear morphology would be involved in the later stages of NET formation, where the mechanistic steps remain unknown. This NETosis step must be of important since it lasts from 30 to 120 minutes and results in cell death.

Twelve out of the fifteen aminothiazoles have a dihydroxyphenyl group at the R^1 position. If the R^1 position is substituted with a methoxy phenyl or dimethoxy phenyl (compound **AT11 and AT12, Table 6**) the inhibition is partially lost. This is also observed when substituted with pyridine (compounds **AT13** and **AT14, Table NS1**). From this, we deduce that the dihydroxylphenyl is essential for activity. With a larger set of 3,4-dihydroxyphenyl R^1 substituted compounds available, significant SAR can be derived regarding the R^3 position (compare entries **AT1**-**AT0, Table 6**). No differences in cell toxicity were observed for the ortho-, meta-, para-phenyl-, compounds **AT3**, **AT4**, **AT5**, (**Table 6**) respectively, they all maintain cells viable. However, there is a slight increase towards the small nuclei phenotype observed for compound **AT3**. Here, a more decondensed phenotype is found. When the hydroxyl is substituted to a methoxy or a phenyl (compounds **AT9** and **AT10**), an increase in cell toxicity of more than 40 % is observed compared to compound **AT3**. All these observations are however overshadowed by the fact that these compounds have a catechol moiety. These dihydroxyphenol moieties, 1, 2- or 1,4- oriented, are known to scavenge ROS, which can account for the activity measured. As stated before, ROS are important initiators of NET formation. However, compound **AT15** does not contain the catechol moiety and does retain NET inhibitory activity. This keeps open the possibility that the aminothiazoles do have a unique mode of action.

In order to measure the ROS scavenging properties of aminothiazoles, an oxidative burst assay with *in situ* using luminol/HRP reagent was performed to test for ROS generation. Most of the compounds stop ROS generation, except for compound **AT8** which maintains a ROS generation of 62%. In addition to the ROS generation experiments, an oxygen consumption assay using a Clark electrode was used. The results clearly showed that most aminothiazoles do consume oxygen for the exception of **AT6** and **AT9**, where the levels of oxygen are lowered to 20%. Combining the results from both assays it is clear that the NET formation inhibition activity of this class of compounds is likely due to ROS scavenging rather than targeting a distinct protein target. This discredits the aminothiazoles as an interesting class of compounds to study in regard to NET formation.

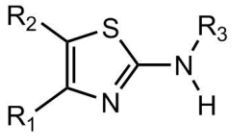

Entry	R1	R2	R3	%Cell Death	%Small Nuclei	%ROS	$\%O_2$	IC_{50}
AT1	3,4-dihydroxyphenyl	H	H	5	66	2	135	28.22
AT2	3,4-dihydroxyphenyl	H	ethyl	24	47	1	107	>100
AT3	3,4-dihydroxyphenyl	H	2-phenol	3	60	0	83	25.10
AT4	3,4-dihydroxyphenyl	H	3-phenol	0	85	0	55	24.65
AT5	3,4-dihydroxyphenyl	H	4-phenol	-1	96	1	91	23.19
AT6	3,4-dihydroxyphenyl	H	2,6-difluorophenyl	1	80	1	20	25.74
AT7	3,4-dihydroxyphenyl	H	4-nitrophenyl	-1	77	1	59	45.10
AT8	3,4-dihydroxyphenyl	H	3-pyridine	0	79	62	90	47.35
AT9	3,4-dihydroxyphenyl	H	2-methoxyphenyl	58	22	1	27	25.12
AT10	3,4-dihydroxyphenyl	H	4-phenoxyphenyl	52	7	1	71	>100
AT11	3-methoxy-4-phenol	H	2,4-difluorophenyl	22	35	1	100	3.12
AT12	3,4-dimethoxyphenyl	H	N,N-dimethyl-4-alanine	29	41	2	120	>100
AT13	3-pyridine	H	4-phenol	31	51	1	103	8.26
AT14	3-pyridine	H	3-pyridine	60	36	10	96	>100
AT15	$-CH_2-CH_2-CH_2-CH_2-$		4-phenol	14	49	10	84	25.00

Table 6. Aminothiazoles inhibit NET formation. Neutrophils were pre-incubated with 100 µM of the compounds for 20 min at 37°C followed by stimulation with 40 nM PMA and further incubation for 240 min to allow NET formation. Cells were stained with SYTOX Green to detect death cells. Nuclear morphology was analyzed upon fixation and permeabilization using automated microscopy. For ROS detection, neutrophils were treated with compounds (100 µM) for 20 min prior to stimulation with 20 nM PMA to induce oxidative burst. ROS were detected *in situ* using luminol/HRP reagent. Oxygen consumption was measured with a Clark electrode after pre-treating the neutrophils with compounds (100 µM) for 20 min. Data shown correspond to percent of generated ROS after 12 min stimulation with PMA (PMA-induced ROS were set to 100%). Data are mean values ± s.d. (N =2, n = 2). AT = Aminothiazole.

8.3 Catechol: an undesired moiety in studying NET formation

Catechol is a moiety that is easily oxidized to highly reactive chemicals within a cellular environment. These reactive species can cause oxidative stress in an uncontrolled manner. Neutrophils rely on ROS generation for several functions such as, activation of pathways, granule maturity, signaling within cells and cell-to-cell communication. Generation of ROS is a highly controlled process. If it takes place in excess it causes tissue and DNA damage, and actives several pathways uncontrollably, such as lipid peroxidation, ROS generation, which results in undesired inflammation (Nathan and Cunningham-Bussel, 2013).

Therefore, there was a decision to investigate the catechol moiety in further detail. As a test-substrate we used pyrotcatechol, which is the smallest example of a catechol. Additionally,

apocynin, a NADPH oxidase inhibitor with a substituted catechol was chosen as a tool to investigate the catechol moiety in neutrophil NET formation (**Figure 23 A-B**). Apocynin is derived from the plant *Apocynum cannabinum* and prevents p47phox from associating to the membrane. Also, apocynin lacks selectivity as it is also known to inhibit MPO and to scavenge hydrogen peroxide (Stefanska and Pawliczak, 2008; t Hart et al., 1990). In the NET assay neutrophils are activated with PMA. PMA in addition to activating PKC, it is involved in the regulation of p47phox (Bey et al., 2004; Fontayne et al., 2002). This protein is a component of NADPH oxidase (Nox) and during screening for NET inhibitors it can be expected to obtain NADPH oxidase inhibitors as hits as well as specific inhibitors of the several Nox proteins, i.e. p47phox, (Kleniewska et al., 2012).

The NET assay and ROS generation experiments were performed using DPI as a positive control. Both compounds, pyrocatechol and apocynin, inhibited NET formation and exhibited a group 1 phenotype. Apocynin, which caused a 80% small nuclei inhibitor was more comparable to DPI than pyrocatechol (**Figure 23 C-D**). Both compounds, pyrocatechol and apocynin, showed no significant toxicity towards neutrophils. It is expected that these compounds have antioxidant properties. In addition, compounds were subjected to ROS production and oxygen consumption assays. Both apocynin and pyrocatechol inhibited ROS productions as effective as DPI (**Figure 23 E**). Both showed excellent levels of oxygen consumption superior to DPI (**Figure 23 F**). This supports the hypothesis that NET formation inhibition activity of molecules with catechol moieties can be directly correlated to their ROS scavenging abilities. Such compounds can be considered undesired moieties in the search of a NET formation inhibitor. Undesired compounds would be avoided in further exploration.

Small molecules with the properties of ROS scavenging or inhibition of ROS production can have serious consequences. A clear example of when it would be advantageous to avoid such undesirable effects is, in patients suffering from chronic granulomatosus disease (CGD). These patients have a genetic mutation in their NADPH oxidase subunits and are unable to effectively produce ROS. Their immune system is compromised because it can neither effectively kill pathogens nor control infections (Winkelstein et al., 2000). The objective of the development of this high-content screen is to learn about NET formation as well as to find an efficient NET formation inhibitor. This requires early exclusion of undesired compounds and a critical view on identifying structural elements that can cause non-specific interaction with cellular processes.

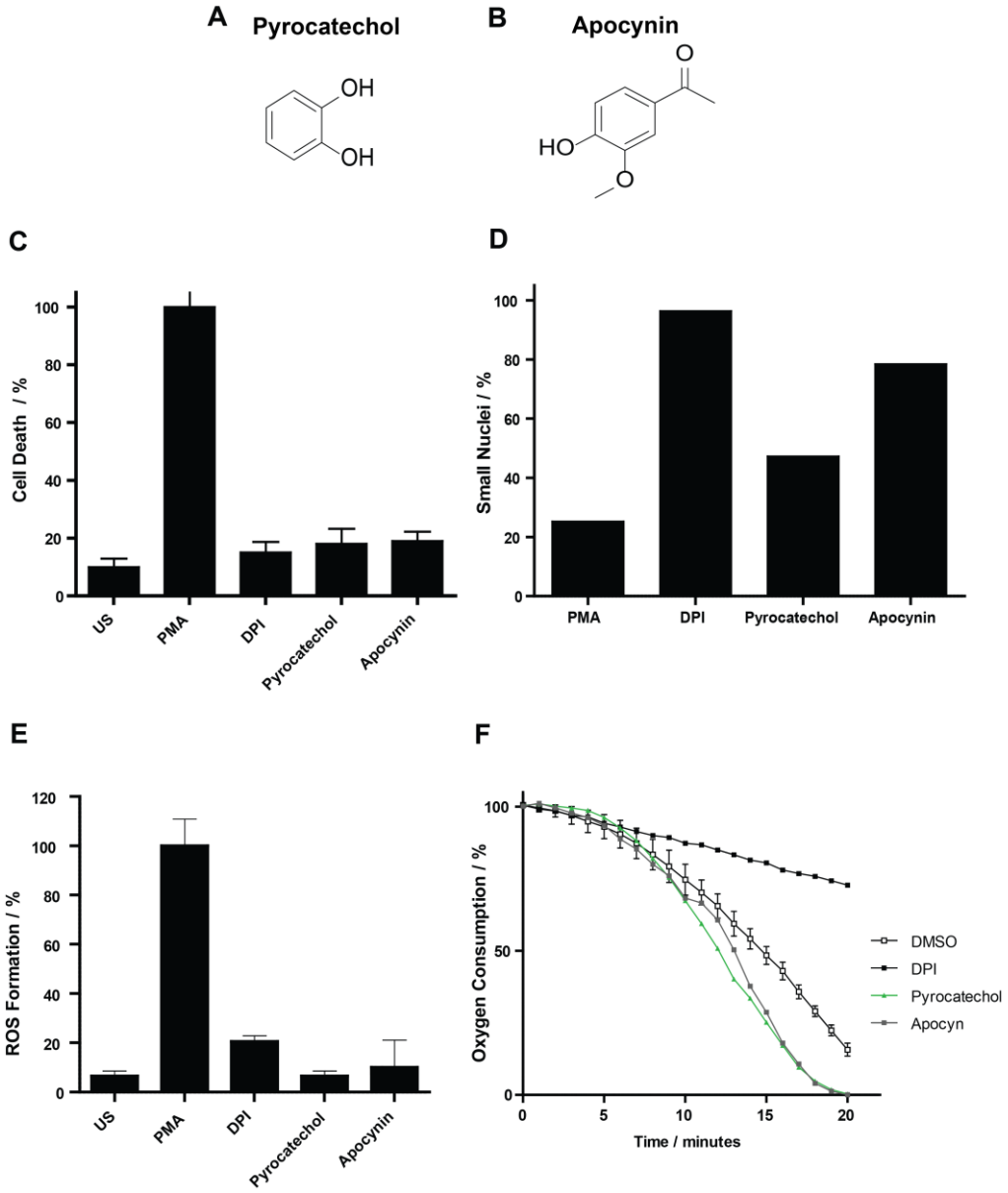

Figure 23. ROS scavengers inhibit NET formation. (A-B) Structure of pyrocatechol and apocynin. (C-D) Pyrocatechol and apocynin inhibit NET formation. Neutrophils were pre-incubated with 100 µM of the compounds for 20 min at 37°C followed by stimulation with 40 nM PMA and further incubation for 240 min to allow NET formation. Cells were stained with SYTOX Green to detect death cells (C). Nuclear morphology was analyzed upon fixation and permeabilization using automated microscopy (D). (E-F) Pyrocatechol and apocynin scavenge ROS. For ROS detection, neutrophils were treated with compounds (30 µM) for 20 min prior to stimulation with 20 nM PMA to induce oxidative burst. ROS were detected *in situ* using luminol/HRP reagent. Data shown corresponds to percentage (related to cells that were treated only with PMA) of generated ROS after 12 min stimulation with PMA (E). Oxygen consumption was measured with a Clark electrode after pre-treating the neutrophils with compounds (30 µM) for 20min (F). Data are mean values ± s.d. (N =2, n = 2).

Chapter 9: Results and Discussion Section 5: Tetrahydroisoquinolines are novel NET formation Inhibitors

9.1 Hypothesis

During the screening of the in-house compound library we identified an additional compound series as novel small-molecule inhibitors of NET formation. These tetrahydroisoquinolines (THIQs) induced, in addition to a group 1 phenotype, a group 2 morphology, which has not previously been investigated further. These compounds can enable the study of NET formation at different stages that is so far not possible with the known NET inhibitors.

9.2 Identification of tetrahydroisoquinolines as NET Inhibitors

Besides aminothiazoles a second compound class, tetrahydroisoquinolines (THIQs), were identified as low micromolar NET formation inhibitors. These compounds induced a group 1 and 2 phenotype (**Figure 24 A-C**). Group 2 phenotype inhibitors, rendering the neutrophils viable and displaying large nuclei, have not been reported in literature. THIQs were found to suppress the PMA-induced NET formation up to 80% at a concentration of 30 µM. They were as effective, to a certain extent, as the well-established NADPH oxidase inhibitor diphenyl iodonium (DPI). Compound **T1** was found to be the most potent compound with an EC_{50} for inhibition of NET formation of 1.9 ± 0.6 µM (**Figure 24 A**). Cells treated with compounds **T1**, **T2**, and **T3** (Table) displayed decondensed nuclei assigned to group 2 indicating that NET formation was arrested at a later stage (**Figure 26**). Compounds **T4**, **T5** and **T6** resulted predominantly in small nuclei, i.e. both lobulated and delobulated. This phenotype indicates inhibition of NET formation at an early stage of NETosis.

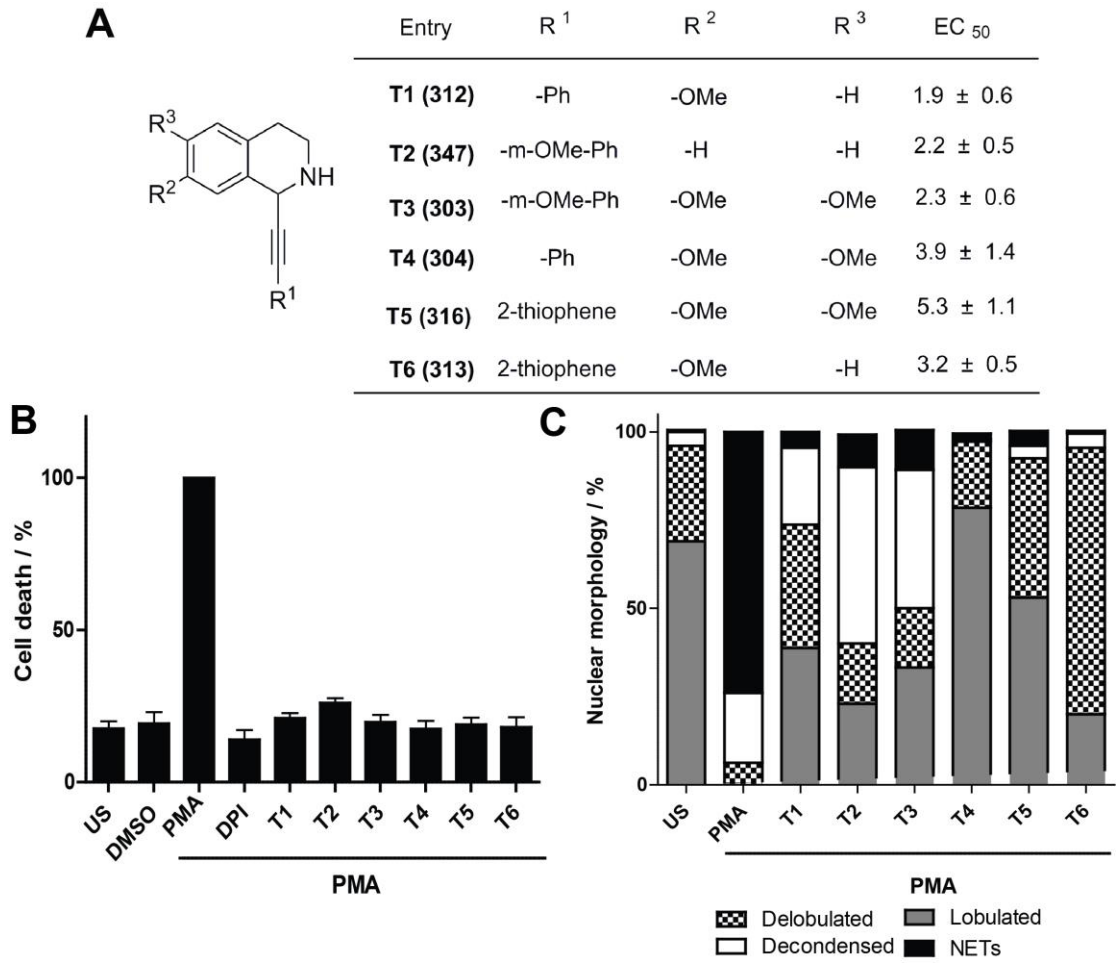

Figure 24. Tetrahydroisoquinolines inhibit NET formation. Structures of tetrahydroisoquinolines that inhibit NET formation and their EC_{50} values for inhibition of NET formation, respectively (A). Neutrophils were pre-incubated with serial dilutions of the compounds for 20 min followed by stimulation with 40 nM PMA and further incubated for 240 min to allow NET formation. Cells were stained with SYTOX Green to detect dead cells and permeabilized for microcopy analysis. EC_{50} were determined using nonlinear regression. (B-C) Neutrophils were pre-incubated with 30 µM of the compounds for 20 min at 37°C followed by stimulation with 40 nM PMA and further incubation for 240 min to allow NET formation. Cells were stained with SYTOX Green to detect death cells (B). Data are mean values ± s.d. (N = 3, n =5). Nuclear morphology was analyzed upon fixation and permeabilization using automated microscopy (C). Data are mean values ± s.d. (N = 3, n = 5). US: unstimulated cells.

A library of 100 THIQ derivatives was synthesized as described previously in collaboration with Tobias Zimmermann (Zimmermann et al., 2013). The library was screened for NET formation inhibition to assess the structure activity relationship (SAR) (**Figure 25**). Major structural changes around the tetrahydroisoquinoline scaffold led to complete loss of activity. Introduction of different substituents around the core scaffold resulted in complete loss of activity (**Figure 25 A**). No substitution was allowed on the nitrogen of the tetrahydroisoquinoline and only methoxy groups were tolerated on the R^2 and R^3 positions. The position that allowed more structural diversity was the R^1 position regarding the substitution pattern on the phenyl ring (**Figure 25 A**). It is noteworthy, that the different functional groups led to different morphology of the nuclei. Small nuclei

phenotypes were induced if a thiophene substituent was present in **T5** and **T6** (**Figure 26**), whereas the m-methoxy-phenyl substituent in **T2** and **T3** (**Figure 26**), led to group 2 phenotypes. The non-substituted phenyl group changed the phenotype dependent on the activators as was the case for compounds **T1** and **T4** (**Figure 26**). Next, we investigated the importance of the stereogenic center. For THIQs **T1**, **T3**, **T4** and **T6**, both *R* and *S* enantiomers were separated by HPLC chromatography on a chiral stationary phase and tested separately. Both isomers displayed similar inhibitory activity showing that stereochemistry was not essential for activity (**Figure 25 B**).

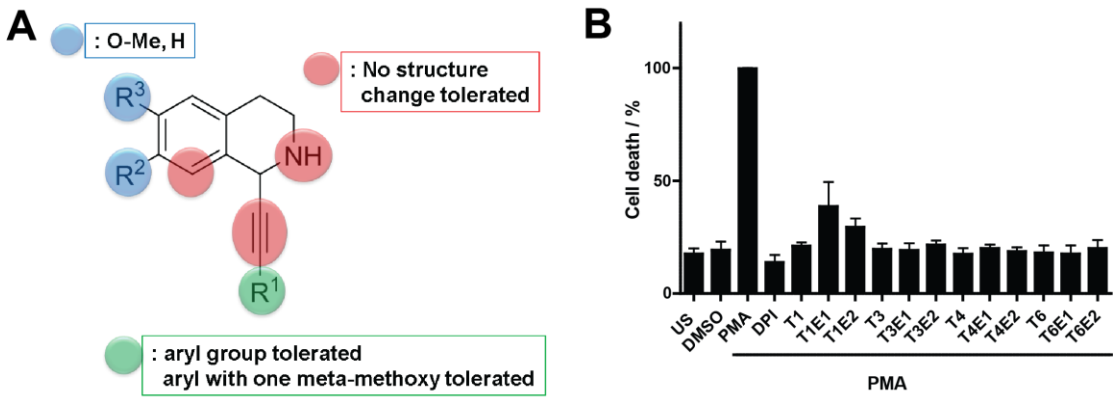

Figure 25. Structure activity relationship of the THIQs for inhibition of NET formation. (A) Structure activity relationship based on NET inhibition and cell death. (B) Separate enantiomers (E1 and E2) of THIQs were assayed at a concentration of 30 µM. Neutrophils were pre-incubated with 30 µM of the compounds for 20 min at 37°C followed by stimulation with 40 nM PMA and further incubation for 240 min to allow NET formation. Cells were stained with SYTOX Green to detect dead cells. Data are mean values ± s.d. (N = 5, n = 3). US: unstimulated cells.

The THIQ compound class is a tool to study NET formation, since one structural change leads to different NET formation inhibition phenotypes. **Figure 26** illustrates how compounds **T1-3** give neutrophils with a large nuclei and **T4-6** give small nuclei when cells were stimulated with PMA. Focusing on these active THIQs, a pattern emerges concerning morphology based on variation applied to the R^1 position. Compounds **T3** and **T2** have a m-methoxyphenyl substituent and display a large nuclei phenotype (illustrated in pink **Figure 26**). Compounds T5 and T6 have a thiazole in the R1 position and both show a small nuclei phenotype (illustrated in blue in the **Figure 26**). Compounds **T1** and **T4** have a non-substituted phenyl group and their phenotype is dependent on the NET formation activator that was used (this will be discussed in more detail below). This possibility of arresting the neutrophil NET formation process at different stages with different THIQs offers a new opportunity for studying this poorly understood type of cell death in a more precise manner.

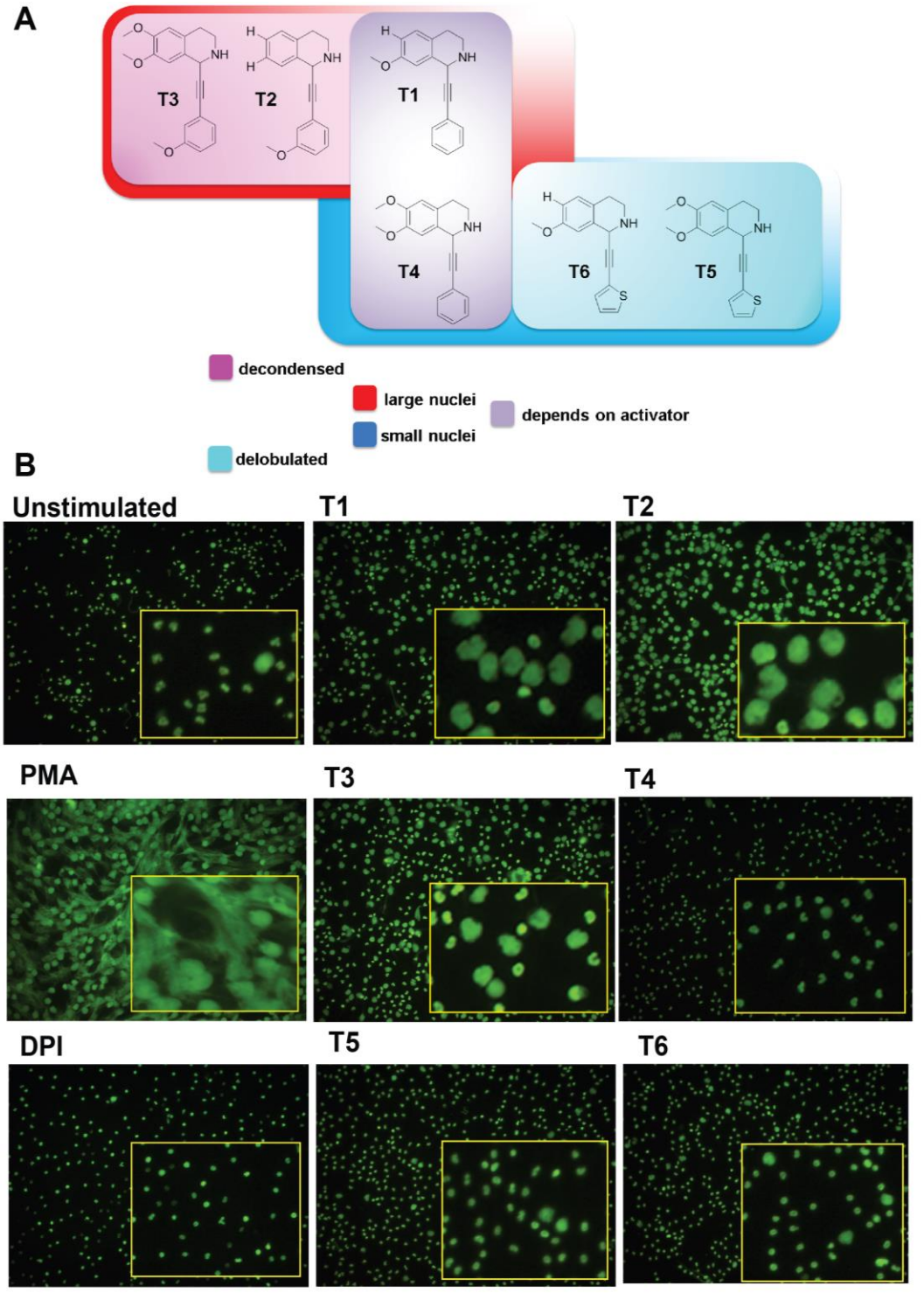

Figure 26. Structure activity relationship of the active THIQs based on their nuclear morphology. Graphic representation of the different phenotypic NET formation inhibitors based on the substitution on R^1 (A). Neutrophils were pre-incubated with 30 µM of the compounds for 20min at 37°C followed by stimulation with 40 nM PMA and further incubation for 240 min to allow NET formation. Cells were stained with SYTOX Green. Nuclear morphology was analyzed upon fixation and permeabilization using automated microscopy (B). US: unstimulated cells

Since PMA is an artificial PKC activator, we investigated the ability of the THIQs to inhibit NET formation using more physiologically relevant PKC activators such as diacylglycerol (DAG) or platelet activation factor (PAF) (Etulain et al., 2015; Hakkim et al., 2011). Upon NET activation with the DAG analog, THIQs successfully suppressed NET formation as detected by a decrease in cell death (**Figure 27**) and by an increase in cells with lobulated nuclei (**Figure 27 B-C**).

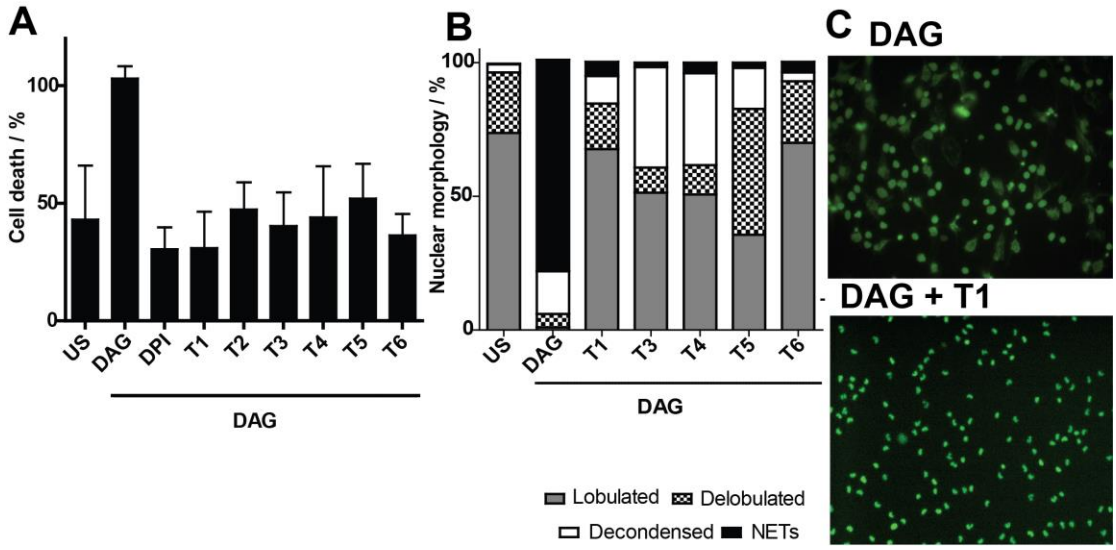

Figure 27. Influence of THIQs on NET formation using DAG as an activator. Neutrophils were pre-treated with the compounds prior to stimulation with 3 µM DAG (A-C). Cells were stained with SYTOX Green to detect dead cells (A) followed by fixation and permeabilization. The detailed nuclear morphology was quantified (B). Representative images of DAG induced NETs with or without treatment with 30 µM **T1**, displaying neutrophil nuclei that were stained with SYTOX Green (C). Data are mean values ± s.d. (N=3, n=3). DAG: Diaglycerol analog: 1–2-dioctanoyl-sn-glycerol, US: unstimulated cells.

Equally, stimulation with PAF halted NET formation by most THIQs as decline in cell death and a decondensed nuclei was observed (**Figure 28**). In both cases, compounds **T3**, **T5**, **T6** maintained their phenotype. These results establish that the THIQs are efficient NET inhibitors when induced by both physiological occurring and non-physiological PKC activators. Compounds retained the same phenotypes with the exception of THIQs **T1** and **T4**.

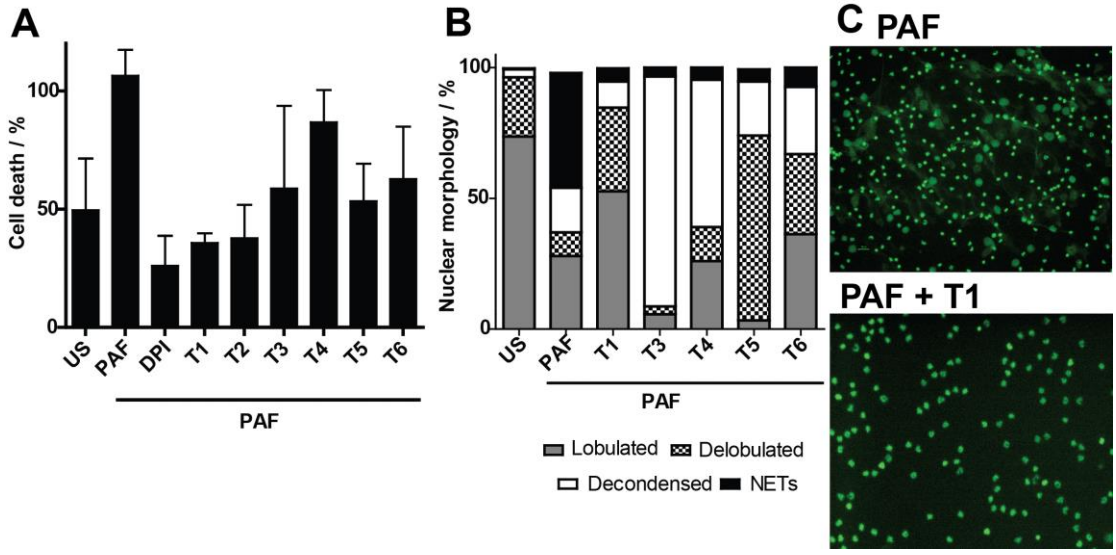

Figure 28. Influence of THIQs on NET formation using PAF as activators. Neutrophils were pre-treated with the compounds prior to stimulation with 3 µM PAF for 240 min (A-C). Cells were stained with SYTOX Green to detect dead cells (A) followed by fixation and permeabilization. The detailed nuclear morphology was quantified (B). Representative images PAF induced NETs with or without treatment with 30 µM **T1**, displaying neutrophil nuclei that were stained with SYTOX Green (C). Data are mean values ± s.d. (N=3, n=3). PAF: Platelet Activating Factor, US: unstimulated cells.

NET formation occurs *in vivo* as a response to pathogenic stimuli, for instance during bacterial infections. *Pseudomonas aeruginosa* was used to investigate inhibition by THIQs in a more complex physiological scenario (Yoo et al., 2014). Upon treatment with the compounds, neutrophils were infected with 100 MOI of *P. aeruginosa* to stimulate NET formation. In the presence of THIQs, cell death was reduced and nuclei displayed a predominant lobulated morphology failing to generate NETs (**Figure 29**).

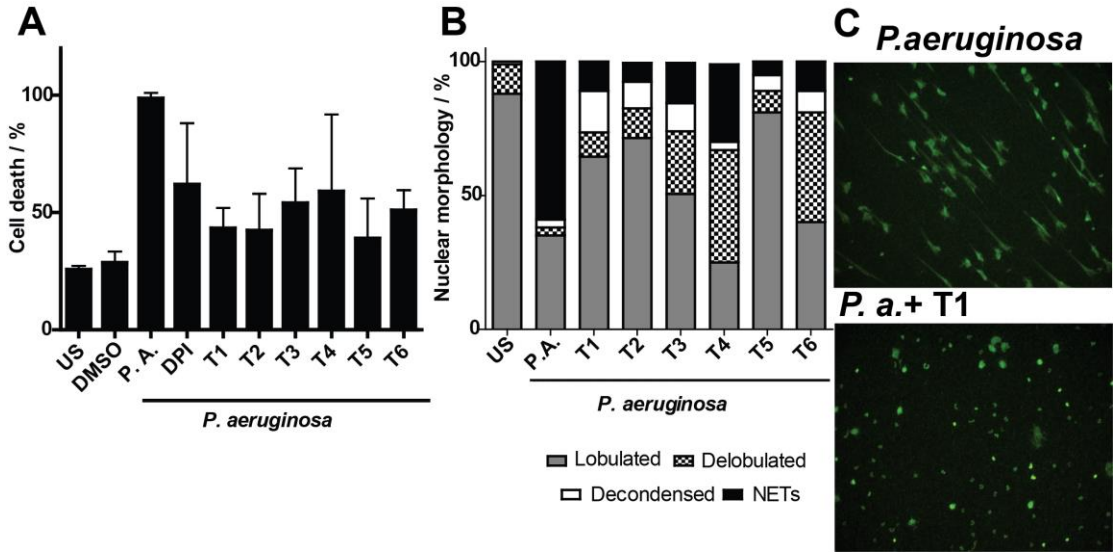

Figure 29. Influence of THIQs on NET formation activated by *P. aeruginosa*. Neutrophils were treated with the compounds prior to stimulation with MOI 100 *P. aeruginosa* (A-C). Cells were stained with SYTOX Green to detect dead cells (A). After fixation and permeabilization, the detailed nuclear morphology was

determined (B). Representative images of *P. aeruginosa* induced NETs with or without treatment with 30 µM **T1**, displaying neutrophil nuclei that were stained with SYTOX Green. In the case of *P. aeruginosa* cells were only fixed (C). Data are mean values ± s.d. (N=3, n=3). *P. a.*: *Pseudomonas aeruginosa*, US: unstimulated cells.

Moreover, the influence of THIQs on NET formation was explored in the presence of glucose oxidase (GO). This enzyme bypasses NADPH oxidase by exogenously generating ROS from glucose, oxygen and water to produce gluconic acid and hydrogen peroxide, thereby inducing NET formation (Fuchs et al., 2007). When GO was added to THIQ-pretreated neutrophils, the extent of cell death induced by GO was reduced by 60% and the nuclear morphology was predominantly decondensed (**Figure 30**). GO-activated NET formation simulates an uncontrolled and escalated NETosis, which is present in several diseases. The fact that the NADPH oxidase inhibitor DPI, does not inhibit the formation of GO-induced NETs (**Figure 30 A**) suggests that the THIQs act downstream of NADPH oxidase. This demonstrates the effectiveness of the THIQs as NET inhibitors. They can inhibit the formation of NETs in the presence of various activators and under physiological conditions.

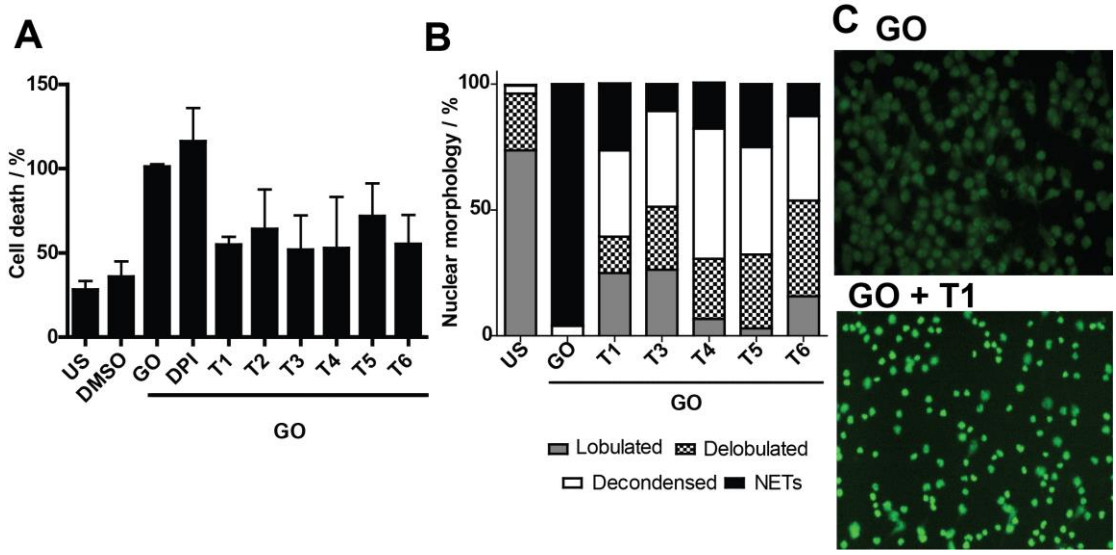

Figure 30. Influence of THIQs on GO activated NET formation. Neutrophils were treated with the compounds prior to stimulation with 100 mU/mL GO (A-C). Cells were stained with SYTOX Green to detect dead cells (A). After fixation and permeabilization, the detailed nuclear morphology was determined (B). Representative images of GO induced NETs with or without treatment with 30 µM **T1**, displaying neutrophil nuclei that were stained with SYTOX Green (C). Data are mean values ± s.d. (N=3, n=3). GO: Glucose Oxidase, US: unstimulated cells.

9.3 Do THIQs interfere with known NET formation mechanisms?

NET formation is a complex process controlled by various essential enzymes, e.g. NADPH oxidase which is responsible for the production of reactive oxygen species (ROS) in the first twenty minutes of the NET formation process (Patel et al., 2010; Urban et al., 2009). ROS are involved in the signaling and the mobilization of granular proteins. Neutrophil granules are very important to NET formation, specifically myeloperoxidase (MPO) (Campos et al., 2007) and nuclear elastase (NE) (Papayannopoulos et al., 2010). MPO, a protein downstream of NADPH oxidase, uses hydrogen peroxide to generate hydrogen hypochlorite (HOCl) to activate NETosis. After the ROS generation during NETosis, NE migrates to the nucleus and degrades histones leading to DNA decondensation. MPO is also known to migrate to the nucleus (Metzler et al., 2011; Papayannopoulos et al., 2010). To investigate where the THIQ compound class interferes with the NET formation machinery, it was crucial to identify the molecular target.

Thus, the influence of THIQs on the oxidative burst was investigated. Interestingly, the compounds did not interfere with ROS formation (**Figure 31**) and the THIQs **T1, T2, T4, and T5** do not scavenge ROS. This suggests that these compounds act downstream of ROS formation. However, compound **T6** weakly inhibited the PMA-induced generation of ROS, while compound **T3** was found to significantly inhibit ROS formation (**Figure 31 A**). All inhibitors of NET formation reported to date inhibit ROS generation upon stimulation with PMA (Fuchs et al., 2007; Metzler et al., 2011; Nishinaka et al., 2011; Palmer et al., 2012; Patel et al., 2010) or using other PKC activator (Hakkim et al., 2011). However, except for compound **T3**, THIQs do not inhibit ROS production within 30 min of NET activation. The THIQ-based NET formation inhibitors allow ROS generation upon initiation of NET formation and therefore, inhibit the process downstream of ROS production. It is crucial to maintain physiological ROS levels and, thus, maintain functional neutrophils when targeting NETs to ensure a sustained immune response in humans.

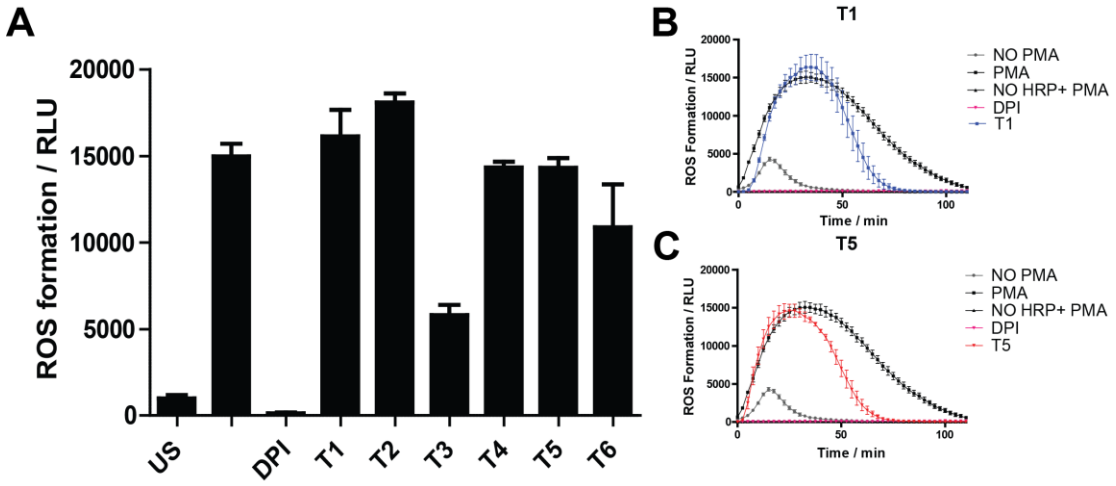

Figure 31. THIQs do not inhibit reactive oxygen species generation. (A-C) Neutrophils were treated with 15 µM of the compounds for 20 min prior to stimulation with 20 nM PMA to induce an oxidative burst. ROS were detected *in situ* using the luminol/HRP reagent every minute for 120 minutes. Data shown correspond to percentage of generated ROS after 30 min stimulation with PMA (A). (B and C) Effect of individual THIQ compounds, T1 (B) and T5 (C) over time on ROS generation. Data are shown as mean values ± s.d. (N=3, n=3). US: unstimulated cells. RLU: relative light units.

Next, we investigated whether THIQs inhibit the enzymes MPO and NE. No inhibition of MPO activity by any of the THIQs could be detected at 15 µM (**Figure 32 A-C**). Additionally, most THIQs did not influence the enzymatic activity of NE (**Figure 32 A and D-E**). Only THIQ **T2** and **T6** reduced the initial activity of NE to 57% and 35% respectively indicating partial inhibition of NE. Until now few proteins have been identified as involved in NETosis, such as the granular proteins myeloperoxidase and neutrophil elastase. Interestingly, most THIQs do not inhibit these granular proteases, suggesting a different mode of action.

A

Inhibitor	MPO inhibition / % (15 µM)	NE inhibition / % (15 µM)
T1	5 ± 0.01	7 ± 0.04
T2	0 ± 0.28	57* ± 0.22
T3	7 ± 0.06	6 ± 0.02
T4	0 ± 0.01	11 ± 0.04
T5	12 ± 0.01	4 ± 0.02
T6	18 ± 0.03	35* ± 0.22

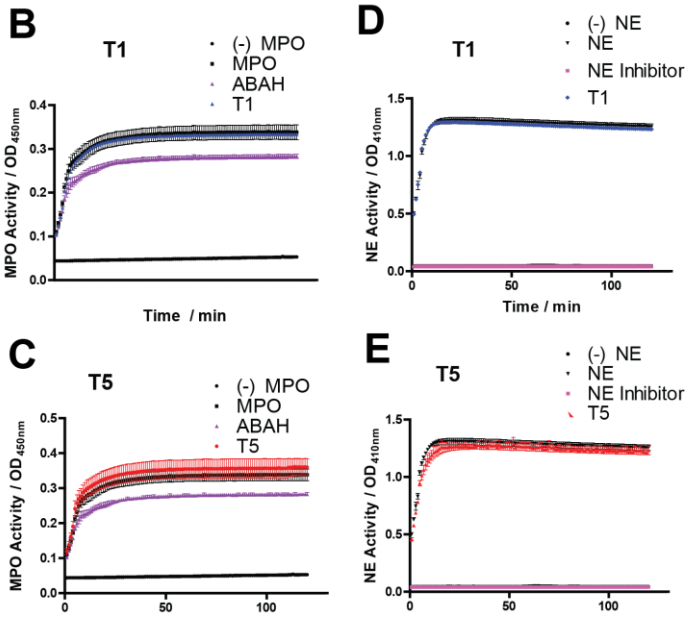

Figure 32. Influence of THIQs on myeloperoxidase (MPO) and neutrophil elastase (NE) activity. (A-C) Influence of THIQs on myeloperoxidase (MPO). (A, D, E) neutrophil elastase (NE) activity. Enzymes were pre-incubated with 15 µM of the compounds for 10 min followed by detection of enzymatic activity with a chromogenic substrate for 2 hours. (B-C) Effect of individual THIQ compounds overtime on MPO activity: T1 (B) and T5 (C). (D-E) Effect of individual THIQ compounds overtime on NE activity: T1 (D) and T5 (E). Data are shown as mean values ± s.d. (N=3, n=3) *: partial inhibition.

To test the cytotoxicity of the compounds, we monitored the release of lactate dehydrogenase (LDH) into the cell culture medium. No cytotoxicity was observed upon incubation of neutrophils with the compounds for 6 h, even at concentrations as high as 200 µM (**Figure 33 A**).

Previously, the involvement of the Raf-MEK-ERK pathway in the process of NET formation was identified (Hakkim et al., 2011). To establish if the THIQs compounds affect MAPK signaling pathway, the phosphorylation of ERK was tested in the presence of the inhibitors. The initial immunoblotting for p-ERK1/2 showed no inhibition of ERK phosphorylation by the compounds (**Figure 33 B**). This result confirmed our hypothesis that the THIQs compounds are not involved in the early stages before NADPH oxidase.

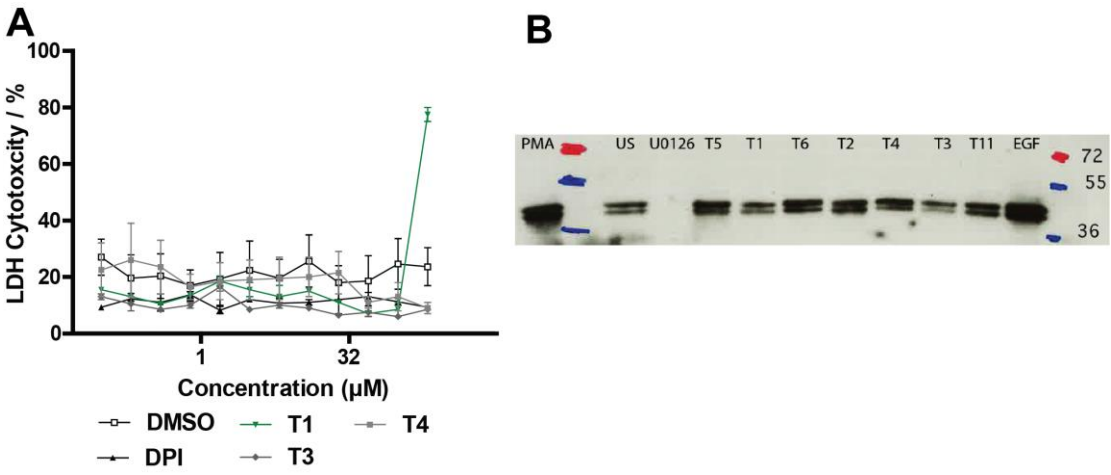

Figure 33. THIQs are not toxic and do not inhibit ERK phosphoralation. (A) Influence of THIQs on the release of LDH . Extracellular LDH activity was determined upon treatment with the compounds or DMSO and DPI as controls for 6 h followed by detection of LDH enzymatic activity using a chromogenic substrate. Data are shown as mean values ± s.d. (N=3, n=3). (B) Detection of ERK phosphorylation via immunoblotting in NET formation. Neutrophils were activated with 40 nM PMA with or without the inhibitors for 90 min prior to cell lysis and immunoblotting for phosphorylated ERK 1 and 2 using anti-p-ERK-1 and 2 antibodies and peroxidase-conjugated goat anti-mouse, or goat anti-rabbit 2nd antibody. (n = 2)

This concluded the series of experiments that link the THIQs to one of the known pathways involved in NET formation. Interestingly, THIQs do not significantly interfere with any of these signaling pathways or proteins. T2 and T6 inhibit NE activity slightly, although when these compounds are compared in detail to the well-established NE inhibitors used as control they are not as effective. The next step was to perform a series of target identification experiments that include proteomic experiments and compound labelling and which will be discussed in further detail in the following chapters.

9.4 THIQs and NET Related Disease

Besides elucidation of the mechanism of NET formation for scientific research purposes, NET formation inhibitors can be used to investigate the involvement of NETs in diseases. As mentioned before, NETs have been related to autoimmune diseases such as systemic lupus erythematosus (SLE) (Garcia-Romo et al., 2011; Hakkim et al., 2010; Lood et al., 2016), rheumatoid arthritis (Dwivedi et al., 2012; Khandpur et al., 2013), chronic granuloma disease (CGD) (Bianchi, Blood 2009 114), and in the pathogenesis of sepsis (Clark et al., 2007). Recently, cancer (Park et al., 2016), preeclampsia (Hahn et al., 2012), thrombosis (Fuchs et al., 2010) and diseases that involve necrotic inflammation (e.g., vasculitis (Kessenbrock et al., 2009) and colitis (Bennike et al., 2015)) where added to the list. A hallmark of many of these disorders is the overproduction and lack of degradation of NETs.

Systemic lupus erythematosus (SLE) is a multifaceted autoimmune disorder. The etiology of SLE is the overproduction of anti-neutrophil cytoplasmic antibodies (ANCA). The main antibody markers are anti-double-stranded (ds) DNA and anti-histones found in patient sera. Recently, another characteristic for SLE was established and that is the over-production of NETs which occurs without stimulus and which is referred to as spontaneous NETs (**Figure 34**). In SLE this is combined with the inability to disintegrate the NET components properly (Podolska et al., 2015; Yu and Su, 2013). This hallmarks SLE as the ultimate NET disease and ideal candidate for NET formation inhibitors as possible treatment. Therefore, SLE patient-derived neutrophils were employed to evaluate the ability of THIQs to inhibit NET formation. These cells where obtained from SLE patients being treated in the Charité under the care of Dr. med. Tobias Alexander.

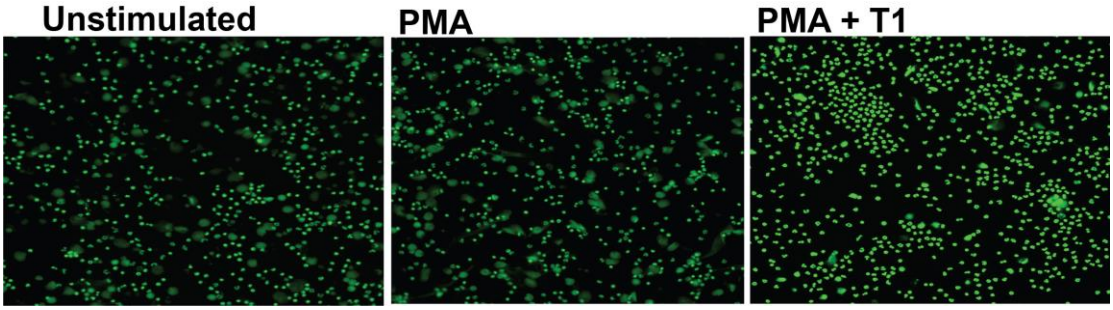

Figure 34. Representative images for spontaneous NET formation in SLE patient cells and the inhibition effect of THIQ T1. Neutrophils were purified from blood of SLE patients. Neutrophils were pre-incubated with 30 µM of the compound T1 for 20 min prior to activation with 40 nM PMA for 240 min to allow NET formation. Cells were stained with SYTOX Green to detect dead cells prior to fixation and permeabilization and image acquisition. PMA-induced NET formation in SLE patient cells as well as inhibition of NET formation by T1 upon PMA-induced NET formation SLE patient cells.

Interestingly, in SLE patient cells the compounds were effective in inhibiting formation of spontaneous NETs by more than 45 % and NETs activated by PMA by more than 68% (**Figure 35**). This change becomes stagering when the THIQ NET inhibition is compared between healthy and SLE patients neutrophils. Specifically, the THIQs reduced neutrophil cell death (**Figure 35 A and C**), together with an increase in cells with lobulated or delobulated nuclei (**Figure 35 B and D**). These results clearly indicate that THIQs are able to inhibit NET formation in neutrophils from patients, most likely at an early stage of the process. Remarkably, THIQs inhibited formation of spontaneous NETs which occur naturally in a patient experiencing a flare. Also, the THIQs inhibit the PMA-NETs, which can be speculated to represent NETosis that occurs in a SLE patient suffering an infection. NET formation inhibitors can offer a novel opportunity for the treatment of SLE without impairing normal functions of neutrophils (i.e. ROS production or granular protein functions).

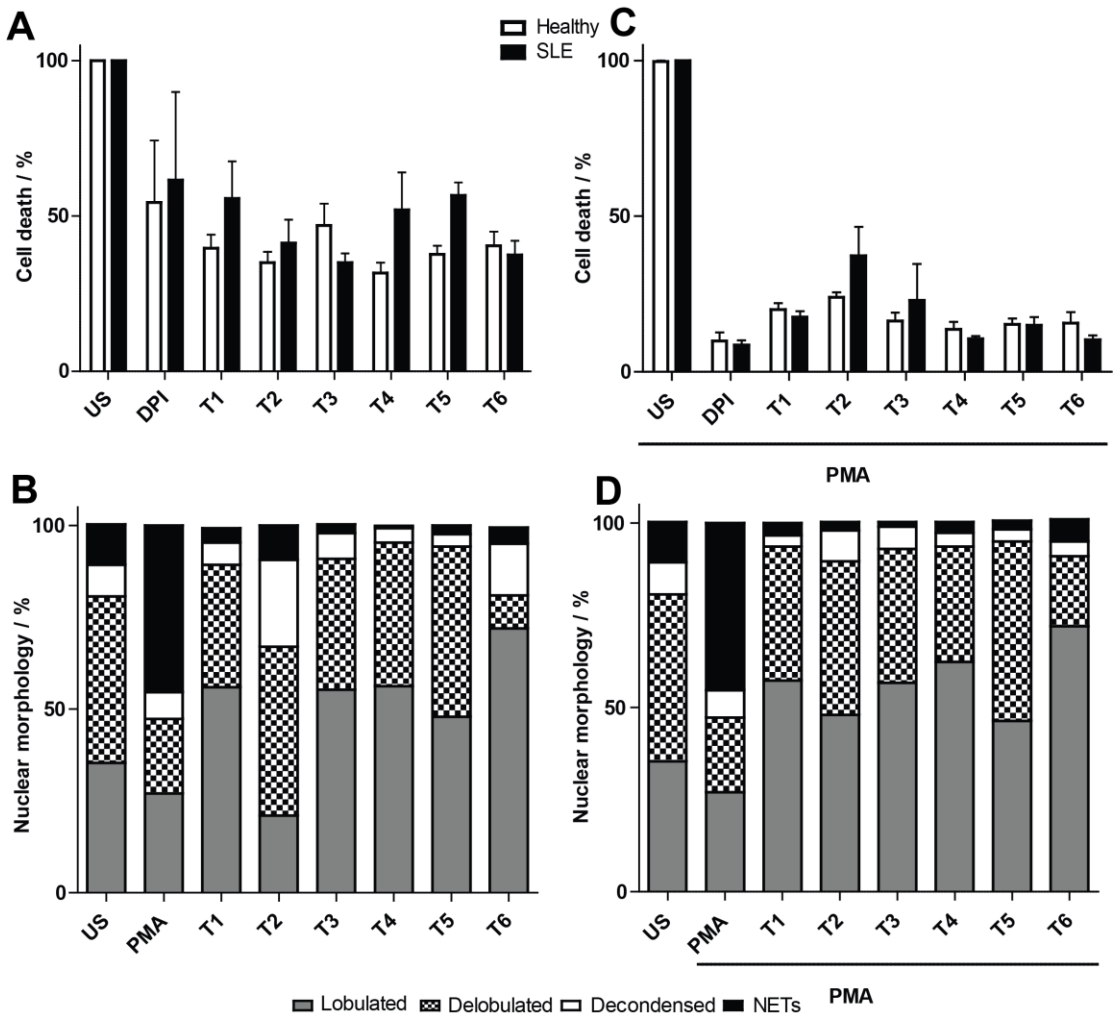

Figure 35. THIQs inhibit NET formation in cells derived from SLE patients. Neutrophils were purified from blood of healthy individuals or SLE patients. The influence of the compounds on spontaneous NET formation was assessed upon incubation with 30 µM of THIQs for 240 min (A). Alternatively, neutrophils were pre-incubated with 30 µM of the compounds for 20 min prior to activation with 40 nM PMA for 240 min to allow NET formation (C). Cells were stained with SYTOX Green to detect dead cells prior to fixation and permeabilization and image acquisition (A and C). Quantification of the nuclear morphology induced by the compounds in SLE patient neutrophils (B and D). Data are mean values ± s.d. (N=3, n=3).

Chapter 10: Results and Discussion Section 6: Target Identification for the Tetrahydroisoquinoline Compound

10.1 Hypothesis

In the previous chapters, the discovery of a new compound class of NET formation inhibitors was described. Tetrahydroisoquinolines (THIQs) were shown to stop NETosis at different stages of the process depending on the chemical structure. The molecular target could not be identified among the known proteins that are involved in NETosis. The next step is to resort to known chemical biological techniques in order to identify the target. We decided to use affinity-based proteomics, i.e. pulldown experiment, as technique to identify the biological target. For this purpose, it is necessary to functionalize THIQs. Besides this proteomics approach, additional techniques were also used in an attempt to identify the THIQ target protein including *in silico* prediction approaches.

10.2 The art of target identification

The field of chemical biology generates large data sets and expanded the “Omics Era” (”Omics” meaning ‘the large study of’) (Di Girolamo et al., 2013). The Omics era started with genomics and the human genome project, which was a large collaboration to sequence the entire human genome (Franzosa et al., 2015). More recently, proteomics and metabolomics were introduced. Metabolomics is the study of metabolites from chemical processes and it is applied in toxicology and environmental sciences. The basic definition of proteomics would be the study of structure and proteins on a large scale, in reality it entails much more (Weinstein, 2001).

Proteomics is an essential tool for chemical biologists aiming to identify the molecular target for a compound of interest. Target identification is a complex science and there is no one correct way to identify a previously unknown small molecule protein target. Often small changes in experimental procedures can make the difference between success and failure. Many parameters have to be taken into consideration in setting up the successful experiment. In the past decade, chemical biologists have developed and improved upon many techniques to troubleshoot issues that arise in the identification of the target for bioactive molecules. Several approaches can be taken, however, the affinity-based proteomics experiment a.k.a. “the pulldown” has rapidly become the go-to-technique for identifying an unknown molecular target (Schenone et al., 2013; Ziegler et al., 2013).

The pulldown is an experiment where the protein of interest is trapped on a solid support and isolated from a complex protein mixture (e.g. cell extract) followed by mass spectroscopy identification (**Figure 36**). The main steps in performing a pulldown are first the chemical preparation of a synthetic tool compound that is equipped with a functional group to allow for attachment to a solid support. Second, the isolation of the desired protein with functionalized active

compound and, finally, the proteomic analysis of the isolated proteins. To correctly identify the target protein several background experiments have to be performed to avoid the identification of false positives or failure to bind the target protein. The established structure activity relationship (SAR) around the chemical compound that is used as tool compound must be studied. This allows for attachment of a linker to the molecule without negatively affecting binding to the target protein. The chemically modified compound, or probe, consists of three main components: the biologically active molecule, a linker, and a functional group. The functional group allows the probe to attach to the solid support, usually polymer beads, which will further permit extensive washings in order to wash away the unbound proteins. The functional group is chosen based on the nature of the investigation. The most common affinity tag is biotin which binds with high affinity to avidin, streptavidin or neutravidin. There are a wide variety of linkers, the most commonly used is an ethyleneglycol of a length of at least three units. The length of the linker needs to be chosen carefully and depends on the size of the molecule of interest. There should be no steric hindrance of the compound-target protein interaction by the solid support (Schenone et al., 2013; Thompson et al., 2012; Ziegler et al., 2013).

Regarding the biochemistry of the pulldown several aspects must be optimized. For example, the biological nature of the sample, i.e. cell lysates; use of stringent washings; control experiments; and possible incorporation of isobaric labels all enable the quantification to be considered and optimized.

For choosing the correct proteomic analysis, understanding the design of the experiment is crucial. Assuming that there is access to an appropriate instrument such as a LC-MS/MS or a GC-MS/MS, instrumental measuring time is the rate determining step. Ideally, qualitative and quantitative data achieved in the shortest time possible is desirable. Over the years analytical protocols have become more sensitive and improved instruments have greatly improved the quality of these experiments. Laboratory techniques and reagents such as isotopic labeling have been developed allowing for the data to be analyzed both qualitatively and quantitatively (Di Girolamo et al., 2013; Rabinowitz et al., 2011; Reaves and Rabinowitz, 2011). Stable isotopes, such as arginine and lysine, can be incorporated in which biomolecules in cells before cell lysis (**Figure 36**). They do not interfere with the physico-chemical properties of the proteins. Isotopes are incorporated into cellular proteins metabolically using labeled essential amino acids in a method called stable isotope labeling by amino acids in cell culture (SILAC). Usually two different types of cell lysates are generated, one with regular growth media called “light” and the other media containing isotope-containing amino acids called “heavy amino acids.” The cells are cultured for usually two or three passing rounds to secure that the amino acids have been incorporated to all the cells. These cells are eventually lysed and the obtained lysates are used in pulldown experiments (Ong et al., 2002). For those cell lines for which cell culture is not possible, *in vitro* labeling such as isotope-coded

affinity tags (ICAT) or isobaric tags for relative and absolute quantification (ITRAQ) is possible (**Figure 36**). For ICAT, the amino acid labeling occurs on the proteins before the trypsin digestion, i.e. during the pulldown in the lysate. In ICAT the label is a deuterium and carbon thirteen (^{13}C) (Gygi et al., 1999). In the case of iTRAQ, the labeling occurs after the trypsin digestion i.e. during the isolation of the peptides. In ITRAQ the labeling occurs on the N-terminus and side chains of peptides with several tags of different masses (Zieske, 2006). For some experiments described in this chapter, the ITRAQ technique was used since neutrophils cannot be maintained in culture longer than twelve hours and there was previous experience with the ITRAQ technique.

10.2.1 Nonspecific Binding

In pulldown experiments, the cell lysate is exposed to the ligand immobilized to solid support. This creates high local concentration of immobilized ligand and will enable binding to high affinity targets but also low affinity proteins present in high concentrations in the cell lysate. Identification of this high-affinity target protein becomes overwhelmed by low-affinity proteins binding non-specifically. This issue becomes a problem when the protein of interest is a low-expressing protein (Ziegler et al., 2013).

Most of the target identification pulldown experiments reported in literature made use of high affinity probes with abundant target proteins. In such a case low affinity proteins are removed during the washing steps or marginalized during analysis by the presence of the high-affinity target protein. The proper use of statistics becomes essential when dealing with both non-specific protein binding and the true target attached to the probe. Several techniques have been developed to discriminate the “false positives” from the true target proteins. For instance, “black lists” have been established where frequent binders are listed that bind to probe. The specifics of the proteome of the used cells can be considered to exclude vastly abundant proteins that can give rise to false positives. Nonetheless, it should always be re-examined if the abundant protein is indeed the target, for example, tubulexin A’s target was tubulin which is an abundant protein (Voigt et al., 2013).

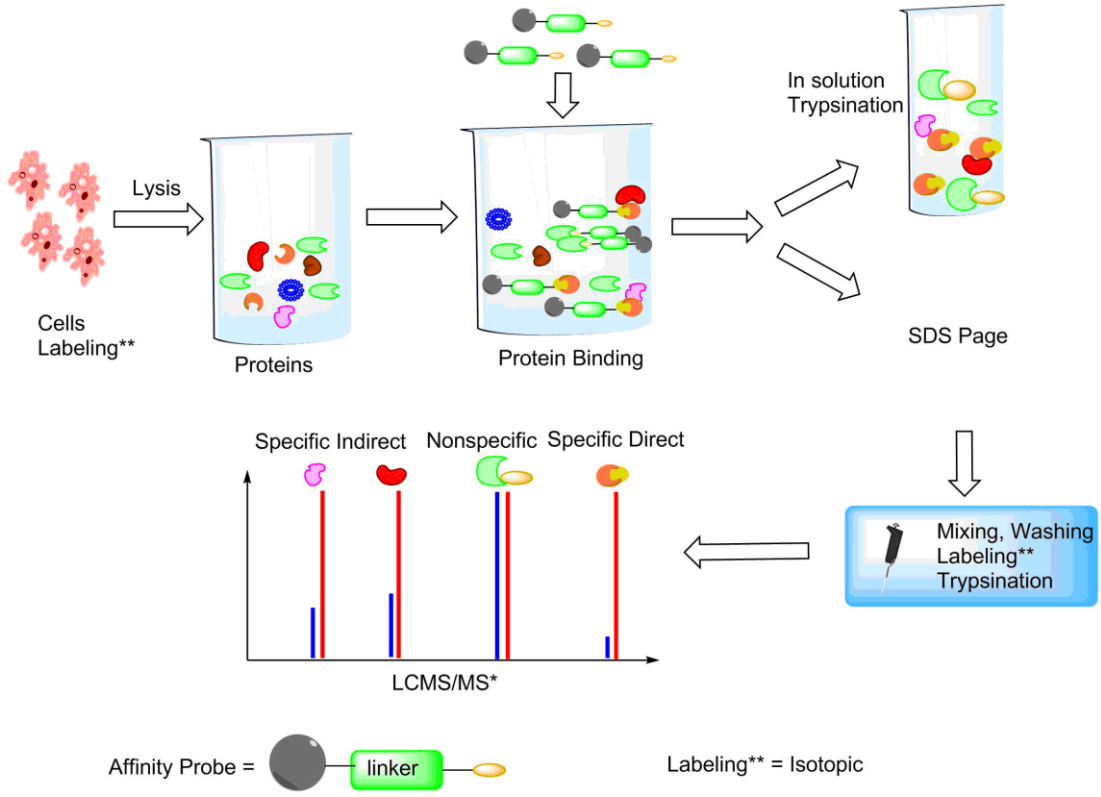

Figure 36. Overview of an affinity-based proteomics. A solid-supported immobilized compound that has affinity for the target protein of interest is synthesized (pulldown probe). During the experiment, a cell lysate is exposed to the pulldown probe allowing for protein binding. The formed complex is washed to remove non-(specific) binding proteins. The protein(s) that did bind to the probe is removed and the elution is subjected to digestion and identification using mass spectroscopy (MS/MS). Isotopic labeling can be incorporated into the cells or on the protein/peptides. The ratios between the isotopic labeled and non-labeled peptides are used to determine the interaction (direct or indirect). Image modified from Schenone, et.al. (Schenone et al., 2013).

10.3 Affinity-based proteomics for NET formation

The known biological pathways for NET formation were examined in the context of the THIQs but none were connected to this compound series. To identify the target(s) of the tetrahydroisoquinoline, pulldown experiments were performed. For this purpose it was necessary to prepare a set of pulldown probes based on the THIQ structure and established SAR as described in chapter 10. The structures of the prepared probes are described in **Figure 36**.

10.3.1 THIQs pulldown probes

From the SAR established around the THIQ scaffold, it can be derived that the R^1 position substitution has little impact on compound activity. This makes this part of the molecule ideal for linker attachment. A triethylene glycol moiety was chosen as a linker unit. The most common affinity tag used for pulldown experiments is biotin which binds with high affinity to avidin. The active probe **P1** (**Figure 37**) is based on compound **T3**, **T4** and **T5**, featuring the most active compounds with a

methoxy group on the R^2 and R^3 position (**Figure 24**). For the design of the inactive control, it is common to use an enantiomer specifically if one is active and the other is inactive. The SAR studies indicated that there was no difference in activity between *R* and *S* enantiomers. However, substitution of the basic nitrogen on the THIQ core resulted in complete loss of activity. Therefore, an intermediate in probe synthesis, a Boc protected version of **T3**, was used as a negative control **P2** (**Figure 37**). Both biotinylated probes were synthesized by Tobias Zimmermann (**Figure 37 A-B**).

The first pulldown results showed no protein to bind specifically to the active probe. Indeed, there were proteins binding to the active probe. However, these proteins also showed affinity for the inactive probe. Therefore, it was hypothesized that the Boc group might fall off during the pulldown experiment. After a series of unsuccessful pulldown experiments with the biotinylated probes (**Figure 37 A-B**), the probe design was reconsidered. It was decided to change the biotin affinity tag for a pulldown construct containing a free amine functional group (**P3**, **Figure 37 C**). This amine probe can bind covalently to N-hydroxysuccinamide (NHS)-coated polymer beads. The new probe is based on the more active THIQ **T1**. This compound has only one methoxy at the R^2 position. For the inactive probe (**P4**), a compound with a methyl group on the nitrogen was prepared. A methyl group is chemically more stable than a Boc group. The synthesis of these compounds is described in the experimental section. In addition to synthesizing the probes required for pulldown experiments, a fluorescently labelled compound (**P5**) was prepared to allow localization and target validation studies. Bodipy was selected as a fluorophore since it has been shown to be less prone to photo-bleaching compared to other known fluorophores (**Figure 37 E-F**).

In addition to the traditional compound-linker-solid support probes, a collaboration with Max Planck-RIKEN Joint center for Systems Chemical Biology provided access to a photo-linked beads. The beads are functionalized with oligo-ethylene glycol linkers with aryldiazirine groups that upon UV irradiation form highly reactive carbenes that react with the added compound in a non-specific manner. This alternative method attaches the small molecule to the solid support via photo-activation. In doing so, the compound is bound to the resin in various conformations of which at least one should still be able to bind the target protein in a high affinity. The principle of this method is illustrated in **Figure 37 E** (Kanoh et al., 2003). This technology has been successfully applied to the target identification for natural products with complicated structures that require long and difficult total synthesis for their preparation or for which no synthesis route is available. The method was developed by the Osada group and colleagues in the RIKEN Global Research Cluster in Wako, Japan. THIQs **T1** and **T3** immobilized on beads by means of this technique by Zimmermann in RIKEN Japan (**Figure 37 D**).

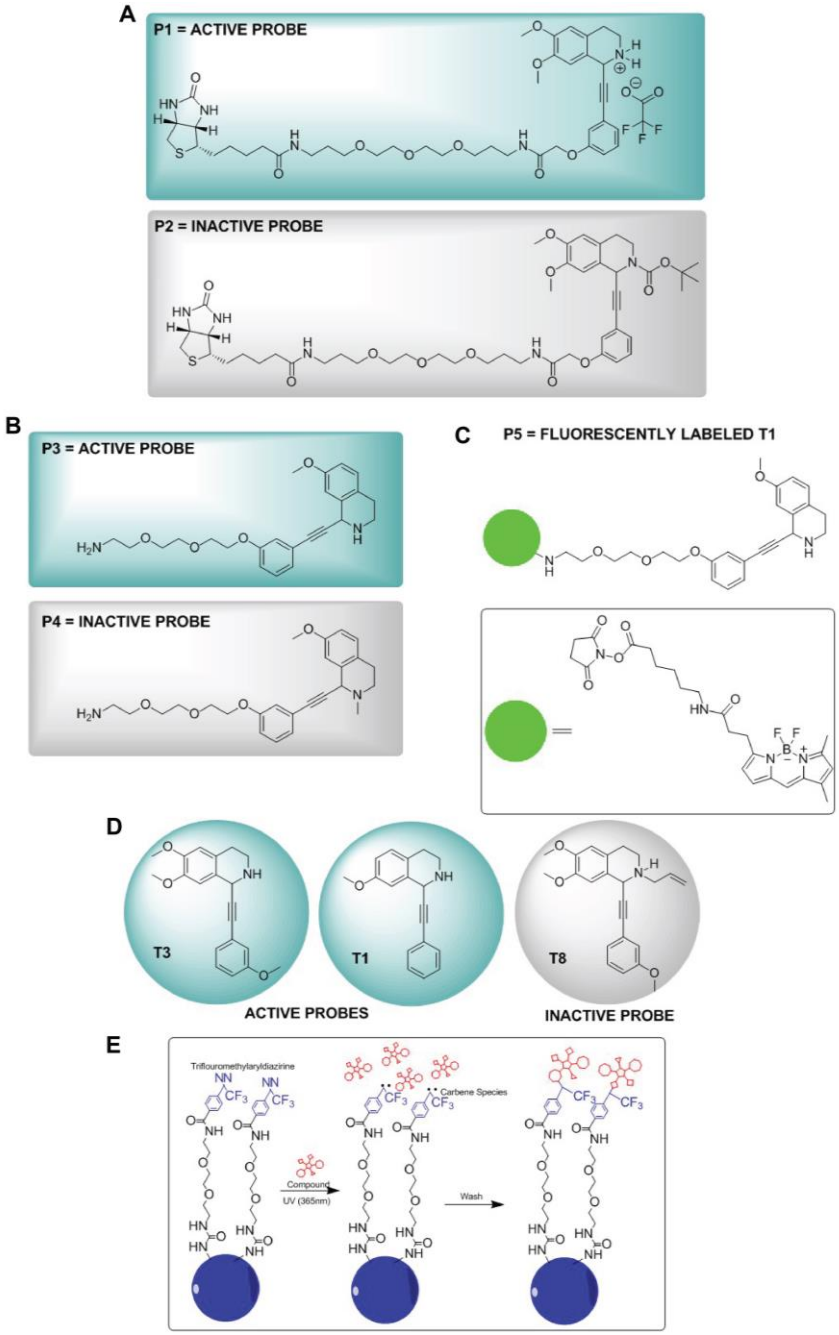

Figure 37. Overview of the THIQs probes. (A) Structures of P1 and P2 biotinylated probes. (B) Structures of P3 and P4 probes for covalent coupling via free amine groups. (C) Structure of P5 the fluorescently labelled THIQ **T1** and bodipy fluorophore structure. (D) THIQs **T1**, **T3, and T8** used for photocrosslinkingg-mediated immobilization to functionalized beads. (E) Scheme to obtained photolinked polymer beads.

10.3.2 Optimization of the affinity-based proteomics

As mentioned above many characteristics of an affinity-based proteomic experiment need optimization.

Features of a pulldown experiment that need to be considered are the nature of the cells, the stringent washings, control experiments and possible incorporation of isobaric labels to aid the analysis. First, the generation of a stable neutrophil lysate is necessary to perform the pulldown. Neutrophils are charged with granules filled with proteases. Once the cells are lysed all the granules are lysed and all proteases are released causing protein degradation. Therefore, **Figure 38 A** shows protein degradation upon cell lysis in the cytoplasmic layer, (low spin supernantant (LSS)) as quickly as within 60 minutes after lysis kept on ice. It was observed that the granular component (high spin supernatant (HSS)) and nuclear component (high spin pellet (HSP)) were affected by degradation by the proteases. After 24 hours on ice, the degradation is more pronounced and it was obvious that the added protease inhibitors were not capable of preventing protein degradation. Eventually, it was found that the serine protease inhibitors phenylmethylsulfonyl fluoride (PMSF) and diisopropylfluorophosphate (DFP) were capable of preventing the significant protein degradation in addition to the known protease inhibitors. However, DFP is extremely toxic and should be used with extreme caution and with an adrenaline shot and medical support in close proximity. No protein degradation was observed upon 24, 48 and 72 hours and even after long storage of up to 5 days on ice (**Figure 38 B**). The stable PMN cell lysate was obtained.

After observation of the initial pulldowns' lack of specificity for the active probe, it was thought that isotopic labeling enabled quantitative proteomics would increase the chances of the identification of the target protein. Alternatively, it was opted for isobaric tagging for relative and absolute quantification (iTRAQ) labeling. This was further optimized by Monica Schmidt at the proteomic facility of the Max Planck Institute for Infection Biology (MPIIB). During iTRAQ, the amine groups of the peptide are labeled with tags that have an added mass of 114-117 Da and appear as one peak in the MS (Ross et al., 2004).

10.4 Affinity-based proteomics results

Mass spectroscopy analysis performed by Dr. Petra Janning from the MPI of Molecular Physiology and Monica Schmidt of the MPI of Infection Biology

Pulldown experiments were performed using lysates of PMA-activated and non-activated neutrophils. As controls, the beads alone or immobilized inactive probe were used. These experiments were processed simultaneously under the same conditions. The beads-only control is expected to enrich proteins that bind to the polymer matrix. Enriched proteins were subjected to

tryptic digest followed by protein identification by means of mass spectrometry. The first round of three experiments were performed with the biotinylated probes. In the second round two independent experiments were performed with the free amine probes. In addition, four experiments were performed with the photo-linked beads. A total of nine pulldown experiments were evaluated. Proteins that were found are summarized in the table in **Figure 38 D.** Unfortunately, no proteins were selectively enriched with the active probe in comparison to the controls. From the proteins list, neutrophil elastase and RAS-related C3 (RAC2) were of interest. Neutrophil elastase was disregarded an elastase activity assay was performed and compound **T1** and **T3** failed to inhibit elastase (data shown in **Figure 32 A and D**). RAC2 was examined by a pulldown experiment followed by immunoblotting and failed to show specificity since the protein was enriched with both, active and inactive probe (**Figure 38 E**).

Consequently, it was hypothesized that the target might not be a cytoplasmic protein. At the time, during the pulldown experiments, the lysates were not prepared to incorporate membrane proteins in the lysates. Another explanation for the unsuccessful target identification using affinity based chromatography. Is that probes were tested in NET assay and activity was lost upon functionalization (**Figure 38 C**). That the pulldown probe fails to pass the cell membrane and maintain the activity is not a requirement to precede with the pulldown experiments. The reason is that during the pulldown procedure the probes will be exposed to the cell lysate and have direct interaction with the proteins found in the cell.

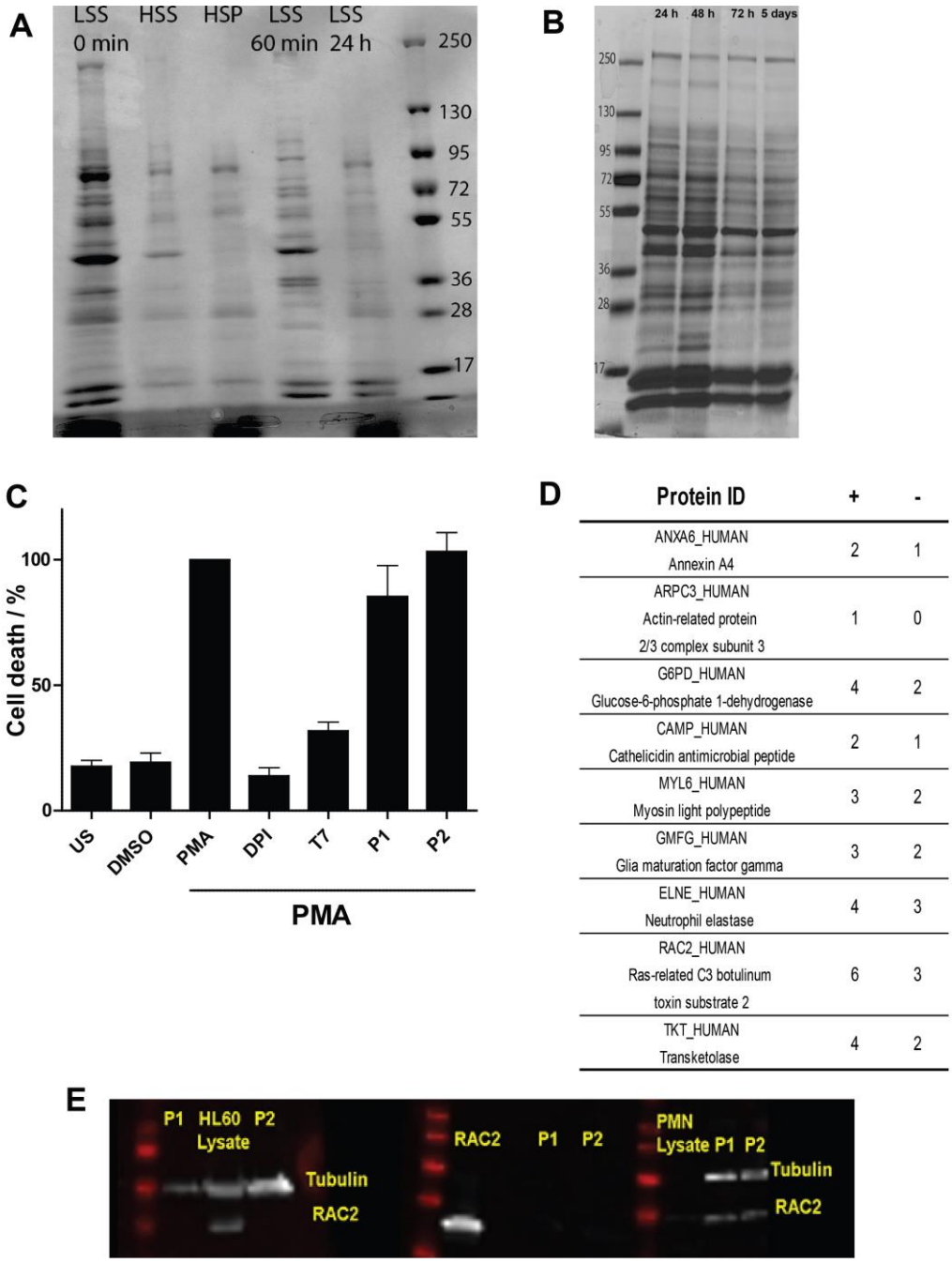

Protein ID	+	-
ANXA6_HUMAN Annexin A4	2	1
ARPC3_HUMAN Actin-related protein 2/3 complex subunit 3	1	0
G6PD_HUMAN Glucose-6-phosphate 1-dehydrogenase	4	2
CAMP_HUMAN Cathelicidin antimicrobial peptide	2	1
MYL6_HUMAN Myosin light polypeptide	3	2
GMFG_HUMAN Glia maturation factor gamma	3	2
ELNE_HUMAN Neutrophil elastase	4	3
RAC2_HUMAN Ras-related C3 botulinum toxin substrate 2	6	3
TKT_HUMAN Transketolase	4	2

Figure 38. THIQs pulldown optimization and results. (A-B) Neutrophil lysate optimization. cytoplasmic proteins, Low Spin Supernatant (LSS), granular proteins, high spin supernantant (HSS), and nuclear proteins, high spin pellet (HSP) (A). Protein degradation inhibited by PMSF and DFP upon addition to neutrophil cell lysate, LSS after 24, 48, 72 h up to 5 days and incubated on ice (B). (C) Pulldown probes did not retain NET inhibitory activity. Neutrophils were pre-incubated with 30 µM of the compounds for 20min at 37°C followed by stimulation with 40 nM PMA and further incubation for 240 min to allow NET formation. Cells were stained with SYTOX Green. US: unstimulated cells. (D) Proteins that were identified the performed enriched by the active (+) or control probe (-). The number indicate how often the protein was identified in total out of 9 independent experiments. (E) RAC2 binds unspecifically to the probes. Detection of RAC2 via immunoblotting. Neutrophils, HL60 lysates and pur RAC2 were subjected to pulldown experiment with a immublotting readout with fluorescence conjugated goat anti-mouse, or goat anti-rabbit 2nd antibody (n = 3).

10.5 Localization studies

In attempt to study the THIQ behavior in cells, localization studies were performed with the fluorescently labeled **P5** (**Figure 37 C**). Neutrophils were subjected to a NET formation time course after activation with PMA. After fixation and permeabilization the slides were with the **P5** compound and nuclear stain DAPI (**Figure 39**). Compound **P5** was found to localized to the neutrophils undergoing NETosis. This is illustrated in the images in **Figure 39** at min 45, highlighted with a red circle, which shows neutrophils which are losing their lobules and becoming rounded, and showing an increased fluorescence. In contrast to the neutrophils that have a lobulated nucleus, which usually indicates that NETosis is yet to start, there is no fluorescence present. After 240min, when NET formation has finished, the fluorescent probe is localized in a ring-like structure around the expanded DNA and not on the actual NETs. If the THIQ target would be a granular protein, such as NE, **P5** would be found on the NETs. This result strongly suggests that THIQs target a protein that is involved in NETosis and not a protein that is a component of NETs.

This result presents a possible explanation for why the protein targeted by THIQs was not identified in the affinity based proteomic experiments. The pulldown probes were performed on unactivated PMNs. During the optimization of the lysate, the focal point was to restrain the proteases. As mentioned before, pulldown experiments are not ideal for identifying proteins that are of low abundancy. From this experiment, it can be speculated that if the target of THIQs is a protein that is only overexpressed when NETosis is undergoing and maintained in low concentration in an unactivated neutrophil the protein concentration would be low.

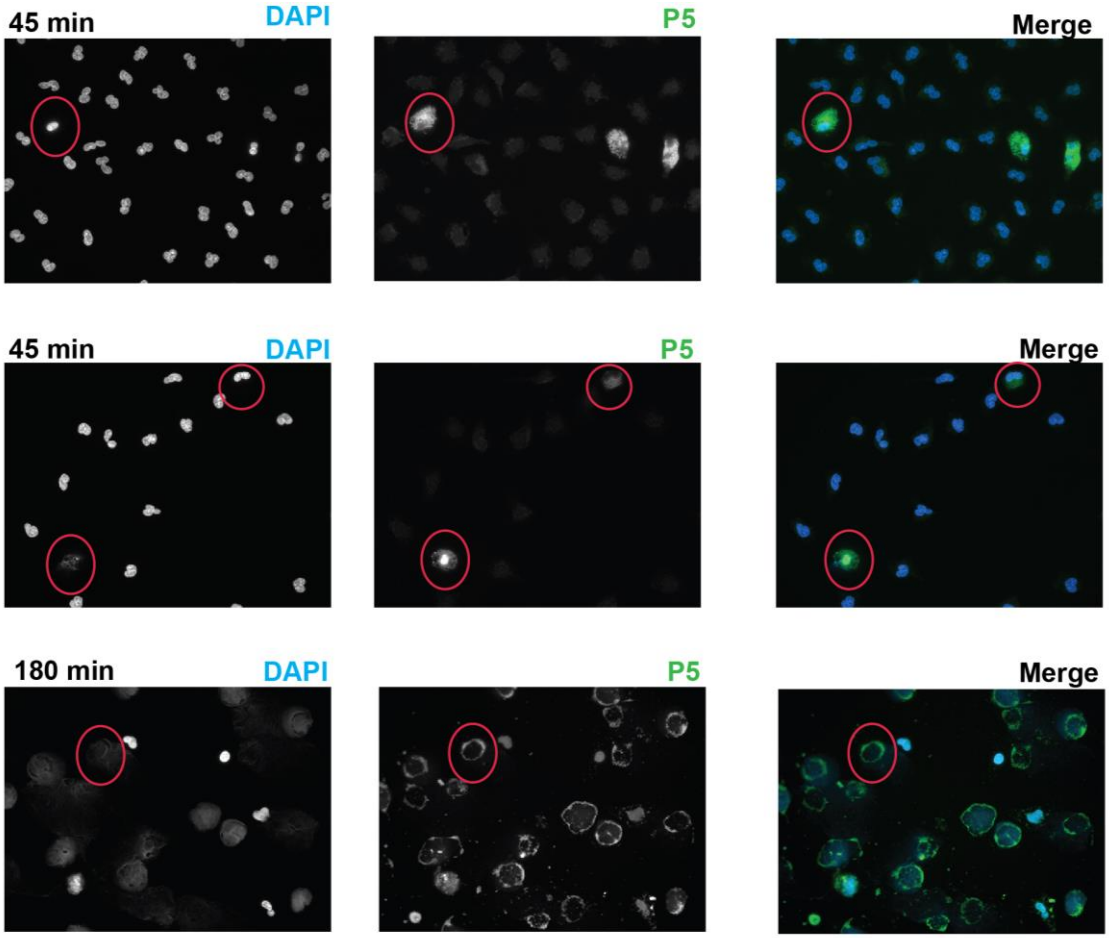

Figure 39. Bodipy-labeled THIQ P5 is enriched in cells that undergo NETosis. Neutrophils were stimulated 40 nM PMA for 45min or 240min allowing NETosis to occur. Followed by fixation and permeabilization, then the slides were blocked with 3% BSA and stained with DAPI (blue) and 1µM P5 (green) 1µM compounds.

10.6 G-protein coupled receptors (GPCR) and NETs

The target identification of the THIQs has proven to be a complicated task, since the conventional affinity-based proteomics approach failed to identify any protein targeted by the compounds. An alternative and relatively simple method is to apply computational inference methods (Schenone et al., 2013). These *in silico* methods make use of known protein-small molecule combinations and the structural features of a compound of interest are related to them. This gives an indication if the compound is likely to have binding affinity for one or several known target proteins. We used the statistic-based similarity ensemble approach (SEA) to investigate THIQ **T1** (Keiser et al., 2007). SEA compares the compound of interest to known ligands for over 1400 different proteins. The program scored the compound a low E-value and the smaller this value is the closer the resemblance to the ligand. For the best NET formation inhibitor THIQ **T1** identified, the

results are given in **Figure 40 A**. The list gives 10 proteins for which **T1** is most likely to be an interaction partner. This list includes eight different GPCRs including the dopamine D5 receptor. The E-value for this receptor is $8.90e^{-6}$ and for the α-adrenergic receptor $9.84e^{-4}$. These GPCRs are both targeted by compounds that were hits in the initial NET screen (**Figure 40 C**). However, the top-of-the-list protein suggested as the target was not a GPCR but an enzyme, quinone reductase with an E-value is $9.58e^{-15}$. The second on the list is a GPCR, the melatonin receptor with an E-value of $2.95e^{-10}$. Additionally to the SEA, flexible alignment studies using computer software MOE (Molecular Operating Environment) program were performed. Here the chemical structure of THIQ **T1** was compared to seratindole (**Figure 40 B**). Seratindole is an antipsychotic drug that targets dopamine, 5-HT2 and adrenogenic receptors. The model shows how the structural features of both molecules aligned in 3-dimentional space. The software places the basic amine of both compounds on top of each other and the flat aromatic rings are easily aligned.

These results strongly suggest that the THIQs may target a GPCR. This would also explain why no target was convincingly identified through pulldown. To identify a membrane protein via a conventional pulldown technique would not be possible unless the appropriate modifications have been taken into experimental consideration. For instance non-denaturing detergents such as NP-40 should be used together with specific centrifugation speeds. During the evaluation of the mass spectroscopy analysis, the membrane proteins are deliberately sought.

From our initial NET formation screen, several GPCR interacting compounds were identified as effective NET formation inhibitors (**Figure 10**). The compounds aminoclodine hydrochloride; apomorphine; and benzazepine hydrobromide were identified as effective inhibitors of NETosis. These compounds target the α_2-adrenergic receptor and also the dopamine receptors. Due to the lack of knowledge considering the relationship between GPCR functions and the process of NET formation these hits were not further investigated. Clearly, there is an undeniable structural similarity between apomorphine and the THIQs. The original hit data was reinvestigated and it was observed that aminoclodine hydrochloride, apomorphine, and benzazepine hydrobromide and THIQs induce the same nuclear morphology of group 2 (i.e. large nuclei) although this data has to be taken with caution since both apomorphine, and benzazepine hydrobromide have a catechol moiety in their chemical structures (**Figure 40 C**). This again supports the hypothesis that GPCRs may be involved to NET formation.

The link between GPCRs (e.g. dopamine, adrenergic, melatonin receptors) and neutrophil functions is a unexplored field. The first report of the involvement of GPCRs, being chemokine receptor (CXCR4), in NET formation was published only recently. It showed that stimulating the cells with integrin and chemokines (CXCL4 or CCL5) simultaneously can induce NET formation in a mice model for acute lung injury (ALI) (Rossaint et al., 2014). Another plausible relation between a

GPCR and NETs can be inferred for the dopamine receptors. These GPCRs, traditionally affecting the brain, were related to high levels of infection of the central nervous system (CNS). Dopamine receptors regulate acute immune responses, investigated in a new field called neuroimmunology (Beck et al., 2004; Mifsud et al., 2011) . As reported previously in the literature, dopamine-receptors are implicated in the assembly of NADPH oxidase. The production of catecholamines by this enzyme bridge the regulation of NFκB and other cytokines in the intensification of the acute inflammation (Kleniewska et al., 2012). Furthermore, a role for catecholamines has been described in phagocytosis by neutrophils and other immune cells during acute inflammation and indicates a cross talk between the nervous system and the immune system (Flierl et al., 2008; Flierl et al., 2007; Flierl et al., 2009). A proposed mechanism for the role of the GPCRs in the context of NETosis in depicted in **Figure 40 D**. Several GPCRs activate through cAMP production the protein kinase A (PKA) and initiate the Raf-MEK-ERK kinase pathway. If the Raf-MEK-ERK pathway is not involved after activating PKA via cAMP production, then a new signaling mechanism is triggered when the PKA is activated. From the compound morphology of the NET inhibitors, it is hypothesized that this novel cAMP mechanism could be involved in a later stage NETosis or as a feedback mechanism to NET formation. This is supported by the data published by Rossaint, et. al., who used chemokines in combination with integrins to activate NETosis in mice neutrophils increasing inflammation, and ultimately causing complications in acute lung injury (Rossaint et al., 2014).

A

#	Code	Reference Name	E-Value	MaxTC
1	NQO2_HUMAN_10000	Quinone reductase 2	9.58e-15	0.35
2	MTR1B_HUMAN_10000	Melatonin receptor 1B	2.95e-10	0.35
3	MTR1A_HUMAN_10000	Melatonin receptor 1A	3.23e-8	0.35
4	DRD5_HUMAN_10000	Dopamine D5 receptor	8.90e-6	0.32
5	ADA2B_RAT_10000	Alpha-2b adrenergic receptor	2.63e-4	0.39
6	ADA2C_RAT_10000	Alpha-2c adrenergic receptor	5.45e-4	0.39
7	ADA2A_RAT_10000	Alpha-2a adrenergic receptor	9.84e-4	0.39
8	DRD1_HUMAN_10000	Dopamine D1 receptor	8.37e-3	0.32
9	KCNA5_HUMAN_10000	Voltage-gated potassium channel subunit Kv1.5	1.60e-2	0.30
10	NMDE3_RAT_10000	Glutamate [NMDA] receptor subunit epsilon 3	4.80e-2	0.38

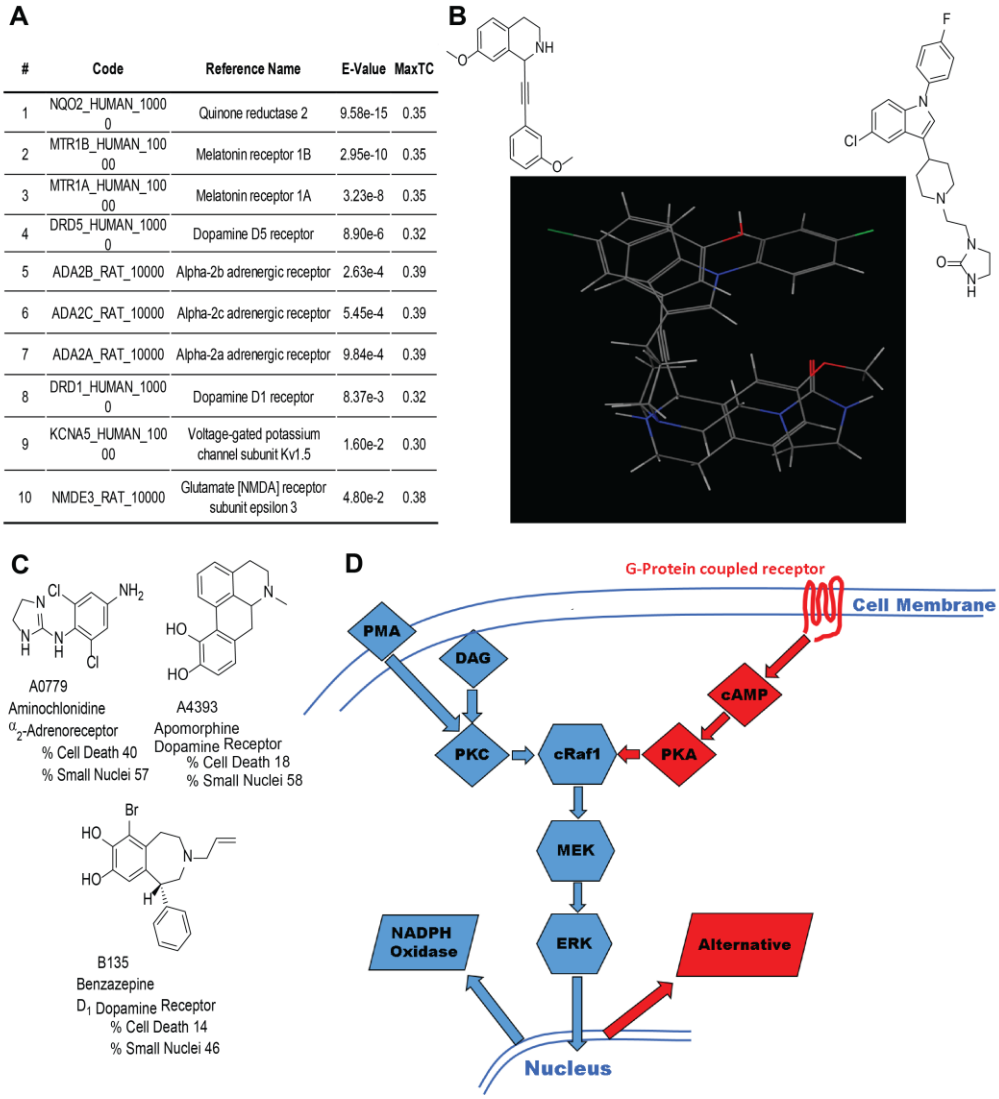

Figure 40. Computational target predictions for THIQ T1 implicate GPCR as targets. (A) SEA results for THIQ compound **T1**. (B) Results of flexible alignment of **T1** (left) and seratindole (right) and their structures. (C) GPCR-targeting hits in the initial NET screen. (D) Illustration of the proposed GPCRs involved mechanism in NET formation.

Next, THIQ **T1** was profiled against a panel of 28 GPCRs for both agonist and antagonist activity. Interestingly, THIQ **T1** was found to be a dopamine receptor D5 antagonist with 59% inhibition at 30 µM. Also, for the melatonin receptor MT2 an antagonist activity was measured with 77% inhibition at 30 µM. The BLT1 receptor was inhibited to 74% at the same concentration. To a lesser extent B2 adrenergic (B2) receptor and calcium (CaS) were antagonized by this compound with 50% and 50%, respectively (**Figure 41 A**). An agonist effect of THIQ **T1** was not significant in any of the receptors tested.

To further investigate these antagonist findings, well-known agonist and antagonist for these particular receptors in the NET formation assay were tested. First, the receptor agonists were tested

for NET formation activation. Melatonin, dopamine, and adenosine failed to significantly activate NET formation at concentrations of 100 µM, 10 µM, 1 µM, and 100 nM (**Figure 41 C-E**). Melatonin, dopamine and adenosine agonists obtained a maximum of 10% NET formation compared to the unstimulated control. The lipid leukotriene B4 (LTB4) was the best activator from all the agonists tested activating NET formation by 50% (**Figure 41 C- E**). This result correlates with the findings of other lipids of the eicosanoid pathway such as arachidonic acid and PAF activate NET formation as well.

In the case of melatonin and adenosine there was a very mild activation of 10% of NET formation. Interestingly, dopamine appears to have an inhibitory effect at higher concentrations. Using this neurotransmitter even more neutrophils were alive and in a lobulated state than the unstimulated neutrophils. Both the quantitative microscopy and the images (**Figure 41 E**) revealed that the melatonin, adenosine and LTB4 compounds induce more variety of morphologies compared to dopamine where the lobulated cells dominate (**Figure 41 C-E**). This inhibitory effect was confirmed when the GPCR agonists were tested for NET formation inhibition. All agonists were tested at 30 µM in the assay and, all compounds showed an inhibitory effect with the exception of LTB4. LTB4 maintains the activity of NET activator rather than NET inhibitor. Dopamine is an effective NET inhibitor causing a group 1 (small nuclei) morphology (**Figure 43 A-B and E-F**). Adenosine, melatonin and dihydrophenylglycine (3,5-DHPG), a glutamate receptor agonist, led to a 40-60% inhibition and a group 2 morphology (decondensated nuclei) (**Figure 41 F-G**). The GPCR agonists were tested for both NET formation activation and inhibition, because this will set the basis for activity of these particular receptors tested in the context of NETosis. The only GPCR that is known to have an effect on neutrophils is the LTB4 receptor which is involved in cell to cell communication in the innate immune system (Sala et al., 2010).

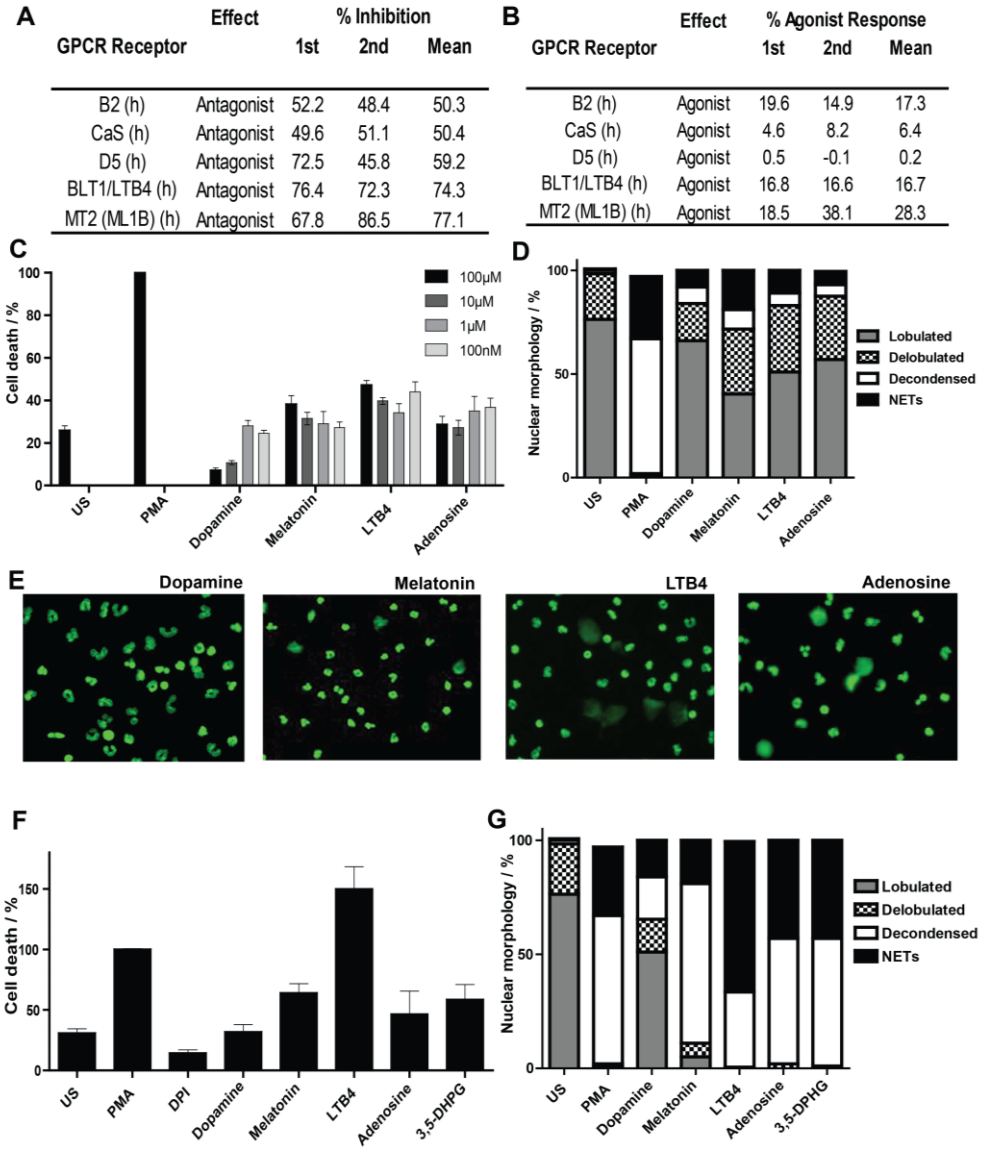

Figure 41. Effect of THIQ T1 on GPCR receptors and effect canonical GPCRs agonists on NET formation. (A-B) THIQ **T1** was profiled against 26 GPCR. (C-G) Influence of the GPCR agonists melatonin, dopamine, and adenosine on NET formation (C and F) cell death (D and G) quantification of the nuclear morphologies. Neutrophils were stimulated with various concentrations of the agonists. (E) Representative images of neutrophils upon treatments with the different agonists and staining with the nuclear dye SYTOX Green. Neutrophils were pre-incubated with 30 µM of the compounds for 20 min at 37°C followed by stimulation with 40 nM PMA and further incubation for 240 min to allow NET formation. Cells were stained with SYTOX Green to detect dead cells. Nuclear morphology was analyzed upon fixation and permeabilization using automated microscopy (D and G). Data are mean values ± s.d. (N = 3, n = 3). Images were acquired using a 20X objective. US: unstimulated cells, LTB4: Leukotriene B4, 3,5-DHPG: dihydroxyphenylglycine.

Also, GPCR antagonists for the melatonin, dopamine, LTB4 and calcium receptors were tested for their effect on NET formation. All antagonists showed a slight inhibitory effect at 30 µM on the PMA-induced NET formation and, more interesting, provoked group 2 nuclear morphology, indicating inhibition of NET formation during the last stage (**Figure 42**). The melatonin antagonists

were the most effective NET formation inhibitors from all the antagonists tested. Luzindole inhibited NET formation with a cell death less than 35% and 70% decondensed nuclei morphology. The other melatonin antagonist tested, K185, also inhibited NETosis with a cell death of 60% and a 70% decondensed nuclei (**Figure 42 A-C**). To find the scientific evidence in the literature to explain why the melatonin antagonists were better NET inhibitors compared to the other GPCR antagonists tested will have to be postponed. Not much is known in the literature of role of melatonin and neutrophils even less when it comes to melatonin and NETs. Both, LY23111 and leukotriene B4 ethanolamide (LTB4-EA) triggered similar nuclear morphology of large nuclei above 50 %. The LTB4 antagonist were the only compounds to show a 10 % of lobulated nuclei the other GPCR antagonists tested had 0 % lobulated nuclei. Nevertheless, the compounds show a high level of cell death (**Figure 42 H-I**). The calcium receptor antagonist, SK96365, and the dopamine receptor antagonist, SCH23330, showed a very similar pattern of cell death of 50% and 50% ratio between small nuclei vs. large nuclei (**Figure 42 D-F and J-L**). Interestingly, the antagonists of the LTB4 receptor showed a clear inhibitory effect.

In the previous paragraphs, GPCR receptor agonists and antagonists were investigated in an attempt to find a correlation between GPCRs and NETosis. In particular, dopamine, melatonin, glutamate have yet to be investigated in more detail regarding their regulatory role on neutrophil function.

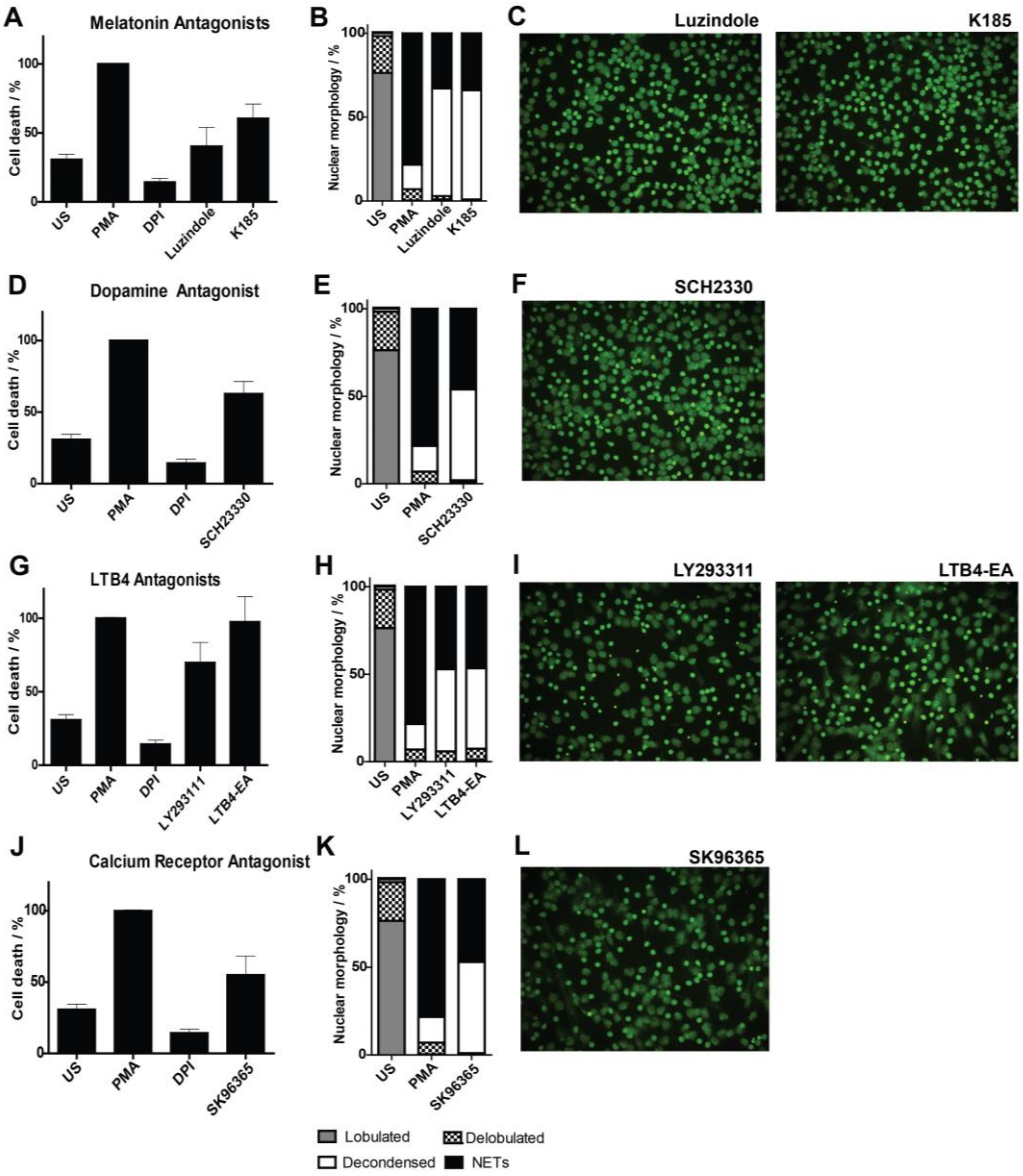

Figure 42. Effects of known GPCRs antagonists on NET formation. Neutrophils were pre-incubated with 30 µM of the antagonists of the melatonin, dopamine, LTB4 and calcium receptors for 20min at 37^{o}C followed by stimulation with 40 nM PMA and further incubation for 240 min to allow NET formation. Cells were stained with SYTOX Green to detect dead cells (A, D, G, and J). Nuclear morphology was analyzed upon fixation and permeabilization using automated microscopy (B, E, H, and K). Data are mean values ± s.d. (N = 3, n = 3). Representative images of neutrophils at different conditions stained with nuclear dye SYTOX Green (C, F, I, and L). Images were acquired using a 20X objective. US: unstimulated cells, LTB4: Leukotriene B4.

Noteworthy is that, the association of dopaminergic receptors with immune cells during acute immune responses is established (Beck et al., 2004). Dopamine receptors are known to be involved in the assembly of the NADPH oxidase. However, the dopamine and apomorphine-mediated inhibition of NET formation most likely results from the suppression of ROS generation. Catecholamines bridge the regulation of NFκB and other cytokines in the intensification of the acute inflammation. Apomorphine and dopamine are known to be involved in radical scavenging due to

the catechol moiety in their structure (Kancheva, Biochimie 2012). The investigation of the dopamine receptor was extended to apormophine and a small library of apormorphine analogs.

It was found that apomorphine inhibited NET formation as effectively as dopamine and both were as potent as the control DPI. There was a difference in the nuclear morphology caused by these compounds. Dopamine led to a group 1 (small nuclei) morphology and apormorphine caused a group 2 (large nuclei) morphology (**Figure 43 B-F**). Since both compound have a catechol moiety it was vital to investigate if the NET formation inhibition was due to the scavenging activity of the catechol moiety rather than a receptor interaction. Both compounds suppressed ROS formation. Determination of oxygen consumption dopamine and apormorphine revealed lack of scavenging of oxygen (as demonstrated for pyrocatechol and apocynin) (**Figure 23 F**). Interestingly, apormorphine showed the same profile as DPI which does not consume oxygen. This result strongly suggests that the oxygen scavenging is not the mechanism of action for these compounds.

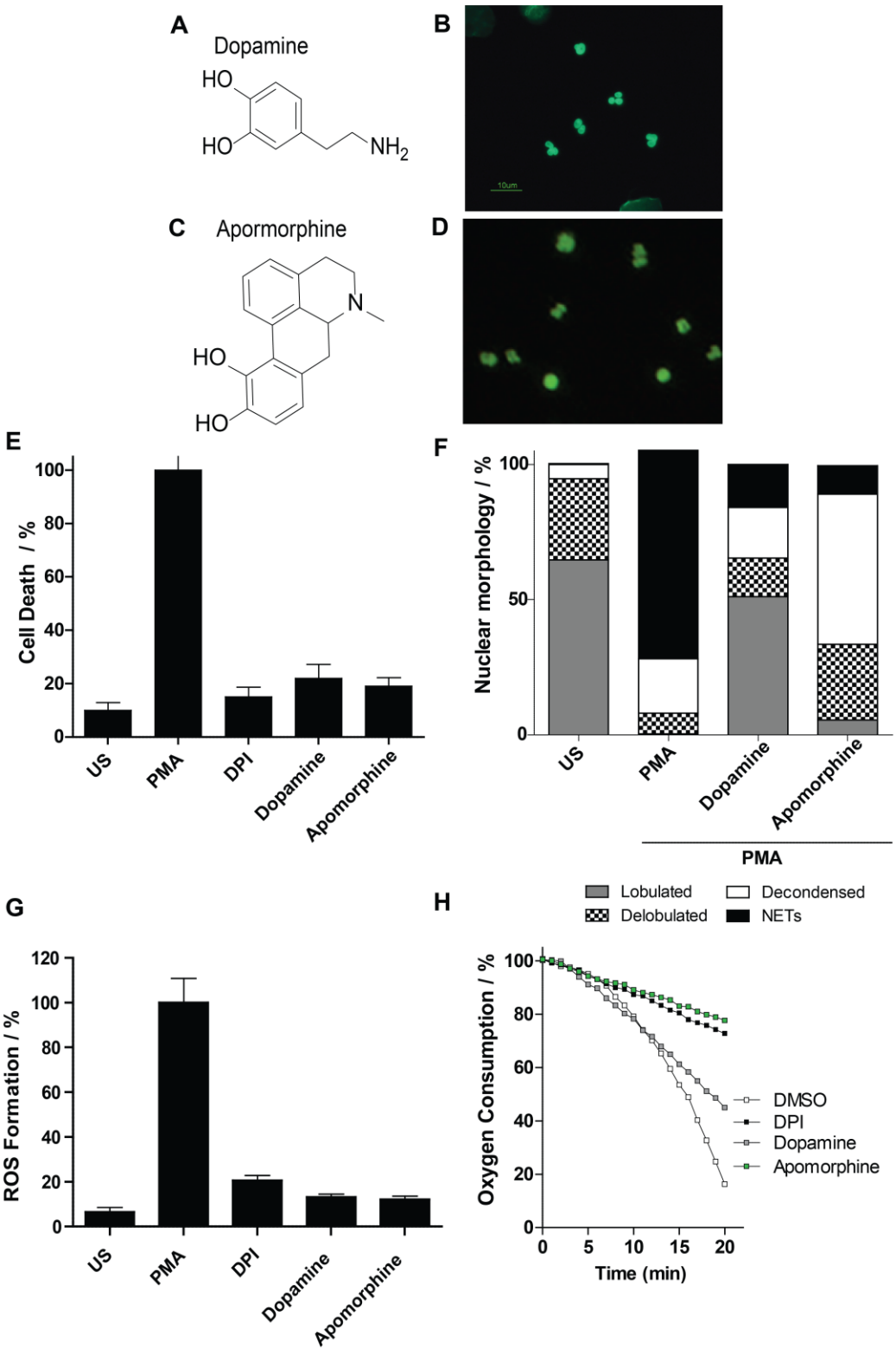

Figure 43. Influence of dopamine and apormorphine on NET formation. (A and B) Structure of dopamine and apormorphine. (B-F) Neutrophils were pre-incubated with 30µM of inhibitor for 20min at 37°C. Followed by PMA (40nM) stimulation and incubated for 240 min to allow NET formation prior to SYTOX Green to detect dead cells. (G) Influence on ROS generation. Neutrophils were stimulated with 40nM PMA to induce oxidative burst upon pre-treatment with compounds for 20 min at a concentration of 15µM for 120min. ROS were detected *in situ* using luminol/HRP reagent. (H) Effect on oxygen consumption. Cells were pre-treated with

30µM of compound and incubated for 20min followed by activation with 40nM PMA. Oxygen consumption was detected using a “Clark-type” electrode for 30min. (N = 3, n = 3).

Considering the structural similarity of the THIQs to apomorphine we decided to study apomorphine and analogues in more detail. Several apomorphine analogs stopped NET formation (**Table 7**). Compounds **A1**, **A2**, **A3**, and **A4** have group 1 morphology. Noteworthy, apomorphine analogue **A5** showed group 2 morphology, same as apormorphine and the THIQs. As for apomorphine, **A1** and **A2**, both inhibit ROS generation. Compounds **A3**, **A4**, **A5** do not inhibit ROS formation. Apomorphine and analogues were never further investigated due to the fact that they contain a catechol moiety. THIQs do have a different mode of action and lack the catechol moiety making them a better compound class to progress compared to the apomorphine-type compounds.

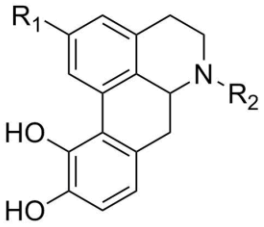

Entry	R1	R2	Cell death / %	Small Nuclei / %	ROS / %
A1	H	Me	10	97	15
A2	H	Pr	11	96	15
A3	H	Allyl	9	99	128
A4	OH	Me	10	98	146
A5	OH	Pr	9	10	101

Table 7. Apomorphine analogs inhibit NET formation. Neutrophils were pre-incubated with 30 µM of the compounds for 20min at 37^{o}C followed by stimulation with 40 nM PMA and further incubation for 240 min to allow NET formation. Cells were stained with SYTOX Green to detect dead cells. Nuclear morphology was analyzed upon fixation and permeabilization using automated microscopy. For ROS detection, neutrophils were incubated with compounds for 20 min prior to stimulation with 20 nM PMA to induce oxidative burst. ROS were detected *in situ* using luminol/HRP reagent. Oxygen consumption was measured with a Clark electrode after pre-treating the neutrophils with compound for 20min. Data shown correspond to percent of generated ROS after 12 min stimulation with PMA. Data are mean values ± s.d. (N =2, n = 2)

Chapter 11: Concluding Remarks and Future Prospects

Neutrophils are the most abundant cells of the innate immune system. Once activated, they communicate with other cells via cytokine excretion and eradicate sites of infection by means of degranulation, phagocytosis and NETosis. The release of NETs, which are composed of chromatin decorated with anti-bacterial granular proteins, leads to a unique form of cell death called NETosis. The onset and progression of NETosis are poorly understood. Instead, perturbation with bioactive small molecules that act rapidly and conditionally offers a chemical-biological alternative to unravel the mechanisms of neutrophil-related processes.

We developed a semi-automated high content phenotypic screen using human neutrophils that is set up for NET formation inhibitor identification. For this purpose, human neutrophils were treated with small molecule compound libraries prior to activation with PMA. The identified small molecule hit compounds were grouped into four categories based on their influence on nuclear morphology and cell viability. Compounds assigned to groups 1 and 2 are of highest interest since the induced phenotypes correspond to inhibition of NET formation. Inspection of morphological changes allowed to postulate the stage of NET formation in which the cells were arrested.

11.1 RAF/MEK/ERK Pathway regulates NETs

Commercially available compound libraries (Sigma) were screened. GW5074, a c-Raf kinase inhibitor was identified as a NET formation inhibitor with group 1 characteristics. The c-Raf protein is part of the MEK/ERK signal transduction pathway. The involvement of the Raf-MEK-ERK pathway in NET formation was confirmed by screening U0126, a MEK inhibitor, and ERK peptide inhibitor. Additionally, the role of the Ras protein was ruled out using indirect Ras-signaling disrupting compounds. All of the indirect inhibitors failed to block NET formation. Therefore, Ras is excluded from the signaling mechanism. The involvement of this pathway in NET formation was confirmed by immunoblotting of the phosphorylated ERK. Consistently, all kinase inhibitors, staurosporine, GW5074, and U0126 blocked ROS formation, implying that they act upstream of NADPH oxidase. We were the first to show the involvement of the Raf-MEK-ERK pathway in the NET formation and its function upstream of NADPH oxidase.

In addition to investigating the location of the Raf-MEK-ERK pathway, there is a link between this signaling pathway and cell survival. Mcl-1, an anti-apoptotic protein, is expressed during early NETosis. This proves that the cell suppresses apoptosis keeping the cell alive and allowing the cell to undergo NET formation. A follow-up on this finding would see if other anti-apoptotic signals are triggered. It is known that anti-apoptotic signals are not only affected by ERK but by other kinases, for instance JNK.

The continuation of this work it would be of interest to investigate the involvement of kinases downstream from ERK and specifically, if there is any role other than regulation of the NADPH oxidase activation. If in NET formation any other regulatory pathways are affected (e.g. cytoskeleton organization and motility), the detail signaling that leads to such large structural changes would be of major interest. Also, what links this signaling mechanism to the eicosanoid pathway and GPCRs signaling cascades needs to be validated. Also the ERK signaling pathway needs to be challenged with better and more specific kinase inhibitors that would better elucidate further into the details of the NET formation mechanism.

11.2 NET Communicate with Eicosanoid Lipids

The eicosanoid pathway was shown to be involved in NET formation. Eicosanoid pathway activator arachidonic acid was identified as triggering NETs, in the similar to diaglycerol and platelet activation factor. Furthermore, it was shown that lipoxygenase (LOX) is required for NETosis by using a selective LOX inhibitor that stopped NETosis and the exclusion of the cyclooxygenase (COX) protein. In addition to the direct involvement of this pathway lipid bodies localize to NETs. Traditionally in innate immunity, lipid signalling is involved in cell-to-cell communication. Our results elucidate a new function in leukocytes, contributing to a novel field of study for neutrophil biology.

As a continuation of this research much is yet to be discovered. In order to complete the mechanism, it needs to be proven that this lipid signalling occurs either upstream or downstream of the known NET formation mechanisms. LOX inhibitors should be challenged with bacterial stimuli and lipid stimuli. In the eicosanoid signalling cascade the downstream product of the LOX protein are lipoxins. Lipoxins are of detrimental importance to neutrophils in cell-to-cell communication and inflammatory response. The information regarding the role of lipoxins in NET formation mechanism is missing. In addition to the LOX signalling it is important to verify the values of lipids in the neutrophils upon activation of NET formation and determine the physiological relevance in an arthritic mouse model.

Additionally, the composition of the lipid bodies is an essential part of the mechanism which is still lacking. I propose that there should be an establishment of a lipidomics investigation upon the establishment of a proper protocol for isolation of lipid bodies. Lipid bodies would be tested to see if they trigger NET generation on unstimulated neutrophils. It would be of value to know the the response of other immune cells and endothelial cells once they are exposed to the lipid bodies.

11.3 Tetraisoquinolines as a New Class of NET formation Inhibitors

After screening the MPI Dortmund in-house-compound library, tetrahydroisoquinolines (THIQs) were identified as a novel class of NET formation inhibitors. Unlike known inhibitors of NET formation (e.g., NADPH oxidase inhibitor DPI, neutrophil elastase inhibitor GW311616A, myeloperoxidase inhibitor ABAH, RAF inhibitor GW5074) these compounds arrest NETosis at an early stage and have a small nuclei with lobulated and delobulated morphology.

THIQs inhibit NETosis at low micromolar concentration independent of the stimulus and at different stages of NET formation. Compound **T1** was found to be most potent with an EC_{50} for inhibition of NET formation of 1.9 ± 0.6 µM with a phenotype of group 2. Treatment with compound **T6** resulted predominantly in cells with small, lobulated and delobulated nuclei. Compounds **T1** and **T6** did not influence ROS formation suggesting that they act downstream of ROS generation. No MPO nor NE inhibitory activity could be detected by these NET inhibitors.

Unraveling the underlying mechanism of action for these THIQs will contribute to a better understanding of NETosis and may provide novel targets and opportunities for therapeutic intervention to treat NET-related diseases. A library of approximately 100 THIQs was synthesized and a SAR was established. Based on the structure activity relationship (SAR) target identification probes were synthesized. Compound **T1** was functionalized with a linker with biotin, free amine or a fluorophore. Pulldown experiments were performed with human neutrophil lysates. Enriched proteins were subjected to tryptic digest followed by protein identification by means of mass spectrometry. Unfortunately, no proteins were identified that were selectively enriched with the active probe in comparison to the control. Computational profiling of THIQ **T1** suggested that the target might be a GPCR. Testing compound **T1** against 28 GPCRs for agonist and antagonist activity resulted in the first positive results regarding the target identification of THIQ **T1**. Also, this established the basis for the novel involvement of GPCRs in NET formation. Interestingly, compound **T1** was identified as an antagonist for dopamine receptor D5, melatonin receptor, and BLT1 receptor. Known GPCR antagonists for these receptors showed an inhibitory effect on NET formation and, more interestingly, they all shared the same group 2 nuclear morphology, although they were not as potent as the THIQs compounds.

Clearly, GPCRs are likely to mediate the THIQs-provoked inhibition of NET formation. However, results are inconclusive with the limited research performed so far. The establishment of a mechanistic role for GPCRs in NETs is missing. The cellular target, or targets, of the THIQs remains to be properly identified. The next target identification experiments should focus on membrane proteins as these were not covered in the pulldown experiments performed. More GPCRs should be validated against more THIQs and EC_{50}s determined, and eventually correlated to the morphology data. Simultaneously, the role of GPCRs should be validated through other means. Neutrophils

should be examined for the expression of the receptors for melatonin, dopamine and any other receptor that is identified as an interacting partner for the THIQs. Additionally, calcium ions and cAMP levels released during NET formation remains to be investigated. These measurements will prove the direct biological link to the identified GPCR on human neutrophils favoring NETs. The link between GPCR activation and Raf-MEK-ERK signaling should be established. Finally, a study on how the feedback and cell communication plays a role in the NET formation signaling pathways is to be pursued.

A hallmark of many immune disorders is the overproduction and lack of degradation of NETs. NET formation inhibitors are considered promising candidates for the treatment of the autoimmune disease systemic lupus erymatosus (SLE). THIQs inhibit NET formation efficiently in non-activated and PMA-activated SLE patient isolated neutrophils. These results clearly indicate that THIQs have great potential as tool compounds and as a starting point for the development of novel small molecule therapeutics. The optimization and efficacy of THIQs should be further pursued and potency ought to be improved. Validation in an appropriate animal model should be pursued. For this, ADME parameters ought to be taken into consideration and optimized to determine if this compound class would be considered for therapeutic use.

The study of the neutrophil NET formation enigma is a perfect example wherein a chemical biology approach can be very successful. An assay protocol was established allowing NET formation to be studied quickly and could be scaled up to a high throughput technique. Novel signalling mechanisms were identified and added to the overall mechanism of NETosis. A novel NET inhibitor compound class was identified and added to the toolbox to study NETs, together with additional biochemical techniques.

Experimental Section

1. General materials and methods

1.1 Laboratory devices

Instrument Name	Manufacturer
Autoklav (Varioklav®400)	Thermo scientific, USA
Axiovert 200M with a Plan-Neofluar 100×/1.3 NA	Carl Zeiss MicroImaging, Inc
Balance (BP301S)	Sartorius, D
CASY Model TT (Cell counter)	Roche, D
Cell –Surelock TM Novex Mini-cell (Device to run precast gel)	Invitrogen
Centrifuge (Centrifuge 5415R)	Eppendorf, D
CO_2- incubator (NUAIRE IR Autoflow and NUAIRE DHD Autoflow)	Integra Biosciences, D
Confocal microscopy TCS-SP Leica and a Fluotar 100× objective lens	Leica
Countess® Automated Cell Counter	Invitrogen Life Technologies
Electrophoresis system (Mini-PROTEAN Elektrophorese System 165-8025)	BioRad, USA
Fluorescence scanner (Typhoon TRIO + TM variable Mode Imager)	GE Healthcare
Fluorometer (Ascent Fluoroskan MTP reader)	Thermo Scientific
Infinite M200 TECAN (Plate reader)	TECAN
Leica DM R upright epifluorescence microscope with Leica 10×/0.3, 20×/0.5, and 40×/0.75 objective	Leica
LI-COR scanner (Odyssey Infrared Imaging System LI-COR)	Biosciences, D
Microscope Leitz (Labovert type 090-122.012)	ERNST LEITZ WETZLAR, D
Monolight 3096 reader (ROS assays)	BD Biosciences
Monolith NT.115 Series	Nanotemper
Neubauer Cell counting chamber	Carl Roth, D
Nikon DXM1200F camera and Nikon ACT-1 software	Nikon

pH - meter (Mettler Toledo FiveEasy)	Mettler Toledo
Power supply device (Power PAC 1000)	BioRad, USA
Semi-dry transfer device (Trans-Blot ®)	SD BioRad, USA
Sonoplus HD2070 (Sonicator for cell lysis)	BANDELIN
Sterile bench (Microflow, Hera Safe type HS12 NUAIRE, class II)	Kendro laboratory, D Integra Biosciences, D
Thermomixer comfort	Eppendorf, D
Ultrasonic bath (EMMI® 30HC)	AMAG, D
UV spectrometer (Biophotometer)	Eppendorf, D
Vacuum concentrator (Concentrator 5301)	Eppendorf, D
VIBRAX VXR (Shaker)	Basic IKA
Vortex devices (Vortex Genie 2)	Carl Roth, D

1.2 General Materials and Reagents

Name	**Details**	**Company**
1,4-Dithio-D,L-threitol hight purity (DTT)	CAS = 3483-12-3, MW = 154.25	Gerbu Biotechnik, D
12% Pierce TM protein gels	10 wells,#25202	Thermoscientific, USA
2-chloroacetamide	CAS = 79-07-2, MW = 93.51, 802412	Merk Millipore
4-20 % Pierce TM protein gels	10 wells, #25204	Thermoscientific, USA
Acetic acid	CAS = 64-19-7	J.T. Baker, Holland
Acetone reagent ACS	CAS = 67-56-1	Sigma Aldrich, D
Acetonitrile HPLC grade	CAS= 75-05-8	Fisher Scientific
Acrylamid 4K- solution 30%		AppliChem , D
$AgNO_3$	CAS = 7761-88-8, MW = 169.87	Sigma Aldrich, D
alpha-cyano-4-hydroxycinnamic acid	CAS = 28166-41-8, MW = 189.17, C2020	Sigma

Name	Details	Company
Amonium persultate analytical grade	CAS= 7727-54-0, MW = 228.2, #13375	Serva, D
BIOCHEMISTRY		
Bio-Rad-protein assay	#500-0006	Bio-Rad laboratories, D
Bromophenol blue-Na salt		Serva, D
Chocolate powder Slim fast		
CL-Xposure TM	Film for WB development, #34091	Thermo scientific, USA
Criterion Precast Gel 12.5 %, 45 µL	5671045	Bio-Rad laboratories, D
Criterion Precast Gel 4-15 %, 15 µL	5671095	Bio-Rad laboratories, D
Criterion Precast Gel 4-15 %, 45 µL	5671083	Bio-Rad laboratories, D
Criterion Precast Gel 4-20 %, 45 µL	5671093	Bio-Rad laboratories, D
$CuSO_4$	CAS= 7758-99-8, MW =249.68	Sigma Aldrich, D
Developing solution for Western blot	#100296	TETENAL-Eukobrom , D
Dimethylsulfoxyde (DMSO) cell culture grade anhydrous	Research Grade D260 276855	Serva, D Sigma Aldrich, D Sigma Aldrich, D
Dodecylsulfate sodium	SDS-b, CAS= 151-21-3, MW = 288.38	Gerbu Biotechnik, D
EDTA- disodium	CAS = 6381-92-6, MW= 372.34	Gerbu Biotechnik, D
Ethanol absolute	CAS = 64-17-5	Sigma Aldrich, D
Ethylenglycol-bis(2-Aminoethylether)-N,N,N',N'-tetraacetic acid (EGTA)	CAS = 67-42-5, MW = 380.35 E3889	Sigma Aldrich, D
Fixing solution for Western blot	#102762	TETENAL-Eukobrom , D
Formaldehyde 37%, for molecular biology	CAS= 7732-18-5, #BP531-500	Fischer Scientific
Glycerol 9%	CAS = 56-81-5	Sigma Aldrich, D
Glycine 99%	CAS= 56-40-6, MW = 75.07	Carl Roth, D
Guanidine hydrochloride	CAS= 50-01-1, MW= 95.53, #369079	CalBiochem, USA

Name	Details	Company
HCl Concentrated 37%	CAS = 7647-01-0	Sigma Aldrich, D
High perfomance extractions disks, C18 Octadecyl	2215	3M Empore
Hydrophilic Streptavidin magnetic beads	S1421S	New england Biolabs
Iodoacetamide	CAS = 144-48-9, MW = 184.96	Sigma Aldrich, USA
KH_2PO_4	CAS= 7778-77-0, MW = 136.09	J.T. Baker Holland
Methanol	CAS = 67-64-1	Sigma Aldrich, D
$MgCl_2$, Magnessium Chloride, (hexahydrant)	CAS = 7791-18-6, MW = 303.3, HNO3.1	Roth
N,N,N', N'-tetramethylethylendiamine, electrophoresis reagent (TEMED)	CAS = 110 – 18-9, MW= 116.21	Sigma Aldrich, D
Na_2CO_3	CAS = 497-19-8, MW = 105.99	Sigma Aldrich, D
Na_2HPO_4 ; $2H_2O$	CAS= 10028-24-7, MW = 177.99	Merck, D
$Na_2S_2O_3$ anhydrous	CAS = 7772-98-7, MW = 158.11	Alfa Aesar
Na_3VO_4	CAS= 13721-39-6, MW= 183.91	Sigma Aldrich, D
NaCl, Sodium Chloride	CAS = 7647-14-5, MW = 58.44	Sigma Aldrich, D
NaF	CAS= 7681-49-4, MW = 41.99	Sigma Aldrich, D
NHS Mag Sepharose	28-9513-80	GE Healthcare
NP-40 Alternative	CAS = 9016-45-9, #492016	CalBiochem , D
PageRuler TM prestained protein ladder plus	#SM1811	Fermentas
PIPES buffer	CAS = 227-057-6, MW = 302.37, 9156.1	Roth
Potassium chloride, KCl	CAS = 7447-40-7, MW = 74.55	J.T. Baker , Holland
PVDF -transfer membrane	Immobilon®-FL	Millipore, USA
RC DC Protein Assay kit	Catalog # 500-0119, -120,-121, -122	Bio-Rad laboratories, D
Sodium HEPES salts	CAS = 75277-39-3, MW = 260.3, #25249	Serva, D
Streptavidin magnetic beads (4	#S1420S	New england Biolabs

Name	Details	Company
mg/ml)		
Super Signal ® West femto Chemiluminescence substrate	34095	Thermo Scientific, USA
Super Signal ® West Pico Chemiluminescence substrate	34087	Thermo Scientific, USA
TBTA 97%, TRIS[(1-benzyl-1H-1,2,3-triazol-4-yl)methyl] amine	CAS= 510758-28-8 , MW= 530.63	Sigma Aldrich, D
t-Butanol	CAS = 75-65-0	Sigma Aldrich, D
TCEP.HCl	CAS = 51805-45-9, MW= 286.65, #20490	Thermo Scientific, USA
TFA for peptide synthesis	CAS= 76-05-1	Carl Roth, D
TRIS-HCl	CAS= 1185-53-1, MW = 121.14	Carl Roth, D
Triton X-100	CAS= 9002-93-1	Serva, D
Trypsin Recombinant	Proteomic analysis, #03 708 969 001	Roche,D
Tween 20	CAS= 9005-64-5	Serva, D
Urea 99%, ACS Reagent	CAS= 57-13-6, MW=60.06	Sigma Aldrich, D
β-Mercaptoethanol	CAS = 60-24-2, MW = 78.13, 39563.01	Serva
CELL CULTURE		
Lipopolysaccharide (LPS) from *Salmonella typhimurium* S-form	581-011	Alexxis/ENZO
Bovine Serum Albumin (BSA) – fatty acid free	CAS = 9048-46-8	Sigma Aldrich, D
Complete Mini EDTA-free protease inhibitor	2683400	Sigma/Roche Diagnostics, D
Costar®Assay plate, sterile, flat bottom,black	#3616	Sigma Aldrich, D
Cytotoxicity Detection Kit (LDH)	11644793001	Roche_Sigma
DMEM	high glucose (4.5g/l) with L-glutamine	PAA, Pasching, A

Name	Details	Company
Endotoxin-free human albumin HSA		Grifols
epidermal Growth Factor (EGF), recombinant human	#PHGO315	Invitrogen, USA
Fetal bovine serum (FBS)	#10270	GIBCO-Invitrogen, D
Hank's Balanced Salt Solution (HBSS)	14170112	GIBCO-Invitrogen, D
Heparin		Ratiopharm, D
HEPES	15630080	GIBCO-Invitrogen, D
Histopaque-1119 gradient	11191	Sigma Aldrich, D
Monolinth NT Protein Labeling kit Green NHS	L002	Nanotemper
Monovette with EDTA		Sarstedt, D
Nunc plates	96-well plates with white walls and clear bottom	Thermo scientific, D
PBS	10010023	GIBCO-Invitrogen, D
Penicillin (10. 000U/ml) – Streptomycin (10 mg/ml) in 0.9% NaCl	10378016	GIBCO-Invitrogen, D
Percoll	17-0891-01	GE Healthcare Life Sciences
RPMI	11875093	GIBCO-Invitrogen, D
RPMI Phenol-free medium	11835030	GIBCO-Invitrogen, D
Sodium pyruvate solution	11360070	GIBCO-Invitrogen, D
Trypan blue solution	CAS = 72-57-1, #93595	Fluka, D
Trypsin-EDTA (1%)	cell culture laboratory grade 15400054	PAA, Pasching, A GIBCO-Invitrogen, D
PROTEINS		
15-lipoxygenase inhibitor I	CAS: 928853-86-5, MW = 313.4 Sc-220625	Santa Cruz
15-lipoxygenase-2 blocking peptide	10004457	Cayman
Arachidonic acid	CAS: 506-32-1, MW = 304.47,	Sigma

Name	Details	Company
	A3555	
Chloro-amidine (TFA salt)	CAS: 1043444-18-3, MW = 424.11, 10599	Caymann
COMPOUNDS		
Cytochalasin B	CAS: 14930-96-2, MW = 479.61 C6762	Sigma
Cytochalasin D	CAS: 22144-77-0, MW = 507.62 C8273	Sigma
Diisopropyl flourophosphate (DFP)	CAS: 55-91-4, MW = 184.15, D0879	Sigma
Formylated methionyl-leucyl-phenylalanine (fmlp)	CAS: 59880-97-6, F3506	Sigma
Glucose oxidase (GO)		Worthington biochemical corporation Miltenyi
Horse Radish Peroxidase (HRP)	1200U/ml	Serval
Luminol	Cat. 11050, 50 mM DMSO	AAT Bioquest,
Myeloperoxidase human	475911	Calbiochem
NE inhibitor, GW311616A	CAS: 197090-44-1, MW = 433.99, G8419	Sigma
NE substrate I	324696	Calbiochem
Neutrophil Elastase, human	324681	Calbiochem
Oil Red O	CAS: 1320-06-5, MW = 408.49, O0625	Sigma
Phenylmethanesulfonyl fluoride (PMSF)	CAS: 329-98-6, MW = 174.11 P7626	Sigma
Phorbol myristate acetate (PMA)	CAS: 16561-29-8, MW = 616.83, P8139	Sigma
Platelet activation factor (PAF)	CAS: 74389-68-7 PAFC-16, #60900 PAFC-16, #511075	Caymann Calbiochem

Name	Details	Company
SYTOX Green	5 mM DMSO, Excitation/Emission: 504/523 nm, S7020	Invitrogen, D
U0126	CAS: 109511-58-2, MW= 380.50, #662005	CalBiochem, USA
U75302	CAS: 119477-85-9, MW = 361.50, sc-201331	Santa Cruz

1.3 Antibodies

IB = Immunoblotting

Antigen	Type	Organism	Company	Concentration used for IB*	Blocking buffer for IB*
CD66b, GPI FITC	Monoclonal	Mouse, MsIgM	BD Pharmigen (555724)		
Anti-α-Tubulin 50 kDa	Monoclonal	Mouse	Sigma Aldrich (T9026)	1:1000 1 : 10000	2%BSA in TBST
CD62L, L-selectin PE	Monoclonal	Mouse Ms IgG1	BD Pharmigen (555544)		
HRP rabbit ImmunoPure® antibody	Secondary	goat anti-rabbit IgG (H+L)	Thermo Scientific (# 31460)	1:10000	TBST
HRP mouse ImmunoPure® antibody	Secondary	goat anti-mouse IgG (H+L)	Pierce (# 31430)	1:10000	TBST
Phospho- p44/42 ERK1/2	Monoclonal	Mouse	Sigma Aldrich (#M8159)	1:1000	5% Skim milk/TBST or 2%Choco/TBST
Phospho- p44/4, ERK1/2	Monoclonal	Rabbit	Cell Signalling (#9101S)	1: 1000	5% Skim milk/TBST 2%BSA in TBST
p44/42 MAPK (ERK 1/2) (Thr202/Tyr204) Total ERK1/2	Monoclonal	Rabbit	Cell signalling (#M4695)	1:1000	5% Skim milk/TBST 2%BSA in TBST

1.4 Buffers and solutions

Buffer	Composition
10X PBS (phosphate buffered saline)	1.37 M NaCl 27 mM KCl 0.1 M Na_2HPO_4 20 mM KH_2PO_4 pH = 7.4
10x Running buffer	250 mM TRIS 2 M Glycine 1 % (w/v) SDS
10X TBS (TRIS-buffered saline)	0.2 M TRIS-HCl 1.5 M NaCl pH = 7.4
5X SDS-PAGE loading buffer	0.225 M TRIS-HCl pH = 6.8 50% glycerol 5% SDS-b 0.05% Bromophenol Blue 700 mM β-Mercaptoethanol
Alkylating solution for protein digestion	55 mM iodacetamide in 25 mM NH_4HCO_3
Ammonium bicarbonate buffer	50 mM ammonium bicarbonate Filter 0.2 µm
APS solution	10 % Ammonium persulfate (w/v)
Binding buffer (TBS) for pulldown using NHS beads	50 m M Tris 150 mM NaCl pH 7.5
Block A buffer for pulldown using NHS beads	0.5 M Ethanolamine 0.5 M NaCl pH 8.3
Block B buffer for pulldown using NHS beads	0.1 M Sodium acetate 0.5 M NaCl

	pH 4.0
C18 Disks	Empore 2215-C18 store in small petri dish seal with parafilm
Cell freezing buffer	90% (v/v) FBS 10% (v/v) DMSO
Chloracetamide Stock*	0.5 M choracetamide in H2O * newly made
Coomassie staining solution for proteomics	Solution A: 2 % (v/v) ortho-Phosphoric acid 10 % (w/v) Ammonium sulphate Solution B: 5 % (w/v) Coomassie Brillant Blue G-250 Solution C: Mix A+B add 20% MeOH (v/v) before use
Coupling buffer A for pulldown using NHS beads	0.15 M Triethanolamine 0.5 M NaCl pH 8.3
Differentiation medium for PLB, NB4, HL60 cells	RPMI with phenol red 5 % (v/v) FBS 1 % (v/v) L-Glutamate 1 % (v/v) penicilium/streptomycin Differentiating agent: 5 µM KN-62 or 1.25% DMSO or 30 ng/mL GCSF or 2 µM ATRA
DTT Stock*	1 M DTT in 50 mM ammonium bicarbonate buffer * newly made
E1 buffer for protein digestion using STAGE Tips	1.1 µL DTT stock 13.75 µL trypsin stock (5 µg/mL) 1085.15 µL urea stock

	Always fresh
E2 buffer for protein digestion using STAGE Tips	11 µL chloroacetamide stock 1089 µL urea stock
Elastase storage buffer	20 mM sodium acetate 100 mM NaCl pH 5.0-6.0 store at -80^{o}C
Equilibration buffer for pulldown using NHS beads	1 mM HCl (ice cold)
Gel casting reagents	3.3 ml H_2O 4.0 ml 30% acrylamide mix 2.5 ml 1.5M TRIS.HCl, pH= 8.8 0.1 ml 10% SDS 0.1 ml 10% ammonium persulfate 0.01 ml TEMED
Granule preparation buffer	20 mM Hepes pH 7.4 100 mM KCl 3 mM NaCl 3 mM $MgCl_2$ 1 mM EGTA 100 mM Sucrose
Granule preparative lysis buffer for pulldown	20 mM HEPES pH7.4 100 mM KCl 3 mM NaCl 3 mM $MgCl_2$ 1 mM EGTA 100 mM Sucrose 0.1% NP40 0.1% Triton X-100 0.1% Tween 20 Complete EDTA free Protease Inhibitor(add freshly) phosphoSTOP (add freshly) 0.1 mM PMSF (add freshly)
Lysis buffer for pulldown	50 mM PIPES (pH 7.4) 50 mM NaCl 5 mM $MgCl_2$ 5 mM EGTA 0.1% NP40 0.1% Triton X-100 0.1% Tween 20

	Complete EDTA free Protease Inhibitor(add freshly) phosphoSTOP (add freshly) DTT orβ-Mercaptoethanol (add freshly)
Membrane stripping buffer	6M guanidine Hydrochloride
MPO storage buffer	20 mM Hepes 100 mM KCl 50% Glycerol
MPO substrate solution	1 mg O-phenylenediamine 10 ml PBS
PBST	PBS + 0.1% Tween 20
Phosphate buffer	10 mM Na_3PO_4 300 mM NaCl pH = 7.4
PMN lysis buffer for pulldown *****	50 mM HEPES pH7.4 150 mM NaCl 5 mM $MgCl_2$ 2 mM $CaCl_2$ 2 mM EGTA 100 mM Sucrose 0.1% NP40 0.1% CHAPS 0.1% Tween 20 Complete EDTA free Protease Inhibitor(add freshly) phosphoSTOP (add freshly) 0.1 mM PMSF (add freshly) * for neutrophil add 1 µL of DFP
PMN washing buffer for pulldown	PMN lysis buffer for pulldown 75 mM of $MgCl_2$ No protease inhibitors, nor fresh additives
Pseudomonas storage buffer	1 mL of LB 20% glycerol Store at -80^{o}C
Reducing solution for protein digestion	50 mM DTT In 25 mM NH_4HCO_3
RIPA buffer	50 mM TRIS pH 7.4 150 mM NaCl 0.25% Sodiumdeoxycholate 1% NP40 Alternative 1 mM EDTA PhosphoStop (add freshly) Complete mini (add freshly)

Separating gel buffer	1,5 M TRIS 0,4 % (w/v) SDS pH = 8.8 (HCl)
Stacking gel buffer	0,5 M TRIS 0,4 % (w/v) SDS pH = 6.8 (HCl)
Starving medium for adherent cancerous cell lines MDCK, HeLa	500 ml DMEM 5 ml L-Glutamate 5 ml non-essential amino acid 5 ml sodium pyruvate 5 ml penicilium/streptomycin
TBST	TBS + 0.1% Tween 20
Thawing medium for NB4, PLB, HL60	RPMI with phenol red 20% (v/v) FBS 1% (v/v) L-Glutamate, 1% (v/v) penicilium/streptomycin
Transfer or blotting buffer	25 mM TRIS.HCl 0.2 M Glycine 50 mM TRIS-HCl pH = 7.4 25% MeOH (add before use)
TRIS Buffer (TBS)	50 mM TRIS pH 7.5 autoclave
Trypsin digestion solution for protein digestion using STAGE Tips (Stock solution, 0,1 µg/µL)	25 µg Trypsin in 250 µL 10 mM HCL. Store at -80 °C for 4 weeks max.
Trypsin stock for protein digestion	0.4 µg/ µL Trypsin in 10 mM HCl store at -20°C
Trysinating solution	
Urea Stock*	1.2 g urea 9 mL 50 mM TRIS-Buffer (pH 7.5)

	*newly made
Wash solution 1 for pulldown	25 mM NH_4HCO_3 Acetonitrile ratio 3:1
Wash solution 2 for pulldown	25 mM NH_4HCO_3 Acetonitrile ratio 1:1
Washing buffer for pulldown	Lysis buffer for pulldown 75 mM of $MgCl_2$ No protease inhibitors, nor fresh additives

2. Mammalian cell culture

During the course of this work, several cell lines and cells isolated from donors were used. All cell culture were approved by safety class S1 and S2. The waste generated was discarded according to required S2 protocol.

2.1 Cell lines

CELL LINE	NAME	ORGANISM	ORIGIN TISSUE	MORPHOLOGY	CELL MEDIUM
HeLa	**"Henrietta Lacks"**	**Human**	**Cervical Cancer**	**Epithelium; Adherent**	DMEM 10% (v/v) FBS 1% (v/v) L-Glutamate 1% (v/v) non-essential amino acids 1% (v/v) sodium pyruvate 1% (v/v) penicilium/streptomycin
HL60	**Human Leukemia**	**Human**	**Myeoloblast**	**Blood cells; Suspension**	RPMI with phenol red 10% (v/v) FBS 1% (v/v) L-Glutamate 1% (v/v) penicilium/streptomycin
NB4	**Human promeolocytic**	**Human**	**Myeoloblast**	**Blood cells; Suspension**	RPMI with phenol red

	leukemia				10% (v/v) FBS 1% (v/v) L-Glutamate 1% (v/v) penicilium/streptomycin
PLB-985	**Human diploid myeloid leukemia**	**Human**	**Myeloblast**	**Blood cells; Suspension**	RPMI with phenol red 10% (v/v) FBS 1% (v/v) L-Glutamate 1% (v/v) penicilium/streptomycin
PLB-MD	**Human diploid myeloid leukemia**	**Human**	**Myeloblast**	**Blood cells; Suspension**	RPMI with phenol red 10% (v/v) FBS 1% (v/v) L-Glutamate 1% (v/v) penicilium/streptomycin

2.1.1 Cell Counting

To count the cells three main methods were used: the hemocytometer, Countess ™, and CASY.

2.1.1.1 Hemocytometer method

10 µL of a mixture (100 µL) containing cells (10 µL) and trypan blue (90 µL) was placed in the hemocytometer and covered with a coverslip. The cells were counted with a 10X objective using a light microscope. The dilution factor was determined and the total cell amount was calculated.

2.1.1.2 Countess ™ method

10 µL of a mixture (100 µL) containing cells (10 µL) and trypan blue (90 µL) was placed in the hemocytometer and covered with a coverslip. The chamber was placed in the Countess slot and the microscope had to be manually focused. The cell number was determined automatically.

2.1.1.3 CASY counting method

CASY cell counting method is similar to the flow cytometer. 10µL of the cells were dissolved in of CASY Buffer (10 mL) in a siliconized CASY tube. The tube was placed into the instrument to count the cells. Using a program incorporated in the instrument, cells were counted automatically and a viability graph was given.

2.1.2 Cell maintenance

Cells were incubated at 37°C at 5% CO_2 until confluence or in the case of suspension cells until concentration of $1x10^6$/mL was reached. The medium monitored via the phenol red used as a pH indicator for nutrients are depleted. For adherent cells, the old medium was discarded. Cells were washed twice with PBS buffer (10 mL) and detached from the surface with trypsin/EDTA solution (5mL).Cells were incubated for 2-5 min at 37°C, 5% CO_2 and immediately re-suspended in 5-10 mL of fresh medium. Cells were pelleted (1250 rpm, 5 min) and resuspended with medium (10 mL) and transferred to a cell culture flask (sterile, 75cm^2) in a 1:13 dilution. For the differentiable cell lines (HL60, NB4, PLB) avoid pH changes since it can start of cell differentiation. Cells were counted and seeded at the appropriate concentration, usually $1.0x10^5$/mL in a 25 cm^2. Cells should not be kept in high passage numbers, such as 24 or for longer than 3 months, after they are thawed.

2.1.1 Long term storage of cells

The lowest passage number is preferred when storing cells or when they have only been a week in culture to make sure that the frozen cells are healthy and non-apoptotic. A minimum of $1.0x10^6$ per mL as final concentration is advised. Once the cells were collected and the supernatant was discarded, cells were washed with PBS twice. The cell pellet was resuspended in freezing buffer (9:1 (v/v) FBS:DMSO). The cell suspension is aliquoted (1-1.5 mL of $1.0x10^6$ cells/ mL) in properly labeled cryotubes. Cells were gradually frozen until and then stored in liquid nitrogen for long term storage.

2.1.2 Defrosting cells

Cells were thawed at room temperature and were rapidly diluted into a 15mL of thawing medium. Certain cell lines require a thawing medium which contains higher concentration FBS (15 or 20 % instead of 10% (v/v)). The FBS concentration varies depending on the cell line. The cells were pelleted (10 min, 800 rpm). The supernatant was removed and cells were placed in growth medium (8 mL, 50 cm^2 flask). For PLB, NB4 and HL60 cells, after thawing the cells were washed three times with thawing medium (RPMI with phenol red 20% (v/v) FBS, 1% (v/v) L-Glutamate, 1% (v/v) penicilium/streptomycin, section 2.2). The cells were incubated in the thawing medium for 3 days. On the third day, cells were passaged into normal growth medium.

2.2 Isolation of human blood cells

2.2.1 Culture conditions

Human neutrophils were used extensively in the work on this thesis. Consequently, it was important to avoid unnecessary centrifugation/vortexing/mechanical steps and to work with them promptly since they have a short life and they are easily pre-activated. Conditions were established to store purified neutrophils for sufficient time to screen the library with a single batch of cells. Neutrophils isolated from donors were viable for 6 hours, when kept at room temperature (approximately 25^oC).

For longer storage, blood could be kept at 4°C before isolation. Notably, storing neutrophils at 4°C should be avoided.

2.2.2 Isolation of human peripheral blood neutrophils

Human neutrophils were isolated from peripheral blood using a density gradient method (Aga et al., 2002). The study was approved by the ethics committee of the Charité Medical Centre, Berlin. Peripheral venous blood from a healthy donor was drawn using heparin (10 U/ml) or heparin containing commercial tubes. Carefully, blood (5-6 mL) was layered tube (15 mL) onto Histopaque-1119 (5 mL, 1:1) using a sterile plastic pipettes. It is important to use sterile plastic pipettes to avoid cell degradation. The blood was centrifuged (20 min, 800*g*) at room temperature. It is important that no "break" is on during the centrifugation and that the acceleration and deceleration is kept to a minimum. Histopaque separates blood into plasma (top phase), peripheral blood mononuclear cells (PBMC) (interphase), neutrophils contaminated with red blood cells (RBC; bottom phase) and RBCs (pellet). The top phase was discarded using a vacuum pump with a sterile glass Pasteur pipette. The red diffused layer (neutrophil-rich phase) was collected and transferred to a sterile falcon tube (15 mL). The red (RBC phase) pellet was discarded. Cells were washed with washing buffer (PBS with 0.5% HSA). Cells were mixed gently and centrifuged (10 min, 300*g*) at room temperature. The supernatants were discarded carefully using a vacuum pump with a sterile glass Pasteur pipette. The pellets were resuspended in the falcon tubes with PBS (2-3 mL). During the spinning cycles, the Percoll-gradients are freshly prepared and can be stored for maximum 2 days at 4°C (important: storage is possible as Percoll dilution or gradient stock, not as a gradient). This is a discontinuous gradient consisting of Percoll-layers with densities of 1.105 g/ml, 1.100 g/ml, 1.093 g/ml, 1.087 g/ml, and 1.081 g/ml.

2.2.2.1 Gradient Preparation

The Percoll gradient stock was prepared with sterile Percoll (36 mL) and sterile 10X PBS (4 mL). The preparation of gradients of 85, 80, 75, 70 and 65% was as follows.

Conc. of Gradient	Gradient Stock	1 x PBS
85%	8.5 ml	1.5 ml
80%	8.0 ml	2.0 ml
75%	7.5 ml	2.5 ml
70%	7.0 ml	3 ml
65%	6.5 ml	3.5 ml

Using sterile pipette in a falcon tube (15 mL), the 85% gradient (2 mL) was added tube, followed by 80% gradient (2 mL) layering very slowly and carefully and continued in this manner in sequential order until gradient 65%. The final tube contained a gradient ranging from 85% to 65% Percoll with the final volume of 10ml. The resuspended cells (2-3 mL max.) are carefully layered onto the gradient. The tubes were centrifuged (20 min, 800 *g*) at room temperature. The interphase between 70-75% Percoll layers are collected and transferred to a fresh tube. This layer looks like a white cloud. The cells were washed with washing buffer in the same manner as indicated before. The tubes are centrifuged (10 min, 200*g*) at room temperature. The pellet is re-suspended with RPMI-HEPES medium (5 mL) and cells are counted.

2.3 Cell differentiation

Cells (PLB, NB4, HL60) were seeded at $1x10^6$/mL in differentiation medium containing 5% FCS RPMI medium supplemented with several different stimulators or combinations of the differentiating agent (Papayannopoulos et al., 2010; Tsuchiya et al., 2010). The cells were allowed to differentiate for different time periods. Every two days the medium was changed. Cells were microscopically inspected for viability. After the differentiation time, cells were centrifuged (5min, 1250 rpm) and washed with PBS (10 mL). Cells were fixed with 4 %PFA and assessed by GIEMSA staining and for neutrophil makers CD15/CD66b using FACS.

2.4 Cytotoxicity Assay

2.4.1 Lactate dehydrogenase (LDH) cytotoxicity assay in immune cells

To detect cytotoxic compounds, a colorimetric assay was employed based on the detection of lactate dehydrogenase (LDH) activity in the extracellular space. Neutrophils ($5x10^4$ cells/mL) were seeded per well in a 96-well plate and incubated with serial dilutions of the compounds (100µL). The controls were the following: background control (assay medium, no cells), spontaneous LDH release (cells alone), substance control (cells with vehicle DMSO) and maximum LDH release (cells treated with Triton X 2%). Cells were incubated (6h, 37°C at 5% CO_2). After incubation, LDH activity was detected according to the manufacturer's instructions. Absorbance was determined at 490 nm using the Monolight 3096 reader.

3 NET Induction and Inhibition

3.1 General Protocol for NET Activation

Neutrophils ($2.5x10^5$ cells) were seeded in a 24-well plate flat bottom. In the case of experiments performed in 96-well plate, $5x10^4$-$5x10^5$ cells were seeded depending on the experiment. Alternatively, 1 $x10^6$ cells were seeded in 6-well flat bottomed plates. Cells were allowed to settle (10-20 min) at room temperature or in some cases at 37°C at 5% CO_2. Neutrophils were activated

with phorbol myristate acetate (PMA). Cells were incubated at 37°C at 5% CO_2 and microscopically monitored until NET formation was complete (process takes 2.5-4h). For SYTOX Green viability and staining, SYTOX Green (2 µM, 10 µL, 10min) was added and samples were incubated (10min). Fluorescence intensity (ex/em 485/518 nm, room temperature) was recorded. For further investigation cells were fixed with PFA (4%, 10 µL) and permeabilized with Triton X-100 (0.01 %, 10 µL). Later, images were acquired on an epifluorescence microscope or using the automated microscope. Image analysis (determination of different nuclear morphologies) was performed using Scan^R software or Cell Profiler (www.cellprofiler.org) (Kamentsky et al., 2011) and Cell Analyzer (www.cellprofiler.org) (Jones et al., 2008) software. For time course experiments, cells were fixed with PFA (4%, 10 µL) at different time points. For microscopy experiments, glass slides were placed on plates and washed with PBS (3mL, 2 times) before the cells were seeded. Cells were seeded (1 $x10^6$ cells), as described above. After NET formation, cells were fixed with PFA (4%, 10 µL) and analyzed according to specific protocols.

3.1.1 NET activation with eicosanoic lipids

The lipids were dissolved in fatty acid-free BSA as a vehicle in medium. Neutrophils (see section 3.1) were activated with 1-3 µM of platelet activating factor (PAF-(C16)), 1-3 µM of 1–2-dioctanoyl-sn-glycerol a potent analog of diacylglycerol (DAG) or 1-3 µM of arachidonic acid. Each lipid was added individually and promptly to avoid decomposition of the lipid. DMSO and unstimulated cells were used as controls. NET formation was shorter using this stimulus.

3.1.2 NET activation with glucose oxidase

Cells (section 3.1) were activated with 100mU/mL of glucose oxidase (GO). NET formation occurred after 1-2 hours after activation.

3.1.3 NET activation with Bacteria

3.1.3.1 *Pseudomonas aeruginosa* PA14

A fresh culture *Pseudomonas aeruginosa* PA14 was made by shaking overnight at 37°C in LB medium (5 mL). The bacterial culture was washed PBS (10 mL) and centrifuged (10 min, 4000 rpm). The bacterial pellet was resuspended in medium (2 mL). The MOI was determined by measuring optical density (OD) (OD = 1 = $1x10^9$ cells/mL). Medium was removed by centrifugation (10 min, 4000 rpm). Bacteria were opsonized (30 min, 37°C) in FBS (10%). Neutrophils ($5x10^4$ cells/well) were seeded in a 24-well plate and the inhibitors were added at concentration pre incubated (30min, 37°C). Neutrophils were activated with MOI of 100 followed by the general protocol described in (3.1) using PMA as control. The general 3.1 protocol, was slightly modified cells were not fixed nor permeabilized. Images were collected immediately and plates are discarded (cannot be preserved for later use due to bacterial overgrowth and safety).

3.1.3.2 *Helicobacter pylori* (experiment performed by Abdul Hakkim)

Helicobacter pylori type 1 strain P12 was grown on brain heart infusion agar plates supplemented with 10 µg/liter of vancomycin, 1 µg/liter of nystatin, and 5 µg/liter of trimethroprim. Plates were incubated at 37 °C in a microaerophilic atmosphere and were sub-cultured every 2 days. Neutrophils were activated with MOI of 100 followed by the general protocol described in (3.1) using PMA as control. The general 3.1 protocol, was slightly modified cells were not fixed nor permeabilized. Images were collected immediately and plates are discarded (cannot be preserved for later use due to bacterial overgrowth and safety).

3.2 General Protocol for NET Inhibition

For the initial screen, compounds were diluted (30 µM, final concentration) in phenol red–free RPMI medium supplemented with 10 mM HEPES. $5x10^4$ neutrophils were seeded per well in a clear bottom 96-well plate in presence of the compounds and pre-incubated (30 min, 37°C at 5% CO_2). Followed by neutrophils activation with PMA (40 nM, 10 µL) to induce NET formation. Unstimulated cells and cells treated with DMSO, 30 µM Diphenylidonium chloride (DPI), or PMA only were used as controls. Cells were incubated (4 h, 37°C at 5% CO_2). For SYTOX Green viability and staining, SYTOX Green (2 µM, 10 µL, 10min) was added and samples were incubated (10min). Fluorescence intensity (ex/em 485/518 nm, room temperature) was recorded. For further investigation cells were fixed with PFA (4%, 10 µL) and permeabilized with Triton X-100 (0.01 %, 10 µL). Later, images were acquired on epifluorescence microscope or using the automated microscope. Image analysis (determination of different nuclear morphologies) was performed using Scan^R software or Cell Profiler (www.cellprofiler.org) (Kamentsky et al., 2011) and Cell Analyzer (www.cellprofiler.org) (Jones et al., 2008) software. A quality control was performed manually.

3.2.1 Automated Protocol for NET Inhibition (experiments performed by Abdul Hakkim)

Library compounds were arrayed by a pipetting robot Zymark SciClone ALH 500 in conjunction with a Tecan EvoWare robot in sterile 384, clear bottom, microtiter plates (MTPs). The final reaction volume 20 µL, neutrophil suspension (10 µL of a 10,000) were seeded in the plates. The cells were allowed to settle (10 min, room temperature) and the compound library was added (100 µM final concentration, 0.2 µL). Followed by PMA (40 nM, 10 µL) addition, DMSO was added as control. For SYTOX Green viability and staining, a mixture (10 µL, 10min, room temperature) containing SYTOX Green (2 µM) and PFA (2%) was added and samples were incubated. Fluorescence intensity (ex/em 485/518 nm, room temperature) was recorded by a Genios Pro MTP reader. To analyze the

nuclear area, cells were permeabilized with Triton X-100 (0.01%). The images (10x objective, 2 images/well, 30 ms exposure, 10 µm offset from the plate bottom) were acquired using GFP channel in a Scan^R automated microscope. The images of DNA staining were analyzed using the Scan^R automated microscopy system.

4 Microscopy

4.1 Immunocytochemistry

Glass slides were placed on 24 well plates and washed with PBS (3mL, 2 times). Neutrophils ($2.0x10^5$ cells) were seeded and allowed to settle (10min, room temperature). The inhibitors were added at the concentration needed and the cells were activated depending on the experiment (section **3.1** and **3.1.1-3.1.3**) and incubated (2.5-4 h, 37^{o}C in 5% CO_2). After NET formation, cells were fixed with PFA (4%, 10 µL, 10 min). Cells were washed twice with washing buffer composed of BSA (3%, 30 µL) in PBS. Cells were permeabilized with a solution of Triton-X (0.5%), BSA (3%) in PBS. Cells were washed three times with washing buffer and blocked with blocking buffer (3% normal donkey serum, 3% cold water fish gelatin, 1% bovine serum albumin, and 0.05% Tween 20 in PBS) (30 µL, 30min, room temperature). After two washes with washing buffer, the cells were incubated with primary antibodies (dilution for the primary antibodies is in the materials table **1.3**, 1hr, 37^{o}C) followed by three washes with washing buffer and incubation with secondary antibodies, which were coupled to fluorophores (45min, 37^{o}C) in the dark. For DNA detection, Hoechst 33342 (1:1000), DAPI (1:1000), or SYTOX Green were used. Specimens were mounted in Mowiol or AquaPoly/Mount and analyzed with epi-fluorescence microscope. Slides were stored at 4^{o}C.

4.2 Quantitative Analysis of Images Using Scan^R (performed by A. Hakkim and protocol modified from his original protocol)

Following image acquisition (**section 3.2.1**), quantitative measurements from each image were performed based on the size of the nuclei and detailed morphology of nucleus during NET formation. For the detection of nuclei with the Scan^R image analysis software an algorithm was applied based on an intensity threshold for the SYTOX signal. The algorithm in the image analysis software detects objects based on an intensity threshold for the fluorescent signal. The sensitivity of the fluorescence was set (200) very low to allow the software to compute multi-lobulated nucleus of naïve neutrophils as single particles. At this threshold (200), the lowest intensities measured/background of zero and a maximum of 4095. After the image acquisition a background correction was performed. The low threshold also increases the object size. The object size and threshold had to be optimized to detect the appropriate morphologies of lobulated nuclei and decondensed nuclei simultaneously. After optimization the sizes were described as follow: lobulated

nuclei are 1000 pixels, delobulated nuclei are 800 pixels, decondensed are 2000 pixels and NETs are <2000 pixels. All detected objects were plotted with Heywood Circularity Factor (HCF) against perimeter and gates were applied separating the different nucleus types. The HCFs were established as follow: lobulated nuclei are 1 to 2, delobulated nuclei are 1, decondensed are 1 and NETs are > 2. To verify that the algorithm was running appropriately it was verified manually to confirm that the quantification represented the images.

4.3 Quantitative analysis using CellProfiler and CellProfiler Analyst

After initial training by Marc Bickle from the screening facility Max Planck Institute of Molecular Cell Biology and Genetics in Dresden, I established the new pipeline using CellProfiler and CellProfiler Analyst (Jones et al., 2008; Kamentsky et al., 2011). CellProfiler is a free image-analysis software provided by the BROAD institute available on http://cellprofiler.org/ The pipeline was trained to recognize the SYTOX green stained nuclei based on the size of the nuclei and detailed morphology of nucleus during NET formation. Images containing predominantly each morphology (lobulated, delobuted, decondensed, NETs) were used to establish the parameters. Based on our previous experience, I used of chemical NET inhibitors to obtain images with the specified nuclear morphologies. The lobulated nuclei were unstimulated cells, the delobulated images were obtained by incubating them with DPI and activating them with PMA following the general NET protocol 3.1. The decondensated nuclei were obtained by incubating the cells with apomorphine and following protocol 3.1. The NET nuclei were obtained by stimulating the cells with PMA. Images were selected to initialize the basic pipeline. This basic pipeline was optimized for each individual microscope that was employed as a constant was the image format which was the .tiff format. To further train each pipeline several images were collected from each particular microscope and the program was trained to detect and the parameters were modified to obtain accurate results. After each experiment, quality control was performed manually to make sure that the pipeline was running smoothly.

5 Enzymatic activity methods

5.1 Determination of ROS Production

ROS production, using an *in situ* horseradish peroxidase-luminol complex, was measured by means of chemiluminescence. Oxidation of luminol-HRP amplified by ROS causes emission of light that allows the detection ROS formation (Liu et al., 1996). Neutrophils (1 x10^6 cells, 50 µL) were seeded per well in a 96-well plate. Compounds were added (30 or 15 µM final concentration, 30 µL) and cells were incubated (30 min, 37^{o}C in 5% CO_2). Followed by the addition a mixture (20 µL) containing luminol (500 µM) and horseradish peroxidase (HRP) (120 U/mL). Finally, neutrophils

were activated PMA (40 nM, 10 µL) and chemiluminescence was continuously recorded (every 2 min, 2 h total) at 37°C.

5.2 Determination of activity neutrophil elastase using chromogenic substrate

Neutrophil elastase (NE) was reconstituted in elastase buffer. Compound (15 µM, 50 µL) and NE (25 ng/mL, 50 µL) dissolved in sodium phosphate buffer were added to the wells of a clear 96-well plate in and incubated (10 min, room temperature). The NE inhibitor G8419 (15 µM, 100 µL) and DMSO were used as controls. The reaction was initiated with NE substrate I in same buffer (12.5 µM, 100 µL). The absorbance was immediately recorded (410 nm, every 1 min, 2 h total, 37°C) using a Monolight 3096 reader.

5.3 Determination of activity of myeloperoxidase using a chromogenic substrate

Myeloperoxidase (MPO) was reconstituted in MPO buffer. Compound (15 µM, 50 µL) and MPO (100 nM, 40 µL) in HBSS buffer were added to the wells of a clear 96-well plate followed by incubation (10 min, room temperature). The MPO substrate (100 µL) was added. DMSO and the MPO inhibitor, 4-aminobenzoic acid hydrazide (ABAH) (15 µM, 50 µL) were used as controls. The reaction was initiated with H_2O_2 (0.5 mM, 10 µL). The absorbance was immediately recorded (450 nm, every 1 min, 2 h total, 37°C) using a Monolight 3096 reader.

6 Biochemical methods

6.1 Preparation of cell lysates

Several methods required the lysis of cells for affinity chromatography experiments, i.e.pulldown. Consequently, several methods were developed and optimization of buffers was needed.

6.1.1 Preparation of human neutrophil cell lysate

Cell lysis of neutrophils is complicated due to large amounts of proteases that are released. To solve this problem it was required to use potent protease inhibitors such as phenylmethanesulfonyl fluoride (PMSF) and diisopropyl flourophosphate (DFP) in different combinations. Before handling DFP is necessary to have the antidote and full knowledge for handling DFP. Details can be found in the book “Prudent practices for handling hazardous chemicals in laboratories, 1980.” DFP is extremely toxic. Atropine antidote together with 2-PAM (pyridine-2-aldoxime) should be present for rapid administration if necessary. DFP is rapidly decomposed in a 2 M NaOH solution. There should be a large container with basic solution available in a HEPA ventilated hood. DFP was the only protease inhibitor capable of stopping protease degradation. During the course of this work, several different lysis buffers were optimized and used for the experiments presented. In the case of western blotting techniques depending on the detection of the protein of interest different lysis

buffers were utilized. For proteomic purposes, optimization of the neutrophil lysate generation was crucial decrease contamination and increase reproducibility. The methods used for PMN cell lysing are described. Every neutrophil lysate was prepared with freshly isolated neutrophils.

6.1.2 Preparation of human neutrophil cell lysate using nitrogen bomb

PMN were isolated from human fresh blood as (**section 2.2.2**). Cells ($5x10^7$-$1x10^8$ cells) were placed in a falcon tube (15mL) and centrifuged (10 min, 800 rpm, room temperature) and washed with PBS (10 mL, ice cold) and centrifuged (10 min, 800 rpm, room temperature). Cells were resuspended in ice chilled granule preparation buffer (2-4 mL). The nitrogen bomb was chilled on ice. An aliquot of cells (2-3µl) were set aside in a glass slide for later microscopic verification of the lysis. Cells were placed in the nitrogen bomb, nitrogen pressure (400 psi, 2-5 min) was applied. Pressure was released and the cell lysate was collected from the nitrogen bomb. The collected lysate was compared via microscopy to the collected aliquot of intact cells to verify proper lysis. The lysate was placed in a siliconized Eppendorf tube, and centrifuged (15 min, 300 x g, -4˚C). This low speed supernatant (LSS, i.e. cytosol fraction) was collected and stored at 4^oC for 4-5days on ice. The LSS from ~$5.3x10^7$/mL produces ~1.9 mg/mL of protein.

6.1.3 Preparation of human neutrophil cell lysate using DFP

PMN were isolated from human fresh blood as (**section 2.2.2**). Cells ($5x10^7$-$1x10^8$ cells) were placed in a falcon tube (15mL) and centrifuged (10 min, 800 rpm, room temperature) and washed with PBS (10 mL, ice cold) and centrifuged (10 min, 800 rpm, room temperature). Protease inhibitors were added freshly to 10mL of neutrophil lysis buffer: 1 tablet of complete EDTA free protease inhibitor, 1 tablet of phosphoSTOP, and 0.1mM PMSF and chilled on ice. Cells were resuspended with lysis buffer (2-4mL, 0-4^oC) in low binding tubes (each tube holds a maximum of 2 mL) and placed on ice. Inside a chemical hood with HEPA filter, DFP (100 µM) was added to each tube by syringe and tubes were incubated (5-10min, 0-4^oC on ice). After the addition of the DFP, the tubes were incubated (30min to 1h, 0-4^oC on ice). Cells were lysed mechanically with a syringe and centrifuged (15min, 13 000 rpm, 4^oC). The supernatant was transferred to a new low binding tube. Protein concentration was determined directly using Lowry method (**section 6.3.2**). Lysates were stored at -80^oC.

6.1.4 Preparation of human neutrophil cell lysates using SDS loading buffer

Neutrophils (1 $x10^6$ cells) were seeded in 6-well plates (flat bottom). Compounds (30 µM, 500 µL) and controls were added and incubated (30 min, 37°C at 5% CO_2). Cells were activated with EGF (200ng/ml) or PMA (40 nM) and incubated (90 min, 37°C at 5% CO_2). The supernatant was

removed, 4x SDS loading buffer was added to the samples directly to lyse the cells avoiding degradation.

6.1.4.1 Neutrophil lysis using DFP

Neutrophils were seeded as explained above (**section 6.1.4**). After incubation with the NET activator and the compounds the medium was removed carefully. Inside a chemical hood with HEPA filter, DFP (100 µM, 5 µL) was added to each well (5-10min, 0-4^{o}C on ice). Chilled RIPA buffer (100 µL) was added to each well. The cells were mechanically removed from the well using a cell scraper and collected in low binding tubes. To remove precipitates, lysates were centrifuged (15 min, 13000 rpm, 4 °C) and transferred to new low binding tubes. Protein concentration was determined using the Lowry method.

6.1.5 Preparation of HL60 cell lysate for pulldown experiments

HL60 cells were allowed to grow to 1x10^{6}/mL in normal grow medium in flask depending on amount of protein needed. Cells were collected by centrifugation (5min, 1250 rpm, room temperature) and resuspended in differentiation medium (RPMI medium supplemented with 1.25% DMSO). Cells were allowed to differentiate for 5 days and the medium was refreshed (every 2 days). After differentiation, cells were centrifuged (5 min, 1250 rpm, room temperature) and washed with PBS (10mL). After removal of the PBS, cells were resuspended in lysis buffer (2mL) that was freshly supplemented with protease inhibitors and transferred to low binding tubes. Cells were incubated (30min to 1h, 0-4^{o}C on ice). Cells were lysed mechanically with a syringe and centrifuged (15min, 13 000 rpm, 4^{o}C). Supernatants were transferred to new low binding tubes and the protein concentration was determined using Lowry method (**section 6.3.2**).

6.2 Cell Fractionation Method

6.2.1 Neutrophil Low Speed Supernatant preparation

Neutrophils were purified as previously described in **section 2.2.2**. Cells (5 x 10^{7} cells/ml to 1x10^{8} cells/mL) were collected centrifuged (10 min, 800 rpm, room temperature) and washed with PBS (10 mL, ice cold) and centrifuged (10 min, 800 rpm, room temperature). Cells were resuspended in ice chilled granule preparation buffer (2-4 mL). The nitrogen bomb was chilled on ice. An aliquot of cells (2-3µl) were set aside in a glass slide for later microscopic verification of the lysis. Cells were placed in the nitrogen bomb, nitrogen pressure (400 psi, 2-5 min) was applied. Pressure is released and the cell lysate is collected from the nitrogen bomb. The collected lysate was compared via microscopy to the collected aliquot of intact cells to verify proper lysis. The lysate was placed in a siliconized Eppendorf tube, and centrifuged (15 min, 300 x g, -4˚C). This low speed supernatant (LSS, i.e. cytosol fraction) was collected and stored at 4^{o}C for 4-5days on ice.

6.2.2 Neutrophil High Speed Supernatant and High Speed Pellet preparation

The high speed supernatant (HSS, cytosol without granules) high speed pellet (HSP, mitochondria membrane and granules) were prepared by collecting the LSS (**section 6.2.1**), followed by ultracentrifugation (1 h, 100,000 x g, 4^{o}C). The HSS section was stored in granule prep buffer. The HSP pellet is resuspended in granule prep buffer (1 mL). HSS/HSP is stable on ice at 4^{o}C for 4-5 days.

6.3 Determination of protein concentration

To determine the protein concentrations of cell lysates two main methods were utilized: the Bradford assay and the Lowry method (**sections 6.3.1-6.3.2**).

6.3.1 Bradford Assay

The Bradford assay measures the protein concentration by means of colorimetry at 595 nm. Bradford stock solution was made and titrated with known concentrations of BSA (0 to 5 µg) using linear regression curve. In a disposable cuvette, Bradford solution (1 mL) and the BSA solution (1 µL) was mixed and incubated (5min) and the absorbance is recorded. Standard curve is determined and the equation was obtained to calculate future protein concentration using this Bradford stock solution. To determine the protein concentration of unknown protein solutions, the stock Bradford solution (1mL) was mixed with protein solution (1 µL) and incubated (5min) and the absorbance is recorded. Using the equation the protein concentration is determined.

6.3.2 RC DC Protein Lowry Assay

The RC DC Protein Assay kit from Biorad was employed. A stock BSA solution (10 mg/mL) was used to obtain a standard curve (BSA concentrations were 0.5 µg/mL to 1.5 µg/mL). The assay was performed according to the manufacturer's instructions. Using linear regression a standard curve was obtained to determine the concentration of the samples. In a 96-well plate, a mixture containing sample and the solutions from the kit (5 µL, 20 µL of solution A, 200 µL of solution B) were mixed and incubated (15 min). The absorbance was recorded within an hour (750 nm, room temperature) using a Monolight 3096 reader.

6.4 SDS-Polyacrylamide gel electrophoresis (SDS-PAGE)

6.4.1 SDS- PAGE gel casting

A casting chamber from Biorad was used to cast the gels. The percentage of the gel was chosen according to the sizes of proteins to be separated. The resolving gel solution was prepared and added first and covered with ethanol to get a straight gel. The gel was polymerized (1 h). In a prompt manner the ethanol layer was removed from the chamber. The gel stacking solution was

added and the loading comb was placed in the gel. Upon polymerization (30-60 min), the gels were used immediately or stored at 4^{o}C in a damp paper to keep moisturized for about 4-5days.

Composition for resolving gel/ stacking gel solution

	12% resolving gel (total = 10mL)	**11% resolving gel (total = 10mL)**	**Stacking gel (total = 1mL)**
Water	3.3mL	3.45 mL	0.68mL
Acrylamide	4.0mL	3.45mL	0.17mL
1.5 M TRIS-HCl, pH = 8.8 0.5M TRIS-HCl, pH = 6.8	2.5mL -	2.5 mL -	- 0.13 mL
10% SDS	0.1mL	0.1mL	0.01 mL
10% Ammonium Persulfate	0.1mL	0.1mL	0.01 mL
TEMED	0.01mL	0.01mL	0.001mL

6.4.2 SDS- PAGE electrophoresis

The samples were loaded onto the apparatus, usually MiniProtean 3 Gel Electrophoresis (Biorad) filled with SDS-running buffer. To avoid contamination with neighboring samples one empty pocket was left empty in-between if possible. The proteins wre separated (100V or 15mA, 15min) followed by an increase in voltage (200V, 35min or 30mA, 45min).

7 Immunoblotting

7.1 Protein transfer

7.1.1 Semi Dry transfer

After SDS-PAGE (**section 6.4**) the gel and filter papers, were pre-wet in cold transfer buffer for 5-10min. If a PVDF membrane was used, it was activated in methanol for 5 min prior to incubation in cold transfer buffer. A “sandwich” is made with two filter papers, PVDF membrane, gel, and two filter papers all wet in transfer buffer. The transfer was performed at 25V for 45min. The successful

transfer was assessed by visual inspection of the pre-stained protein ladder on the membrane and using staining with Ponceau S.

7.1.2 Wet Blotting transfer

The wet blotting technique is preferred when proteins are large. In advance two liters of transfer buffer was prepared and cooled to 4^{o}C. It also follows the same principle of section 7.1.1. The sandwich was placed vertically and additionally to the filter paper also sponges were used. Everything was be kept under buffer at all times to avoid air bubbles. The transfer was performed under stirring (4^{o}C, 100V for 1.5-2 h or 20V overnight).

7.2 Blocking of the membrane

After the protein transfer (**section 7.1.1-2**), the membranes need to be blocked to retain the proteins on the membrane. Membranes were placed in blocking buffer and shaken (1 h, room temperature). The blocking solution is highly dependent on the antibody and detection method. A common blocking buffer was 5% skim milk in TBST was used for HRP-based detection; for antibody detection by means of fluorescence LICOR blocking buffer was used.

7.3 Immunodetection of proteins immobilized on membranes

7.3.1 General protocol for detection using HRP-conjugated antibodies

After blocking (**section 7.2**) membranes were incubated with the primary antibody which was diluted at a concentration specified by manufacturer, typically in BSA (2%, in TBST), and incubated (1 at room temperature, or overnight at 4°C). The membrane was washed TBST (5 times, for 5 min/time) while shaking. The membrane was incubated with the secondary HRP-labelled antibody (1 h, room temperature) while shaking. Prior to development the membrane was washed again with TBST (3 time, 5 min/time) and TBS (1 time, 10 min/time). For detection, SuperSignal ® West Pico or Femto was used according to the manufacturer's instruction. Membranes were later detected by exposing them to an X-ray film or scanned using Odyssey Infrared Imaging System LI-COR, (Biosciences).

7.3.2 General protocol for detection by fluorophore-coupled antibody

After blocking (**section 7.2**) membranes were incubated with the primary antibody which was diluted at a concentration specified by manufacturer in LICOR blocking buffer with 0.1% Tween-20 avoiding light, and incubated (1 at room temperature, or overnight at 4°C). The membrane was washed PBST (5 times, for 5 min/time) while shaking. The membrane was incubated with the

secondary HRP-labelled antibody (LICOR blocking buffer with 0.1% Tween-20, 1 h, room temperature) while shaking. Prior to development the membrane was washed again with PBST (3 time, 5 min/time) and PBS (1 time, 10 min/time). Membranes were scanned using Odyssey Infrared Imaging System LI-COR, (Biosciences).

7.4 Detection of ERK phosphorylation via immunoblotting in NET formation

Neutrophils were seeded in 6-well at plate flat bottom 1 x10^6 cells and were activated with EGF or PMA in presence of inhibitors and controls without for 90 min at 37°C at 5% CO_2. The supernatant was removed, followed by addition of protease inhibitors to the samples following procedure in **section 6.1.4.1**. An equal amount of protein in each sample was separated (11% SDS/PAGE) and transferred to PVDF membrane. Membranes were blocked (5% skim milk/TBST) and probed with monoclonal mouse anti-p-ERK-1 and 2 (Sigma) and a polyclonal, rabbit anti-total ERK (Sigma). Membranes followed the general protocol on **section 7.3.1**.

8 Target identification methods

Protein target identification experiments consist of fishing for the protein by immobilizing the compound via a linker on to solid support (i.e. NHS beads). This enables to isolation of protein-compound complexes and identification of protein targets using mass spectroscopy.

8.1 Pulldown Experiments

8.1.1 Pulldown using biotinylated probes

Homogenized streptavidin magnetic beads (500 µL) were collected in a siliconized tube and washed with PBS (500 µl, 2min, room temperature). The biotinylated compound was diluted in PBS (500 µL, 10 µM). Compound was added to the beads and incubated (30min, room temperature, gentle rotation). After the incubation, beads were collected with magnetic separator and washed with PBS (500 µL). Cell lysate obtained in **section 6.1.3** (500 µL, 1 mg/ml) was added to the beads and incubated (1 h, 4°C, gentle rotation). The beads were washed with lysis buffer containing 75mM $MgCl_2$ without β-mercaptoethanol (2 times, 10 min/time, gently rotation) followed by additional washings with PBS (2 times, 10 min/time, gently rotation). This removes unspecific binders. For direct mass spectroscopy analysis, beads were collected and resuspendend in PBS (500 µL) and given to Monika Schmid directly. For in solution trypsin digestion the protocol in **section 8.2.2** was followed. Alternatively, the beads were boiled in SDS loading buffer (50 µL, 95^{o}C, 5 min, shaking) to release proteins from the solid support. The supernatant was collected in a new siliconized tube. In a Criterion precast gel 4-20% Gel (Biorad) SDS-PAGE, 40-45µl of the protein in SDS buffer were loaded on the gel and electrophoresis was performed. Gels were digested as described in **section 8.2.1**.

8.1.2 Pulldown using probes with free amine

Homogenized NHS magnetic beads (25 µL) were collected in a siliconized tube. Beads were collected with a magnetic separator and they were equilibrated with equilibration buffer (500µL, ice-cold 1 mM HCl, **section 1.4**). After removal of the equilibration buffer, the probe was coupled in coupling buffer (500µl, 10 µM probe, in 0.15M triethanolamine, 0.5M NaCl, pH. 8.3) and incubated (1h, room temperature, gentle rotation). After the incubation, beads were collected followed by blocking with blocking buffer A (500µL, 0.5M ethanolamine, 0.5M NaCl, pH = 8.3). Upon removal of buffer A, beads were washed with blocking buffer B (500µL, 0.1M sodium acetate, 0.5M NaCl, pH = 4.0). These washing steps (alternating blocking buffer A and B) were performed 3 more times. During the second addition of blocking buffer A beads were incubated (15min, slow rotation). After the last addition of blocking buffer B, beads were washed with binding buffer (500µL, 50mM TRIS, 150mM NaCl, pH.= 7.5). After the washing, cell lysate obtained in **section 6.1.3** (500 µL, 1 mg/ml) was added to the beads and incubated (1 h, 4°C, gentle rotation). The beads were washed with lysis buffer containing 75mM $MgCl_2$ without β-mercaptoethanol (2 times, 10 min/time, gently rotation) followed by additional washings with PBS (2 times, 10 min/time, gently rotation). For direct mass spectroscopy analysis, beads were collected and resuspendend in PBS (500 µL) and given to Monika Schmid directly. For in solution trypsin digestion the protocol in **section 8.2.2** was followed. Alternatively, the beads were boiled in SDS loading buffer (50 µL, 95^{o}C, 5 min, shaking) to release proteins from the solid support. The supernatant was collected in a new siliconized tube. In a Criterion precast gel 4-20% Gel (Biorad) SDS-PAGE, 40-45µl of the protein in SDS buffer were loaded on the gel and electrophoresis was performed. Gels were digested as described in **section 8.2.1**.

8.1.3 Pulldown using of photochemically-bound compound beads

The functionalization of the beads has been performed via immobilization using photo-crosslinking. These beads were made by Tobias Zimmermann at the RIKEN Global Research Cluster in Wako, Japan. following the established protocol developed by Osada and colleagues (Kanoh et al., 2003).

In a siliconized tube, homogenized beads (200 µL) were collected and washed with PBS (500 µL). It is important to note that these beads are not magnetic, in every step beads are allowed to settle and the buffers are carefully removed. After the removal of PBS, Cell lysate obtained in **section 6.1.3** (500 µL, 1 mg/ml) was added to the beads and incubated (1 h, 4°C, gentle rotation). The beads were washed with lysis buffer containing 75mM $MgCl_2$ without β-mercaptoethanol (2 times, 10 min/time, gently rotation) followed by additional washings with PBS (2 times, 10 min/time, gently rotation). For direct mass spectroscopy analysis, beads were collected and resuspendend in PBS (500 µL) and given to Monika Schmid directly. For in solution trypsin digestion the protocol in **section 8.2.2** was followed. Alternatively, the beads were boiled in SDS loading buffer (50 µL, 95^{o}C, 5 min, shaking) to release proteins from the solid support. The supernatant was collected in a new

siliconized tube. In a Criterion precast gel 4-20% Gel (Biorad) SDS-PAGE, 40-45µl of the protein in SDS buffer were loaded on the gel and electrophoresis was performed. Gels were digested as described in **section 8.2.1**.

8.2 Protein digestion methods for mass spectrometry analysis

8.2.1 SDS gel trypsin digestion

After the electrophoresis, the gel is placed in a Coomassie staining solution for proteomics (**section 1.4**) and gently shaking (overnight, room temperature). The gel was destained with water until the background was clear. An image was collected of the Coomassie stained gel. Gel was cut in 10-15 consecutive pieces (approximately 2mm in size) using a clean scalpel and placed into a siliconized tube. Gel pieces were covered with wash solution 1 (200 µL, 25 mM NH_4HCO_3 with acetonitrile in ratio 3:1, **section 1.4**) followed by incubation with shaking (30 min, 450 rpm, 37 °C). The washing solution was replaced with wash solution 2 (200 µL, 25 mM NH_4HCO_3 with acetonitrile in ratio 1:1 **section 1.4**) and samples were shaken (30 min, 450 rpm, 37 °C). If necessary, the washing steps were repeated until the spots were completely destained. The following step was the reduction of the disulfide bonds in the proteins with freshly prepared reducing solution (100 µL, 50 mM DTT in 25 mM NH_4HCO_3, **section 1.4**) was added to the destained gel pieces and incubated with shaking (45min, 450 rpm, 37 °C). After the reduction solution was removed, the gel pieces were alkylated (100 µL, 55 mM iodacetamide in 25 mM NH_4HCO_3, **section 1.4**) incubated in the dark (1-2 h, room temperature). The alkylation solution was removed and the gel pieces were washed while shaking with wash solution 2 (2 x 15 min, 450 rpm, room temperature). The wash solution 2 was completely removed, followed by the addition of acetonitrile (30 µL, 10 min) under the hood while the proteins were dried and the acetonitrile was removed using vacuum concentrator. To trypsinate the proteins, trypsination solution (15-30 µL, Trypsin stock solution:25 mM NH_4HCO_3, 9:1) was added to the dried gel spots and incubated (15 min, room temperature) and additional buffer is added (25 µL, 25 mM NH_4HCO_3) was added to the spots and samples were incubated while shaking (overnight, 30 °C). The tubes were placed in iced ultra-sonic bath for 30 min to extract the peptides. The peptide solution was collected in a new siliconized tube and TFA (3-5 µL, 10%) was added. The extraction procedure was repeated. The solution was collected in the same tubes as before. The peptides were dried in a vacuum concentrator and submitted for LC-MS/MS analysis.

8.2.2 In solution trypsin digestion and stage tip purification

After the beads were collected in the pulldown experiment (**section 8.1**), E1 fresh buffer (100 µL, E1 = 1.1 µL DTT stock + 13.75 µL trypsin stock (5 µg/mL) + 1085.15 µL urea stock, **section 1.4**) was added to the beads and incubated (1 h, room temperature, 350 rpm). The supernatant was transferred to new siliconized tube. Beads were collected and E2 buffer was added (100 µL, E2 = 11 µL chloracetamide stock + 1089 µL urea stock) and incubated (2 min, room temperature, 350

rpm). The supernatants were collected and combined. The tubes were placed in a thermomixer and incubated (overnight, 350 rpm, 37°C to RT). The reaction was stopped with TFA (2 µL). For the generation of STAGE tips, two C18 filter disks were placed in a small petri-dish and stored sealed to avoid contaminations (Wisniewski et al., 2009). Using a STAGE tip syringe the layer of C18 filter disks were punctured through. The material was transferred to a yellow tip (1-200 µL) and pressed into the tip as far as possible. The yellow tip was placed onto an adapter on the top of a 150 µL tube. The tips were activated MeOH (100 µL), followed by an equilibration step with buffer A (100 µL, 2 times, buffer A = 0.1% formic acid in water, **section 1.4**) and centrifuged (3 min, 5000 rpm). The pulldown sample was loaded (100 µL) followed by short incubation (1 min) and centrifuged (5 min, 5000 rpm). The tips were washed by adding buffer A (100 µL) and centrifuged (10 min, 2500 rpm). The peptides were eluted by adding buffer B (20 µL, 2 times, 1 min/time, buffer B = 20 % H_2O + 80 % acetonitrile + 0.1% formic acid, **section 1.4**) and centrifuging (3 min, 5000 rpm). The peptides were dried in a vacuum concentrator and submitted for LC-MS/MS analysis.

8.2.3 Mass spectrometry analysis

Proteins enriched during the pulldowns were identified by means of mass spectrometry at two mass spectrometry facilities: Mass Spectrometry at the Max Planck Institute in Dortmund supervised by Petra Janning and Core Facility for Protein analysis at the Max Planck Institute for Infection Biology operated by Monika Schmid. For comparative purposes, Monika Schmid and Petra Janning coordinated their protocols.

Samples were subjected to analysis using GC-MS/MS at the MPI for Infection Biology performed by Monika Schmid. Alternatively, samples were subjected to analysis using LC-MS/MS at the MPI of Molecular Physiology supervised by Dr. Petra Janning.

8.3 Target validation experiment

8.3.1 Protein binding of RAC2 detection via immunobloting

The pulldown experiments using beads was performed as described in **sections 8.1**. Cell lysates were collected according to **section 6.1.3** and HL60 **section 6.1.5**, or pure RAC2 protein were used to perform the pulldown. Once the SDS is gels is done the RAC2 antibody (Millipore), at concentration indicated by manufacturer, immunoblot is performed following protocol from **section 7.3**. The membranes were developed using chemiluminescence procedure and femto detection was usually required.

9 *In silico* target prediction

9.1 Similarity ensemble approach (SEA)

The Similarity ensemble approach (SEA, http://sea.bkslab.org) relates proteins to their ligands based on their chemical similarity. It is collaboration project by the Keiser and Shoichet groups. The tetraisoquinolines were subjected to this analysis (Keiser et al., 2007).

9.2 Flexible alignment with Molecular Operating Environment (MOE)

Flexible alignment for tetrahydroisoquinolines were subjected to alignments with known antagonist of GPCRs, i.e. Seratindol known 5-HT_2 and dopamine, adregenic receptor binder, performed with Molecular Operating Environment (MOE) Software Package.

10 GPCR screening

Based on the *in-silico* predictions, GPCR were suggested as a potential targets for the tetrahydroisoquinolines. After careful consideration a list GPCR of potential targets was generated and the most potent compound **T1** was subjected to GPCR screening at the company CEREP. The purpose of this study was to test **T1** in binding and cellular and nuclear receptor functional assays.

11 Synthetic Chemistry

11.1 Synthesis of probes P3, P4 and P5

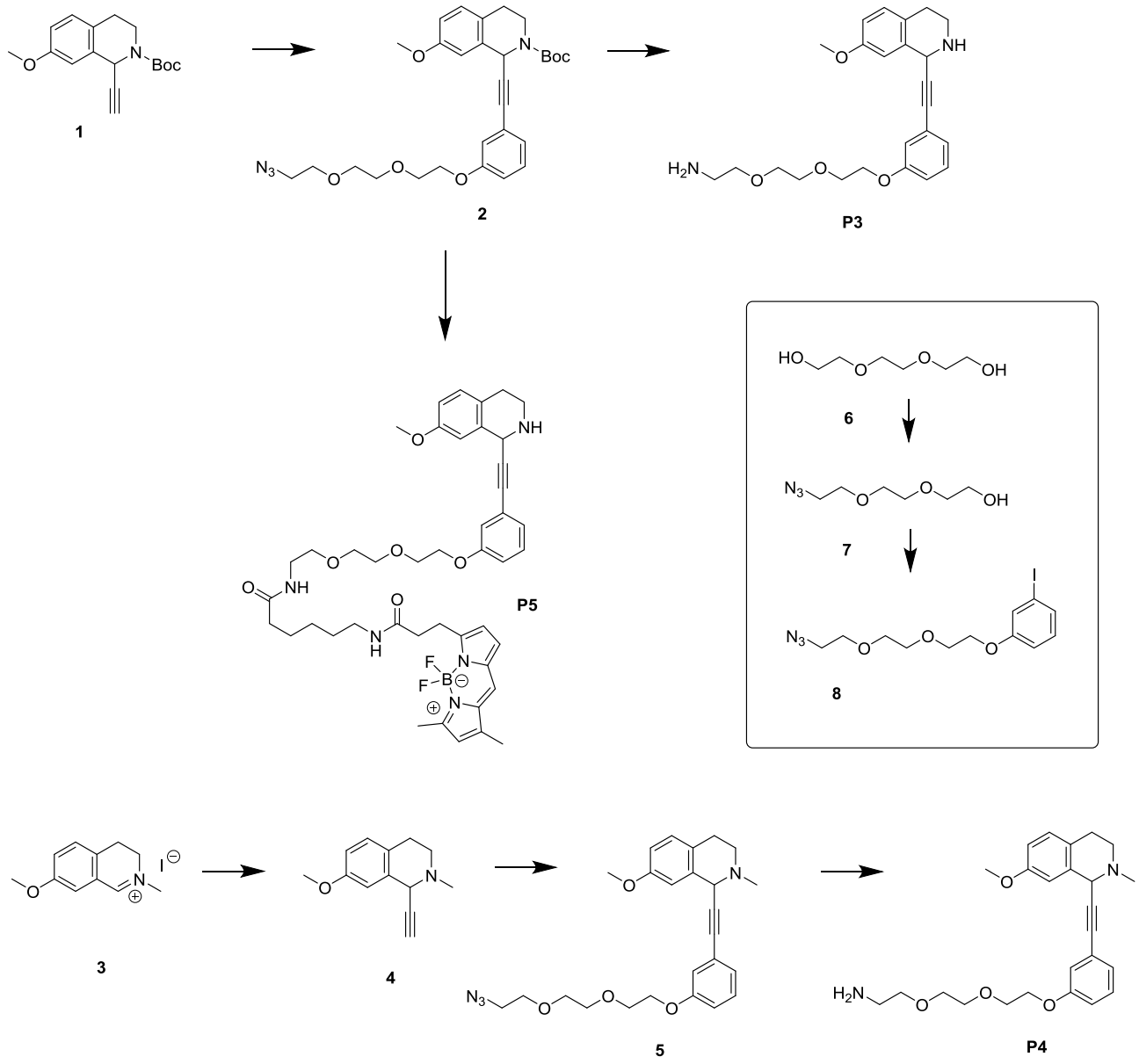

Scheme 1: Synthesis of probes **P3**, **P4**, and **P5**.

All chemicals were obtained from Acros, Aldrich, Alfa Aesar or Merck and were used without further purification. Solvents were used as received. 1H and 13C NMR spectra were recorded on a Varian Mercury 400- or a Bruker DRX 500 NMR spectrometer. Chemical shifts are reported in δ values relative to residual solvent peaks (Abbreviations: s: singlet, bs: broad singlet, bd: broad doublet, d: doublet, dd: doublet of doublets, dt: doublet of triplets, t: triplet, q: quartet, m: multiplet). Column chromatography was performed using silica gel for chromatography (0.035-0.070 mm, 60A) purchased from Acros Organic. Compounds on TLC were visualized by UV and/or basic KMnO4

staining. High resolution mass spectra (HR-MS, 70 eV) were measured on a Thermo Orbitrap, coupled to a Thermo Accela nano-HPLC machine, using electron spray ionization (ESI). Analytical HPLC-MS data were recorded on an Agilent HPLC (1100 series) coupled to a Finnigan LCQ ESI spectrometer, using a Nucleodur C18 gravity column, ID 4 mm, length 125 mm, particle size 3 µm from Macherey-Nagel. A gradient was applied beginning at 10% acetonitrile and ending at 90% after 15 min, followed by 3 min at 90% acetonitrile; finally, the column was washed for 5 min with 100% acetonitrile. The column was equilibrated for 3 min with 10% acetonitrile. All RP-HPLC solvents contained TFA (0.1% v/v). Preparative HPLC purifications were performed with an Agilent 1100 series instrument, connected to an Agilent MSD VL mass spectrometer andequipped with a fraction collector. All RP-HPLC solvents contained TFA (0.1% v/v) and products with basic amines were isolated as a TFA salt.

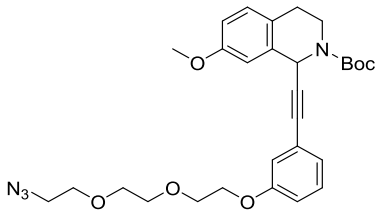

tert-butyl 1-((3-(2-(2-(2-azidoethoxy)ethoxy)ethoxy)phenyl)ethynyl)-7-methoxy-3,4-dihydroisoquinoline-2(1H)-carboxylate (2) 70 mg (0.24 mmol) **1** was dissolved in 4 ml dry THF. 113 mg (0.3 mmol) **8** in 2 ml THF, 70 µl (0.5 mmol) TEA and 4 mg (0.024 mmol) CuI were added and argon was bubbled through the solution for 5 minutes before adding 20 mg (0.024 mmol) $Pd(PPh_3)_4$ and the RM was stirred overnight at 65 ºC. The RM was concentrated and the product was purified over silica(cHex/EtOAc 7:3) obtaining 86 mg (66%) **2.** ^{1}H-NMR (400 MHz, $CDCl_3$): δ 7.15 (t, J = 7.9 Hz, 2H), 7.05 (d, J = 8.4 Hz, 2H), 6.97 (d, J = 7.6 Hz, 2H), 6.92 (s, 2H), 6.89 – 6.82 (m, 4H), 6.78 (dd, J = 8.4, 2.6 Hz, 2H), 4.11 (dt, J = 11.1, 5.6 Hz, 10H), 3.87 – 3.81 (m, 4H), 3.80 (s, 6H), 3.72 (dd, J = 5.9, 3.0 Hz, 4H), 3.67 (dd, J = 6.9, 3.7 Hz, 9H), 3.41 – 3.32 (m, 5H), 2.89 (s, 2H), 2.73 (d, J = 15.7 Hz, 2H), 1.51 (s, 19H): ^{13}C NMR (101 MHz, $CDCl_3$): δ 171.26, 158.64, 158.36, 130.17, 129.41, 124.74, 124.10, 117.57, 115.67, 114.12, 112.26, 88.73, 77.57, 77.25, 76.93, 71.04, 70.31, 69.97, 67.71, 60.56, 55.59, 50.90, 28.67, 27.91, 27.13, 21.21, 14.39. ESI HRMS calculated for $C_{29}H_{37}O_6N_4$ $[M+H]^+$ = 537.27076. Mass found $[M+H]^+$ = 537.27176.

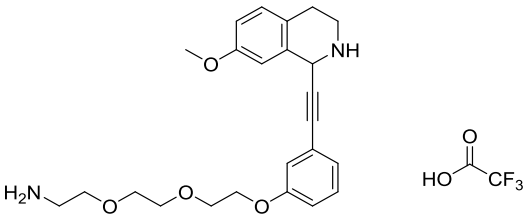

2-(2-(2-(3-((7-methoxy-1,2,3,4-tetrahydroisoquinolin-1-yl)ethynyl)phenoxy)ethoxy)ethoxy)ethan-1-amine (P3) 60 mg (0.11 mmol) **2** was dissolved in THF and 30 mg (0.11 mmol) PPh_3 was added. The RM was stirred overnight at RT. 50 µl water was added and the RM was stirred overnight. The RM was evaporated to dryness and the residue was dissolved in 2.5 ml DMF obtaining a 0.044M solution of the reduced azide. 1 ml of the solution was treated with 1 ml 2.0 M HCl in ether (2 mmol) and the RM was stirred overnight. The RM was evaporated to dryness and the product was purified using preparative HPLC obtaining 14 mg **P3** (61% yield) as a TFA salt. ^{1}H NMR (400 MHz, $CDCl_3$): δ 8.39 – 7.89 (m, 3H), 7.22 – 7.16 (m, 2H), 7.08 (d, J = 8.6 Hz, 4H), 7.02 (d, J = 7.7 Hz, 2H), 6.96 (d, J = 2.5 Hz, 2H), 6.89 (d, J = 8.3 Hz, 2H), 6.85 (dd, J = 8.5, 2.6 Hz, 2H), 5.50 (s, 2H), 4.17 – 4.05 (m, 4H), 3.79 (d, J = 8.2 Hz, 11H), 3.64 (dd, J = 12.5, 5.4 Hz, 18H), 3.42 (s, 3H), 3.02 (d, J = 15.5 Hz, 10H), 2.48 (s, 13H). ^{13}C NMR (101 MHz, $CDCl_3$): δ 159.25, 158.73, 130.40, 130.14, 129.83, 124.91, 123.25, 122.45, 118.94, 116.71, 115.77, 112.40, 88.64, 82.46, 70.75, 70.24, 69.88, 67.67, 66.85, 55.86, 48.19, 40.52, 39.89, 24.72. ESI HRMS calculated for $C_{24}H_{31}O_4N_2$ $[M+H]^+$ = 411.22783. Mass found $[M+H]^+$ = 411.22814.

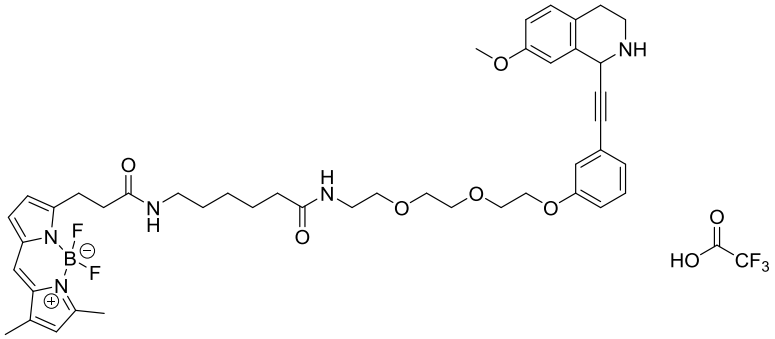

6-(3-(5,5-difluoro-7,9-dimethyl-5H-5l4,6l4-dipyrrolo[1,2-c:2',1'-f][1,3,2]diazaborinin-3-yl)propanamido)-N-(2-(2-(2-(3-((7-methoxy-1,2,3,4-tetrahydroisoquinolin-1-yl)ethynyl)phenoxy)ethoxy)ethoxy)ethyl)hexanamide (P5) 0.5 ml of a 0.044M solution of Boc protected **P3** in DMF was treated with 15 mg (0.025 mmol) bodipy-OSu and 5 µl (0.036 mmol) TEA. The RM was stirred overnight in a dark reaction vial. 250 µl 2M HCl in ether (0.5 mmol) added and the RM was stirred overnight at RT. The mixture was concentrated and taken up in methanol. The product was purified using preparative HPLC and 10 mg **P5** (55 % yield) was obtained as a white

solid. ESI HRMS calculated for $C_{44}H_{55}O_6N_5BF_2$ $[M+H]^+$ = 798.42080. Mass found $[M+H]^+$ = 798.42095.

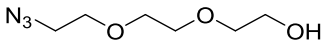

2-(2-(2-azidoethoxy)ethoxy)ethanol (7) 38.6 g (257 mmol) triethylene glycol (**6**) was dissolved in 250 mL anhydrous THF under argon atmosphere and cooled to 0 ^{0}C. 5.0 mL methanesulfonyl chloride (64.4 mmol) and 9.0 mL TEA (64.4 mmol) were added dropwise. The RM was allowed to stir at room temperature overnight under an argon atmosphere. The reaction mixture was concentrated and the residue was dissolved in 250 mL dry ethanol. 20.9 g sodium azide (322.0 mmol) was added and the reaction mixture was heated to reflux for 6 hours. After cooling to room temperature the mixture was concentrated and dissolved in water. The product was extracted with DCM (3x), and the combined organic fractions were dried over magnesium sulfate, filtered, and concentrated to yield 5.1 g **7** as a sticky oil (45% yield from methanesulfonyl chloride). R_f = 0.20 (100% EtOAc); ^{1}H-NMR(400 MHz, $CDCl_3$) δ: 3.77 (t, J = 5.8 Hz, 2H), 3.72 – 3.66 (m, 6H), 3.64 (t, J = 5.8 Hz, 2H), 3.39 (t, J = 5.0 Hz, 2H), 1.57 (s, 1H).

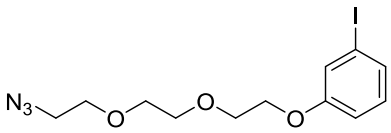

2-(2-(2-(3-((6,7-dimethoxy-1,2,3,4-1-(2-(2-(2-azidoethoxy)ethoxy)ethoxy)-3-iodobenzene (8)
2.0 g (11.4 mmol) **7**, 2.1 g (11.4 mmol) tosyl chloride were dissolved in 10 mL pyridine. The RM was stirred overnight at RT under argon. The RM was poured into sat. $NaHCO_3$(aq) (60 mL) and was extracted with EtOAc (3x 50 mL). The combined EtOAc was dried over $MgSO_4$(s) and evaporated. The residue was dissolved in 20 mL DMF and 2.8 g 3-iodophenol (12.5 mmol), 4.1 g cesium carbonate (12.5 mmol) and 0.36 g potassium iodide (2.3 mmol) were added. The RM was stirred for 8 hours at RT. The RM was diluted with EtOAc (150 mL) and washed with sat. $NaHCO_3$(aq) (100 mL). The EtOAc was dried over $MgSO_4$(s) and evaporated to dryness. The residue was purified over silica (cHex/EtOAc 7:3) obtaining 2.0 g (46 % yield) **8**.

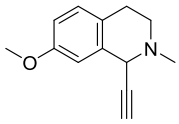

1-ethynyl-7-methoxy-2-methyl-1,2,3,4-tetrahydroisoquinoline (4) 300 mg iodine salt **3** (0.99 mmol) was dissolved in 3 mL dry THF under argon. The RM was cooled to 0°C and 5.9 mL 0.5 M ethynyl magnesiumbromide solution (2.97 mmol) was added dropwise. The RM was stirred 30 min. and allowed to reach RT. The RM was diluted with EtOAc (20 mL) and washed with sat. $NaHCO_3$(aq) (50 mL). The EtOAc was dried over $MgSO_4$(s) and evaporated to dryness obtaining 147 mg (73 % yield) **4**.

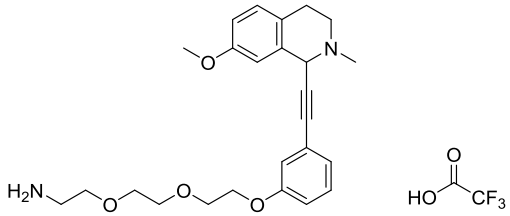

2-(2-(2-(3-((7-methoxy-2-methyl-1,2,3,4-tetrahydroisoquinolin-1-yl)ethynyl)phenoxy)ethoxy)ethoxy)ethan-1-amine (P4) 24 mg (0.11mmol) **4** was dissolved in 1 ml THF. 67 mg (0.15mmol) iodide in 0.5 ml THF, 31 µl (0.22 mmol) TEA and 2 mg (0.011 mmol) CuI were added and argon was bubbled through the solution before adding 12 mg (0.011mmol) $Pd(PPh_3)_4$ and the RM was stirred overnight at 65 °C. The solution was treated with 1 ml 2.0 M HCl in ether (2 mmol) and the RM was stirred overnight. The RM was evaporated to dryness and the product was purified using preparative HPLC obtaining 14 mg **P4** (30 % yield) as a TFA salt. ^{1}H NMR (400 MHz, $CDCl_3$): δ 8.25 – 7.94 (m, 15H), 7.20 (d, J = 8.1 Hz, 8H), 7.11 (d, J = 9.3 Hz, 7H), 7.02 (d, J = 8.0 Hz, 14H), 6.94 (s, 8H), 6.89 (d, J = 6.4 Hz, 14H), 5.73 – 5.65 (m, 2H), 5.62 – 5.44 (m, 6H), 4.11 (s, 16H), 3.80 (d, J = 7.6 Hz, 44H), 3.74 – 3.60 (m, 55H), 3.59 – 3.45 (m, 9H), 3.31 – 3.14 (m, 11H), 3.09 (s, 23H), 3.02 (s, 20H).^{13}C NMR (101 MHz, $CDCl_3$): δ 159.54, 158.90, 130.63, 130.13, 125.10, 122.14, 121.62, 118.47, 117.56, 116.34, 112.73, 70.74, 70.29, 69.88, 67.64, 66.88, 55.85, 48.42, 40.03. ESI HRMS calculated for $C_{25}H_{33}O_4N_2$ $[M+H]^+$ = 425.24348. Mass found $[M+H]^+$ = 425.24385.

References

Adamson, B., Norman, T.M., Jost, M., Cho, M.Y., Nunez, J.K., Chen, Y., Villalta, J.E., Gilbert, L.A., Horlbeck, M.A., Hein, M.Y., *et al.* (2016). A Multiplexed Single-Cell CRISPR Screening Platform Enables Systematic Dissection of the Unfolded Protein Response. Cell *167*, 1867-1882 e1821.
Aga, E., Katschinski, D.M., van Zandbergen, G., Laufs, H., Hansen, B., Muller, K., Solbach, W., and Laskay, T. (2002). Inhibition of the spontaneous apoptosis of neutrophil granulocytes by the intracellular parasite Leishmania major. J Immunol *169*, 898-905.
Agarwal, P., Beahm, B.J., Shieh, P., and Bertozzi, C.R. (2015). Systemic Fluorescence Imaging of Zebrafish Glycans with Bioorthogonal Chemistry. Angewandte Chemie *54*, 11504-11510.
Ali, H., Richardson, R.M., Tomhave, E.D., DuBose, R.A., Haribabu, B., and Snyderman, R. (1994). Regulation of stably transfected platelet activating factor receptor in RBL-2H3 cells. Role of multiple G proteins and receptor phosphorylation. J Biol Chem *269*, 24557-24563.
Altmann, K.H., Buchner, J., Kessler, H., Diederich, F., Krautler, B., Lippard, S., Liskamp, R., Muller, K., Nolan, E.M., Samori, B., *et al.* (2009). The state of the art of chemical biology. Chembiochem *10*, 16-29.
Altmeier, S., Toska, A., Sparber, F., Teijeira, A., Halin, C., and LeibundGut-Landmann, S. (2016). IL-1 Coordinates the Neutrophil Response to C. albicans in the Oral Mucosa. PLoS Pathog *12*, e1005882.
Amulic, B., Cazalet, C., Hayes, G.L., Metzler, K.D., and Zychlinsky, A. (2012). Neutrophil function: from mechanisms to disease. Annu Rev Immunol *30*, 459-489.
Bardoel, B.W., Kenny, E.F., Sollberger, G., and Zychlinsky, A. (2014). The balancing act of neutrophils. Cell Host Microbe *15*, 526-536.
Basu, S., Hodgson, G., Zhang, H.H., Katz, M., Quilici, C., and Dunn, A.R. (2000). "Emergency" granulopoiesis in G-CSF-deficient mice in response to Candida albicans infection. Blood *95*, 3725-3733.
Beck, G., Brinkkoetter, P., Hanusch, C., Schulte, J., van Ackern, K., van der Woude, F.J., and Yard, B.A. (2004). Clinical review: immunomodulatory effects of dopamine in general inflammation. Crit Care *8*, 485-491.
Beiter, K., Wartha, F., Albiger, B., Normark, S., Zychlinsky, A., and Henriques-Normark, B. (2006). An endonuclease allows Streptococcus pneumoniae to escape from neutrophil extracellular traps. Curr Biol *16*, 401-407.
Bennett, L., Palucka, A.K., Arce, E., Cantrell, V., Borvak, J., Banchereau, J., and Pascual, V. (2003). Interferon and granulopoiesis signatures in systemic lupus erythematosus blood. J Exp Med *197*, 711-723.
Bennike, T.B., Carlsen, T.G., Ellingsen, T., Bonderup, O.K., Glerup, H., Bogsted, M., Christiansen, G., Birkelund, S., Stensballe, A., and Andersen, V. (2015). Neutrophil Extracellular Traps in Ulcerative Colitis: A Proteome Analysis of Intestinal Biopsies. Inflamm Bowel Dis *21*, 2052-2067.
Bey, E.A., Xu, B., Bhattacharjee, A., Oldfield, C.M., Zhao, X., Li, Q., Subbulakshmi, V., Feldman, G.M., Wientjes, F.B., and Cathcart, M.K. (2004). Protein kinase C delta is required for p47phox phosphorylation and translocation in activated human monocytes. J Immunol *173*, 5730-5738.
Bianchi, M., Hakkim, A., Brinkmann, V., Siler, U., Seger, R.A., Zychlinsky, A., and Reichenbach, J. (2009). Restoration of NET formation by gene therapy in CGD controls aspergillosis. Blood *114*, 2619-2622.
Bolt, H.M., Hengstler, J.G., and Stewart, J. (2009). Analysis of Reactive Oxygen Species. Excli J *8*, 241-245.
Bon, R.S., Guo, Z., Stigter, E.A., Wetzel, S., Menninger, S., Wolf, A., Choidas, A., Alexandrov, K., Blankenfeldt, W., Goody, R.S., *et al.* (2011). Structure-guided development of selective RabGGTase inhibitors. Angewandte Chemie *50*, 4957-4961.
Borregaard, N. (2010). Neutrophils, from marrow to microbes. Immunity *33*, 657-670.
Brinkmann, V., Reichard, U., Goosmann, C., Fauler, B., Uhlemann, Y., Weiss, D.S., Weinrauch, Y., and Zychlinsky, A. (2004). Neutrophil extracellular traps kill bacteria. Science *303*, 1532-1535.
Brinkmann, V., and Zychlinsky, A. (2007). Beneficial suicide: why neutrophils die to make NETs. Nat Rev Microbiol *5*, 577-582.
Brogden, K.A. (2005). Antimicrobial peptides: pore formers or metabolic inhibitors in bacteria? Nat Rev Microbiol *3*, 238-250.
Bucci, M., Goodman, C., and Sheppard, T.L. (2010). A decade of chemical biology. Nature chemical biology *6*, 847-854.
Buchanan, J.T., Simpson, A.J., Aziz, R.K., Liu, G.Y., Kristian, S.A., Kotb, M., Feramisco, J., and Nizet, V. (2006). DNase expression allows the pathogen group A Streptococcus to escape killing in neutrophil extracellular traps. Curr Biol *16*, 396-400.

Bugl, S., Wirths, S., Muller, M.R., Radsak, M.P., and Kopp, H.G. (2012). Current insights into neutrophil homeostasis. Ann N Y Acad Sci *1266*, 171-178.
Bugl, S., Wirths, S., Radsak, M.P., Schild, H., Stein, P., Andre, M.C., Muller, M.R., Malenke, E., Wiesner, T., Marklin, M.*, et al.* (2013). Steady-state neutrophil homeostasis is dependent on TLR4/TRIF signaling. Blood *121*, 723-733.
Cagnol, S., and Chambard, J.C. (2010). ERK and cell death: mechanisms of ERK-induced cell death--apoptosis, autophagy and senescence. FEBS J *277*, 2-21.
Caie, P.D., Walls, R.E., Ingleston-Orme, A., Daya, S., Houslay, T., Eagle, R., Roberts, M.E., and Carragher, N.O. (2010). High-content phenotypic profiling of drug response signatures across distinct cancer cells. Mol Cancer Ther *9*, 1913-1926.
Campanelli, D., Detmers, P.A., Nathan, C.F., and Gabay, J.E. (1990). Azurocidin and a homologous serine protease from neutrophils. Differential antimicrobial and proteolytic properties. J Clin Invest *85*, 904-915.
Campos, E., Montella, C., Garces, F., Baldoma, L., Aguilar, J., and Badia, J. (2007). Aerobic L-ascorbate metabolism and associated oxidative stress in Escherichia coli. Microbiology *153*, 3399-3408.
Canny, G., and Levy, O. (2008). Bactericidal/permeability-increasing protein (BPI) and BPI homologs at mucosal sites. Trends Immunol *29*, 541-547.
Capodici, C., Pillinger, M.H., Han, G., Philips, M.R., and Weissmann, G. (1998). Integrin-dependent homotypic adhesion of neutrophils. Arachidonic acid activates Raf-1/Mek/Erk via a 5-lipoxygenase-dependent pathway. J Clin Invest *102*, 165-175.
Carvalho, L.O., Aquino, E.N., Neves, A.C., and Fontes, W. (2015). The Neutrophil Nucleus and Its Role in Neutrophilic Function. J Cell Biochem *116*, 1831-1836.
Chang, P.V., Prescher, J.A., Sletten, E.M., Baskin, J.M., Miller, I.A., Agard, N.J., Lo, A., and Bertozzi, C.R. (2010). Copper-free click chemistry in living animals. Proceedings of the National Academy of Sciences of the United States of America *107*, 1821-1826.
Chou, R.C., Kim, N.D., Sadik, C.D., Seung, E., Lan, Y., Byrne, M.H., Haribabu, B., Iwakura, Y., and Luster, A.D. (2010). Lipid-cytokine-chemokine cascade drives neutrophil recruitment in a murine model of inflammatory arthritis. Immunity *33*, 266-278.
Chow, O.A., von Kockritz-Blickwede, M., Bright, A.T., Hensler, M.E., Zinkernagel, A.S., Cogen, A.L., Gallo, R.L., Monestier, M., Wang, Y., Glass, C.K.*, et al.* (2010). Statins enhance formation of phagocyte extracellular traps. Cell Host Microbe *8*, 445-454.
Clark, S.R., Guy, C.J., Scurr, M.J., Taylor, P.R., Kift-Morgan, A.P., Hammond, V.J., Thomas, C.P., Coles, B., Roberts, G.W., Eberl, M.*, et al.* (2011). Esterified eicosanoids are acutely generated by 5-lipoxygenase in primary human neutrophils and in human and murine infection. Blood *117*, 2033-2043.
Clark, S.R., Ma, A.C., Tavener, S.A., McDonald, B., Goodarzi, Z., Kelly, M.M., Patel, K.D., Chakrabarti, S., McAvoy, E., Sinclair, G.D.*, et al.* (2007). Platelet TLR4 activates neutrophil extracellular traps to ensnare bacteria in septic blood. Nat Med *13*, 463-469.
Cohen, A.S., Dubikovskaya, E.A., Rush, J.S., and Bertozzi, C.R. (2010). Real-time bioluminescence imaging of glycans on live cells. Journal of the American Chemical Society *132*, 8563-8565.
Cooper, P.R., Palmer, L.J., and Chapple, I.L. (2013). Neutrophil extracellular traps as a new paradigm in innate immunity: friend or foe? Periodontol 2000 *63*, 165-197.
Cronstein, B.N., and Weissmann, G. (1995). Targets for antiinflammatory drugs. Annu Rev Pharmacol Toxicol *35*, 449-462.
Cyster, J.G. (2005). Chemokines, sphingosine-1-phosphate, and cell migration in secondary lymphoid organs. Annu Rev Immunol *23*, 127-159.
Dancey, J.T., Deubelbeiss, K.A., Harker, L.A., and Greenaway, J. (1976). Section preparation of human marrow for light microscopy. J Clin Pathol *29*, 704-710.
Deevska, G.M., and Nikolova-Karakashian, M.N. (2017). The expanding role of sphingolipids in lipid droplet biogenesis. Biochim Biophys Acta.
Dekker, F.J., Rocks, O., Vartak, N., Menninger, S., Hedberg, C., Balamurugan, R., Wetzel, S., Renner, S., Gerauer, M., Scholermann, B.*, et al.* (2010). Small-molecule inhibition of APT1 affects Ras localization and signaling. Nature chemical biology *6*, 449-456.
Di Girolamo, F., Lante, I., Muraca, M., and Putignani, L. (2013). The Role of Mass Spectrometry in the "Omics" Era. Curr Org Chem *17*, 2891-2905.

Dickinson, B.C., and Chang, C.J. (2011). Chemistry and biology of reactive oxygen species in signaling or stress responses. Nature chemical biology *7*, 504-511.
Douda, D.N., Khan, M.A., Grasemann, H., and Palaniyar, N. (2015). SK3 channel and mitochondrial ROS mediate NADPH oxidase-independent NETosis induced by calcium influx. Proceedings of the National Academy of Sciences of the United States of America *112*, 2817-2822.
Doweyko, A.M., and Doweyko, L.M. (2009). What is next for small-molecule drug discovery? Future medicinal chemistry *1*, 1029-1036.
Dwivedi, N., Upadhyay, J., Neeli, I., Khan, S., Pattanaik, D., Myers, L., Kirou, K.A., Hellmich, B., Knuckley, B., Thompson, P.R.*, et al.* (2012). Felty's syndrome autoantibodies bind to deiminated histones and neutrophil extracellular chromatin traps. Arthritis Rheum *64*, 982-992.
Edenius, C., Haeggstrom, J., and Lindgren, J.A. (1988). Transcellular conversion of endogenous arachidonic acid to lipoxins in mixed human platelet-granulocyte suspensions. Biochem Biophys Res Commun *157*, 801-807.
Eder, J., Sedrani, R., and Wiesmann, C. (2014). The discovery of first-in-class drugs: origins and evolution. Nat Rev Drug Discov *13*, 577-587.
El Benna, J., Han, J., Park, J.W., Schmid, E., Ulevitch, R.J., and Babior, B.M. (1996). Activation of p38 in stimulated human neutrophils: phosphorylation of the oxidase component p47phox by p38 and ERK but not by JNK. Arch Biochem Biophys *334*, 395-400.
Emerit, I., and Cerutti, P.A. (1981). Tumour promoter phorbol-12-myristate-13-acetate induces chromosomal damage via indirect action. Nature *293*, 144-146.
Erlanson, D.A., Fesik, S.W., Hubbard, R.E., Jahnke, W., and Jhoti, H. (2016). Twenty years on: the impact of fragments on drug discovery. Nat Rev Drug Discov *15*, 605-619.
Etulain, J., Martinod, K., Wong, S.L., Cifuni, S.M., Schattner, M., and Wagner, D.D. (2015). P-selectin promotes neutrophil extracellular trap formation in mice. Blood *126*, 242-246.
Evans, T.J., Buttery, L.D., Carpenter, A., Springall, D.R., Polak, J.M., and Cohen, J. (1996). Cytokine-treated human neutrophils contain inducible nitric oxide synthase that produces nitration of ingested bacteria. Proceedings of the National Academy of Sciences of the United States of America *93*, 9553-9558.
Faurschou, M., and Borregaard, N. (2003). Neutrophil granules and secretory vesicles in inflammation. Microbes Infect *5*, 1317-1327.
Favata, M.F., Horiuchi, K.Y., Manos, E.J., Daulerio, A.J., Stradley, D.A., Feeser, W.S., Van Dyk, D.E., Pitts, W.J., Earl, R.A., Hobbs, F.*, et al.* (1998). Identification of a novel inhibitor of mitogen-activated protein kinase kinase. J Biol Chem *273*, 18623-18632.
Flierl, M.A., Rittirsch, D., Huber-Lang, M., Sarma, J.V., and Ward, P.A. (2008). Catecholamines-crafty weapons in the inflammatory arsenal of immune/inflammatory cells or opening pandora's box? Mol Med *14*, 195-204.
Flierl, M.A., Rittirsch, D., Nadeau, B.A., Chen, A.J., Sarma, J.V., Zetoune, F.S., McGuire, S.R., List, R.P., Day, D.E., Hoesel, L.M.*, et al.* (2007). Phagocyte-derived catecholamines enhance acute inflammatory injury. Nature *449*, 721-725.
Flierl, M.A., Rittirsch, D., Nadeau, B.A., Sarma, J.V., Day, D.E., Lentsch, A.B., Huber-Lang, M.S., and Ward, P.A. (2009). Upregulation of phagocyte-derived catecholamines augments the acute inflammatory response. PloS one *4*, e4414.
Fontayne, A., Dang, P.M., Gougerot-Pocidalo, M.A., and El-Benna, J. (2002). Phosphorylation of p47phox sites by PKC alpha, beta II, delta, and zeta: effect on binding to p22phox and on NADPH oxidase activation. Biochemistry *41*, 7743-7750.
Franzosa, E.A., Hsu, T., Sirota-Madi, A., Shafquat, A., Abu-Ali, G., Morgan, X.C., and Huttenhower, C. (2015). Sequencing and beyond: integrating molecular 'omics' for microbial community profiling. Nat Rev Microbiol *13*, 360-372.
Fremont, L. (2000). Biological effects of resveratrol. Life Sci *66*, 663-673.
Fuchs, T.A., Abed, U., Goosmann, C., Hurwitz, R., Schulze, I., Wahn, V., Weinrauch, Y., Brinkmann, V., and Zychlinsky, A. (2007). Novel cell death program leads to neutrophil extracellular traps. Journal of Cell Biology *176*, 231-241.
Fuchs, T.A., Brill, A., Duerschmied, D., Schatzberg, D., Monestier, M., Myers, D.D., Jr., Wrobleski, S.K., Wakefield, T.W., Hartwig, J.H., and Wagner, D.D. (2010). Extracellular DNA traps promote thrombosis. Proceedings of the National Academy of Sciences of the United States of America *107*, 15880-15885.

Futerman, A.H., and Hannun, Y.A. (2004). The complex life of simple sphingolipids. EMBO Rep *5*, 777-782.
Garcia-Romo, G.S., Caielli, S., Vega, B., Connolly, J., Allantaz, F., Xu, Z., Punaro, M., Baisch, J., Guiducci, C., Coffman, R.L.*, et al.* (2011). Netting neutrophils are major inducers of type I IFN production in pediatric systemic lupus erythematosus. Sci Transl Med *3*, 73ra20.
Goldmann, O., and Medina, E. (2012). The expanding world of extracellular traps: not only neutrophils but much more. Front Immunol *3*, 420.
Gunzer, M. (2014). Traps and hyper inflammation - new ways that neutrophils promote or hinder survival. Br J Haematol *164*, 189-199.
Gygi, S.P., Rist, B., Gerber, S.A., Turecek, F., Gelb, M.H., and Aebersold, R. (1999). Quantitative analysis of complex protein mixtures using isotope-coded affinity tags. Nat Biotechnol *17*, 994-999.
Hahn, S., Giaglis, S., Hoesli, I., and Hasler, P. (2012). Neutrophil NETs in reproduction: from infertility to preeclampsia and the possibility of fetal loss. Front Immunol *3*, 362.
Hakkim, A., Fuchs, T.A., Martinez, N.E., Hess, S., Prinz, H., Zychlinsky, A., and Waldmann, H. (2011). Activation of the Raf-MEK-ERK pathway is required for neutrophil extracellular trap formation. Nature chemical biology *7*, 75-77.
Hakkim, A., Furnrohr, B.G., Amann, K., Laube, B., Abed, U.A., Brinkmann, V., Herrmann, M., Voll, R.E., and Zychlinsky, A. (2010). Impairment of neutrophil extracellular trap degradation is associated with lupus nephritis. Proceedings of the National Academy of Sciences of the United States of America *107*, 9813-9818.
Hampton, M.B., Kettle, A.J., and Winterbourn, C.C. (1998). Inside the neutrophil phagosome: oxidants, myeloperoxidase, and bacterial killing. Blood *92*, 3007-3017.
Haney, S.A., LaPan, P., Pan, J., and Zhang, J. (2006). High-content screening moves to the front of the line. Drug Discov Today *11*, 889-894.
Harris, E.S., McIntyre, T.M., Prescott, S.M., and Zimmerman, G.A. (2000). The leukocyte integrins. J Biol Chem *275*, 23409-23412.
Hayyan, M., Hashim, M.A., and AlNashef, I.M. (2016). Superoxide Ion: Generation and Chemical Implications. Chem Rev *116*, 3029-3085.
Hoiby, N., Ciofu, O., and Bjarnsholt, T. (2010). Pseudomonas aeruginosa biofilms in cystic fibrosis. Future Microbiol *5*, 1663-1674.
Honda, Z., Takano, T., Gotoh, Y., Nishida, E., Ito, K., and Shimizu, T. (1994). Transfected platelet-activating factor receptor activates mitogen-activated protein (MAP) kinase and MAP kinase kinase in Chinese hamster ovary cells. J Biol Chem *269*, 2307-2315.
Horvath, P., Aulner, N., Bickle, M., Davies, A.M., Nery, E.D., Ebner, D., Montoya, M.C., Ostling, P., Pietiainen, V., Price, L.S.*, et al.* (2016). Screening out irrelevant cell-based models of disease. Nat Rev Drug Discov *15*, 751-769.
Jankowski, A., Scott, C.C., and Grinstein, S. (2002). Determinants of the phagosomal pH in neutrophils. J Biol Chem *277*, 6059-6066.
Jankun, J., Wyganowska-Swiatkowska, M., Dettlaff, K., Jelinska, A., Surdacka, A., Watrobska-Swietlikowska, D., and Skrzypczak-Jankun, E. (2016). Determining whether curcumin degradation/condensation is actually bioactivation (Review). Int J Mol Med *37*, 1151-1158.
Jones, T.R., Kang, I.H., Wheeler, D.B., Lindquist, R.A., Papallo, A., Sabatini, D.M., Golland, P., and Carpenter, A.E. (2008). CellProfiler Analyst: data exploration and analysis software for complex image-based screens. BMC Bioinformatics *9*, 482.
Jorch, S.K., and Kubes, P. (2017). An emerging role for neutrophil extracellular traps in noninfectious disease. Nat Med *23*, 279-287.
Kamentsky, L., Jones, T.R., Fraser, A., Bray, M.A., Logan, D.J., Madden, K.L., Ljosa, V., Rueden, C., Eliceiri, K.W., and Carpenter, A.E. (2011). Improved structure, function and compatibility for CellProfiler: modular high-throughput image analysis software. Bioinformatics *27*, 1179-1180.
Kanoh, N., Kumashiro, S., Simizu, S., Kondoh, Y., Hatakeyama, S., Tashiro, H., and Osada, H. (2003). Immobilization of natural products on glass slides by using a photoaffinity reaction and the detection of protein-small-molecule interactions. Angewandte Chemie-International Edition *42*, 5584-5587.
Kapoor, S., Waldmann, H., and Ziegler, S. (2016). Novel approaches to map small molecule-target interactions. Bioorg Med Chem *24*, 3232-3245.

Kato, K., Clark, G.D., Bazan, N.G., and Zorumski, C.F. (1994). Platelet-activating factor as a potential retrograde messenger in CA1 hippocampal long-term potentiation. Nature *367*, 175-179.
Keiser, M.J., Roth, B.L., Armbruster, B.N., Ernsberger, P., Irwin, J.J., and Shoichet, B.K. (2007). Relating protein pharmacology by ligand chemistry. Nat Biotechnol *25*, 197-206.
Kessenbrock, K., Krumbholz, M., Schonermarck, U., Back, W., Gross, W.L., Werb, Z., Grone, H.J., Brinkmann, V., and Jenne, D.E. (2009). Netting neutrophils in autoimmune small-vessel vasculitis. Nat Med *15*, 623-625.
Khandpur, R., Carmona-Rivera, C., Vivekanandan-Giri, A., Gizinski, A., Yalavarthi, S., Knight, J.S., Friday, S., Li, S., Patel, R.M., Subramanian, V.*, et al.* (2013). NETs are a source of citrullinated autoantigens and stimulate inflammatory responses in rheumatoid arthritis. Sci Transl Med *5*, 178ra140.
Klebanoff, S.J. (2005). Myeloperoxidase: friend and foe. J Leukoc Biol *77*, 598-625.
Kleniewska, P., Piechota, A., Skibska, B., and Goraca, A. (2012). The NADPH oxidase family and its inhibitors. Arch Immunol Ther Exp (Warsz) *60*, 277-294.
Knight, J.S., Zhao, W., Luo, W., Subramanian, V., O'Dell, A.A., Yalavarthi, S., Hodgin, J.B., Eitzman, D.T., Thompson, P.R., and Kaplan, M.J. (2013). Peptidylarginine deiminase inhibition is immunomodulatory and vasculoprotective in murine lupus. J Clin Invest *123*, 2981-2993.
Kostic, M., Crews, C.M., Hertweck, C., Shokat, K., and Suga, H. (2016a). Cell Chemical Biology: Home of Exciting Chemical Biology. Cell chemical biology *23*, 1-2.
Kostic, M., Crews, C.M., Hertweck, C., Shokat, K., and Suga, H. (2016b). Voices of Chemical Biology: Charting the Next Decade. Cell chemical biology *23*, 199.
Kruger, P., Saffarzadeh, M., Weber, A.N., Rieber, N., Radsak, M., von Bernuth, H., Benarafa, C., Roos, D., Skokowa, J., and Hartl, D. (2015). Neutrophils: Between host defence, immune modulation, and tissue injury. PLoS Pathog *11*, e1004651.
Kuhns, D.B., Alvord, W.G., Heller, T., Feld, J.J., Pike, K.M., Marciano, B.E., Uzel, G., DeRavin, S.S., Priel, D.A., Soule, B.P.*, et al.* (2010). Residual NADPH oxidase and survival in chronic granulomatous disease. N Engl J Med *363*, 2600-2610.
Kusters, J.G., van Vliet, A.H., and Kuipers, E.J. (2006). Pathogenesis of Helicobacter pylori infection. Clin Microbiol Rev *19*, 449-490.
Lackey, K., Cory, M., Davis, R., Frye, S.V., Harris, P.A., Hunter, R.N., Jung, D.K., McDonald, O.B., McNutt, R.W., Peel, M.R.*, et al.* (2000). The discovery of potent cRaf1 kinase inhibitors. Bioorg Med Chem Lett *10*, 223-226.
Lande, R., Ganguly, D., Facchinetti, V., Frasca, L., Conrad, C., Gregorio, J., Meller, S., Chamilos, G., Sebasigari, R., Riccieri, V.*, et al.* (2011). Neutrophils activate plasmacytoid dendritic cells by releasing self-DNA-peptide complexes in systemic lupus erythematosus. Sci Transl Med *3*, 73ra19.
Lande, R., Gregorio, J., Facchinetti, V., Chatterjee, B., Wang, Y.H., Homey, B., Cao, W., Wang, Y.H., Su, B., Nestle, F.O.*, et al.* (2007). Plasmacytoid dendritic cells sense self-DNA coupled with antimicrobial peptide. Nature *449*, 564-569.
Lee, W.L., Harrison, R.E., and Grinstein, S. (2003). Phagocytosis by neutrophils. Microbes Infect *5*, 1299-1306.
Liu, L., Dahlgren, C., Elwing, H., and Lundqvist, H. (1996). A simple chemiluminescence assay for the determination of reactive oxygen species produced by human neutrophils. J Immunol Methods *192*, 173-178.
Lominadze, G., Powell, D.W., Luerman, G.C., Link, A.J., Ward, R.A., and McLeish, K.R. (2005). Proteomic analysis of human neutrophil granules. Mol Cell Proteomics *4*, 1503-1521.
Lood, C., Blanco, L.P., Purmalek, M.M., Carmona-Rivera, C., De Ravin, S.S., Smith, C.K., Malech, H.L., Ledbetter, J.A., Elkon, K.B., and Kaplan, M.J. (2016). Neutrophil extracellular traps enriched in oxidized mitochondrial DNA are interferogenic and contribute to lupus-like disease. Nat Med *22*, 146-153.
Mackay, H.J., and Twelves, C.J. (2007). Targeting the protein kinase C family: are we there yet? Nat Rev Cancer *7*, 554-562.
Martin, C., Burdon, P.C., Bridger, G., Gutierrez-Ramos, J.C., Williams, T.J., and Rankin, S.M. (2003). Chemokines acting via CXCR2 and CXCR4 control the release of neutrophils from the bone marrow and their return following senescence. Immunity *19*, 583-593.
Mayadas, T.N., Cullere, X., and Lowell, C.A. (2014). The multifaceted functions of neutrophils. Annu Rev Pathol *9*, 181-218.

Mehlem, A., Hagberg, C.E., Muhl, L., Eriksson, U., and Falkevall, A. (2013). Imaging of neutral lipids by oil red O for analyzing the metabolic status in health and disease. Nat Protoc *8*, 1149-1154.
Melo, R.C., D'Avila, H., Bozza, P.T., and Weller, P.F. (2011a). Imaging lipid bodies within leukocytes with different light microscopy techniques. Methods Mol Biol *689*, 149-161.
Melo, R.C., D'Avila, H., Wan, H.C., Bozza, P.T., Dvorak, A.M., and Weller, P.F. (2011b). Lipid bodies in inflammatory cells: structure, function, and current imaging techniques. J Histochem Cytochem *59*, 540-556.
Metzler, K.D., Fuchs, T.A., Nauseef, W.M., Reumaux, D., Roesler, J., Schulze, I., Wahn, V., Papayannopoulos, V., and Zychlinsky, A. (2011). Myeloperoxidase is required for neutrophil extracellular trap formation: implications for innate immunity. Blood *117*, 953-959.
Metzler, K.D., Goosmann, C., Lubojemska, A., Zychlinsky, A., and Papayannopoulos, V. (2014). A myeloperoxidase-containing complex regulates neutrophil elastase release and actin dynamics during NETosis. Cell Rep *8*, 883-896.
Mifsud, K.R., Gutierrez-Mecinas, M., Trollope, A.F., Collins, A., Saunderson, E.A., and Reul, J.M. (2011). Epigenetic mechanisms in stress and adaptation. Brain Behav Immun *25*, 1305-1315.
Moraes, L.A., Giner, R.M., Paul-Clark, M.J., Perretti, M., and Perrett, D. (2004). An isocratic HPLC method for the quantitation of eicosanoids in human platelets. Biomed Chromatogr *18*, 64-68.
Mulcahy, H., Charron-Mazenod, L., and Lewenza, S. (2008). Extracellular DNA chelates cations and induces antibiotic resistance in Pseudomonas aeruginosa biofilms. PLoS Pathog *4*, e1000213.
Nathan, C. (2006). Neutrophils and immunity: challenges and opportunities. Nature Reviews Immunology *6*, 173-182.
Nathan, C., and Cunningham-Bussel, A. (2013). Beyond oxidative stress: an immunologist's guide to reactive oxygen species. Nat Rev Immunol *13*, 349-361.
Nauseef, W.M., and Borregaard, N. (2014). Neutrophils at work. Nat Immunol *15*, 602-611.
Nemeth, T., and Mocsai, A. (2012). The role of neutrophils in autoimmune diseases. Immunology letters *143*, 9-19.
Niedel, J.E., Kuhn, L.J., and Vandenbark, G.R. (1983). Phorbol diester receptor copurifies with protein kinase C. Proceedings of the National Academy of Sciences of the United States of America *80*, 36-40.
Nishinaka, Y., Arai, T., Adachi, S., Takaori-Kondo, A., and Yamashita, K. (2011). Singlet oxygen is essential for neutrophil extracellular trap formation. Biochemical and biophysical research communications *413*, 75-79.
Nwe, K., and Brechbiel, M.W. (2009). Growing applications of "click chemistry" for bioconjugation in contemporary biomedical research. Cancer biotherapy & radiopharmaceuticals *24*, 289-302.
O'Donnell, B.V., Tew, D.G., Jones, O.T., and England, P.J. (1993). Studies on the inhibitory mechanism of iodonium compounds with special reference to neutrophil NADPH oxidase. Biochem J *290 (Pt 1)*, 41-49.
Olins, A.L., and Olins, D.E. (2004). Cytoskeletal influences on nuclear shape in granulocytic HL-60 cells. BMC Cell Biol *5*, 30.
Olins, A.L., and Olins, D.E. (2005). The mechanism of granulocyte nuclear shape determination: possible involvement of the centrosome. Eur J Cell Biol *84*, 181-188.
Ong, S.E., Blagoev, B., Kratchmarova, I., Kristensen, D.B., Steen, H., Pandey, A., and Mann, M. (2002). Stable isotope labeling by amino acids in cell culture, SILAC, as a simple and accurate approach to expression proteomics. Mol Cell Proteomics *1*, 376-386.
Palmer, L.J., Cooper, P.R., Ling, M.R., Wright, H.J., Huissoon, A., and Chapple, I.L. (2012). Hypochlorous acid regulates neutrophil extracellular trap release in humans. Clinical and experimental immunology *167*, 261-268.
Papayannopoulos, V., Metzler, K.D., Hakkim, A., and Zychlinsky, A. (2010). Neutrophil elastase and myeloperoxidase regulate the formation of neutrophil extracellular traps. J Cell Biol *191*, 677-691.
Papayannopoulos, V., and Zychlinsky, A. (2009a). NETs: a new strategy for using old weapons. Trends Immunol *30*, 513-521.
Papayannopoulos, V., and Zychlinsky, A. (2009b). NETs: a new strategy for using old weapons. In Trends Immunol, pp. 513-521.
Park, J., Wysocki, R.W., Amoozgar, Z., Maiorino, L., Fein, M.R., Jorns, J., Schott, A.F., Kinugasa-Katayama, Y., Lee, Y., Won, N.H.*, et al.* (2016). Cancer cells induce metastasis-supporting neutrophil extracellular DNA traps. Sci Transl Med *8*, 361ra138.

Parker, H., Dragunow, M., Hampton, M.B., Kettle, A.J., and Winterbourn, C.C. (2012). Requirements for NADPH oxidase and myeloperoxidase in neutrophil extracellular trap formation differ depending on the stimulus. J Leukoc Biol *92*, 841-849.
Patel, S., Kumar, S., Jyoti, A., Srinag, B.S., Keshari, R.S., Saluja, R., Verma, A., Mitra, K., Barthwal, M.K., Krishnamurthy, H.*, et al.* (2010). Nitric oxide donors release extracellular traps from human neutrophils by augmenting free radical generation. Nitric Oxide *22*, 226-234.
Petrides, P.E., and Nauseef, W.M. (1998). Molecular and clinical aspects of neutrophil peroxidase deficiency: multidisciplinary approaches on an international scale. J Mol Med (Berl) *76*, 659-660.
Pilsczek, F.H., Salina, D., Poon, K.K., Fahey, C., Yipp, B.G., Sibley, C.D., Robbins, S.M., Green, F.H., Surette, M.G., Sugai, M.*, et al.* (2010). A novel mechanism of rapid nuclear neutrophil extracellular trap formation in response to Staphylococcus aureus. J Immunol *185*, 7413-7425.
Podolska, M.J., Biermann, M.H., Maueroder, C., Hahn, J., and Herrmann, M. (2015). Inflammatory etiopathogenesis of systemic lupus erythematosus: an update. Journal of inflammation research *8*, 161-171.
Porto, B.N., and Stein, R.T. (2016). Neutrophil Extracellular Traps in Pulmonary Diseases: Too Much of a Good Thing? Front Immunol *7*, 311.
Prescott, S.M., Zimmerman, G.A., Stafforini, D.M., and McIntyre, T.M. (2000). Platelet-activating factor and related lipid mediators. Annu Rev Biochem *69*, 419-445.
Rabinowitz, J.D., Purdy, J.G., Vastag, L., Shenk, T., and Koyuncu, E. (2011). Metabolomics in drug target discovery. Cold Spring Harbor symposia on quantitative biology *76*, 235-246.
Reaves, M.L., and Rabinowitz, J.D. (2011). Metabolomics in systems microbiology. Current opinion in biotechnology *22*, 17-25.
Reddy, K.V., Yedery, R.D., and Aranha, C. (2004). Antimicrobial peptides: premises and promises. Int J Antimicrob Agents *24*, 536-547.
Reeves, E.P., Lu, H., Jacobs, H.L., Messina, C.G., Bolsover, S., Gabella, G., Potma, E.O., Warley, A., Roes, J., and Segal, A.W. (2002). Killing activity of neutrophils is mediated through activation of proteases by K+ flux. Nature *416*, 291-297.
Remijsen, Q., Vanden Berghe, T., Wirawan, E., Asselbergh, B., Parthoens, E., De Rycke, R., Noppen, S., Delforge, M., Willems, J., and Vandenabeele, P. (2011). Neutrophil extracellular trap cell death requires both autophagy and superoxide generation. Cell Res *21*, 290-304.
Rivera, A., Siracusa, M.C., Yap, G.S., and Gause, W.C. (2016). Innate cell communication kick-starts pathogen-specific immunity. Nat Immunol *17*, 356-363.
Roberts, P.J., and Der, C.J. (2007). Targeting the Raf-MEK-ERK mitogen-activated protein kinase cascade for the treatment of cancer. Oncogene *26*, 3291-3310.
Ross, P.L., Huang, Y.N., Marchese, J.N., Williamson, B., Parker, K., Hattan, S., Khainovski, N., Pillai, S., Dey, S., Daniels, S.*, et al.* (2004). Multiplexed protein quantitation in Saccharomyces cerevisiae using amine-reactive isobaric tagging reagents. Mol Cell Proteomics *3*, 1154-1169.
Rossaint, J., Herter, J.M., Van Aken, H., Napirei, M., Doring, Y., Weber, C., Soehnlein, O., and Zarbock, A. (2014). Synchronized integrin engagement and chemokine activation is crucial in neutrophil extracellular trap-mediated sterile inflammation. Blood *123*, 2573-2584.
Rubinsztein, D.C., Codogno, P., and Levine, B. (2012). Autophagy modulation as a potential therapeutic target for diverse diseases. Nat Rev Drug Discov *11*, 709-730.
Saitoh, T., Komano, J., Saitoh, Y., Misawa, T., Takahama, M., Kozaki, T., Uehata, T., Iwasaki, H., Omori, H., Yamaoka, S.*, et al.* (2012). Neutrophil extracellular traps mediate a host defense response to human immunodeficiency virus-1. Cell Host Microbe *12*, 109-116.
Sala, A., Folco, G., and Murphy, R.C. (2010). Transcellular biosynthesis of eicosanoids. Pharmacol Rep *62*, 503-510.
Saladino, R., Gualandi, G., Farina, A., Crestini, C., Nencioni, L., and Palamara, A.T. (2008). Advances and challenges in the synthesis of highly oxidised natural phenols with antiviral, antioxidant and cytotoxic activities. Current medicinal chemistry *15*, 1500-1519.
Savige, J., Davies, D., Falk, R.J., Jennette, J.C., and Wiik, A. (2000). Antineutrophil cytoplasmic antibodies and associated diseases: a review of the clinical and laboratory features. Kidney Int *57*, 846-862.
Scapini, P., and Cassatella, M.A. (2014). Social networking of human neutrophils within the immune system. Blood *124*, 710-719.

Schenone, M., Dancik, V., Wagner, B.K., and Clemons, P.A. (2013). Target identification and mechanism of action in chemical biology and drug discovery. Nature chemical biology *9*, 232-240.
Schroeder, B.O., Wu, Z., Nuding, S., Groscurth, S., Marcinowski, M., Beisner, J., Buchner, J., Schaller, M., Stange, E.F., and Wehkamp, J. (2011). Reduction of disulphide bonds unmasks potent antimicrobial activity of human beta-defensin 1. Nature *469*, 419-423.
Schultz, J., and Kaminker, K. (1962). Myeloperoxidase of the leucocyte of normal human blood. I. Content and localization. Arch Biochem Biophys *96*, 465-467.
Segal, A.W., Dorling, J., and Coade, S. (1980). Kinetics of fusion of the cytoplasmic granules with phagocytic vacuoles in human polymorphonuclear leukocytes. Biochemical and morphological studies. J Cell Biol *85*, 42-59.
Seger, R.A. (2010). Chronic granulomatous disease: recent advances in pathophysiology and treatment. Neth J Med *68*, 334-340.
Shelef, M.A., Tauzin, S., and Huttenlocher, A. (2013). Neutrophil migration: moving from zebrafish models to human autoimmunity. Immunol Rev *256*, 269-281.
Simard, F.A., Cloutier, A., Ear, T., Vardhan, H., and McDonald, P.P. (2015). MEK-independent ERK activation in human neutrophils and its impact on functional responses. J Leukoc Biol *98*, 565-573.
Stark, M.A., Huo, Y., Burcin, T.L., Morris, M.A., Olson, T.S., and Ley, K. (2005). Phagocytosis of apoptotic neutrophils regulates granulopoiesis via IL-23 and IL-17. Immunity *22*, 285-294.
Stefanska, J., and Pawliczak, R. (2008). Apocynin: molecular aptitudes. Mediators Inflamm *2008*, 106507.
Steinberg, B.E., and Grinstein, S. (2007). Unconventional roles of the NADPH oxidase: signaling, ion homeostasis, and cell death. Sci STKE *2007*, pe11.
Stigter, E.A., Guo, Z., Bon, R.S., Wu, Y.W., Choidas, A., Wolf, A., Menninger, S., Waldmann, H., Blankenfeldt, W., and Goody, R.S. (2012). Development of selective, potent RabGGTase inhibitors. J Med Chem *55*, 8330-8340.
Sundberg, S.A. (2000). High-throughput and ultra-high-throughput screening: solution- and cell-based approaches. Current opinion in biotechnology *11*, 47-53.
t Hart, B.A., Simons, J.M., Knaan-Shanzer, S., Bakker, N.P., and Labadie, R.P. (1990). Antiarthritic activity of the newly developed neutrophil oxidative burst antagonist apocynin. Free Radic Biol Med *9*, 127-131.
Tamaoki, T., Nomoto, H., Takahashi, I., Kato, Y., Morimoto, M., and Tomita, F. (1986). Staurosporine, a potent inhibitor of phospholipid/Ca++dependent protein kinase. Biochem Biophys Res Commun *135*, 397-402.
Tellis, C.C., and Tselepis, A.D. (2014). Pathophysiological role and clinical significance of lipoprotein-associated phospholipase A(2) (Lp-PLA(2)) bound to LDL and HDL. Curr Pharm Des *20*, 6256-6269.
Thirumurugan, P., Matosiuk, D., and Jozwiak, K. (2013). Click chemistry for drug development and diverse chemical-biology applications. Chem Rev *113*, 4905-4979.
Thompson, A.D., Makley, L.N., McMenimen, K., and Gestwicki, J.E. (2012). The three cornerstones of chemical biology: innovative probes, new discoveries, and enabling tools. ACS Chem Biol *7*, 791-796.
Toker, A. (2005). The biology and biochemistry of diacylglycerol signalling. Meeting on molecular advances in diacylglycerol signalling. EMBO Rep *6*, 310-314.
Tsuchiya, M., Piras, V., Giuliani, A., Tomita, M., and Selvarajoo, K. (2010). Collective dynamics of specific gene ensembles crucial for neutrophil differentiation: the existence of genome vehicles revealed. PloS one *5*, e12116.
Urban, C.F., Ermert, D., Schmid, M., Abu-Abed, U., Goosmann, C., Nacken, W., Brinkmann, V., Jungblut, P.R., and Zychlinsky, A. (2009). Neutrophil extracellular traps contain calprotectin, a cytosolic protein complex involved in host defense against Candida albicans. PLoS Pathog *5*, e1000639.
van der Linden, M., and Meyaard, L. (2016). Fine-tuning neutrophil activation: Strategies and consequences. Immunology letters.
Vieira, O.V., Botelho, R.J., and Grinstein, S. (2002). Phagosome maturation: aging gracefully. Biochem J *366*, 689-704.
Voigt, T., Gerding-Reimers, C., Ngoc Tran, T.T., Bergmann, S., Lachance, H., Scholermann, B., Brockmeyer, A., Janning, P., Ziegler, S., and Waldmann, H. (2013). A natural product inspired tetrahydropyran collection yields mitosis modulators that synergistically target CSE1L and tubulin. Angewandte Chemie *52*, 410-414.

von Kockritz-Blickwede, M., and Nizet, V. (2009). Innate immunity turned inside-out: antimicrobial defense by phagocyte extracellular traps. J Mol Med (Berl) *87*, 775-783.
Walker, B.A., Hagenlocker, B.E., and Ward, P.A. (1991). Superoxide responses to formyl-methionyl-leucyl-phenylalanine in primed neutrophils. Role of intracellular and extracellular calcium. J Immunol *146*, 3124-3131.
Walker, M.J., Hollands, A., Sanderson-Smith, M.L., Cole, J.N., Kirk, J.K., Henningham, A., McArthur, J.D., Dinkla, K., Aziz, R.K., Kansal, R.G.*, et al.* (2007). DNase Sda1 provides selection pressure for a switch to invasive group A streptococcal infection. Nat Med *13*, 981-985.
Walker, T.S., Tomlin, K.L., Worthen, G.S., Poch, K.R., Lieber, J.G., Saavedra, M.T., Fessler, M.B., Malcolm, K.C., Vasil, M.L., and Nick, J.A. (2005). Enhanced Pseudomonas aeruginosa biofilm development mediated by human neutrophils. Infect Immun *73*, 3693-3701.
Warnatsch, A., Ioannou, M., Wang, Q., and Papayannopoulos, V. (2015). Inflammation. Neutrophil extracellular traps license macrophages for cytokine production in atherosclerosis. Science *349*, 316-320.
Weinrauch, Y., Drujan, D., Shapiro, S.D., Weiss, J., and Zychlinsky, A. (2002). Neutrophil elastase targets virulence factors of enterobacteria. Nature *417*, 91-94.
Weinstein, J.N. (2001). Searching for pharmacogenomic markers: the synergy between omic and hypothesis-driven research. Dis Markers *17*, 77-88.
Wetzel, S., Bon, R.S., Kumar, K., and Waldmann, H. (2011). Biology-oriented synthesis. Angewandte Chemie *50*, 10800-10826.
Wetzel, S., Klein, K., Renner, S., Rauh, D., Oprea, T.I., Mutzel, P., and Waldmann, H. (2009). Interactive exploration of chemical space with Scaffold Hunter. Nature chemical biology *5*, 581-583.
Williams, R. (2006). Killing controversy. J Exp Med *203*, 2404.
Winkelstein, J.A., Marino, M.C., Johnston, R.B., Jr., Boyle, J., Curnutte, J., Gallin, J.I., Malech, H.L., Holland, S.M., Ochs, H., Quie, P.*, et al.* (2000). Chronic granulomatous disease. Report on a national registry of 368 patients. Medicine (Baltimore) *79*, 155-169.
Winterbourn, C.C., Hampton, M.B., Livesey, J.H., and Kettle, A.J. (2006). Modeling the reactions of superoxide and myeloperoxidase in the neutrophil phagosome: implications for microbial killing. J Biol Chem *281*, 39860-39869.
Wisniewski, J.R., Zougman, A., and Mann, M. (2009). Combination of FASP and StageTip-based fractionation allows in-depth analysis of the hippocampal membrane proteome. J Proteome Res *8*, 5674-5678.
Wu, T., and Mohan, C. (2007). Three pathogenic determinants in immune nephritis--anti-glomerular antibody specificity, innate triggers and host genetics. Front Biosci *12*, 2207-2211.
Wymann, M.P., and Schneiter, R. (2008). Lipid signalling in disease. Nat Rev Mol Cell Biol *9*, 162-176.
Wymann, M.P., Zvelebil, M., and Laffargue, M. (2003). Phosphoinositide 3-kinase signalling--which way to target? Trends Pharmacol Sci *24*, 366-376.
Yedgar, S., Krimsky, M., Cohen, Y., and Flower, R.J. (2007). Treatment of inflammatory diseases by selective eicosanoid inhibition: a double-edged sword? Trends Pharmacol Sci *28*, 459-464.
Yipp, B.G., and Kubes, P. (2013). NETosis: how vital is it? Blood *122*, 2784-2794.
Yoo, D.G., Floyd, M., Winn, M., Moskowitz, S.M., and Rada, B. (2014). NET formation induced by Pseudomonas aeruginosa cystic fibrosis isolates measured as release of myeloperoxidase-DNA and neutrophil elastase-DNA complexes. Immunology letters *160*, 186-194.
Yost, C.C., Weyrich, A.S., and Zimmerman, G.A. (2010). The platelet activating factor (PAF) signaling cascade in systemic inflammatory responses. Biochimie *92*, 692-697.
Yousefi, S., Gold, J.A., Andina, N., Lee, J.J., Kelly, A.M., Kozlowski, E., Schmid, I., Straumann, A., Reichenbach, J., Gleich, G.J.*, et al.* (2008). Catapult-like release of mitochondrial DNA by eosinophils contributes to antibacterial defense. Nat Med *14*, 949-953.
Yousefi, S., Mihalache, C., Kozlowski, E., Schmid, I., and Simon, H.U. (2009). Viable neutrophils release mitochondrial DNA to form neutrophil extracellular traps. Cell Death Differ *16*, 1438-1444.
Yousefi, S., and Simon, H.U. (2016). NETosis - Does It Really Represent Nature's "Suicide Bomber"? Front Immunol *7*, 328.
Yu, Y., and Su, K. (2013). Neutrophil Extracellular Traps and Systemic Lupus Erythematosus. J Clin Cell Immunol *4*.

Ziegler, S., Pries, V., Hedberg, C., and Waldmann, H. (2013). Target identification for small bioactive molecules: finding the needle in the haystack. Angewandte Chemie *52*, 2744-2792.
Zieske, L.R. (2006). A perspective on the use of iTRAQ reagent technology for protein complex and profiling studies. J Exp Bot *57*, 1501-1508.
Zimmermann, T.J., Burger, M., Tashiro, E., Kondoh, Y., Martinez, N.E., Gormer, K., Rosin-Steiner, S., Shimizu, T., Ozaki, S., Mikoshiba, K.*, et al.* (2013). Boron-based inhibitors of acyl protein thioesterases 1 and 2. Chembiochem *14*, 115-122.

Acknowledgements

Primarily, I would like to thank Prof. Dr. Dr. Herbert Waldmann for this a life changing opportunity of being the first in my family to pursue a doctorate degree. For making it possible to study in Germany in such an interesting and challenging topic. For his supervision and scientific freedom, making this period a genuine learning experience at all levels, supporting my project, inspiring input, challenging discussions, for keeping me focused allowing me to develop as an independent researcher and for the non-scientific lessons like pouring a proper German 7 min. beer. It has been an honor to work with such a brilliant mind and see it in action.

I sincerely thank Prof. Arturo Zychlinsky for taking me into his group as one of the lab members. For his supervision and suggestions regarding the biological relevance of my project. For opportunity of working and meeting important people and inspiration of successful Mexican. Por abrirme la puertas de su hogar. Muy agradecida.

In would like to acknowledge Dr. Carsten Watzl for being part of my PhD defense. For a very satisfying scientific discussion, Thank you.

I sincerely thank Dr. Luis Martinez for showing me the dark side…for being my first mentor who made this experience possible by supporting me and all the letters of recommendation he made for me.

I am most grateful to Dr. Gemma Triola for being there for me scientifically and personally. For all the discussions, for guidance…y por motivarme. For always being there when I needed you the most. Gracias nena.

I would like to thank Dr. Slava Ziegler for keeping track of me in such a complicated situation and all in my projects. For extensive suggestions, discussions, support, and guidance. For taking your time in to revise my thesis and paper in your busy schedule.

Dr. Juana de Diego for all the support in and out of the lab. For teaching me and educational discussion for being a human encyclopedia. Dr. Alejandro Sanchez for teaching me all the techniques that I was lacking and being my idea buddy. Gracias a los dos.

I would like to acknowledge the people with whom I collaborated: Dr. Abdul Hakkim Rahamathullah for a fantastic job in setting the basis for my project; Dr. Tobias J. Zimmmermann for the cool-teamwork in the chemistry; LDC- Dr. Axel Chondras, Dr. Matthias Baumann and Peter Habenberger for the work on Hedgehog Project; Dr. Tashiro-san, for their work in the microtubule inhibition project; Collaboration with RIKEN Advanced Science Institute. Thanks to the Dortmund Proteomics analytic team, Dr. Petra Janning, Andreas Brockmeyer; Berlin Proteomics team Dr. Monica Schimidt.

I would like to thank the MPI-Dortmund and MPI-Berlin administration teams. Specially Gaby Gresch and Johana Schutz for being so patient and helping me out with all the traveling tickets; Cornelia Heinz and Dr. Bärbel Raupach for organizing all that it took to be part of the lab.

I am very grateful of having been part of the IMPRS-family; I am thankful for Dr. Waltraud Hofmann-Goody and Christa Hornemann, for the lovely conversations and encouragement; Prof. Dr. Martin Engelhard for all his support. Many thanks for the financial support and all the means to do my work promptly. For allowing me to organize the IMPRS Sympossium 2010, it was an exciting time and a great learning experience.

I would like to thank all my colleagues of the chemical biology department, the AKW, and the infection biology department for providing a great working environment. In particular I want to thank my past and present lab-mates of that always made the lab a fun place to work: chemistry A3.11. Dr. Sebastian Koch, Dr. Luc Eberhard, Dr. Tobias Zimmermann, Dr. Peter Schröder, Melanie Schwalfenberg, Dr. Maria Pascual, Janine Schulte-Zweckel, Sho, and Federica Rosi. Biology lab A3.17 Dr. Verena Pries, Christine Novak, Dr. Tuyen Tran, Dr. Marion Rusch, Dr. Kirsten Tschapalda and Dr. Philipp Küchler. My last office A3.28 Michael Winzler, Dr. Tom Mejuch, Dr. Lucas Robke, Dr. Philipp Küchler, Janine Schulte-Zweckel, Dr. Luca Laria..thanks for having me in the office

My labmates in Berlin

To all the lifelong friends that I made during my life in Germany. Melanie, Kristina G., Gloria, Kirsten, Bahar, Gemma, Cat, Luca, Jacqui, Anouk, Philipp, Natalie, and Sven for being a positive influence in my life and showing me that being me is good. All of you for going with me in adventures I would not be the person I am today without your touch in my life and my best cheerleaders.

Martijn, they are no words to express all the gratitude and the love you make me feel. For being the toughest critic of my work, my best friend, confidant, teacher in and out the lab, for all the great chemistry input and making my phd time the best and the hardest time of my life.

Finalmente, quiero agradecer le a mi grande familia. A mis padres Daniel y Elvira por apoyarme incondicionalmente y hacer mi educacion una prioridad en mi vida. Al llegar a este nivel no podria hacerlo sin su apoyo y su motivacion. Mamá gracias por todas esas cartas que hicieron los momentos mas dificiles, possibles. Papá gracias por todas sus palabras de aliento y los viajes a casa.

A mis hermanos Daniel y Aztlan que gracias a ellos siempre mantego mis pies firmes en la tierra. Y por ser mis amigos y mis guardianes siempre.

Abuelita Sofia por ser ese roble que hace nuestra familia fuerte. Tia Irma por inspirarme de que no hay edad para encontrar una nueva carrera. Tia Maty le das sentido a mi trabajo, d.e.p. A mis tios, tias, primas y primos a los Rey y a los Martinez por manterme motivada y sentirme ser miembro de la familia.

A mis amigos de toda la vida, a mis nenas Rocio y Karina, por siempre recibirme y hablar conmigo como si nunca me hubiera ido. A los punkers, no importa en la parte del mundo donde me encuentre siempre me reciben con los brazos abiertos y por algunos que han venido a visitarme Menny, Hashish ahahhaha, Ramon. A los que fueron a la casa: Menny, Marina, Shaba, Nora Ivet, Yadira, Chikis, gracias por ayudarme a practicar mis primeras platicas en español.

A mis sobrin@s Leonardo, Danielito, Chantal, Victoria, Oscarito, Valentina, Mateo, Mael e Ira que son nuestro futuro y me dan mucho aliento al verlos crecer.

Y a todas las personas que me han ayudado a lo largo de mi vida.To all my mentors throughout my life Gracias, Vielen Dank, Dankie wel, my sincerest thanks…My life will never be the same ☺

Declaration

Hiermit versichere ich an Eides statt, dass ich die vorliegende Arbeit selbständig und nur mit den angegeben Hilfsmitteln angefertigt habe.

I hereby declare that I performed the work presented independently and did not use any other but the indicated aids.

Nijmegen, NL, August 2017

Nancy E. Martinez